RADIOLOGY AND ONCOLOGY

vol.48 no.4
december 2014

Halaven®
eribulin

NOVA SMER DO PODALJŠANJA **CELOKUPNEGA PREŽIVETJA**

Eisai

Prva in edina samostojna kemoterapija,
ki v primerjavi z ostalimi možnostmi zdravljenja
z enim zdravilom, pri bolnicah s predhodno že
večkratno zdravljenim metastatskim rakom dojke,
dokazano značilno podaljša celokupno preživetje.[1,2]

- **Halaven** (eribulin): ne-taksanski zaviralec dinamike mikrotubulov, prvo zdravilo iz nove skupine kemoterapevtikov, imenovanih *halihondrini*.
- Zdravilo HALAVEN je indicirano za zdravljenje bolnic z lokalno napredovalim ali metastatskim rakom dojke, ki je napredoval po vsaj enem režimu kemoterapije za napredovalo bolezen. Predhodna zdravljenja morajo vključevati antraciklin in taksan, bodisi kot adjuvantno zdravljenje ali za zdravljenje metastatskega raka dojke, razen če to zdravljenje za bolnice ni bilo primerno.[1]
- Priporočeni odmerek 1,23 mg/m^2, intravensko, v obliki 2- do 5-minutne infuzije, 1. in 8. dan vsakega 21-dnevnega cikla.
- Ena 2 ml viala vsebuje 0,88 mg eribulina.
- Raztopina, pripravljena za uporabo, redčenje ni potrebno.

SKRAJŠAN POVZETEK GLAVNIH ZNAČILNOSTI ZDRAVILA

HALAVEN 0,44 mg/ml raztopina za injiciranje (eribulin)
TERAPEVTSKE INDIKACIJE: Zdravljenje lokalno napredovalega ali metastatskega raka dojke, ki je napredoval po vsaj enem režimu kemoterapije za napredovalo bolezen vključno z antraciklinom in taksanom (adjuvantno zdravljenje ali zdravljenje metastatskega raka dojke), razen če to ni bilo primerno. **ODMERJANJE IN NAČIN UPORABE:** Halaven se daje v enotah, specializiranih za dajanje citotoksične kemoterapije, in le pod nadzorom usposobljenega zdravnika z izkušnjami v uporabi citotoksičnih zdravil. Odmerjanje: Priporočeni odmerek eribulina v obliki raztopine je 1,23 mg/m^2 i.v. v obliki 2- do 5-minutne infuzije 1. in 8. dan vsakega 21-dnevnega cikla. Bolnikom je lahko slabo ali bruhajo. Treba je razmisliti o antiemetični profilaksi, vključno s kortikosteroidi. *Preložitev odmerka med zdravljenjem*: Dajanje Halavena je treba preložiti, če se pojavi kaj od naslednjega: absolutno število nevtrofilcev (ANC) < 1 x 10^9/l, trombociti < 75 x 10^9/l ali nehematološki neželeni učinki 3. ali 4. stopnje. *Zmanjšanje odmerka med zdravljenjem*: Za priporočila za zmanjšanje odmerka ob pojavu hematoloških ali nehematoloških neželenih učinkov glejte celoten povzetek glavnih značilnosti zdravila. Okvara jeter zaradi zasevkov: Priporočeni odmerek pri blagi okvari jeter (stopnje A po Child-Pughu) je 0,97 mg/m^2 v obliki 2- do 5-minutne i.v. infuzije 1. in 8. dan 21-dnevnega cikla. Priporočeni odmerek pri zmerni okvari jeter (stopnje B po Child-Pughu) je 0,62 mg/m^2 v obliki 2- do 5-minutne i.v. infuzije 1. in 8. dan 21-dnevnega cikla. Pri hudi okvari jeter (stopnje C po Child-Pughu) se pričakuje, da je treba dati še manjši odmerek eribulina. Okvara jeter zaradi ciroze: Zgornje odmerke se lahko uporabi za blago do zmerno okvaro, vendar se priporoča skrbno nadziranje, saj bo odmerke morda treba ponovno prilagoditi. Okvara ledvic: Pri hudi okvari ledvic (očistek kreatinina < 40 ml/min) bo morda treba odmerek zmanjšati. Priporoča se skrbno nadziranje varnosti. Način uporabe: Odmerek se lahko razredči z do 100 ml 0,9 % raztopine natrijevega klorida (9 mg/ml) za injiciranje. Ne sme se ga redčiti v 5 % infuzijski raztopini glukoze. Pred dajanjem glejte navodila glede redčenja zdravila v celotnem povzetku glavnih značilnosti zdravila ter se prepričajte, da obstaja dober periferni venski dostop ali prehodna centralna linija. Ni znakov, da bi eribulin povzročal mehurje ali dražil. V primeru ekstravazacije mora biti zdravljenje simptomatsko. **KONTRAINDIKACIJE:** Preobčutljivost na zdravilno učinkovino ali katerokoli pomožno snov. Dojenje. **POSEBNA OPOZORILA IN PREVIDNOSTNI UKREPI:** Mielosupresija je odvisna od odmerka in se kaže kot nevtropenija. Pred vsakim odmerkom eribulina je treba opraviti pregled celotne krvne slike. Zdravljenje z eribulinom se lahko uvede le pri bolnikih z vrednostmi ANC ≥ 1,5 x 10^9/l in s trombociti > 100 x 10^9/l. Bolnike, pri katerih se pojavijo febrilna nevtropenija, huda nevtropenija ali trombocitopenija, je treba zdraviti v skladu s priporočili v celotnem povzetku glavnih značilnosti zdravila. Hudo nevtropenijo se lahko zdravi z uporabo G-CSF ali enakovrednim zdravilom v skladu s smernicami. Bolnike je treba skrbno nadzirati za znake periferne motorične in senzorične nevropatije. Pri razvoju hude periferne nevrotoksičnosti je treba odmerek prestaviti ali zmanjšati. Če začnemo zdravljenje pri bolnikih s kongestivnim srčnim popuščanjem, z bradiaritmijami ali sočasno z zdravili, za katera je znano, da podaljšujejo interval QT, vključno z antiaritmiki razreda Ia in III, in z elektrolitskimi motnjami, je priporočljivo spremljanje EKG. Pred začetkom zdravljenja s Halavenom je treba popraviti hipokaliemijo in hipomagneziemijo in te elektrolite je treba občasno kontrolirati med zdravljenjem. Eribulina ne smemo dajati bolnikom s prirojenim sindromom dolgega intervala QT. To zdravilo vsebuje majhne količine etanola (alkohola), manj kot 100 mg na odmerek. Eribulin je pri podganah embriotoksičen, fetotoksičen in teratogen. Halavena se ne sme uporabljati med nosečnostjo, razen kadar je to nujno potrebno. Ženske v rodni dobi naj ne zanosijo v času, ko same ali njihov moški partner dobivajo Halaven, in naj med zdravljenjem in še do 3 mesece po njem uporabljajo učinkovito kontracepcijo. Moški naj se pred zdravljenjem posvetujejo o shranjevanju sperme zaradi možnosti nepopravljive neplodnosti. **INTERAKCIJE:** Eribulin se izloča do 70 % prek žolča. Sočasna uporaba učinkovin, ki zavirajo jetrne transportne beljakovine, kot so beljakovine za prenos organskih anionov in beljakovine, odporne na številna zdravila, z eribulinom se ne priporoča (npr. ciklosporin, ritonavir, sakvinavir, lopinavir in nekateri drugi zaviralci proteaze, efavirenz, emtricitabin, verapamil, klaritromicin, kinin, kinidin, dizopiramid itd). Sočasno zdravljenje z indukcijskimi učinkovinami, kot so rifampicin, karbamazepin, fenitoin, šentjanževka, lahko povzroči znižanje koncentracij eribulina v plazmi, zato je ob sočasni uporabi induktorjev potrebna previdnost. Eribulin je blag inhibitor encima CYP3A4. Priporočljiva je previdnost in spremljanje glede neželenih učinkov pri sočasni uporabi snovi, ki imajo ozko terapevtsko okno in se odstranjujejo iz telesa predvsem preko CYP3A4 (npr. alfentanil, ciklosporin, ergotamin, fentanil, pimozid, kinidin, sirolimus, takrolimus). **NEŽELENI UČINKI:** Povzetek varnostnega profila Neželeni učinek, o katerem najpogosteje poročajo v zvezi s Halavenom, je supresija kostnega mozga, ki se kaže kot nevtropenija, levkopenija, anemija, trombocitopenija s pridruženimi okužbami. Poročali so tudi o novem začetku ali poslabšanju že obstoječe periferne nevropatije. Med neželenimi učinki, o katerih poročajo, je toksičnost za prebavila, ki se kaže kot anoreksija, navzea, bruhanje, driska, zaprtost in stomatitis. Med drugimi neželenimi učinki so utrujenost, alopecija, zvečani jetrni encimi, sepsa in mišičnoskeletni bolečinski sindrom. Seznam neželenih učinkov: *Zelo pogosti (≥ 1/10):* nevtropenija (57,0 %) (3./4. stopnje: 49,7 %), levkopenija (29,3 %) (3./4. stopnje: 17,3 %), anemija (20,6 %) (3./4. stopnje: 2,0 %), zmanjšan apetit (21,9 %) (3./4. stopnje: 0,7 %), periferna nevropatija (35,6 %) (3./4. stopnje: 7,6 %), glavobol (17,2 %) (3./4. stopnje: 0,8 %), dispnea (13,9 %) (3./4. stopnje: 3,1 %), kašelj (13,6 %) (3./4. stopnje: 0,6 %), navzea (33,8 %) (3./4. stopnje: 1,1 %), zaprtost (19,6 %) (3./4. stopnje: 0,6 %), driska (17,9 %) (3./4. stopnje: 0,8 %), bruhanje (17,6 %) (3./4. stopnje: 0,9 %), alopecija, artralgija in mialgija (19,4 %) (3./4. stopnje: 1,1 %), bolečina v hrbtu (13,0 %) (3./4. stopnje: 1,5 %), bolečina v udu (10,0 %) (3./4. stopnje: 0,7 %), utrujenost/astenija (47,9 %) (3./4. stopnje: 7,8 %), pireksija (20,4 %) (3./4. stopnje: 0,6 %), zmanjšanje telesne mase (11,3 %) (3./4. stopnje: 0,3 %). *Pogosti (≥ 1/100 do < 1/10):* okužba sečil (8 %) (3./4. stopnje: 0,5 %), pljučnica (1,2 %) (3./4. stopnje: 0,8 %), ustna kandidiaza, ustni herpes, okužba zgornjih dihal, nazofaringitis, rinitis, limfopenija (4,9 %) (3./4. stopnje: 1,4 %), febrilna nevtropenija (4,7 %) (3./4. stopnje: 4,5 %), trombocitopenija (4,3 %) (3./4. stopnje: 0,7 %), hipokaliemija (6,1 %) (3./4. stopnje: 1,7 %), hipomagneziemija (2,9 %) (3./4. stopnje: 0,2 %), dehidracija (2,8 %) (3./4. stopnje: 0,5 %), hiperglikemija, hipofosfatemija, nespečnost, depresija, disgevzija, omotičnost (7,9 %) (3./4. stopnje: 0,5 %), hipoestezija, letargija, nevrotoksičnost, obilnejše solzenje (6,0 %) (3./4. stopnje: 0,1 %), konjunktivitis, vrtoglavica, tahikardija, vročinski valovi, orofaringealna bolečina, epistaksa, rinoreja, bolečina v trebuhu, stomatitis (9,3 %) (3./4. stopnje: 0,8 %), suha usta, dispepsija (5,9 %) (3./4. stopnje: 0,2 %), gastroezofagealna refluksna bolezen, razjede v ustih, distenzija trebuha, zvišanje alanin-aminotransferaze (7,6 %) (3./4. stopnje: 2,1 %), zvišanje aspartat-aminotransferaze (7,4 %) (3./4. stopnje: 1,5 %), zvišanje gama-glutamiltransferaze (1,8 %) (3./4. stopnje: 0,9 %), hiperbilirubinemija (1,5 %) (3./4. stopnje: 0,3 %), izpuščaj, pruritus (3,9 %) (3./4. stopnje: 0,1 %), bolezni nohtov, nočno potenje, suha koža, eritem, hiperhidroza, bolečina v kosteh (9,6 %) (3./4. stopnje: 1,7 %), mišični spazmi (5,1 %) (3./4. stopnje: 0,1 %), mišično-skeletna bolečina in mišično-skeletna bolečina v prsih, mišična oslabelost, disurija, vnetje sluznice (8,3 %) (3./4. stopnje: 1,1 %), periferni edem, bolečina, mrzlica, bolečina v prsih, gripi podobna bolezen. *Občasni (≥ 1/1.000 do < 1/100):* sepsa (0,5 %) (3./4. stopnje: 0,2 %), nevtropenična sepsa (0,1 %) (3./4. stopnje: 0,1 %), herpes zoster, tinitus, globoka venska tromboza, pljučna embolija, hepatotoksičnost (1,0 %) (3./4. stopnje: 0.6 %), palmarno-plantarna eritrodisestezija, hematurija, proteinurija, odpoved ledvic. *Redki (≥ 1/10.000 do < 1/1.000):* diseminirana intravaskularna koagulacija, intersticijska pljučna bolezen, pankreatitis, angioedem. Za popoln opis neželenih učinkov glejte celoten povzetek glavnih značilnosti zdravila. Vrsta ovojnine in vsebina: viala z 2 ml raztopine. **Režim izdaje: H Imetnik dovoljenja za promet:** Eisai Europe Ltd, European Knowledge Centre, Mosquito Way, Hatfield, Hertfordshire, AL10 9SN, Velika Britanija
HAL-270614, julij 2014
Pred predpisovanjem in uporabo zdravila prosimo preberite celoten povzetek glavnih značilnosti zdravila!

Viri: (1) Povzetek glavnih značilnosti zdravila Halaven, junij 2014; (2) Cortes J *et al. Lancet* 2011; 377: 914–23.

PharmaSwiss
Choose More Life

Odgovoren za trženje v Sloveniji:
PharmaSwiss d.o.o., Brodišče 32, 1236 Trzin
telefon: +386 1 236 47 00, faks: +386 1 283 38 10
HAL-0714-01, julij 2014

RADIOLOGY AND ONCOLOGY

December 2014
Vol. 48 No. 4
Pages 331-425
ISSN 1318-2099
UDC 616-006
CODEN: RONCEM

Publisher
Association of Radiology and Oncology

Affiliated with
Slovenian Medical Association – Slovenian Association of Radiology, Nuclear Medicine Society,
Slovenian Society for Radiotherapy and Oncology, and Slovenian Cancer Society
Croatian Medical Association – Croatian Society of Radiology
Societas Radiologorum Hungarorum
Friuli-Venezia Giulia regional groups of S.I.R.M.
Italian Society of Medical Radiology

Aims and scope
Radiology and Oncology is a journal devoted to publication of original contributions in diagnostic and interventional radiology, computerized tomography, ultrasound, magnetic resonance, nuclear medicine, radiotherapy, clinical and experimental oncology, radiobiology, radiophysics and radiation protection.

Editorial office

Radiology and Oncology
Zaloška cesta 2
P. O. Box 2217
SI-1000 Ljubljana
Slovenia
Phone: +386 1 5879 369
Phone/Fax: +386 1 5879 434
E-mail: gsersa@onko-i.si

Reader for English

Vida Kološa

Secretary

Mira Klemenčič

Zvezdana Vukmirović

Design

Monika Fink-Serša, Samo Rovan, Ivana Ljubanović

Layout

Matjaž Lužar

Printed by

Tiskarna Ozimek, Slovenia

Published quarterly in 400 copies

Beneficiary name: DRUŠTVO RADIOLOGIJE IN ONKOLOGIJE
Zaloška cesta 2
1000 Ljubljana
Slovenia

Beneficiary bank account number: SI56 02010-0090006751
IBAN: SI56 0201 0009 0006 751
Our bank name: Nova Ljubljanska banka, d.d.,
Ljubljana, Trg republike 2,
1520 Ljubljana; Slovenia

SWIFT: LJBASI2X

Subscription fee for institutions EUR 100, individuals EUR 50

The publication of this journal is subsidized by the Slovenian Research Agency.

Indexed and abstracted by:
Science Citation Index Expanded (SciSearch®)
Journal Citation Reports/Science Edition
Scopus
PubMed
PubMed Central
EMBASE/Excerpta Medica
DOAJ
Open J-gate
Chemical Abstracts
Biomedicina Slovenica
Summon by Serial Solutions (ProQuest)

This journal is printed on acid- free paper

On the web: ISSN 1581-3207
http://www.degruyter.com/view/j/raon
http://www.radioloncol.com

contents

RADIOLOGY AND ONCOLOGY is covered in Science Citation Index Expanded (SciSearch®),Journal Citation Reports/Science Edition, Scopus, PubMed, PubMed Central, DOAJ, EMBASE/Excerpta Medica, Open J-gate, Chemical Abstracts, Biomedicina Slovenica, Summon by Serial Solutions (ProQuest)

research article

Accuracy of ^{18}F-flurodeoxyglucose-positron emission tomography/computed tomography in the staging of newly diagnosed nasopharyngeal carcinoma: a systematic review and meta-analysis

Balamurugan A. Vellayappan[1], Yu Yang Soon[1], Arul Earnest[2], Qing Zhang[3], Wee Yao Koh[1], Ivan Weng Keong Tham[1], Khai Mun Lee[1]

[1] Department of Radiation Oncology, National University Cancer Institute, National University Health System, National University of Singapore, Singapore

[2] Centre for Quantitative Medicine, Office of Clinical Sciences, Duke-NUS Graduate Medical School, Singapore

[3] Department of Radiation Oncology, Sixth Hospital of Jiao Tong University, Shanghai, People's Republic of China

Radiol Oncol 2014; 48(4): 331-338.

Received: 9 October 2013
Accepted: 14 January 2014

Correspondence to: Balamurugan Vellayappan, M.D., Department of Radiation Oncology, National University Cancer Institute, National University Health System, National University of Singapore, 1E Kent Ridge Road, NUHS Tower Block, Singapore 119228. E-mail: balamurugan_A_vellayappan@nuhs.edu.sg

Disclosure: No potential conflicts of interest were disclosed.

Background. The specific role of 18F-flurodeoxyglucose-positron emission tomography/computed tomography (FDG-PET/CT) in staging of nasopharyngeal carcinoma (NPC) remains to be validated. A systematic review and meta-analysis were performed to assess the accuracy of staging FDG-PET/CT for newly diagnosed NPC.

Methods. We searched various biomedical databases and conference proceedings for relevant studies. We determined the pooled sensitivities and specificities, diagnostic odds ratios (DOR) and constructed summary receiver operating characteristic (SROC) curves using the hierarchical regression model.

Results. 15 relevant studies including 851 patients were identified. Five addressed primary tumor (T), nine addressed regional lymph nodes (N) and seven addressed distant metastasis (M). The combined sensitivity estimate for FDG-PET/CT in T classification was 0.77 (95% confidence interval [CI] 0.59-0.95). For N classification, combined sensitivity was 0.84 (95% CI 0.76-0.91), specificity was 0.90 (95% CI 0.83-0.97), DOR was 82.4 (23.2-292.6) and Q*-index was 0.90. For M classification, the combined sensitivity estimate was 0.87 (95% CI 0.74-1.00), specificity was 0.98 (95% CI 0.96-1.00), DOR was 120.9 (43.0-340.0) and Q*-index was 0.89.

Conclusions. FDG-PET/CT showed good accuracy in N and M but not T classification for newly diagnosed NPC. FDG-PET/CT, together with Magnetic resonance imaging (MRI) of the nasopharynx, should be part of the routine staging investigations.

Key words: nasopharyngeal carcinoma; PET/CT; staging; accuracy; meta-analysis

Introduction

In 2008, there were approximately 84400 new cases of nasopharyngeal carcinoma (NPC) and 51600 deaths from the disease worldwide.[1] The geographical disparities in the burden of NPC are noteworthy, with incidence rates highest in East and Southeast Asia and lowest in Central America.[1]

NPC may spread locally to involve the parapharyngeal soft tissue, base of skull or intracranial structures. The nasopharynx has a rich lymphatic plexus; 75% of patients present with enlarged cer-

vical nodes, 80% of whom have bilateral involvement.[2] NPC has a relatively high incidence of systemic metastasis (up to 41%) when compared with the other head and neck tumors (5%–24%). The most common sites of metastases are bone (20%), lung (13%), and liver (9%).[3]

NPC is staged non-surgically and treated primarily with radiotherapy (with or without chemotherapy). Accurate staging is essential as it influences the choice of treatment modalities, radiotherapy planning and prognosis. Combined modality treatment, as well as larger treatment volumes, invariably leads to greater toxicities. Although FDG-PET/CT is sometimes used in the clinical management of NPC in preference to other imaging modalities, such computed tomography or bone scans, the magnitude of benefit of using FDG-PET/CT, if any, is unclear. Indications for its use in the clinic have been rather empirical than standardized in many centres, often in the setting of a diagnostic dilemma affecting treatment options after the use of conventional imaging modalities.

The American Joint Committee on Cancer (AJCC) T (Primary tumor) N (Regional lymph nodes) M (Distant Metastasis) system is one of the most widely used staging system internationally.[4] Conventional staging modalities may include MRI of the head and neck, contrast enhanced CT scans, liver ultrasound (US) and whole body radionuclide bone scan (WBBS). For M classification, one series reported the sensitivity and specificity for conventional workup (chest X-Ray, liver US, WBBS) to be 0.33 and 0.90 respectively; the same series reported CT of the thorax and abdomen with WBBS to be 0.67 and 0.92 respectively.[5]

The National Comprehensive Cancer Network (NCCN) guidelines recommend gadolinium-enhanced MRI of the nasopharynx and neck as well as CT scan (if indicated, for T and N classifications). It recommends imaging of distant metastases in the chest, liver and bones (which may include PET scan and/or CT) for patients with N2-3 disease. It also suggests that FDG-PET/CT scan may be considered for patients with Stage III and IV disease.[6]

The use of FDG-PET/CT has superseded standalone FDG-PET studies, by offering both functional and anatomic imaging, (for the initial staging and post-treatment assessments for a wide range of cancers).[7] Published individual studies in the medical literature have reported increased accuracy especially in detection of metastases but are less conclusive on local and regional staging. The role of FDG-PET/CT in the overall staging of pre-treated NPC remains to be validated. To our knowledge, only one systematic review and meta-analysis of six studies examining the accuracy of FDG-PET/CT in detection of distant metastasis in pre-treated NPC showed it to have a high sensitivity of 88% and specificity of 97% for M classification.[8] However, there were some limitations of this meta-analysis. Firstly, it did not address the accuracy of PET/CT scan for T and N classifications. Additionally, it excluded several publications in languages other than English[9,10] and finally, new data[11,12] have been published since the meta-analysis.

The aim of our study was to perform a systematic review and meta-analysis of all relevant publications to determine the accuracy of FDG-PET/CT in the TNM staging of newly diagnosed treatment naïve NPC patients, with reference to conventional modalities and/or clinical follow up.

Materials and methods

Identification and eligibility of relevant studies

We included studies, without language restriction, that determined the sensitivity and specificity of FDG-PET/CT for TNM staging of pre-treated (biopsy proven) nasopharyngeal cancer, when compared to conventional staging modalities (i.e. MRI or CT scan of head and neck for T and N classifications, biopsy or clinical follow up of suspected metastases to regional lymph nodes or distant sites).

We searched MEDLINE, Cochrane CENTRAL register of controlled trials, Cochrane Database of systematic reviews, Chinese national knowledge infrastructure (CNKI) and China Biomedical Literature Disc (CBMDisc) from date of inception to September 2011 and meeting proceedings of American Society for Radiation Oncology (ASTRO) and American Society of Clinical Oncology (ASCO) from 2000 to September 2011).

We used a search algorithm that included the following terms: (*1*) PET OR 18F-FDG PET OR positron emission tomography; (*2*) nasopharyngeal cancer OR nasopharyngeal carcinoma OR cancer of the nasopharynx OR lymphoepithelioma; (*3*) staging OR detection OR lymph node OR metastasis OR TNM.

FDG-PET only studies were excluded. For N and M classifications, studies that did not provide sufficient information to construct 2 x 2 table for sensitivity and specificity calculations were excluded. For T classification, we chose to analyze the sensitivity of FDG-PET/CT, in comparison to the

reference standard. (*i.e* verifying false positive and true negative results in a non-surgically staged tumor would be impossible, and likely not reported in published studies).

The most recent publication was chosen when data was presented in more than one publication.

Two reviewers (B.V and S.Y.Y) independently judged study eligibility and disagreements were resolved by discussion and if necessary by a third reviewer (L.K.M)

The study was approved by institutional board committee and was carried out according to the Helsinki declaration.

Data extraction

Two reviewers (B.V and S.Y.Y) extracted data from each eligible study independently using a standardized data extraction form and any disagreements were resolved by discussion or by appeal to a third reviewer (L.K.M).

Reviewers were not blinded with regard to information about the journal name, the authors, country of origin or the year of publication; as this has been shown to be unnecessary.[13] In addition, we recorded the following information: study design (retrospective/prospective), sample size, age and gender distribution, stage of patients included and reference tests used to define extent of disease. Publications looking at more than one aspect of classification were treated independently. In particular, we extracted the number of cases that were true positive, false negative, true negative and false positive. True positive was defined as both FDG-PET/CT and the reference test detecting presence of disease; true negative where neither test detected disease; false positive where FDG-PET/CT detected disease but not the reference test and false negative where FDG-PET/CT failed to show disease detected by the reference test.

The methodological quality of each study was also independently assessed by B.V and S.Y.Y using the QUADAS tool.[14] This scale contains 14 items that examine potential sources of bias in diagnostic studies in a systematic evidence-based manner. Higher scores are suggestive of lower risk of bias in the study's methodology. Sensitivity analyses were performed after exclusion of retrospective studies, or studies with high risk of bias (QUADAS <10).

Statistical analysis

The accuracy of FDG-PET/CT in the staging of newly diagnosed NPC was determined by the combined estimates of sensitivity and specificity, pooled diagnostic odds ratio (DOR), summary receiver operating characteristic (SROC) curves and Q*-index. The degree of heterogeneity among the included studies was assessed visually (forest plots) and statistically (chi-square tests and I2 statistic). When significant heterogeneity was observed (P <0.05), a random effects model was applied. A random effects meta-regression model was used to compare sub-group estimates.

The traditional ROC graph explores the effect of varying thresholds on sensitivity and specificity from a single study, unlike each data point in the SROC graph which represents a separate study. Thus, the SROC graph gives us a global estimate of the diagnostic test's performance and illustrates the tradeoff between sensitivity and specificity.[15] Q*-index is the best statistical summary method to reflect the diagnostic value. It is defined by the point where sensitivity and specificity are equal, which is the point closest to the ideal top-left corner of the SROC curve.[16] The diagnostic odds ratio is a single indicator of test accuracy that combines data from sensitivity and specificity into a single number. It is the ratio of the odds of a positive test in a patient with disease relative to the odds of a positive test in a patient without disease and has a value that ranges from 0 to infinity, with higher values indicating better discriminatory test performance i.e. accuracy. A value of 1.0 indicates that the test does not discriminate between patients with and without the disease.[17]

Subgroups to be analyzed were determined a-priori, with the following reasons:

T classification. Contrast enhanced MRI is considered to the current gold standard for soft tissue involvement and intracranial extension.[18] A subgroup analysis was performed considering studies, which utilized MRI to be the only acceptable reference test (versus MRI or CT or clinical findings). This may be viewed as a non-inferiority comparison or concordance of FDG-PET/CT to MRI.

N classification. FDG-PET/CT may over or underestimate the involvement of retropharyngeal and paraphayngeal lymph nodes; possibly because of poor distinction from the primary nasopharyngeal tumour.[11] A subgroup analysis was done for studies looking primarily at cervical lymph nodal involvement versus non-cervical lymph nodes (*i.e.* retro/parapharyngeal). As neck dissection is not part of standard staging, it is unlikely to have histopathology as the reference standard. We performed a subgroup analysis to see if there was a

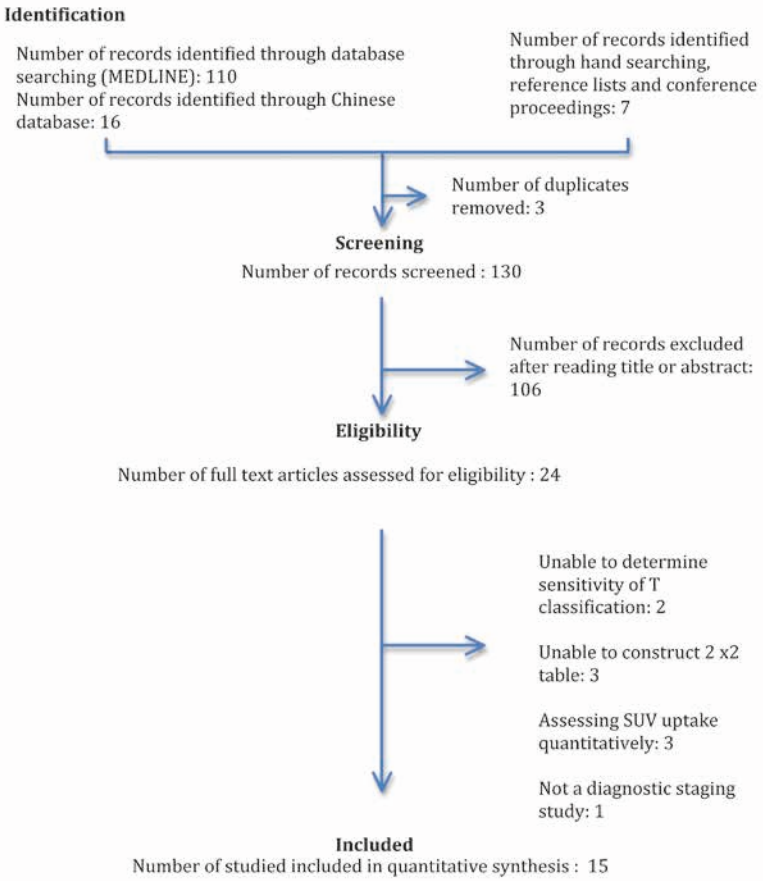

FIGURE 1. Flow of information through the different phases of a systematic review (as per PRISMA statement).

difference between studies that required histology versus those that did not.

M classification. We performed a subgroup analysis to determine if there was a difference between studies which relied solely on clinical follow-up as the reference standard versus those which required histology.

Analyses were performed using META-DISC version 1.4 (XI Cochrane Colloquium; Barcelona, Spain)[16] and STATA version 11.2 (Stata Corp, College Station, Tx, USA) and level of significance set at 5%.

Results

Study selection and description

We identified 15 studies including 851 patients using the search strategy summarized in Figure 1. Five studies addressed the local extent of the primary tumor (T).[11,19-22] Nine studies dealt with regional nodal classification, including retropharyngeal lymph nodal involvement (N).[10,11,19,20,23-27] Seven studies dealt with distant metastatic classification (M).[5,9-12,19, 28] One study was excluded from (M) as it potentially had overlapping data sets.[20]

Nine studies were published in the English language.[5,9,11,12,19-21,27,28] One study was published as an abstract form.[10] The characteristics of the 15 studies are summarized in Table 1. 220 patients were included in the analysis of T classification, 559 patients in N classification and 385 in M classification. The mean age of the participants was 46.8 years and approximately 70.5% were male. All studies except three included patients of all stages.[11,21,22]

Formal critical appraisal indicated that the methodological quality was high in three studies (QUADAS score ≥13),[11,20,26] moderate in seven studies (QUADAS score 10-12)[5,11,19,22,23,25,27] and low in five studies (QUADAS <10).[9,10,12,19,21] Studies looking at more than one aspect of classification were assessed independently for quality. Most studies had a suboptimal design or insufficient description with regards to question 12 (100% no or unclear), question 11 (63% no or unclear) and question 4 (74% no or unclear).

All studies had a cross sectional design and ten of the 15 studies were conducted prospectively.[5,20-28]

Accuracy

T classification. Based on the combined data from five available studies that evaluated the T-classification our analysis revealed a sensitivity of 0.77(95% CI 0.59-0.95) while no specificity level could be ascertained (Figure 2). Four (of the five) studies did not report false positive results hence preventing us from calculating the specificity for T classification.[19-22] Subgroup analysis revealed the sensitivity of FDG-PET/CT was lower when compared to MRI alone; however, this was not statistically significant (0.65 vs. 0.86, P=0.214). The sensitivity results on T classification were similar with exclusion of the two low quality studies,[19,21] or the two retrospective studies.[11,19]

N classification. The combined sensitivity estimate for N classification is 0.84 (95% CI 0.76-0.91) and specificity 0.90 (95% CI 0.83-0.97). The pooled DOR for N classification was 82.4 (23.2-292.6). The Q*-index was 0.90 (SE 0.03) (Figure 3). The reference standards used for N classification varied amongst studies. MRI neck was the most frequently used reference standard.[11,24,26,27] Two studies relied on clinical follow up to be their reference standard,[23,25] and 2 other studies required histological confirmation though fine needle aspiration of involved cervical nodes.[10,20] One study used contrast enhanced

TABLE 1. Characteristics of included studies

Class.	Author (year)	Sample size	Design	Age (years)	Male (%)	Patient population	Reference Test	Quadas
T	Chen (2006)[19]	20	R	46.3	70	All comers	nasoscopy and CT/MR	8
	King (2008)[11]	52	R	50	73	Stage III-IV	MRI	13
	Ng (2009)[20]	111	P	48.9	75.6	All comers	MRI	13
	Wu (2011)[21]	12	P	49	66.7	All comers, looking at intracranial and intraorbital extension (T4)	MRI/CT and clinical finding	9
	Cai (2011)[22]	25	P	50	64	Locally advanced NPC (at least T3)	MRI/CT and clinical findings	12
N	Hu (2005)[23]	105	P	43	78	All comers	Followup for 9 months	10
	Su (2006)[24]	53	P	40	68	All comers	MRI – looking at retropharyngeal LN	11
	Chen (2006)[19]	20	R	46.3	70	All comers	CT	8
	Zhang (2006)[25]	116	P	NR	79.3	All comers	Followup for 9 months	10
	Tang (2007)[26]	87	P	43	72.8	All comers	MRI - looking at para/ retropharyngeal LN	13
	Lin (2008)[27]	68	P	41	58.5	All comers	MRI neck	11
	King (2008)[11]	52	R	50	73	Stage III-IV	MRI neck	12
	Ng (2009)[20]	17	P	48.9	75.6	All comers	FNA	13
	Lin (2009)[10]	41	R	NR	NR	All comers	FNA	7
M	Chen (2006)[19]	20	R	46.3	70	All comers	Histological proof, or clinical followup for 6 months	11
	Wang (2007)[9]	18	R	52	60.5	All comers	Histological proof, or clinical followup for 17 months (median)	9
	King (2008)[11]	52	R	50	73	Stage III-IV	Histological proof, or clinical followup for 12 months	12
	Chua (2009)[5]	78	P	50	76.9	All comers	Histological proof, or clinical followup for 6 months	11
	Ng (2009)[28]	150	P	48.1	74	All comers	Histological proof, or clinical followup for 12 months	11
	Lin (2009)[10]	41	R	NR	NR	All comers	Clinical followup (time not specified)	6
	Iaguru (2011)[12]	26	R	47.3	69.2	All comers	Clinical followup (time not specified)	9

FNA = fine needle aspirate cytology; M = distant metastasis; N = regional lymph nodes; NPC = nasopharyngeal carcinoma; NR = not reported; P = prospective; R = retrospective; T = primary tumor

CT to be their reference standard[19], which is considered to be inferior to MRI.[29,30]

The effect on sensitivity was significantly lower for studies assessing retro/parapharyngeal nodal involvement (0.94 vs. 0.44, $p<0.001$) whereas specificity did not differ significantly (0.85 vs. 1.00, $P=0.305$). There was no significant difference in sensitivity or specificity between studies that required histological confirmation (0.93 vs. 0.82, $P=0.666$; 0.82 vs. 0.91, $P=0.533$). The sensitivity and specificity results on N classification were similar with exclusion of two low quality studies,[10,19] or the three retrospective studies.[10,11,19]

M classification. The combined sensitivity estimate for M classification is 0.87 (95% CI 0.74-1.00), and specificity 0.98 (95% CI 0.96-1.00). The pooled DOR for M classification is 120.9 (43.0-340.0). The Q*-index is 0.92 (SE 0.02) (Figure 4). All studies used either histological proof or clinical follow up (range 6-17 months) to define true positive and true negative lesions. Two studies used clinical follow up alone,[10,12] and the duration was not reported. The mean time of follow up for the remaining studies was 12 months. Subgroup analysis did not show any significant differences for pooled sensitivity or specificity (1.00 vs. 0.84, $P= 0.996$; 0.99 vs. 0.98, $P=0.531$). Sensitivity analysis showed that the results on M classification were similar with exclusion of the three low quality studies,[9,10,12] or the five retrospective studies.[9-12,19]

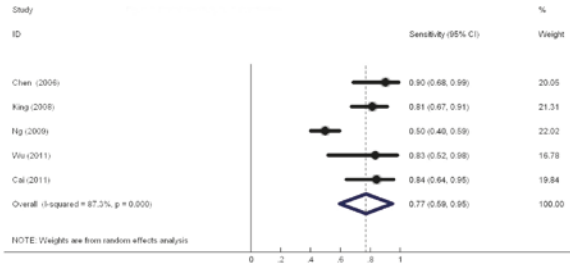

FIGURE 2. Pooled sensitivity for T classification.

Discussion

This meta-analysis suggests that FDG-PET/CT has excellent sensitivity and specificity compared to conventional staging modalities for N and M but not for T classification of NPC. We observed that FDG-PET/CT might be less accurate to determine involvement of para/retropharyngeal lymph nodes, although this estimate may be imprecise owing to relatively small number of studies.

Compared to other published meta-analyses investigating the accuracy of FDG-PET/CT, our results showed similar results for M classification but superior results for N classification. Nevertheless, we should note there are intrinsic differences. Kyazs *et al*. looked at the utility of FDG-PET (without combined CT) for cervical nodal metastasis in squamous cell head and neck cancer, referencing it against surgical specimens.[31] The review did not find good evidence to support the routine use of pretreatment evaluation FDG PET. They reported an overall sensitivity and specificity of 0.79 and 0.86 respectively. The sensitivity was significantly lower in the clinically negative neck (0.50).

The variation in reported results may be due to the improved accuracy of integrated FDG-PET/CT versus stand-alone FDG-PET, differing reference standards (conventional methods versus surgical specimen) and differing primaries (NPC *versus* non-NPC). Our results did not differ after the inclusion of Chinese language publications for M classification, as previously reported by Xu and colleagues.[8]

The strengths of this study are that it addresses a pragmatic question, incorporates recently published data, includes Chinese language based publications, has a standardized study quality assessment, and has a pre-planned sub-group analysis to address potential sources of heterogeneity. Additionally, sensitivity analyses showed consistent results, suggesting the robustness of the findings.

There are some limitations of this meta-analysis. Firstly, our review was based on published results and not individual patient data. Secondly,

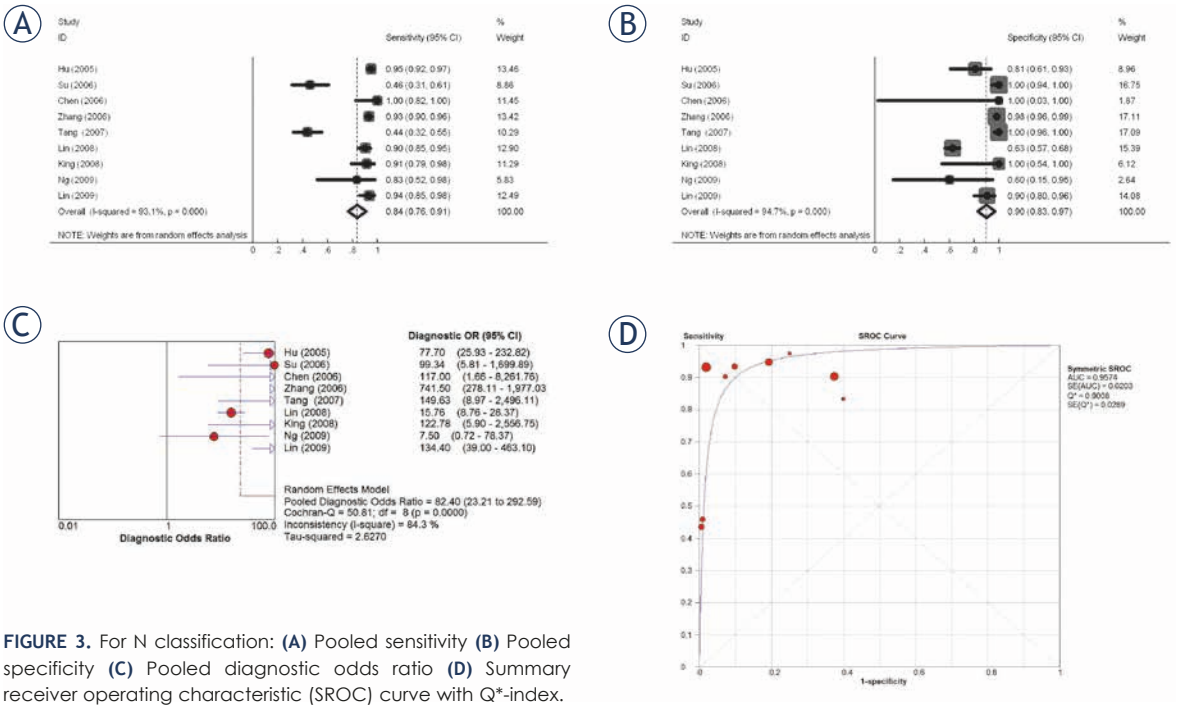

FIGURE 3. For N classification: **(A)** Pooled sensitivity **(B)** Pooled specificity **(C)** Pooled diagnostic odds ratio **(D)** Summary receiver operating characteristic (SROC) curve with Q*-index.

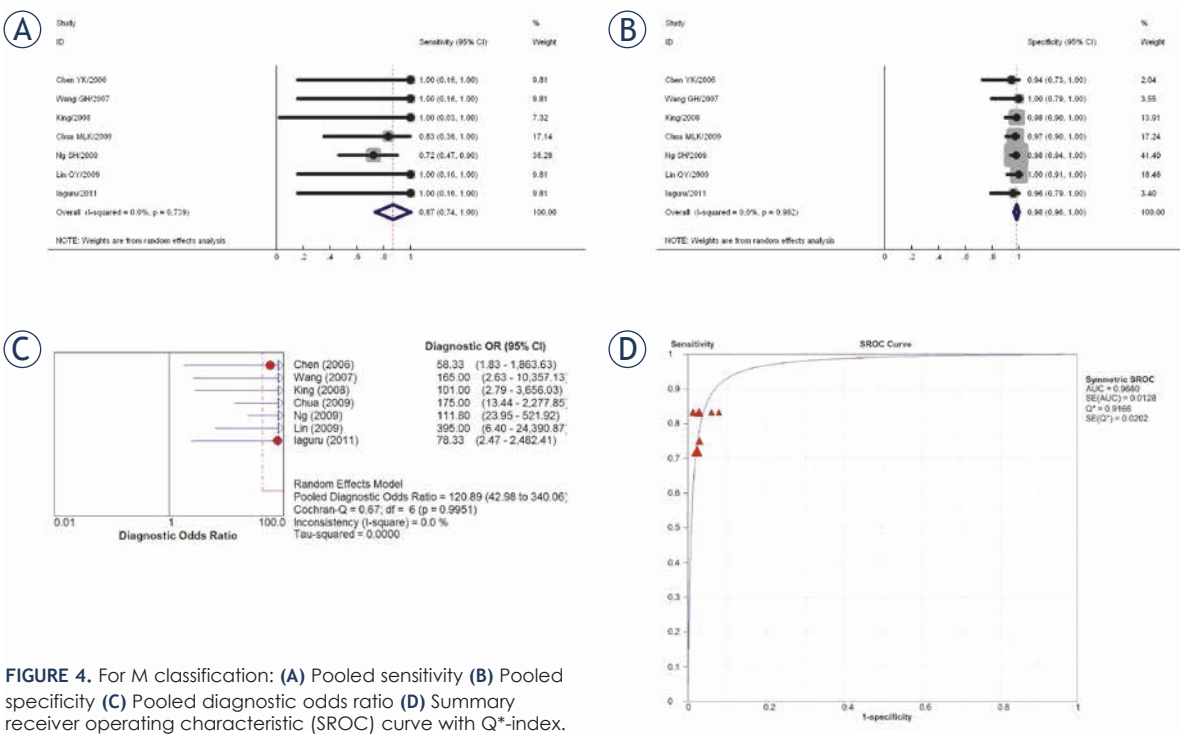

FIGURE 4. For M classification: **(A)** Pooled sensitivity **(B)** Pooled specificity **(C)** Pooled diagnostic odds ratio **(D)** Summary receiver operating characteristic (SROC) curve with Q*-index.

the imaging reference standards used for T and N classifications were heterogeneous and subject to interpretation. The follow up time for M classification varied (6-17 months) and there was no consistent follow up strategy. Lastly, the included studies were heterogeneous in design though the majority of the studies were of low-moderate risk of bias based on the QUADAS assessment.

In conclusion, FDG-PET/CT showed good accuracy in N and M but not T classification for newly diagnosed pre-treated NPC. While head and neck MRI is still recommended for T classification, FDG-PET/CT is accurate for clinical staging of regional nodes and distant disease and can be considered as an alternative standard of care wherever available. The diagnostic superiority of FDG-PET/CT over conventional staging modalities for detection of metastatic disease makes for more accurate disease prognostication and optimization of treatment strategy. The additional information derived from the FDG-PET/CT can also potentially aid neck nodal target delineation. FDG-PET/CT, together with MRI of the head and neck, has become part of the routine staging investigations for NPC at our centre. Future research should investigate the accuracy of FDG-PET/MRI as a single staging modality for NPC.[32, 33]

References

1. Jemal A, Bray F, Center MM, Ferlay J, Ward E, Forman D. Global cancer statistics. *CA Cancer J Clin* 2011; **61**: 69-90.
2. Chong VF, Ong CK. Nasopharyngeal carcinoma. *Eur J Radiol* 2008; **66**: 437-47.
3. Sham JS, Choy D, Choi PH. Nasopharyngeal carcinoma: the significance of neck node involvement in relation to the pattern of distant failure. *Br J Radiol* 1990; **63**: 108-13.
4. Edge SB, Byrd DR, Compton CC, Fritz AG, Greene FL, Trotti AM 3rd. *AJCC Cancer Staging Manual.* 7th edition. New York: Springer; 2009.
5. Chua ML, Ong SC, Wee JT, Ng DC, Gao F, Tan TW, et al. Comparison of 4 modalities for distant metastasis staging in endemic nasopharyngeal carcinoma. *Head Neck* 2009; **31**: 346-54.
6. NCCN guidelines for treatment of cancer by site. Head and neck cancers. Available from: http://www.nccn.org./professionals/physician_gls/f_guidelines.asp#head-and-neck, Accessed on 09 October, 2013
7. Lardinois D, Weder W, Hany TF, Kamel EM, Korom S, Seifert B, et al. Staging of non-small-cell lung cancer with integrated positron-emission tomography and computed tomography. *N Engl J Med* 2003; **348**: 2500-7.
8. Xu GZ, Guan DJ, He ZY. (18)FDG-PET/CT for detecting distant metastases and second primary cancers in patients with head and neck cancer. A meta-analysis. *Oral Oncol* 2011; **47**: 560-5.
9. Wang GH, Lau EW, Shakher R, Binns DS, Hogg A, Drummond E, et al. [Clinical application of (18)F-FDG PET/CT to staging and treatment effectiveness monitoring of nasopharyngeal carcinoma]. [Chinese]. *Ai Zheng* 2007; **26**: 638-42.
10. Lin Q, Zhao H, Zhao J, Lin C. Comparison of diagnostic value between 18F-FDG PET/CT and MRI in nasopharyngeal carcinoma. *Journal of Jilin University* 2009; **35**: 1163-66.

11. King AD, Ma BB, Yau YY, Zee B, Leung SF, Wong JK, et al. The impact of 18F-FDG PET/CT on assessment of nasopharyngeal carcinoma at diagnosis. *Br J Radiol* 2008; **81**: 291-8.
12. Iagaru A, Mittra ES, Gambhir SS. FDG-PET/CT in cancers of the head and neck: what is the definition of whole body scanning? *Mol Imaging Biol* 2011; **13**: 362-7.
13. Berlin JA. Does blinding of readers affect the results of meta-analyses? University of Pennsylvania Meta-analysis Blinding Study Group. *Lancet* 1997; **350**: 185-6.
14. Whiting P, Rutjes AW, Reitsma JB, Bossuyt PM, Kleijnen J. The development of QUADAS: a tool for the quality assessment of studies of diagnostic accuracy included in systematic reviews. *BMC Med Res Methodol* 2003; **3**: 25.
15. Moses LE, Shapiro D, Littenberg B. Combining independent studies of a diagnostic test into a summary ROC curve: data-analytic approaches and some additional considerations. *Stat Med* 1993; **12**: 1293-316.
16. Zamora J, Abraira V, Muriel A, Khan K, Coomarasamy A. Meta-DiSc: a software for meta-analysis of test accuracy data. *BMC Med Res Methodol* 2006; **6**: 31.
17. Glas AS, Lijmer JG, Prins MH, Bonsel GJ, Bossuyt PM. The diagnostic odds ratio: a single indicator of test performance. *J Clin Epidemiol* 2003; **56**: 1129-35.
18. Goh J, Lim K. Imaging of nasopharyngeal carcinoma. *Ann Acad Med Singapore* 2009; **38**: 809-16.
19. Chen YK, Su CT, Ding HJ, Chi KH, Liang JA, Shen YY, et al. Clinical usefulness of fused PET/CT compared with PET alone or CT alone in nasopharyngeal carcinoma patients. *Anticancer Res* 2006; **26**: 1471-7.
20. Ng SH, Chan SC, Yen TC, Chang JT, Liao CT, Ko SF, et al. Staging of untreated nasopharyngeal carcinoma with PET/CT: comparison with conventional imaging work-up. *Eur J Nucl Med Mol Imaging* 2009; **36**: 12-22.
21. Wu HB, Wang QS, Wang MF, Zhen X, Zhou WL, Li HS. Preliminary study of 11C-choline PET/CT for T staging of locally advanced nasopharyngeal carcinoma: comparison with 18F-FDG PET/CT. *J Nucl Med* 2011; **52**: 341-6.
22. Cai L, Zhang W, Chen Y, Huang Z. Value of ^{18}F-FDG PET/CT and MRI for evaluating skull bone metastasis in nasopharyngeal cancer. *Chongqing Medical Journal* 2011; **40**: 771-73.
23. Hu WH, Zhang GY, Liu LZ, Wu HB, Li L, Gao YH, et al. [Comparison between PET-CT and MRI in diagnosing nodal metastasis of nasopharyngeal carcinoma]. [Chinese]. *Ai Zheng* 2005; **24**: 855-60.
24. Su Y, Zhao C, Xie CM, Lu LX, Sun Y, Han F, et al. [Evaluation of CT, MRI and PET-CT in detecting retropharyngeal lymph node metastasis in nasopharyngeal carcinoma]. [Chinese]. *Ai Zheng* 2006; **25**: 521-5. Zhang GY, Hu WH, Liu LZ, Wu HB, Gao YH, Li L, et al. [Comparison between PET/CT and MRI in diagnosing lymph node metastasis and N staging of nasopharyngeal carcinoma]. [Chinese]. *Zhonghua Zhong Liu Za Zhi* 2006; **28**: 381-4.
25. Tang LL, Ma J, Chen Y, Zong JF, Sun Y, Wang Y, et al. [The values of MRI, CT, and PET-CT in detecting retropharyngeal lymph node metastasis of nasopharyngeal carcinoma]. [Chinese]. *Ai Zheng* 2007; **26**: 737-41.
26. Lin XP, Zhao C, Chen MY, Fan W, Zhang X, Zhi SF, et al. [Role of 18F-FDG PET/CT in diagnosis and staging of nasopharyngeal carcinoma]. [Chinese]. *Ai Zheng* 2008; **27**: 974-8.
27. Ng SH, Chan SC, Yen TC, Chang JT, Liao CT, Ko SF, et al. Pretreatment evaluation of distant-site status in patients with nasopharyngeal carcinoma: accuracy of whole-body MRI at 3-Tesla and FDG-PET-CT. *Eur Radiol* 2009; **19**: 2965-76.
28. Olmi P, Fallai C, Colagrande S, Giannardi G. Staging and follow-up of nasopharyngeal carcinoma: magnetic resonance imaging versus computerized tomography. *Int J Radiat Oncol Biol Phys* 1995; **32**: 795-800.
29. Rumboldt Z, Gordon L, Bonsall R, Ackermann S. Imaging in head and neck cancer. *Curr Treat Options Oncol* 2006; **7**: 23-34.
30. Kyzas PA, Evangelou E, Denaxa-Kyza D, Ioannidis JP. 18F-fluorodeoxyglucose positron emission tomography to evaluate cervical node metastases in patients with head and neck squamous cell carcinoma: a meta-analysis. *J Natl Cancer Inst* 2008; **100**: 712-20.
31. Zaidi H, Del Guerra A. An outlook on future design of hybrid PET/MRI systems. *Med Phys* 2011; **38**: 5667-89.
32. Loeffelbein DJ, Souvatzoglou M, Wankerl V, Martinez-Moller A, Dinges J, Schwaiger M, et al. PET-MRI Fusion in Head-and-Neck Oncology: Current Status and Implications for Hybrid PET/MRI. *J Oral Maxillofac Surg* 2012; **70**: 473-83.

research article

Searching for primaries in patients with neuroendocrine tumors (NET) of unknown primary and clinically suspected NET: evaluation of Ga-68 DOTATOC PET/CT and In-111 DTPA octreotide SPECT/CT

Nils Friedemann Schreiter[1], Ann-Mirja Bartels[1], Vera Froeling[3], Ingo Steffen[1], Ulrich-Frank Pape[2], Alexander Beck[3], Bernd Hamm[3], Winfried Brenner[1], Rainer Röttgen[1,3]

[1] Department of Nuclear Medicine, Charité – Universitätsmedizin Berlin, Augustenburger Platz 1, 13353 Berlin, Germany
[2] Department of Gastroenterology, Charité – Universitätsmedizin Berlin, Augustenburger Platz 1, 13353 Berlin, Germany
[3] Department of Radiology, Charité – Universitätsmedizin Berlin, Augustenburger Platz 1, 13353 Berlin, Germany

Radiol Oncol 2014; 48(4): 339-347.

Received: 28 October 2013
Accepted: 23 February 2014

Correspondence to: Dr. med. Nils F. Schreiter, Klinik für Nuklearmedizin, Charité Campus Virchow Klinikum, Augustenburger Platz 1, 13353 Berlin, Germany. E-mail: nils.schreiter@charite.de

Disclosure: No potential conflicts of interest were disclosed.

Background. To evaluate the clinical efficacy of In-111 DTPA octreotide SPECT/CT and Ga-68 DOTATOC PET/CT for detection of primary tumors in patients with either neuroendocrine tumor of unknown primary (NETUP) or clinically suspected primary NET (SNET).

Patients and methods. A total of 123 patients were included from 2006 to 2009, 52 received Ga-68 DOTATOC PET/CT (NETUP, 33; SNET, 19) and 71 underwent In-111 DTPA octreotide SPECT/CT (50; 21). The standard of reference included histopathology or clinical verification based on follow-up examinations.

Results. In the NETUP group Ga-68 DOTATOC detected primaries in 15 patients (45.5%) and In-111 DTPA octreotide in 4 patients (8%) ($p < 0.001$); in the SNET group, only 2 primaries could be detected, all by Ga-68 DOTATOC. In patients with NETUP, primary tumors could be found significantly more often than in patients with SNET ($p = 0.01$). Out of these 21 patients 14 patients were operated.

Conclusions. Ga-68 DOTATOC PET/CT is preferable to In-111 DTPA octreotide SPECT/CT when searching for primary NETs in patients with NETUP but should be used with caution in patients with SNET.

Key words: NET; CUP; Ga-68 DOTATOC PET/CT; In-111 DTPA octreotide SPECT; clinically suspected NET

Introduction

Neuroendocrine tumors (NET) are a rare heterogeneous group of tumors with an increasing incidence.[1-3] Arising from the endocrine cells of the diffuse neuroendocrine system of the human body, NET can occur in different body regions.[4,5] With the density of neuroendocrine cells varying between different body tissues, primary NET are most common in the gastrointestinal tract and in the bronchopulmonary system.[6,7] Cases where histology suggests metastasis from NET without a known primary tumor are categorized as cancer of unknown primary (CUP). CUP patients constitute 7.6-15% of NET study populations [2,4,7-9], while NET account for less than 5% of all CUP.[10] NET patients with an unknown primary (NETUP) have a poorer prognosis than other NET patients.[6] Kirshborn *et al.* reported a 10-year survival rate of 22%.[6,8] Surgical management is the only curative approach and should always be considered as a treatment option even when resection appears to be difficult and metastasis is present.[11-14]

Excellent diagnostic imaging is pivotal for op-

TABLE 1. Patient population: number of patients in each group; men/women; age (mean, median, range)

	Ga-68 DOTATOC	In-111-DTPA	All patients (n=123)
All patients (n = 123)	52 (m,18;w,34) age: 55.5;57;13-83	71 (m,29;w,42) age: 58.9;62;22-81	123 (m,47;w,76) age: 57.5;59;13-83
NETUP (n = 83)	33 (m,13;w,20) age: 56.3;56;32-83	50 (m,24;w,26) age: 61.3;66;30-81	83 (m,46;w,37) age: 59.3;59;30-83
SNET (n = 40)	19 (m,5;w,14) age: 54.1;64;13-77	21 (m,5;w,16) age: 53.2;54;22-72	40 (m,10;w,30) age: 53.7;56.5;3-77

NETUP = neuroendocrine tumor of unknown primary; SNET = clinicaly suspected primary NET

timal surgical planning. The most important imaging modalities proposed in the European neuroendocrine tumor society (ENETS) Consensus Guidelines are computed tomography (CT), magnetic resonance imaging (MRI), ultrasonography (US), contrast-enhanced US (CEUS), endoscopic US (EUS), and intraoperative US (IOUS).[15] Because these modalities provide complementary information, most NET patients undergo diagnostic workup with a combination of imaging tests. NET cells are characterized by an increased expression of somatostatin receptors, making somatostatin receptor imaging a promising option for detecting NET.[16-21] In-111 DTPA octreotide SPECT/CT is currently the standard technique for performing somatostatin receptor imaging.[22] A promising alternative is somatostatin receptor PET/CT using tracers such as Ga-68 DOTATOC, Ga-68 DOTATATE, or Ga-68 DOTANOC. The tracer we used in this study, Ga-68 DOTATOC, was found to be more sensitive and specific than In-111 DTPA octreotide[17], resulting in the detection of more NET lesions.[23] Moreover, Ga-68 DOTATOC reduces patients' radiation exposure and can be produced at low costs by specialized centers.[24,25] However, as with the other PET tracers mentioned above and unlike In-111 DTPA octreotide, Ga-68 DOTATOC is not a fully approved drug in the EU and USA.

New developments in molecular NET imaging range from the combination of F-18 FDG and Ga-68 DOTATOC to characterize different tumors and their aggressiveness to promising new tracers such as Glucagon-Like-Peptide-1 (GLP-1) receptor or somatostatin receptor antagonists tracers.[26,27] Depending on the clinical problem not all examinations need to have the best tumor detection or the best tumor to background ratio. If a clinician wants to be informed about the somatostatin receptor expression of a disseminated NET before planning his therapy it is not necessary to use the examination with the best lesion detection. The results of our study should help to decide which examination should be used in the search for NET primaries.

In the present study, we evaluate the performance of Ga-68 DOTATOC PET/CT and In-111 DTPA octreotide SPECT/CT in detecting unknown NET primaries. A distinction is made between patients with NETUP and patients with clinically suspected NET (SNET). Our aim is to determine whether the reported advantages of Ga-68 DOTATOC PET/CT for staging of NET will lead to a therapeutically relevant increase in the detection of NET primaries.

Patients and methods

Ethical adherence

The retrospective study was approved by the institutional ethics review board. Procedures were followed in accordance with the Helsinki Declaration.

Inclusion criteria

We consecutively included all patients with NETUP as diagnosed on the basis of histology of metastasis or patients with SNET who underwent diagnostic workup with Ga-68 DOTATOC PET/CT or In-111 DTPA octreotide SPECT/CT at our department over a four-year period beginning in 2006. The clinical diagnosis of SNET was established at the ENETS Center of our hospital. Patients were randomly referred for Ga-68 DOTATOC PET/CT or In-111 DTPA SPECT/CT by the referring physicians according to availability.

Exclusion criteria

All patients in whom the primary was already confirmed by another modality were excluded. Each patient was assigned to only one group, ensuring independent groups for statistical analysis. In patients who underwent either one of the two study modalities (SPECT/CT or PET/CT) without result and who were examined later on by the other modality, only the first examination was included in the analysis. In a second approach the group of patients who underwent both examinations was analyzed separately.

Patient population

A total of 123 patients were included, 40 (32.5%) with SNET and 83 (67.5%) with NETUP. Table 1

summarizes the patient population. Search for the primary was performed using In-111 DTPA octreotide SPECT/CT in 71 (57.7%) patients and Ga-68 DOTATOC PET/CT in 52 (42.3%) patients. In the In-111 DTPA octreotide SPECT/CT group, 21 patients (29.6%) had SNET and 50 (70.4%) NETUP. In the Ga-68 DOTATOC PET/CT group, there were 19 patients (36.5%) with SNET and 33 (63.5%) with NETUP.

Patients in the In-111 DTPA octreotide group (42 women, 29 men) had a mean age of 58.9 years (median, 62; range, 22-81 years). Mean age in the Ga-68 DOTATOC PET/CT group (34 women; 18 men) was 55.5 years (median, 57; range, 13-83 years).

The mean interval from initial diagnosis/suspected NET to the study examination (calculated for 71 patients for whom the date of initial diagnosis was available) was 13.8 months (median, 4.5 months; range, 0-202 months) for In-111 DTPA octreotide (n = 42), and 11.7 months (median, 6 months; range, 0-64 months) for Ga-68 DOTATOC PET/CT (n = 29).

In the group of SNET the indication for somatostatin receptor imaging was based on the clinic of the patients. Out of 40 patients, 15 patients had flush symptoms, 17 patients diarrhea, 7 patients hypoglycemia, 3 patients hyperglycemia, 5 patients intestinal ulcerations, and 2 patients an ectopic ACTH syndrome. Six patients had a multiple endocrine neoplasia type 1 (MEN1) syndrome.

Ga-68 DOTATOC PET/CT

PET/CT examinations were performed on a Biograph 16 scanner (Siemens AG, Germany). Ga-68 DOTATOC was prepared as described by Zhernesekov et al.[28] The mean Ga-68 DOTATOC activity administered per patient was 112.5 MBq (median, 106 MBq; range, 66-200 MBq). The PET scan was acquired at approx. 1 hour after administration in 5–6 bed positions using a 168 × 168 acquisition matrix. Iterative reconstruction was performed with a scatter correction using the ordered subset expectation maximization technique (OSEM) with 5 iterations and 8 subsets. The transaxial field of view (FOV) was 585 mm and the axial FOV 162 mm. Non-contrast CT or venous phase CT was used for attenuation correction. For the triphasic CT protocol, 80-100 ml Ultravist 370 (Bayer Schering, Germany) was administered, using bolus tracking for acquisition of an arterial phase (approx. 24s delay), a portal venous phase (approx. 45s delay) for an upper abdominal scan with 16 × 0.75 mm slice thickness, and a venous phase (approx. 70s delay) for an upper abdominal scan with 16 × 1.5 mm slice thickness. PET/CT was performed with a triphasic CT protocol in 40 patients, a venous phase alone in 4 patients, and unenhanced CT in 8 patients. The CT dose parameters were: 230 effective mAs and 120 kV.

In-111-DTPA octreotide SPECT/CT

SPECT/CT and scintigraphy examinations were performed on a Hawkeye SPECT/CT system (GE Healthcare, USA). The patients were administered 180-200 MBq In-111 DTPA octreotide, provided by an external supplier (Covidien, Petten, The Netherlands). Whole-body scintigraphic series were acquired 4 h, 24 h, and 48 h after tracer injection with a SPECT/CT acquisition of the upper abdomen after 24 h, and a repeated scan after 48 h, if needed. When whole body scintigraphy detected unclear lesions outside the upper abdomen, additional SPECT/CT images of that region were acquired. Planar whole body images were acquired with continuous table feed of 5 cm/min. SPECT imaging was performed with 360°, 60 frames (30 sec/frame), 6° angulation, 128 × 128 matrix, and a 540 × 400 mm FOV. Iterative reconstruction was performed with a scatter correction using OSEM with 2 iterations and 10 subsets. The CT scan of the SPECT/CT protocol was performed with low-dose technique (1 cm slice thickness) with 35 effective mAs and 140 kV. The low dose scan was also used for attenuation correction of SPECT.

Analysis

All image data were analyzed by an experienced resident and a senior physician on a Centricity PACS Radiology RA 1000 Workstation (GE Healthcare, USA). The readers recorded the detection of primary NET lesions, primary NET lesions in additional sites, and sites with multiple tumors. For each primary NET lesion detected, the maximum standardized uptake value (SUVmax) was determined by placing a region of interest (ROI) in transaxial attenuation-corrected PET image. SUV was calculated according the formula:

$$SUV = \frac{(Q1/Qinj)}{BW}$$

where Q1 is the activity within the lesion in mCi/ml, Qinj the activity injected in mCi, and BW the patient's body weight adapted standardization value in grams. PET and CT images were analyzed separately.

Data were compiled and analyzed using Excel (Microsoft, USA) and SPSS Statistics 19 (IBM, USA).

TABLE 2. Numbers of true positive NET primaries by modality (In-111-DTPA octreotide SPECT and Ga-68 DOTATOC PET/CT, not including primaries detected by CT only) and by patient groups

	Ga-68 DOTATOC	In-111-DTPA	All patients (n=123)	p-Value
All patients (n = 123)	17/52 (32.7%)	4/71 (7.1%)	21/123 (17.1%)	<0.001
NETUP (n = 83)	15/33 (45.5%)	4/50 (8%)	19/83 (22.3%)	<0.001
SNET (n = 40)	2/19 (10.5%)	0/21	2/40 (5%)	0.573
p-Value	0.01	0.185	0.014	

NETUP = neuroendocrine tumor of unknown primary; SNET = clinicaly suspected primary NET

TABLE 3. Primary tumor sites detected based on In-111-DTPA or Ga-68 DOTATOC imaging excluding sites detected by CT only

	lesions (n = 24) / patients (n = 21)
Duodenum	4
Jejunum	4
Ileum	8
Pancreas	8
Other	0

TABLE 4. Sites of metastasis and histologic grades

	Ga-68 DOTATOC (n=33)	In-111-DTPA (n = 50)	Total (n =83)
Metastatic site			
Liver	23 (69.7%)	33 (66%)	66 (79.5%)
Bones	7 (21.2%)	9 (18%)	16 (19.3%)
Lymph nodes	19 (57.6%)	23 (46%)	42 (50.6%)
Lungs	2 (6.1%)	3 (6%)	5 (6%)
Other	3 (9.1%)	8 (16%)	11 (13.3%)
Histologic grade			
Grade 1	16 (48.5%)	21 (42%)	37 (44,6%)
Grade 2	5 (15.2%)	4 (8%)	9 (10.8%)
Grade 3	6 (18.2%)	8 (16%)	14 (16.9%)
Unknown	6 (18.2%)	17 (34%)	23 (27.7%)

Differences in the detection of primaries between patient groups were evaluated for statistical significance using the two-sided Fisher´s exact test. A p-value of less than 0.05 was considered statistically significant.

Reference standard

For patients with true positive findings (including patients with primaries detected by CT only and patients with positive second examination after inconclusive first examination (n = 30) who were subsequently operated on, histopathology of surgical specimens was used as the standard of reference (available for 18 patients). In the other patients (n = 12), follow-up examinations using MRI, CT, Ga-68 DOTATOC PET/CT, In-111 DTPA octreotide SPECT/CT, and other imaging modalities such as endosonography and endoscopy were used for reference. For confirmation of true positive primaries in patients without a histopathologic examination, the mean follow-up period was 21.4 months (median, 16 range, 6-52 months).

The mean follow-up period in patients with false positive primaries (n = 6) was 24.3 months (median, 15.5 months; range, 8-63 months). In three patients, false positive findings in the rectum and ileum were additionally ruled out by colonoscopy.

Results

Comparison of detection rates

Disregarding CT only positive lesions Ga-68 DOTATOC PET/CT detected markedly more primaries than In-111 DTPA octreotide SPECT/CT: (17/52 (32.7%) versus 4/71 (5.6%); $p < 0.001$). In the NETUP group Ga-68 DOTATOC detected 15/33 primaries (45.5%), significantly more than In-111 DTPA with 4/50 detected primaries (8%) ($p < 0.001$). In the 40 patients with SNET, Ga-68 DOTATOC detected 2/19 primaries (10.5%), while In-111 DTPA octreotide SPECT detected no primary. Due to the small number of cases, no significance could be reached ($p = 0.573$).

The difference in the detection rate of primaries with Ga-68 DOTATOC between NETUP and SNET was significant ($p = 0.01$). Out of these 21 patients with true positive primary detection 14 patients were operated.

One primary tumor sites was detected by multiphasic CT only, in a patient with NETUP. Table 2 lists primary tumor sites detected by patient groups for PET and SPECT rating tumors detected by CT only as undetected.

False positive findings

There were 2/52 (3.8%) false positive findings in Ga-68 DOTATOC PET/CT versus 4/71 (5.6%) in the In-111 DTPA octreotide SPECT/CT group (all patients with CUP). The difference was statistically not significant ($p = 0.651$).

Primary tumor detection

In 21 patients a primary localisation could be detected, due to the injected radiotracer. There were

three cases of multiple primary tumors; three patients were diagnosed with PET/CT only. Two patients had primary tumors at two sites, one in the pancreas and duodenum, the other in the jejunum and ileum. One patient had two primary tumors in the jejunum. An overview of primary tumor localizations is given in Table 3. All primary tumors detected had a mean SUVmax of 15.7 (median, 10.5; range, 1.1-64.6). In two patients with SPECT/CT a subsequent PET/CT could detect multiple primary tumors. One patient had a primary tumor in the ileum and an additional primary tumor in the pancreas which could be seen in the CT only.

Metastatic sites and histologic differentiation

The distribution of metastatic sites and of histologic grades was similar for both modalities. The data are summarized in Table 4.

Patients examined with both modalities

Seventeen patients underwent Ga-68 DOTATOC PET/CT after In-111 DTPA octreotide SPECT/CT:

- Fifteen patients had unsuccessful In-111 DTPA octreotide SPECT/CT followed by Ga-68 DOTATOC PET/CT. In these patients primary tumors were detected by PET/CT in 7 patients by PET and in one patient by CT only.
- In two patients whose primary tumors were detected by In-111 DTPA SPECT/CT, a Ga-68 DOTATOC PET/CT was performed for improved localization. In these patients a primary localization was detected by both modalities. In one of these patients Ga-68 DOTATOC PET/CT found an additional primary tumor localization.
- Three patients underwent In-111 DTPA octreotide SPECT/CT after Ga-68 DOTATOC PET/CT:
- No primary tumor could be detected by both modalities in these patients.

Examples of patients who underwent both examinations are shown in figures 1-3.

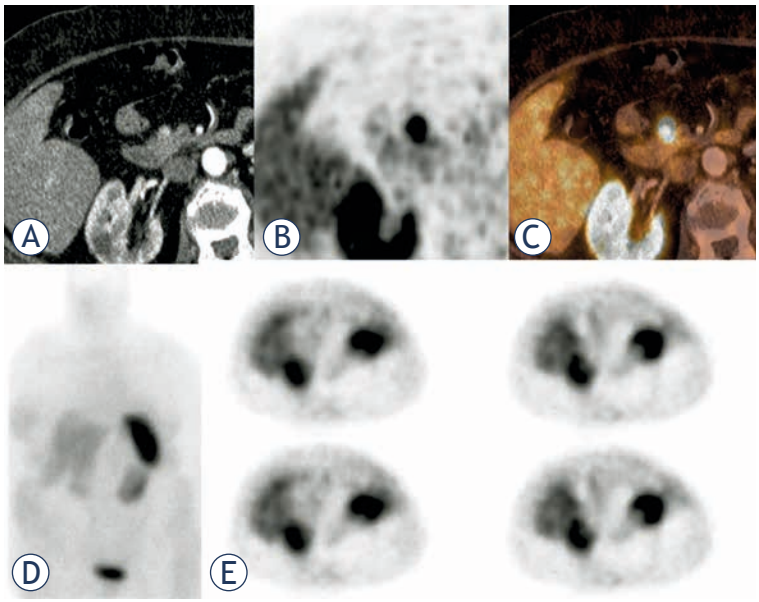

FIGURE 1. (A-C) Insulinoma presenting as a hyperperfused **(A)** Ga-68 DOTATOC positive lesion **(B)** in the pancreatic head **(C)**. In the In-DTPA octreotide scintigraphy **(D)** and SPECT **(E)** performed 3 days earlier no lesion could be found.

Discussion

Arising from cells of the diffuse neuroendocrine system, NET primaries can develop in different regions of the body.[4] NET are rare, and only a small proportion of NET patients have cancer of unknown primary. However, the true prevalence of CUP in NET patients is likely to be higher due to documentation bias.[10] Bias may result, for instance, when a suspected tumor is documented as a definitive diagnosis. Reported percentages must therefore be interpreted with caution. Identification of CUP by a suitable imaging modality is important because it can markedly improve patient survival. Surgery is the method of first choice in most patients with a locoregionally confined NET primary.[29] Recent data suggest that even patients with nonresectable NET liver metastasis may benefit from resection of the primary tumor.[29-31] In our study population, surgery was also a very common treatment in those patients in whom the study modalities identified a primary tumor. The sites of NETUP include the bronchi, stomach, pancreas, colon, and rectum[10], and different imaging modalities are available to search for the primary. A clear guideline-based diagnostic strategy for identifying NETUP however does not exist. Therefore, it stands to reason to use the guidelines that exist for other CUP for orientation. The performance of different imaging modalities in identifying CUP varies with the location in which the tumor is ultimately found. For instance, EUS has excellent detection rates for tumors located in the head of pancreas[32], while it is naturally not suitable for identifying primaries in the lungs. Somatostatin receptor imaging offers the advantage of enabling whole-body evaluation. It has gained a central role in staging NET. In-111 DTPA octreotide is the current standard for somatostatin receptor imaging[22]

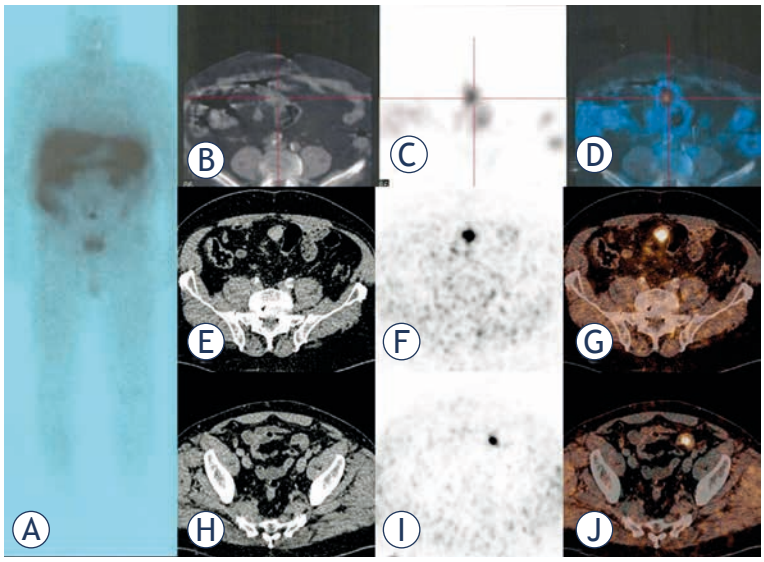

FIGURE 2. (A) In-111 DPTA octreotide detected one suspicious lesion located in the ileum **(B-D)** in a patient with NET liver metastases. Ga-68 DOTATOC PET/CT confirmed the lesion **(E-G)**, but could visualise also an additional lesion in the ileum undetected by In-111 DTPA octreotide **(H-J)**.

and, unlike PET tracers, has been approved for marketing in the USA and Europe. The effective dose to a patient examined with In-111 DTPA octreotide SPECT/CT (12 mSv/222 MBq In-111 DTPA octreotide) is higher compared to a patient examined with Ga-68 DOTATOC PET/CT (2,5 mSV/110 MBq Ga-68 DOTATOC) including a low dose CT for attenuation correction.[24,25] With superior detection rates having been reported for PET tracers[17,23], we expected them to be superior to In-111 DTPA octreotide in the search for primary NET when we planned our study. However, it was difficult to estimate how much better they would perform on the basis of the available data in literature.

To the best of our knowledge, there are only two published studies that focus on somatostatin receptor imaging in NETUP.[33,34] Savelli *et al*., using In-111 pentetroide scintigraphy and SPECT, reported detection of primary NET in 14/36 (39%) patients with CUP.[34] Prasad *et al.* used Ga-68 DOTANOC, identifying 35 NET primaries in 59 patients with CUP (59%).[33] Our detection rates for In-111 DTPA octreotide and Ga-68 DOTATOC PET/CT, 8% and 45.5%, are lower for both modalities. One important reason for this discrepancy is that populations of CUP patients are very heterogeneous with the difficulty of identifying primary tumors varying with the extent of disease, the time of first diagnosis, the number and type of prior diagnostic tests, and the clinical experience of physicians referring CUP patients. Another factor already mentioned above is how reliably and carefully the results of imaging studies are documented; this is especially important when investigating patients with SNET. We had six cases of false positive findings. The divergence of our reported detection rates is especially obvious for In-111 DTPA octreotide SPECT/CT in comparison with the study of Savelli *et al*. This we consider mainly attributable to the fact that Savelli *et al*. performed their study much earlier, *i.e*., between 1996 and 2000.[33] Since then, there have been important technical advances, resulting in much better detection rates for MRI and CT. Hence, patients undergoing In-111 DTPA octreotide SPECT/CT today, which has not evolved much during the same period, have occult primaries after negative MR and CT imaging that are much more difficult to detect. The highest detection rate of 86.7% for occult primary tumors was reported by Wang *et al*., who focused on surgical exploration for NETUP, identifying 6/7 tumors with laparoscopy and 7/8 tumors with laparotomy in patients with well-differentiated NET liver metastases.[29] CT and somatostatin receptor scintigraphy performed poorly with regard to the detection of primary NETUP in the gastrointestinal tract, detecting only 34.6% and 26.2%, respectively.[29] These data were acquired between 1993 and 2008, *i.e*., predominantly later than in the study by Savelli *et al*. However, the 26.2% of primaries detected with somatostatin receptor scintigraphy also include tumors already detected by another test. Hence, the number of primary tumors first diagnosed with somatostatin receptor scintigraphy is actually lower in this study.

With Ga-68 DOTATOC and Ga-68 DOTANOC having slightly different affinity profiles for somatostatin receptor subtypes[35], it is conceivable that the choice of tracer also may influence detection rates of NET primaries. However, this assumption remains hypothetical as we are not aware of a study comparing Ga-68 DOTATOC and Ga-68 DOTANOC in the same patient population. For comparable imaging modalities detection rates for NETUP are mainly of interest in relative terms and not absolute terms. There is good comparability of In-111 DTPA octreotide SPECT/CT and Ga-68 DOTATOC PET/CT with both being whole-body imaging modalities targeting somatostatin receptors.

In our study, Ga-68 DOTATOC PET/CT had a much better detection rate than In-111 DTPA octreotide SPECT/CT, suggesting that Ga-68 DOTATOC PET/CT should be preferred when searching for primary tumors in NETUP patients. Despite the

cautionary remarks regarding the comparability of CUP patient populations made above, we think that for the purpose of our study comparability is adequate. Both imaging modalities were performed at the same center, reducing a possible bias that might result from greater heterogeneity of center specific procedures in a retrospective multicenter approach. Despite random assignment of the patients to either group, there is some indication that primary tumor detection might have been even more difficult in the Ga-68 DOTATOC PET/CT group: the Ga-68-DOTATOC PET/CT group included 15 patients with prior unsuccessful In-111 DTPA octreotide SPECT/CT, while there were only 3 patients with unsuccessful Ga-68-DOTATOC PET/CT in the In-111 DTPA octreotide SPECT/CT group. Other factors influencing the difficulty of identifying a primary NET include primary tumor localization within the body and the severity of disease as indicated by the degree of histologic differentiation and possibly the number and site of metastases. The primary tumor sites are difficult to compare between the two groups in our study due to the small number of tumors detected with In-111 DTPA octreotide SPECT/CT. The distribution of metastatic sites provides no evidence of a disadvantage for either group in this regard.

Tumor histology is an important factor influencing the detectability of lesions by somatostatin receptor imaging. This is because poorly differentiated NET have fewer somatostain receptors.[36,37] Histologic grading of NETUP is still under debate.[38] One grading system differentiates between low-grade and high-grade tumors.[10,38] We used the 2010 WHO criteria, distinguishing well-differentiated low-grade (ENETS G1), intermediate grade (ENETS G2), and poorly differentiated high-grade tumors (ENETS G3).[39] With regard to detectability based on histology, there was no advantage large enough to explain the markedly higher primary tumor detection rate of PET/CT.

The vast majority of nuclear medicine departments perform In-111 DTPA SPECT/CT without contrast medium administration for the CT scan, while most Ga-68 DOTATOC PET/CT examinations are performed with contrast administration because it has been shown to improve tumor detection.[40,41] To preclude distortion, we also did a comparison of both modalities classifying only those examinations as successful in which the primary tumor was also visible on PET and rated primary tumors visible on CT only as undetected by PET/CT. This comparison was also done because the contrast administration protocols in the PET/CT examinations were not fully uniform. Such cases of lesions being detectable in the CT only would not exist under ideal conditions with patients undergoing prior CT scans within a short interval before somatostatin receptor imaging. However, it is difficult to enforce fully standardized protocols for prior examinations. The cases of primary tumors detected only by CT indicate that contrast-enhanced CT provides additional information, making lesion detection more reliable.

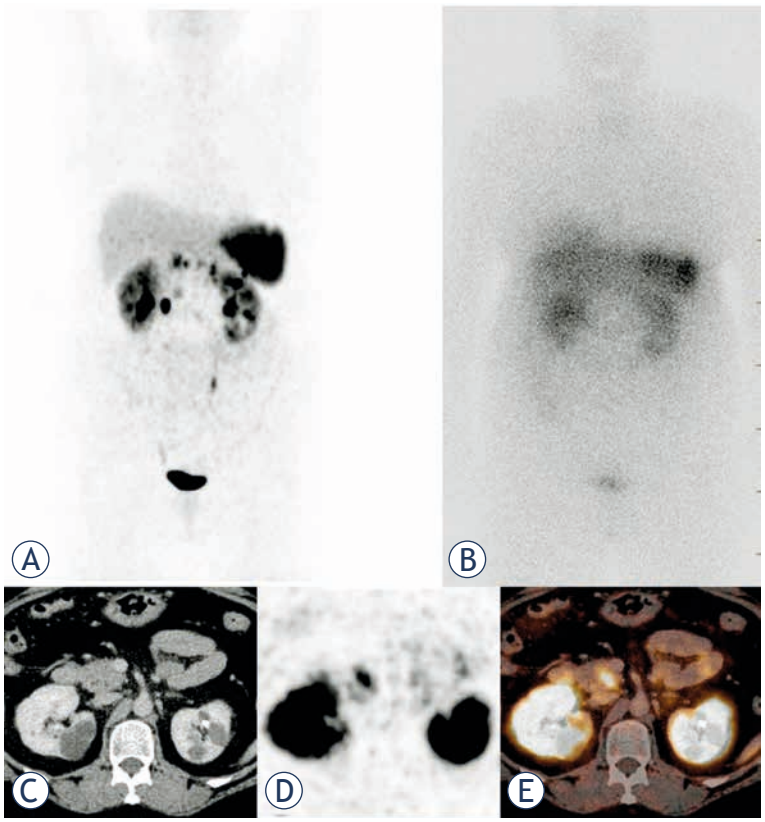

FIGURE 3. Patient with MEN1 and several NET lesions in the Ga-68 DOTATOC MIP**(A)**, which were not visible in the In-111 octreotide scintigraphy performed a few days before **(B)**, Ga-68 DOTATOC PET/CT images of the lesion in the pancreatic head **(C-E)**.

Ga-68 DOTATOC PET/CT also performed better in the direct comparison of those patients who underwent both imaging modalities. However, these results must be interpreted with great caution as there was usually a time interval between the two examinations. Interestingly, two of the four patients in whom the primary tumor was detected by In-111-DTPA octreotide SPECT additionally underwent Ga-68 DOTATOC PET/CT to improve lesion localization.

Enteropancreatic NET may occur in multiple locations.[7,42-45] One possible reason is that the specific stem cells of these NET may be induced

to undergo malignant transformation in different body regions by exposure to an exogenous growth factor.[7] In a study by Katona *et al*. investigating inactivation of the X-chromosome, the majority of multilocular NET lesions of the enteropancreatic axis were found to arise independently, while some originated as a single clone with subsequent local and discontinuous metastases.[43] In our study, some patients in whom a primary was detected had multilocular lesions. Hence, we must reconsider our concept of a single primary tumor giving rise to metastatic disease. The term CUP does not fully apply to cases of multiple NET lesions arising independently. This terminological inaccuracy must be born in mind when interpreting the results of CUP studies. An optimal imaging modality for initiating adequate therapeutic management is especially important when multilocular NET lesions are present. In this respect, somatostatin receptor PET/CT is more suitable than In-111 DTPA octreotide SPECT/CT due to its higher sensitivity as suggested by our results (multilocular NET lesions were only detected with PET/CT).

The detection rate for primary tumors was much lower in patients with SNET compared to patients with NETUP. A clinical diagnosis without histologic confirmation is highly examiner dependent. Recent studies suggest that only approx. 20% of all NET patients have typical symptoms such as Zollinger-Ellison or carcinoid syndrome.[12,46,47] The majority of all NET patients have nonspecific symptoms.[46,48-51] It is therefore likely that not all patients with SNET actually had NET. This is why strict criteria for ordering somatostatin receptor imaging must be used in this subset. Ga-68 DOTATOC PET/CT should be preferred in this subgroup, one reason being the lower radiation exposure. Somatostatin receptor imaging appears to be useful in patients with MEN 1 and the respective clinical presentation, as suggested by successful detection of primary tumors in three patients with MEN 1 in our study.

Our study is limited by the retrospective design, which is less accurate than a prospective study with regard to the data obtained on the number of prior examinations, date of first diagnosis, or histologic grade. A prospective study design also allows stricter randomization and better standardization of imaging procedures. An advantage of the retrospective design is the inclusion of a relatively large number of patients with this rare tumor entity. In a prospective setting, this would require a long study period for recruitment, during which tracers may become outdated.

A further limitation is that both examinations were not performed in the same collective of patients for reasons of radiation protection. However, the collectives of patients were quite comparable and there were no patient characteristics strongly favoring the Ga-68 DOTATOC patient group.

Another constriction is that histology was not available for all patients, which commonly limits other studies[33,34] and was due to the fact that it is ethically precluded to operate on patients without an apparent clinical benefit for the sole reason of obtaining biopsy material. The large number of patients operated on, because the primary tumor was identified, is an advantage of our study compared to similar studies in the literature.

In conclusion, our results show that Ga-68 DOTATOC PET/CT has better detection rates compared with In-111 DTPA octreotide SPECT/CT and should be preferred to search for unknown primaries in patients with NETUP. Ideally, the protocol should include a contrast-enhanced CT scan to further improve performance. In patients with SNET, somatostatin receptor imaging should be used with caution. Its use, again preferably Ga-68 DOTATOC PET/CT, is justified only after a meticulous clinical examination which strongly suggests NET as reason for the underlying symptoms.

References

1. Hoyer D, Bell GI, Berelowitz M, Epelbaum J, Feniuk W, Humphrey PP, et al. Classification and nomenclature of somatostatin receptors. *Trends Pharmacol Sci* 1995; **16:** 86-8.
2. Janson ET, Sorbye H, Welin S, Federspiel B, Gronbaek H, Hellman P, et al. Nordic Guidelines 2010 for diagnosis and treatment of gastroenteropancreatic neuroendocrine tumours. *Acta Oncol* 2010; **49:** 740-56.
3. Reubi JC. Peptide receptors as molecular targets for cancer diagnosis and therapy. *Endocr Rev* 2003; **24:** 389-427.
4. Pape UF, Berndt U, Muller-Nordhorn J, Bohmig M, Roll S, Koch M, et al. Prognostic factors of long-term outcome in gastroenteropancreatic neuroendocrine tumours. *Endocr Relat Cancer* 2008; **15:** 1083-97.
5. Rindi G, Leiter AB, Kopin AS, Bordi C, Solcia E. The "normal" endocrine cell of the gut: changing concepts and new evidences. *Ann N Y Acad Sci* 2004; **1014:** 1-12.
6. Hauso O, Gustafsson BI, Kidd M, Waldum HL, Drozdov I, Chan AK, et al. Neuroendocrine tumor epidemiology: contrasting Norway and North America. *Cancer* 2008; **113:** 2655-64.
7. Modlin IM, Lye KD, Kidd M. A 5-decade analysis of 13,715 carcinoid tumors. *Cancer* 2003; **97:** 934-59.
8. Kirshbom PM, Kherani AR, Onaitis MW, Feldman JM, Tyler DS. Carcinoids of unknown origin: comparative analysis with foregut, midgut, and hindgut carcinoids. *Surgery* 1998; **124:** 1063-70.
9. Quaedvlieg PF, Visser O, Lamers CB, Janssen-Heijen ML, Taal BG. Epidemiology and survival in patients with carcinoid disease in The Netherlands. An epidemiological study with 2391 patients. *Ann Oncol* 2001; **12:** 1295-300.
10. Spigel DR, Hainsworth JD, Greco FA. Neuroendocrine carcinoma of unknown primary site. *Semin Oncol* 2009; **36:** 52-9.

11. Fendrich V, Bartsch DK. Surgical treatment of gastrointestinal neuroendocrine tumors. *Langenbecks Arch Surg* 2011; **396:** 299-311.

12. Fischer L, Mehrabi A, Buchler MW. Neuroendocrine tumors of the duodenum and pancreas. Surgical strategy. *Chirurg* 2011; **82:** 583-90.

13. Norton JA, Fraker DL, Alexander HR, Gibril F, Liewehr DJ, Venzon DJ, et al. Surgery increases survival in patients with gastrinoma. *Ann Surg* 2006; **244:** 410-9.

14. Plockinger U, Rindi G, Arnold R, Eriksson B, Krenning EP, de Herder WW, et al. Guidelines for the diagnosis and treatment of neuroendocrine gastrointestinal tumours. A consensus statement on behalf of the European Neuroendocrine Tumour Society (ENETS). *Neuroendocrinology* 2004; **80:** 394-424.

15. Sundin A, Vullierme MP, Kaltsas G, Plockinger U. ENETS Consensus Guidelines for the Standards of Care in Neuroendocrine Tumors: radiological examinations. *Neuroendocrinology* 2009; **90:** 167-83.

16. Hofmann M, Maecke H, Borner R, Weckesser E, Schoffski P, Oei L, et al. Biokinetics and imaging with the somatostatin receptor PET radioligand (68) Ga-DOTATOC: preliminary data. *Eur J Nucl Med* 2001; **28:** 1751-7.

17. Kowalski J, Henze M, Schuhmacher J, Macke HR, Hofmann M, Haberkorn U. Evaluation of positron emission tomography imaging using [68Ga]-DOTA-D Phe(1)-Tyr(3)-Octreotide in comparison to [111In]-DTPAOC SPECT. First results in patients with neuroendocrine tumors. *Mol Imaging Biol* 2003; **5:** 42-8.

18. Kwekkeboom D, Krenning EP, de Jong M. Peptide receptor imaging and therapy. *J Nucl Med* 2000; **41:** 1704-13.

19. Lebtahi R, Cadiot G, Sarda L, Daou D, Faraggi M, Petegnief Y, et al. Clinical impact of somatostatin receptor scintigraphy in the management of patients with neuroendocrine gastroenteropancreatic tumors. *J Nucl Med* 1997; **38:** 853-8.

20. Lebtahi R, Le Cloirec J, Houzard C, Daou D, Sobhani I, Sassolas G, et al. Detection of neuroendocrine tumors: 99mTc-P829 scintigraphy compared with 111In-pentetreotide scintigraphy. *J Nucl Med* 2002; **43:** 889-95.

21. Vick C, Zech CJ, Hopfner S, Waggershauser T, Reiser M. Imaging of neuroendocrine tumors of the pancreas. *Radiologe* 2003; **4:** 293-300.

22. Rambaldi PF, Cuccurullo V, Briganti V, Mansi L. The present and future role of (111)In pentetreotide in the PET era. *Q J Nucl Med Mol Imaging* 2005; **49:** 225-35.

23. Buchmann I, Henze M, Engelbrecht S, Eisenhut M, Runz A, Schafer M, et al. Comparison of 68Ga-DOTATOC PET and 111In-DTPAOC (Octreoscan) SPECT in patients with neuroendocrine tumours. *Eur J Nucl Med Mol Imaging* 2007; **34:** 1617-26.

24. Hartmann H, Zophel K, Freudenberg R, Oehme L, Andreeff M, Wunderlich G, et al. [Radiation exposure of patients during 68Ga-DOTATOC PET/CT examinations]. *Nuklearmedizin* 2009; **48:** 201-7.

25. Schreiter NF, Brenner W, Nogami M, Buchert R, Huppertz A, Pape UF, et al. Cost comparison of (111)In-DTPA-octreotide scintigraphy and (68)Ga-DOTATOC PET/CT for staging enteropancreatic neuroendocrine tumours. *Eur J Nucl Med Mol Imaging* 2012; **39:** 72-82.

26. Fani M, Del Pozzo L, Abiraj K, Mansi R, Tamma ML, Cescato R, et al. PET of somatostatin receptor-positive tumors using 64Cu- and 68Ga-somatostatin antagonists: the chelate makes the difference. *J Nucl Med* 2011; **52:** 1110-8.

27. Toumpanakis C, Kim MK, Rinke A, Bergestuen DS, Thirlwell C, Khan MS, et al. Combination of cross-sectional and molecular imaging studies in the localization of gastroenteropancreatic neuroendocrine tumors. *Neuroendocrinology* 2014; **99:** 63-74.

28. Zhernosekov KP, Filosofov DV, Baum RP, Aschoff P, Bihl H, Razbash AA, et al. Processing of generator-produced 68Ga for medical application. *J Nucl Med* 2007; **48:** 1741-8.

29. Wang SC, Parekh JR, Zuraek MB, Venook AP, Bergsland EK, Warren RS, et al. Identification of unknown primary tumors in patients with neuroendocrine liver metastases. *Arch Surg* 2010; **145:** 276-80.

30. Givi B, Pommier SJ, Thompson AK, Diggs BS, Pommier RF. Operative resection of primary carcinoid neoplasms in patients with liver metastases yields significantly better survival. *Surgery* 2006; **140:** 891-7.

31. Hellman P, Lundstrom T, Ohrvall U, Eriksson B, Skogseid B, Oberg K, et al. Effect of surgery on the outcome of midgut carcinoid disease with lymph node and liver metastases. *World J Surg* 2002; **26:** 991-7.

32. Khashab MA, Yong E, Lennon AM, Shin EJ, Amateau S, Hruban RH, et al. EUS is still superior to multidetector computerized tomography for detection of pancreatic neuroendocrine tumors. *Gastrointest Endosc* 2011; **73:** 691-6.

33. Prasad V, Ambrosini V, Hommann M, Hoersch D, Fanti S, Baum RP. Detection of unknown primary neuroendocrine tumours (CUP-NET) using (68)Ga-DOTA-NOC receptor PET/CT. *Eur J Nucl Med Mol Imaging* 2010; **37**: 67-77.

34. Savelli G, Lucignani G, Seregni E, Marchiano A, Serafini G, Aliberti G, et al. Feasibility of somatostatin receptor scintigraphy in the detection of occult primary gastro-entero-pancreatic (GEP) neuroendocrine tumours. *Nucl Med Commun* 2004; **25:** 445-9.

35. Breeman WA, de Blois E, Sze Chan H, Konijnenberg M, Kwekkeboom DJ, Krenning EP. (68)Ga-labeled DOTA-peptides and (68)Ga-labeled radiopharmaceuticals for positron emission tomography: current status of research, clinical applications, and future perspectives. *Semin Nucl Med* 2011; **41:** 314-21.

36. Cimitan M, Buonadonna A, Cannizzaro R, Canzonieri V, Borsatti E, Ruffo R, et al. Somatostatin receptor scintigraphy versus chromogranin A assay in the management of patients with neuroendocrine tumors of different types: clinical role. *Ann Oncol* 2003; **14:** 1135-41.

37. Rodrigues M, Gabriel M, Heute D, Putzer D, Griesmacher A, Virgolini I. Concordance between results of somatostatin receptor scintigraphy with 111In-DOTA-DPhe 1-Tyr 3-octreotide and chromogranin A assay in patients with neuroendocrine tumours. *Eur J Nucl Med Mol Imaging* 2008; **35:** 1796-802.

38. Stoyianni A, Pentheroudakis G, Pavlidis N. Neuroendocrine carcinoma of unknown primary: a systematic review of the literature and a comparative study with other neuroendocrine tumors. *Cancer Treat Rev* 2011; **37:** 358-65.

39. Klimstra DS, Modlin IR, Coppola D, Lloyd RV, Suster S. The pathologic classification of neuroendocrine tumors: a review of nomenclature, grading, and staging systems. *Pancreas* 2010; **39:** 707-12.

40. Schreiter NF, Nogami M, Steffen I, Pape UF, Hamm B, Brenner W, et al. Evaluation of the potential of PET-MRI fusion for detection of liver metastases in patients with neuroendocrine tumours. *Eur Radiol* 2012; **22:** 458-67.

41. Ruf J, Schiefer J, Furth C, Kosiek O, Kropf S, Heuck F, et al. 68Ga-DOTATOC PET/CT of neuroendocrine tumors: spotlight on the CT phases of a triple-phase protocol. *J Nucl Med* 2011; **52:** 697-704.

42. Berge T, Linell F. Carcinoid tumours. Frequency in a defined population during a 12-year period. *Acta Pathol Microbiol Scand A* 1976; **84:** 322-30.

43. Katona TM, Jones TD, Wang M, Abdul-Karim FW, Cummings OW, Cheng L. Molecular evidence for independent origin of multifocal neuroendocrine tumors of the enteropancreatic axis. *Cancer Res* 2006; **66:** 4936-42.

44. Saha S, Hoda S, Godfrey R, Sutherland C, Raybon K. Carcinoid tumors of the gastrointestinal tract: a 44-year experience. *South Med J* 1989; **82:** 1501-5.

45. Watson RG, Johnston CF, O'Hare MM, Anderson JR, Wilson BG, Collins JS, et al. The frequency of gastrointestinal endocrine tumours in a well-defined population--Northern Ireland 1970-1985. *Q J Med* 1989; **72:** 647-57.

46. Fischer L, Kleeff J, Esposito I, Hinz U, Zimmermann A, Friess H, et al. Clinical outcome and long-term survival in 118 consecutive patients with neuroendocrine tumours of the pancreas. *Br J Surg* 2008; **95:** 627-35.

47. O'Toole D, Salazar R, Falconi M, Kaltsas G, Couvelard A, de Herder WW, et al. Rare functioning pancreatic endocrine tumors. *Neuroendocrinology* 2006; **84:** 189-95.

48. Arnold R. Endocrine tumours of the gastrointestinal tract. Introduction: definition, historical aspects, classification, staging, prognosis and therapeutic options. *Best Pract Res Clin Gastroenterol* 2005; **19:** 491-505.

49. Dralle H, Krohn SL, Karges W, Boehm BO, Brauckhoff M, Gimm O. Surgery of resectable nonfunctioning neuroendocrine pancreatic tumors. *World J Surg* 2004; **28:** 1248-60.

50. Schurr PG, Strate T, Rese K, Kaifi JT, Reichelt U, Petri S, et al. Aggressive surgery improves long-term survival in neuroendocrine pancreatic tumors: an institutional experience. *Ann Surg* 2007; **245:** 273-81.

51. Vagefi PA, Razo O, Deshpande V, McGrath DJ, Lauwers GY, Thayer SP, et al. Evolving patterns in the detection and outcomes of pancreatic neuroendocrine neoplasms: the Massachusetts General Hospital experience from 1977 to 2005. *Arch Surg* 2007; **142:** 347-54.

research article

The role of elastosonography, gray-scale and colour flow Doppler sonography in prediction of malignancy in thyroid nodules

Idil Gunes Tatar[1], Aydin Kurt[1], Kerim Bora Yilmaz[2], Mehmet Doğan[3], Baki Hekimoglu[1], Sema Hucumenoglu[4]

[1] Department of Radiology, Ankara Diskapı Training and Research Hospital, Ankara, Turkey
[2] Department of General Surgery, Ankara Diskapi Training and Research Hospital, Ankara, Turkey
[3] Department of Pathology, Dr. Abdurrahman Yurtaslan Ankara Oncology Training and Research Hospital, Ankara, Turkey
[4] Ankara Research and Training Hospital, Department of Pathology, Ankara, Turkey

Radiol Oncol 2014; 48(4): 348-353.

Received 6 November 2013
Accepted 27 January 2014

Correspondence to: Idil Gunes Tatar, M.D., Department of Radiology, Ankara Diskapi Training and Research Hospital, 06110, Diskapi-Altında, Ankara, Turkey. Phone: +90 312 596 2616; Fax: +90 312 230 7649; E-mail: idilttr@yahoo.com

Disclosure: No potential conflicts of interest were disclosed.

Background. Ultrasound is as a noninvasive method commonly used in the work-up of thyroid nodules. This study aimed to evaluate the usefulness of sonographic and elastosonographic parameters in the discrimination of malignancy.

Patients and methods. 150 thyroid nodules were evaluated by gray-scale, Doppler and elastosonography. The cytological analysis revealed that 141 nodules were benign and 9 were malignant.

Results. Orientation of the nodule was the only sonographic parameter associated with malignancy (p = 0.003). In the strain ratio analysis the best cut-off point was 1.935 to discriminate malignancy (p = 0.000), with 100% sensitivity, 76% specificity, 100% negative predictive value, 78.5% positive predictive value and 78% accuracy rate. There was a statistically significant correlation between the elasticity score and malignancy (p = 0.001). Most of the benign nodules had score 2 and 3, none of them displayed score 5. On the other hand, none of the malignant nodules had score 1 and 2, most of them displaying score 5.

Conclusions. A change in the diagnostic algorithm of the thyroid nodules should be considered integrating the elastosonographic analysis.

Key words: ultrasound; Doppler; elastosonography; thyroid, malignancy

Introduction

Thyroid nodules are recognised if palpated by the patient, during physical examination or by a radiological assessment. Studies reveal that 2.7–17% of the thyroid nodules are malignant whereas the majority is benign.[1] The best way to differentiate between malignant and benign thyroid nodules is the cytological evaluation of the material sampled by fine-needle aspiration (FNA).[2] Considering the high prevalence of thyroid nodules, it is not feasible to evaluate all thyroid nodules by FNA. In contemporary guidelines, ultrasound (US) evaluation is recommended as a noninvasive method for the management of thyroid nodules.[3-5] US is the main tool in the risk analysis of both palpable and non-palpable thyroid nodules and their selection for FNA cytology (FNAC).[6] Nevertheless, it has some limitations in differentiating between benign and malignant thyroid nodules resulting from the inconsistency of sensitivity, specificity, positive and negative predictive values of sonographic features in the published studies.[7]

Malignant thyroid nodules are usually stiff on palpation.[8] Stiffness of the nodule is determined by its cellularity and can be detected by ultrasound

elastography (USE). USE, which was first suggested by Ophir *et al*., analyses the elasticity of a nodule by measuring the amount of distortion which takes place when the nodule is compressed.[9-12] When compression is applied to the thyroid tissue, it produces the strain which is defined as the displacement of tissue in vertical direction, and the amount of strain is bigger in softer tissue compared to harder tissue. There are two kinds of evaluations performed by USE. One is based on the elasticity scores (ES) and the other is based on the strain ratio (SR) measurements.

The aim of this study is to evaluate the usefulness of gray-scale and colour flow Doppler US parameters, ES and SR in the differentiation of benign versus malignant thyroid nodules.

Patients and methods

In total 200 patients with thyroid nodules who were referred to the radiology department for FNAC by the general surgery department were assessed for eligibility. After obtaining the approval of the institutional ethical board committee, informed consent was taken from the participants. Seventeen patients refused to participate; furthermore, 13 patients with nodules having egg shell calcifications, >50% cystic component detected by US and thyroiditis, three patients with hematologic diseases and other comorbidities related with complications at the FNA were excluded from the study. From the remaining 167 patients 5 patients refused to undergo FNAC. The study sample included 162 patients (mean age 49 years; range, 20–83 years; 132 females and 30 males). Patients were examined by US and USE prior to FNAC. The patient flow of the study is summarized in Figure 1.

All patients were examined by conventional US and USE using a linear transducer 8–13 MHz (Logos EUB 8500; Hitachi, Tokyo, Japan). All sonographic examinations were conducted by a sonographer with 15 years of sonography experience. The patients were requested to lie down in the supine position with the neck slightly extended. Carotid arteries were avoided if it was possible.

Gray-scale images were first obtained for each nodule. The following US parameters were evaluated: location (right lobe, left lobe, isthmus), internal structure (solid, cystic, mixed), echo structure (hyperechoic, isoechoic, or hypoechoic compared to normal thyroid parenchyme), margin (smooth, microlobulated, irregular), presence or absence of calcifications (none, microcalcifications which are defined as hyperechoic spots small than 2 mm, macrocalcifications, mixed), orientation (parallel, nonparallel), and halo sign (presence or absence).

Colour flow Doppler patterns were defined as type 1: no internal blood flow, type 2: perinodular blood flow and absent or little internal blood flow and type 3: significant internal and absent or little perinodular blood flow.

An intermittent light pressure was applied until the pressure was standardized until a sinusoid was formed between two predetermined lines to maintain the pressure at the optimal level. Sonograms

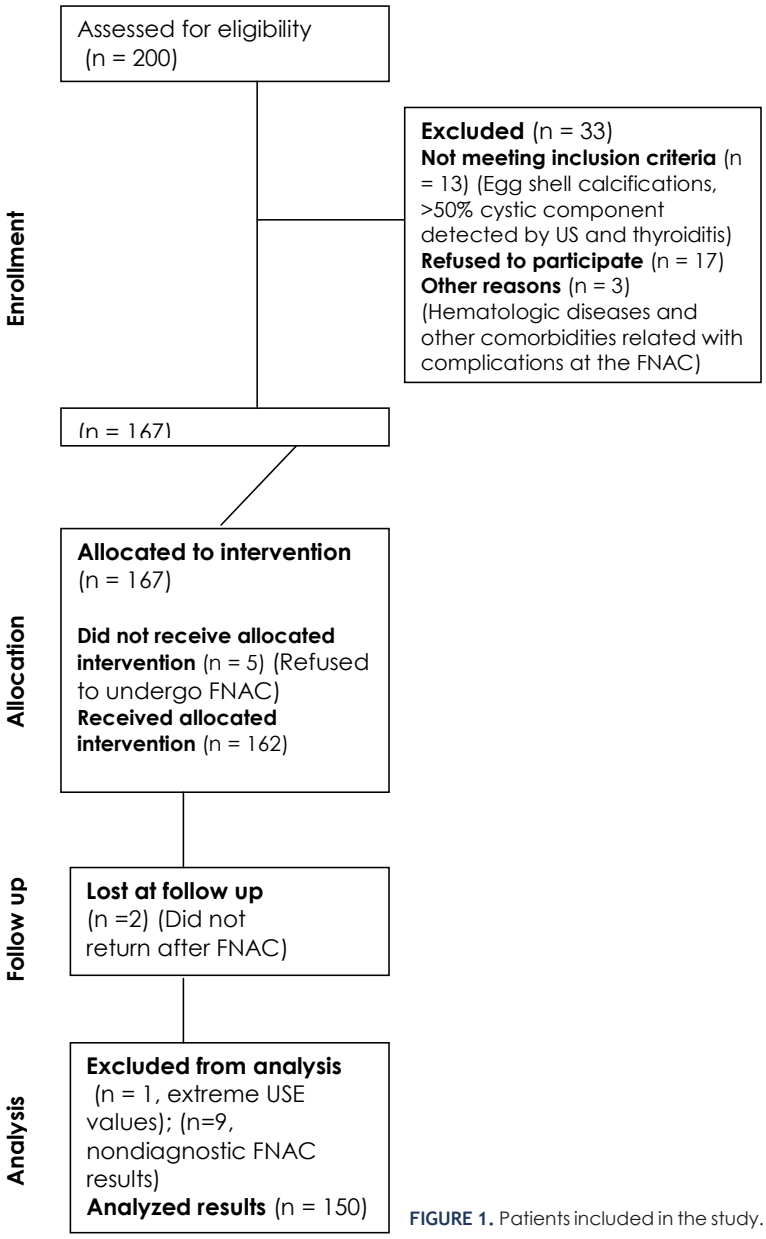

FIGURE 1. Patients included in the study.

FNAC = fine-needle aspiration cytology; USE = ultrasound elastorgaphy

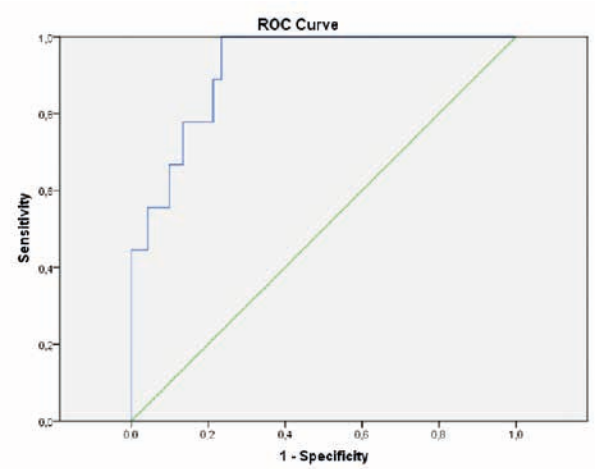

FIGURE 2. ROC curve analysis of the strain ratio measurements of thyroid nodules by elastosonography.

and elastograms were displayed next to each other for the identification of the nodule. The nodule and surrounding thyroid parenchymal tissue was evaluated.

A region-of-interest (ROI) box with an adjustable size covering the majority of the nodule was placed (average strain represented as A) taking the adjacent normal thyroid parenchymal tissue preferably which has the same depth and the same size as the reference (average strain represented as B). Strain ratio (B/A) which reflects the stiffness of the lesion was calculated for each nodule.

An elastogram based on a colour scale was displayed on the B-mode image which ranges from red to blue. Red colour represents tissues with greatest elasticity meaning softest components, whereas blue colour represents tissue with no strain meaning hardest components. Each nodule was given an ES based on a five-point scale developed by Rago *et al*.[13] ES 1 indicated homogenously elastic nodule. ES 2 indicated predominantly elastic nodule. ES 3 indicated elasticity only at the periphery of the nodule. ES 4 indicated absence of intranodular elasticity. ES 5 indicated absence of elasticity in the nodule or in the posterior shadowing. In the literature nodules having scores 4 or 5 were classified as suspicious for malignancy.

FNA was done under US guidance by the same radiologist at the end of the sonographic examination. Half of the aspirate was dried in the air, and the rest was fixed with alcohol and stained with Papanicolaou and Giemsa. The materials were interpreted by an experienced cytologist. The sufficiency of material was determined according to the guidelines of the Papanicolaou Society.[14] The pathologist was blind to the sonographic findings.

To eliminate false-positive results, 9 patients with cytologic malignancies underwent surgery. The surgical material was fixed with formalin, embedded in paraffin and was stained by hematoxylin and eosin.

Fisher Exact Chi-Square test was used for categorical data analysis and Mann Whitney-U test for numerical data analysis. Receiver operating characteristic curve analysis was used to calculate the best cut-off value of the SR. Sensitivity, specificity, and accuracy rate, positive predictive value and negative predictive value were calculated for SR calculations. P values less than 0.05 were accepted as significant.

Results

Among 162 patients who underwent FNAC, two patients were lost during the follow-up. Nine patients with nondiagnostic FNAC results and one patient with extreme USE results were excluded from the study. Finally the statistical analysis was done on 150 patients. According to FNAC results 141 of the nodules were benign. Six nodules had malignant cytology results and pathology proved to be papillary carcinoma in five of them and follicular carcinoma in the remaining one. Three nodules had undetermined cytology findings and pathology proved to be papillary carcinoma in one of them and follicular carcinoma in the other two.

Sex and age of the patients were not associated with malignancy with p values being equal to 0.562 and 0.571, respectively.

Gray-scale US features associated with malignancy

Location, structure, echogenicity, margin, presence or absence of calcifications and halo sign, vascularity of the nodule were not related to malignancy. Orientation of the nodule was the only sonographic parameter associated with malignancy ($p = 0.003$). In addition, 93.6% of the benign nodules had parallel orientation whereas 55.6% of the malignant nodules displayed parallel orientation (i.e. transverse diameter greater than vertical diameter).

SR is calculated by dividing the mean strain of the adjacent normal thyroid parenchymal tissue by the mean intranodular strain. By using the receiver operating characteristic analysis, the best cut-off point was found to be 1.935 to differentiate benign from malignant nodules with 95% confidence interval ($p = 0.000$, AUC = 0.920) (Figure 2). The

sensitivity, specificity, negative predictive value, positive predictive value and accuracy rate of the SR analysis were 100%, 76%, 100%, 78.5% and 78% respectively.

There was a statistically significant correlation between the ES and cytology of the nodules (p = 0.001). When the elasticity scores of the benign nodules were analysed most of the benign nodules had ES 2 and 3. Among the benign nodules 2 nodules displayed ES 1 (1.4%); 69 nodules showed ES 2 (48.9%) (Figure 3); 56 nodules had ES 3 (39.7%) and 14 nodules revealed ES 4 (9.9%). None of the benign nodules displayed ES 5. On the other hand, none of the malignant nodules had ES 1 and 2, most of them displaying an ES 5. Among the malignant nodules 2 nodules displayed ES 3 (22.2%); 3 nodules had ES 4 (33.3%) (Figure 4); 4 nodules showed ES 5 (44.4%).

Discussion

The literature asserts that sonographic features and elastosonographic evaluation have variable diagnostic performances in the discrimination of benign and malignant nodules. In a retrospective multicenter study nonparallel orientation, spiculated margin, marked hypoechogenicity, microcalcification and macrocalcification were found to be associated with malignancy.[15] Yet, Iannuccilli *et al*., declared that the presence of intrinsic microcalcification, which is defined as a "snowstorm" pattern of calcification which has 100% specifity for malignancy, was the only statistically significant feature associated with malignancy.[7]

The use of USE for improving the diagnostic accuracy of sonographic examination of the thyroid nodules was first described by Lyshchik *et al*.[16] Authors prospectively evaluated the role of USE for discriminating malignancy and found that SR value greater than 4 had the highest association with malignancy (p < 0.001); with 96% specificity and 82% sensitivity.[16]

In a recent meta-analysis published by Razavi *et al*., which evaluated twenty four studies USE was concluded to be more sensitive and specific compared to each of the ultrasound features.[17] In the retrospective research conducted by Moon *et al*., USE alone and the combination of USE and gray-scale US, demonstrated inferior performance in the differentiation of malignant versus benign thyroid nodules compared to gray-scale US features.[18] Other studies have also demonstrated that USE is superior to US or the addition of USE to US, increased the diagnostic performance of US findings was higher.[19,20] Bojunga *et al*., carried out a meta-analysis of USE studies for the discrimination of malignant thyroid nodules. USE exhibited a mean sensitivity of 92% and a specificity of 90% for the diagnosis of malignant thyroid nodules. A wide range of specificity was noted in different studies. Authors explained that USE could be used with high sensitivity in the management of thyroid nodules and might be a useful tool in conjunction with or even instead of FNAC for the selection of patients for surgery.[21]

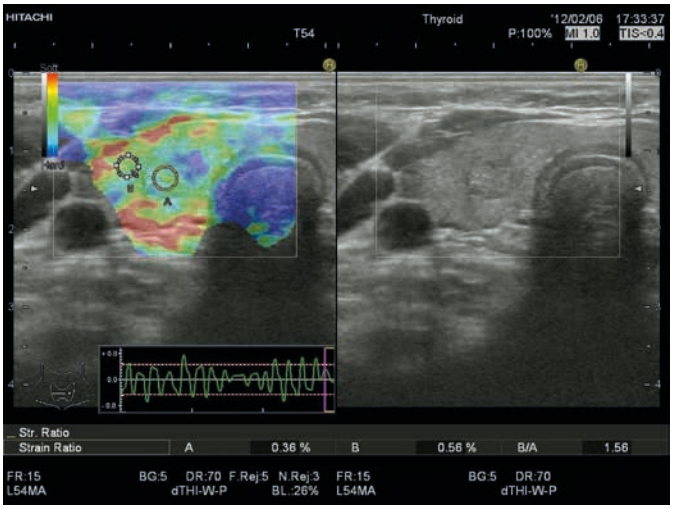

A

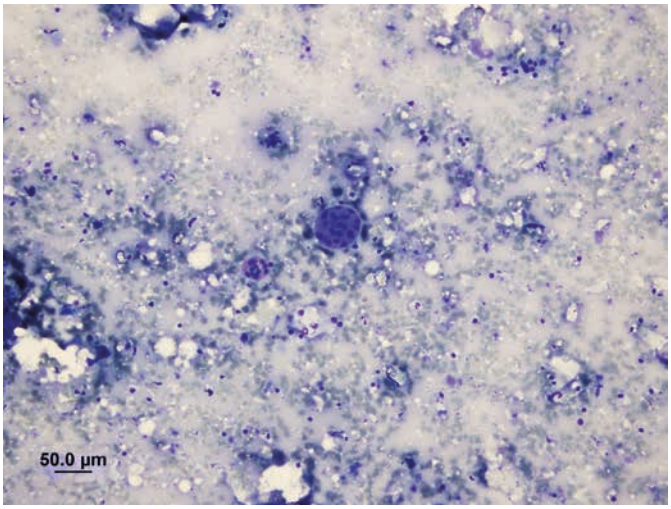

B

FIGURE 3. A Elastosonographic evaluation of an isoechoic solid nodule measuring 6.7 x 5.4 mm with well-defined margins, parallel orientation and peripheral halo in the right lobe of the thyroid gland of a 44 year-old female patient. Region of interest of the nodule is represented by A, region of interest of the adjacent thyroid parenchyme is represented by B. Elasticity score interpretation was 2, strain ratio measurement was 1.56. **B** Fine needle aspiration cytology revealed benign thyrocyte group forming low cellularity macrofollicule formation (May-Grunwald giemsa stain, X200).

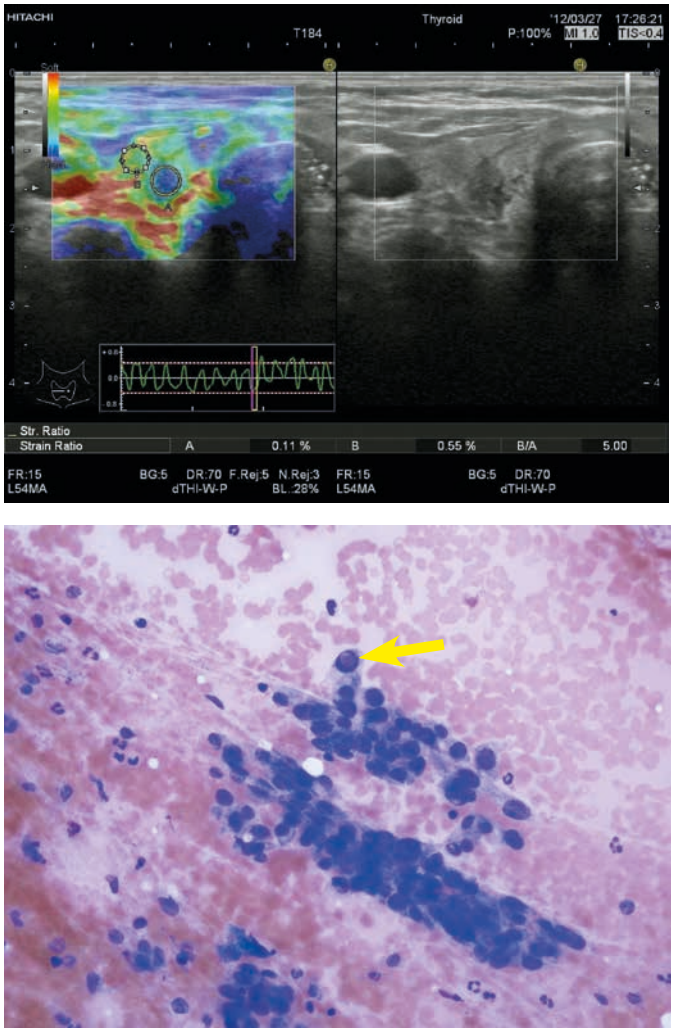

FIGURE 4. A Elastosonographic evaluation of a hypoechoic, solid nodule measuring 6 x 8 mm with irregular margins, antiparallel orientation in the right lobe of the thyroid gland of a 53 year-old female patient. Region of interest of the nodule is represented by A, region of interest of the adjacent thyroid parenchyme is represented by B. Elasticity score interpretation was 4, strain ratio measurement was 5. **B** Fine needle aspiration cytology revealed papillary carcinoma cells with atypical nuclei containing intranuclear inclusion bodies (arrow) (May-Grunwald giemsa stain, x400). Histopathology proved to be papillary carcinoma.

In the literature various cut-off values have been suggested for the discrimination of malignancy in SR analysis. Ning *et al*., concluded that the best cut-off point of SR was 4.2 for the discrimination of malignancy.[22] In the study of Xing *et al*., the best cut-off values for large and small nodules were different, i.e. for nodules that are larger than 1 cm, the cut-off value was 3.98 whereas for the ones equal or smaller than 1 cm the cut-off value was 4.21. Authors also concluded that SR analysis demonstrated better diagnostic performance compared to the 4 scale ES method.[23] Kagoya *et al*. indicated that SR value greater than 1.5 was found as the predictor of malignancy, with 90% sensitivity and 50% specificity.[24]

In our study, the distribution of the strain ratio value confirmed that benign nodules are much softer than the malignant ones and the best cut-off value was found to be 1.925. We have also established a statistically significant correlation between the ES and pathology of the nodules. None of the benign nodules demonstrated ES 5 and none of the malignant nodules showed ES 1 and 2. Antiparallel orientation was the only gray-scale US feature associated with malignancy. In the light of the results; taller than wide shape, ES 3, 4 and especially 5, SR greater than 1.925 were associated with malignancy. Presence of at least one of these findings should prompt the FNAC analysis in the primary evaluation of the thyroid nodules.

USE can also be beneficial in the management of patients with FNAC with nondiagnostic or indeterminate results, which constitute the major limitation of FNAC of thyroid nodules. A nondiagnostic cytology can be obtained in cystic or hemorrhagic lesions due to lack of adequate number of cells for diagnosis. In 10 to 20% of all FNA materials, although the collected material is insufficient, cytology is classified as indeterminate, meaning that differentiation between follicular adenoma and follicular carcinoma or the follicular variant of a papillary thyroid carcinoma is not made.[25] Among patients with FNA resulting in indeterminate lesion, 25% end up with a final diagnosis of malignancy on histology.[26]

Rago *et al*., carried out a study to investigate the role of USE in the presurgical diagnosis of nodules with indeterminate or nondiagnostic cytology.[27] For indeterminate lesions the sensitivity and specificity of USE were 96.8% and 91.8%, respectively. For nodules with nondiagnostic cytology USE had a sensitivity of 87.5% and a specificity of 86.7%. Authors showed that USE could be a valuable method for the discrimination of malignancy in nodules with indeterminate or nondiagnostic cytology and it eventually contributes to the selection of patients for surgery. USE evaluation of such lesions can not only help decrease the unnecessarily use of FNAC but also increases the diagnostic ability. In diagnostic algorithm of the clinicians crucial problems such as repeating biopsies and delays in diagnosis can be prevented with the help of USE.

A limitation of our study is the low prevalence of malignant nodules. Larger prospective studies are needed to confirm our results. For the nodules

with indeterminate or nondiagnostic cytology a study with a larger cohort is necessary to evaluate the role of USE in the selection of patients for surgery.

Conclusions

Nonparallel orientation of the nodule can be used as a gray-scale US criterion indicative of malignancy. In the USE evaluation elasticity scores 3, 4 and especially 5; strain ratio measurements greater than 1.925 are suggestive of malignancy.

A change in the diagnostic algorithm of the thyroid nodules should be considered integrating the USE analysis. Accordingly, in the diagnostic work-up of the thyroid nodules, USE evaluation should take part in the standard protocol in clinical practice for the decision and evaluation period of the treatment.

Acknowledgement

We would like to thank to Dr. Erdal Cosgun from Hacettepe University Department of Biostatistics for his support in the statistical analysis of the study.

References

1. Frates MC, Benson CB, Doubilet PM, Kunreuther E, Contreras M, et al. Prevalence and distribution of carcinoma in patients with solitary and multiple thyroid nodules on sonography. *J Clin Endocrinol Metab* 2006; **91:** 3411-7.
2. Castro MR, Gharib H Thyroid fine-needle aspiration biopsy: progress, practice, and pitfalls. *Endocr Pract* 2003; **9:** 128-36.
3. Pacini F, Schlumberger M, Dralle H, Elisei R, Smit JW, Wiersinga W. European consensus for the management of patients with differentiated thyroid carcinoma of the follicular epithelium. *Eur J Endocrinol* 2006; **154:** 787-803.
4. Gharib H, Papini E, Valcavi R, Baskin HJ, Crescenzi A, Dottorini ME, et al. American Association of Clinical Endocrinologists and Associazione Medici Endocrinologi medical guidelines for clinical practice for the diagnosis and management of thyroid nodules. *Endocr Pract* 2006; **12:** 63-102.
5. Cooper DS, Doherty GM, Haugen BR, Kloos RT, Lee SL, Mandel SJ, et al. Revised American Thyroid Association management guidelines for patients with thyroid nodules and differentiated cancer. *Thyroid* 2009; **19:** 1167-214.
6. Gharib H, Papini E, Paschke R, Duick DS, Valcavi R, Hegedüs L, et al. American Association of Clinical Endocrinologists, Associazione Medici Endocrinologi, and European Thyroid Association medical guidelines for clinical practice for the diagnosis and management of thyroid nodules. *J Endocrinol Invest* 2010; **33:** 1-50.
7. Iannuccilli JD, Cronan JJ, Monchik JM. Risk for malignancy of thyroid nodules as assessed by sonographic criteria. *J Ultrasound Med* 2004; *23:* 1455-64.
8. Gharib H, Papini E, Paschke R, Duick DS, Valcavi R, Hegedüs L, et al. American Association of Clinical Endocrinologists, Associazione Medici Endocrinologi, and European Thyroid Association Medical Guidelines for Clinical Practice for the Diagnosis and Management of Thyroid Nodules. *Endocr Pract* 2010; **16:** 1-43.
9. Dighe M, Bae U, Richardson ML, Dubinsky TJ, Minoshima S, Kim Y. Differential diagnosis of thyroid nodules with US elastography using carotid artery pulsation. *Radiology* 2008; **248:** 662-9.
10. Ophir J, Cespedes I, Ponnekanti H, Yazdi Y, Li X. Elastography: a quantitative method for imaging the elasticity of biological tissues. *Ultrason Imaging* 1991; **13:** 111-34.
11. Chaturvedi P, Insana MF, Hall TJ. Ultrasonic and elasticity imaging to model disease-induced changes in soft-tissue structure**.** *Med Image Anal* 1998; **2:** 325-38.
12. Adriaenssens N, Belsack D, Buyl R, Ruggiero L, Breucq C, De Mey J, et al. Ultrasound elastography as an objective diagnostic measurement tool for lymphoedema of the treated breast in breast cancer patients following breast conserving surgery and radiotherapy. *Radiol Oncol* 2012; **46:** 284-95.
13. Rago T, Santini F, Scutari M, Pinchera A, Vitti P. Elastography: new developments in ultrasound for predicting malignancy in thyroid nodules. *J Clin Endocrinol Metab* 2007; **92:** 2917-22.
14. Guidelines of the Papanicolaou Society of Cytopathology for the Examination of Fine-Needle Aspiration Specimens from Thyroid Nodules. The Papanicolaou Society of Cytopathology Task Force on Standards of Practice. *Mod Pathol* 1996; **9:** 710-5.
15. Moon WJ, Jung SL, Lee JH, Na DG, Baek JH, Lee YH, et al. Benign and malignant thyroid nodules: US differentiation-multicenter retrospective study. *Radiology* 2008; **247:** 762–70.
16. Lyshchik A, Higashi T, Asato R, Tanaka S, Ito J, Mai JJ. Thyroid gland tumor diagnosis at US elastography. *Radiology* 2005; **237:** 202-11.
17. Razavi SA, Hadduck TA, Sadigh G, Dwamena BA. Comparative effectiveness of elastographic and B-mode ultrasound criteria for diagnostic discrimination of thyroid nodules: a meta-analysis. *AJR Am J Roentgenol* 2013; **200:** 1317-26.
18. Moon HJ, Sung JM, Kim EK, Yoon JH, Youk JH, Kwak JY. Diagnostic performance of gray-scaleUS and elastography in solid thyroid nodules. *Radiology* 2012; **262:** 1002-13.
19. Shuzhen C. Comparison analysis between conventional ultrasonography and ultrasound elastography of thyroid nodules. *Eur J Radiol* 2012; **81:** 1806-11.
20. Trimboli P, Guglielmi R, Monti S, Misischi I, Graziano F, Nasrollah N, et al. Ultrasound sensitivity for thyroid malignancy is increased by real-time elastography: a prospective multicenter study. *J Clin Endocrinol Metab* 2012; **97:** 4524-30.
21. Bojunga J, Herrmann E, Meyer G, Weber S, Zeuzem S, Friedrich-Rust M. Real-time elastography for the differentiation of benign and malignant thyroid nodules: a meta-analysis. *Thyroid* 2010; **20:** 1145-50.
22. Ning CP, Jiang SQ, Zhang T, Sun LT, Liu YJ, Tian JW. The value of strain ratio in differential diagnosis of thyroid solid nodules. *Eur J Radiol* 2012; **81:** 286-91.
23. Xing P, Wu L, Zhang C, Li S, Liu C, Wu C. Differentiation of benign from malignant thyroid lesions: calculation of the strain ratio on thyroid sonoelastography. *J Ultrasound Med* 2011; **30:** 663-9.
24. Kagoya R, Monobe H, Tojima H. Utility of elastography for differential diagnosis of benign and malignant thyroid nodules. *Otolaryngol Head Neck Surg* 2010; **143:** 230–234.
25. Lewis CM, Chang KP, Pitman M, Faquin WC, Randolph GW. Thyroid fine-needle aspiration biopsy: variability in reporting. *Thyroid* 2009; **19:** 717-23.
26. Rago T, Di Coscio G, Basolo F, Scutari M, Elisei R, Berti P, et al. Combined clinical, thyroid ultrasound and cytological features help to predict thyroidmalignancy in follicular and Hurthle cell thyroid lesions: resultsfrom a series of 505 consecutive patients. *Clin Endocrinol* 2007; **66:** 13-20.
27. Rago T, Scutari M, Santini F, Loiacono V, Piaggi P, Di Coscio G, et al. Useful tool for refining the presurgical diagnosis in thyroid nodules with indeterminate or nondiagnostic cytology. *J Clin Endocrinol Metab*; 2010; **95:** 5274-80.

research article

Differential S-phase progression after irradiation of p53 functional versus non-functional tumour cells

Friedo Zölzer[1,2], Tamare Mußfeldt[1], Christian Streffer[1]

[1] Institute of Medical Radiobiology, Medical Faculty, University Duisburg-Essen, Germany

[2] Department of Radiology, Toxicology and Civil Protection, Faculty of Health and Social Studies, University of South Bohemia in České Budějovice, Czech Republic

Radiol Oncol 2014; 48(4): 354-360.

Received 24 April 2014
Accepted 24 July 2014

Correspondence to: Dr. Friedo Zölzer, Department of Radiology, Toxicology and Civil Protection, Faculty of Health and Social Studies, University of South Bohemia in České Budějovice, Emy Destinové 46, 37005 České Budějovice, Czech Republic. E-mail: zoelzer@zsf.jcu.cz

Disclosure: No potential conflicts of interest were disclosed.

Background. Many pathways seem to be involved in the regulation of the intra-S-phase checkpoint after exposure to ionizing radiation, but the role of p53 has proven to be rather elusive. Here we have a closer look at the progression of irradiated cells through S-phase in dependence of their p53 status.

Materials and methods. Three pairs of tumour cell lines were used, each consisting of one p53 functional and one p53 non-functional line. Cells were labelled with bromodeoxyuridine(BrdU) immediately after irradiation, they were then incubated in label-free medium, and at different times afterwards their position within the S-phase was determined by means of flow cytometry.

Results. While in the p53 deficient cells progression through S-phase was slowed significantly over at least a few hours, it was halted for just about an hour in the p53 proficient cells and then proceeded without further delay or even at a slightly accelerated pace.

Conclusions. It is clear from the experiments presented here that p53 does play a role for the progress of cells through the S-phase after X-ray exposure, but the exact mechanisms by which replicon initiation and elongation is controlled in irradiated cells remain to be elucidated.

Key words: x-rays; intra-S-phase checkpoint; flow cytometry, relative movement

Introduction

The crucial importance of the tumour suppressor protein p53 for the regulation of cell cycle progression after irradiation has been known for more than two decades. It was the papers of Kastan *et al*.[1] and Kuerbitz *et al*.[2] at the beginning of the 1990s that alerted radiation biologists to the fact that the G_1-checkpoint was under the control of p53. The checkpoint itself, *i.e.* a radiation induced block of cell cycle progression before the entry into the S-phase had already been described in 1953 by Howard and Pelc[3] for plant cells, and 15 years later by Little[4] for human cells. Afterwards, the G_1-checkpoint had somewhat fallen into oblivion as in many tumour cell lines it was not observed, which Kastan's discovery explained by the fact that it required functionality of p53, often lost at later stages of tumour development. Although the capability to halt cell cycle progression for a few hours after irradiation should give cells additional time for repair before entry into the S-phase, a functional p53 does not necessarily convey greater radioresistence.[5] Other factors, such as the checkpoint control in later phases of the cell cycle, clearly also play a role. There is, however, a clear advantage of cells capable of a G_1-block in terms of how they proceed through the following S-phase: after a few hours of extra repair time cells have no problems completing replication of their previously damaged DNA,

whereas cells incapable of such a halt tend to fail at some point during replication.[6]

Historically, greater attention has been given to the G_2-checkpoint. It was observed first by Howard and Pelc[3] in plant cells, and a decade later by Terasima and Tolmach[7] in human cells. As for a possible role of p53 in controlling this checkpoint, the reports in the literature are somewhat contradictory. Cells deficient in p53 are capable of arresting cell cycle progression before entry into mitosis.[1] We have demonstrated recently that while the accumulation of cells in the G_2-compartment after irradiation can be different in p53 functional and non-functional tumour cell lines, the delay of the G_2-phase itself is completely independent of the p53 status.[8] Some authors have claimed, however, that manipulation of the p53 expression can have an effect on the G_2-checkpoint.[9,10] Others have suggested that p53 plays a role in the maintenance of the arrest 2 – 10 hours after radiation.[11,12] It would seem, therefore, that both p53-dependent and p53-independent pathways play a role.[13,14] Supposedly, the function of the G_2-checkpoint is to allow for the repair of DNA damage before mitosis. This is in agreement with the observation that abrogation of the block, *e.g.* by high concentrations of caffeine, usually sensitizes cells to radiation[15,16], although that does not seem to be the case with all cell types.[17] Again, the interplay of different checkpoints may be of relevance here. Interestingly, although the length of the G_2-phase delay did not correlate with radiation sensitivity as such, the number of unrejoined chromosome breaks was significantly elevated if the checkpoint was attenuated.[18]

And finally, regarding the role of p53 in the regulation of S-phase, there does not seem to be a great number of studies directly addressing the issue.[19] Radiation induced delays in the S-phase have been described and their regulation has been analysed since Painter and Young discovered radioresistant DNA synthesis in Ataxia telangiectasia cells in 1980[20], but it was not until a decade and a half later that authors began to speak of an S-phase damage checkpoint.[21,22] This checkpoint seemed to be independent of p53. At least in some cases, however, p53 apparently did have an influence on how and when cells proceeded through replication (see below). Thus, the role of p53 in the regulation of the S-phase checkpoint "seems much more elusive" than its role for the G_1- and G_2-phases and "the details … are awaiting future studies", as Fei and El-Deiry stated in their review 2003.[23] That is still true 10 years later.

In general, when one looks at the regulation of S-phase after DNA damage, a rather complex, sometimes confusing picture presents itself. Two checkpoints can be distinguished, one involving stalled replication forks (called the "replication checkpoint") and another activated by double strand breaks (called the "intra-S-phase checkpoint").[24,25] Replication forks can be stalled because of nucleotide starvation or because of inhibition of key replication enzymes, but also by certain types of DNA damage. In all of these cases, patches of single-stranded DNA appear to be the key signal, causing first the activation of ATR, which in turn leads to the phosphorylation of Dbf4 (directly) and Cdc7 (indirectly via activation of Chk1). The thus modified Cdc7/Dbf4 complex is now unable to initiate replication at hitherto unfired origins, but at the same time it protects the integrity of the stalled replication fork.[26] Part of this process, namely the phosphorylation of Dbf4, can also be initiated by ATM, which is activated as a consequence of double strand break induction. Dbf4 is thus at the same time one of the components of the "replication checkpoint" and the "intra-S-phase checkpoint", the latter being also under the influence of three more pathways.[27-29] The first of these leads from ATM activation to the phosporylation of Smc1[30] and Smc3[31], associated proteins responsible for the maintenance of chromatin structure. The other two depend on the activation of either Chk1 (by ATR) or Chk2 (by ATM). Both of these checkpoint kinases can either directly phosphorylate Cdc25A, causing its degradation and thus preventing activation of Cdk2, which in turn blocks the formation of the pre-replication complexes and the firing of new origins.[32,33] Or they can work through p53 which has a number of ways to influence replication: it causes the activation of killin, a nuclear inhibitor of DNA replication[34,35]; it has an influence on Cdc25A through a factor called ATF3, described as a transcriptional repressor[36]; it represses the transcription of Cdc25A through p21[37], and finally it inhibits Cdk2 through p21 directly.[38]

In order to clarify how irradiated cells progress through the S-phase in the presence or absence of a functional p53, we compared 6 human tumour cell lines that had earlier been characterized as to their p53 status, their capability to control the G_1-checkpoint and their tendency to fail during S-phase when irradiated in G_1. We labelled cells in S-phase with the help of BrdU and followed their movement through the S- and G_2-phases using a pulse-chase protocol. Clear differences between p53 functional and non-functional cells became ob-

vious in this study, which suggest that the importance of p53 protein for the intra-S checkpoint has to be re-evaluated.

Materials and methods

Cell lines

The following human tumour cell lines were used[6]:

- Be11: A human melanoma cell line originally isolated in Dr. Malaise's laboratory at the Institute Gustave-Roussy, Villejuif, France[39]; the cells have a DNA index of 1.6 and are only slightly pigmented.
- MeWo: A human melanoma cell line originally isolated by Dr. Fogh's group in the Sloan-Kettering Institute for Cancer Research, New York[40]; the subline used in our institute has a DNA index of 1.6 and is no longer pigmented.
- 4197: A squamous carcinoma cell line derived from a tumour in the lower jaw of a 55-year-old male patient; it was established in 1987 from a biopsy taken at the department of maxillofacial surgery at the University Clinics in Essen; the cells have a DNA index of 1.0.
- 4451: A squamous carcinoma cell line derived from a recurrent tumour in the lower jaw of a 46-year-old male patient; it was established in 1988 from a biopsy taken at the aforementioned department; the cells have a DNA index of 1.5.
- EA14: A human malignant glioma cell line isolated in the Department of Radiotherapy at the University Clinics Essen[45]; the cells have a DNA index of 1.3.
- U87: A human malignant glioma cell line isolated by Ponten and Macintyre at the Wallenberg Laboratory, Uppsala, Sweden; the cells have a DNA index of 1.0.

All six cell lines have been characterized with respect to their p53 status. In our own study of the first four[41], we used a number of indirect methods suggesting that Be11 and 4197 were p53 wild types, but MeWo and 4451 were p53 mutants.[41] Since then, MeWo and 4451 have been confirmed as mutants by direct DNA sequencing.[42,43] The observation that Be11 and 4197 are p53 wild-types has been corroborated by analysis of their p21 expression after radiaton exposure, which is intact.[44] The latter two cell lines have been studied by others.[46] Both of them were reported to have a p53 wild-type gene sequence. However, a strong increase of p53 and p21 expression after irradiation was observed only in EA14, whereas U87 showed a much reduced increase in p53 and no increase at all in p21. We therefore designated Be11, 4197, and EA14 as p53 functional, but MeWo, 4451, and U87 as p53 non-functional.

Culture conditions and treatment

The cells were routinely cultured in Minimal Essential Medium with Eagle's salts, supplemented with 20% fetal calf serum. They were subcultured twice a week and routinely checked for mycoplasma contamination. For the experiments, cells from an exponentially growing culture were seeded into small culture flasks (25 m^2, 5 ml medium, 250,000 cells). After 24 h, they were exposed to X-rays (Stabilipan' Siemens, 240kV, 0.5mm Cu filter, 15mA, 1Gy/min). All culture flasks, including sham irradiated controls, were taken from the incubator at the same time and kept together while successively treated in the adjacent room.

Two-parameter flow cytometry[47]

Immediately after radiation exposure, 50µl of bromodeoxyuridine (BrdU) solution (1mM) was added to the flasks (final concentration 10µM), and the flasks were incubated for 30 min. The medium was then removed, the flasks washed twice, and the cells were further incubated in the absence of BrdU. Cells were trypsinized at 2 hour intervals (up to 10 hours after irradiation) and fixed in 96% ethanol.

The immunofluorescence staining for flow cytometry analysis has been described in detail elsewhere.[48] Briefly, cells were incubated in a pepsin solution to isolate nuclei and then in 2 N HCl to partly denature the DNA. They were then incubated with anti-BrdU mouse IgG (Becton Dickinson, 1:20) followed by goat anti-mouse IgG FITC-conjugate (DuPont, 1:100). The DNA was stained with propidium iodide (PI). Green (FITC) and red (PI) fluorescence after 488-nm laser excitation were recorded with a FACScan flow cytometer (Becton Dickinson) and plotted in two-parameter scattergrams. Ten thousand events were recorded; the coefficient of variation of the DNA histograms was about 5%.

Data analysis

Relative movement (RM) values were calculated as the mean DNA fluorescence of the BrdU labelled undivided cells (those that had not yet passed through mitosis, Figure 1) less the DNA fluorescence of the cells in G_1 divided by the difference in DNA fluorescence of the cells in $G_1$and G_2[47, 49]:

$$RM = \frac{F_{lab} - F_{G1}}{F_{G2} - F_{G1}}$$

Each experiment was carried out four times with each cell line. All values given below are means and standard errors of the mean from interexperimental variation.

Results

The pulse-chase method which we employed here allowed us to follow the progression of labelled cells through S-phase in the course of several hours after irradiation. At the time of radiation exposure, S-phase cells were positioned, on average, at about half the distance between the G_1 and G_2-peaks. They then moved towards the G_2-peak and after a few hours, having undergone mitosis, began to reappear in G_1. Earlier research has shown that when the Relative Movement (the mean position of labelled cells between the G_1 and G_2-peaks) is plotted against time after labelling, it initially increases with a slope of $1/T_S$, where T_S is the duration of S-phase; when the first cells have passed through mitosis, the slope is reduced by a factor of 2.[47,49] As shown in Figure 2, this was the case for all cell lines in the absence of irradiation. The "break-point" in the curves occurred mostly around 6 h, which is in reasonable agreement with estimates for their transit time through the G_2-and M-phases.[8,50] From the increase of the Relative Movement in the first hours after labelling we obtained values for the duration of the unperturbed S-phase between 14 h (MeWo) and 20 h (Be11). Table 1 suggests that there was no obvious connection with the p53 status.

Important differences between p53 functional and non-functional cells were seen, however, after irradiation. In the p53 functional cells, progression through the S-phase was halted for just a short time and then proceeded without further delay or even at a slightly accelerated pace. An initial delay was also seen, for 4197 and EA14, in unirradiated cells, but it was prolonged after radiation exposure. In p53 non-functional cells, on the other hand, progression through the S-phase was significantly slowed down over at least a few hours. In the case of 4451, the slow-down was particularly dramatic, but progression returned to normal after 4 h.

Within the first two pairs of cell lines, the p53 proficient ones were more radioresistant in terms of cell survival, so that it seemed advisable to also employ higher doses with them as compared to the p53 deficient ones (6 Gy for Be11, 8 Gy for 4197 leading

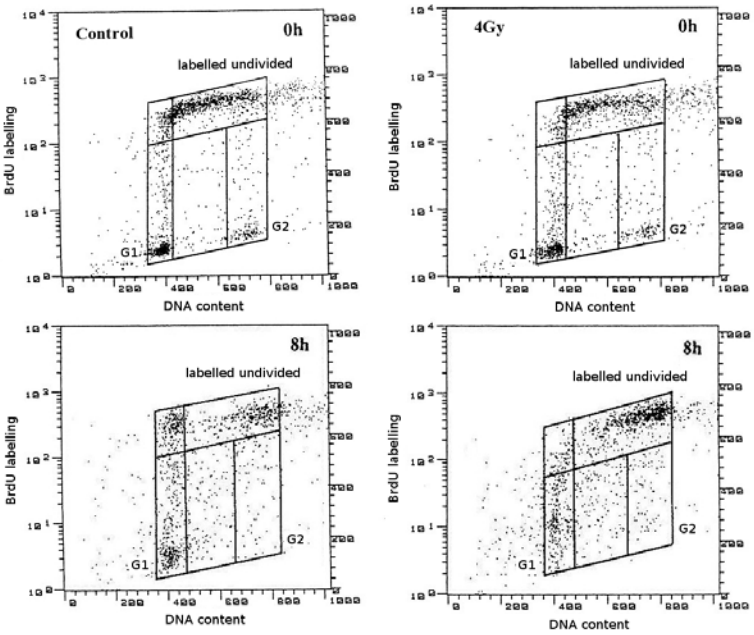

FIGURE 1. Examples of scattergrams of control cultures and cultures exposed to 4 Gy of X-rays, labelled with BrdU and kept in BrdU-free medium for the times indicated (MeWo) (FL1-H: BrdU incorporation (FITC), FL3-H: DNA content (PI))

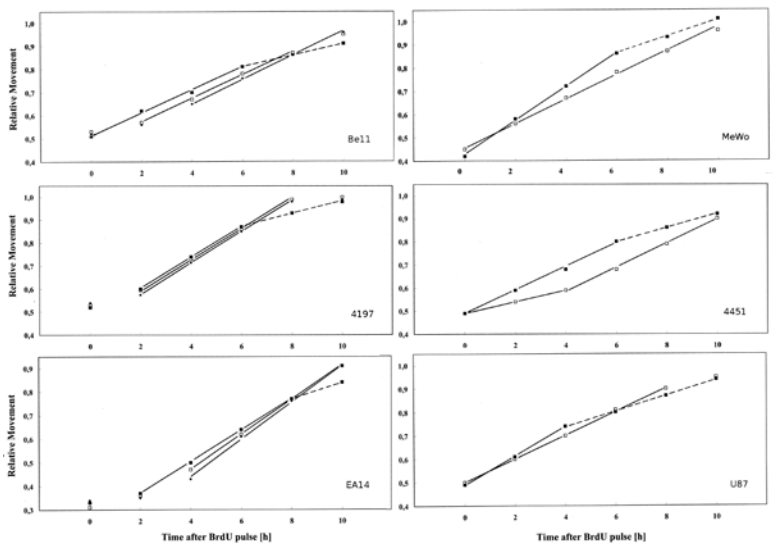

FIGURE 2. "Relative Movement" as a function of time after radiation exposure in p53 functional (Be11, 4197, EA14) and p53 non-functional (MeWo, 4451, U97) cell lines. Error bars omitted for clarity. See Table 1 for means and standard errors of the mean from interexperimental variation. The extensions of the solid lines indicate which data points were included in the regression analysis. The broken lines depict the second, shallower component of the "Relative Movement" curves (see text).

TABLE 1. Duration of S-phase and delay per unit dose calculated from data shown in Figure 2

Cell line	Dose [Gy]	Duration of S-phase [h]	Delay [h/Gy] [c]
Be11	0	20.4 ±1.6 [b]	
	4	0.8 ± 0.6 [a] + 19.8 ± 2.0 [b]	- 0.15 ± 0.27
	6	1.2 ± 0.6 [a] + 19.4 ± 2.1 [b]	- 0.17 ± 0.18
MeWo	0	13.7 ± 1.1 [b]	
	4	17.5 ± 0.9 [b]	0.95 ± 0.35
4197	0	0.8 ± 0.4 [a] + 15.4 ± 2.6 [b]	
	4	1.0 ± 0.6 [a] + 15.1 ± 2.4 [b]	- 0.08 ± 0.12
	8	1.2 ± 0.8 [a] + 14.8 ± 1.7 [b]	- 0.07 ± 0.08
4451	0	19.6 ± 1.2 [b]	
	4	(0 – 4 h) 40.7 ± 4.5 [b]	5.28 ± 1.36
		(6 – 10 h) 19.2 ± 2.2 [b]	- 0.10 ± 0.23
EA14	0	1.4 ± 0.5 [a] + 14.9 ± 0.4 [b]	
	4	1.9 ± 1.0 [a] + 13.6 ± 1.5 [b]	- 0.33 ± 0.19
	8	2.6 ± 0.4 [a] + 12.6 ± 0.5 [b]	- 0.29 ± 0.09
U87	0	16.0 + 1.6 [b]	
	4	19.6 ± 1.1 [b]	0.90 ± 0.58

[a] The smaller figures are the initial lags immediately after irradiation

[b] The larger figures are the durations of S-phase calculated from the slopes m of the "Relative Movement" curves (T_S = 1/m)

[c] Delays calculated from the slopes m of the "Relative Movement" curves (T_S = 1/m), i.e. neglecting the initial lags

to the same cell survival as 4 Gy in MeWo and 4415, resp.[41]). Not even with these higher doses, however, was their progression through the S-phase (after the initial short delay) significantly reduced. The same was the case with EA14 (where we also applied 8 Gy in spite of it being more radiosensitive than its counterpart U87[46]). We therefore concluded that the absence of a strong radiation effect on S-phase progression in the p53 functional cell lines was real and not due to their different radiosensitivity as compared to the p53 non-functional cell lines.

Discussion

It must be emphasized that any conclusion that may be drawn here about the progression through S-phase in relation to p53 function, is restricted to cells which are in S-phase at the time of irradiation. This is due to the fact that labelling was done immediately after radiation exposure. For MeWo, we have some data from an earlier study where we looked at the Relative Movement of cells labelled 24 or 48 h after irradiation and we could still see a significant slow-down in S-phase at these times, although the G_2-block had been completely overcome.[47] No such experiments have been undertaken for any of the other cell lines used in the present investigation.

For cells in S-phase, then, it is clear that a functional p53 suppresses further DNA synthesis for no more than a short period, but permits progression through the S-phase at a normal pace afterwards. In cells that are p53 non-functional, DNA synthesis is slowed down for at least a couple of hours, in two of our three cell lines for the whole duration of the S-phase. Whether the p53 effect is on replicon initiation or on elongation in already initiated replicons is impossible to tell from our data. A complete halt of replication for 1-2 hours in p53 proficient cell lines would suggest that both are affected, but with up to 100 000 origins of replication in a human cell one would probably not notice if elongation in a few already initiated replicons was finished and just the firing of new origins prevented. Indeed, experiments in which the direct block of viral origin by p53 binding was studied after γ-irradiation, it was found that initiation was completely shut down, but elongation continued unabated even though the template must still have been damaged.[51] This agrees with the conclusion of a much earlier study.[20]

On the other hand, an investigation of the different effects of irradiation on DNA synthesis in normal and Li-Fraumeni fibroblasts clearly showed that in the absence of p53 both initiation and elongation were slowed down.[52] Although the experiments described in that study focused on overall DNA synthesis and were not designed to distinguish between a slow-down of progression through S-phase and a reduced entry of cells into S-phase, the findings reported seem to be in very good agreement with our data. In normal cells, DNA synthesis was shut down within an hour or two after irradiation, then recovered, and again decreased after about 6 hours. The latter effect was ascribed to less cells entering S-phase because of the G_1-block. In p53-deficient fibroblasts, the initial drop in DNA synthesis was also present, but it lasted longer then in normal cells, recovered more fully and was not followed by a dramatic drop at later times, presumably because cells were not blocked in G_1. Importantly, normal fibroblasts seemed to shut down only initiation, while both initiation and elongation were affected in p53-deficient cells.[52]

By which mechanism p53 suppresses replicon initiation and by which means both replicon initiation and elongation are suppressed in p53-deficient cells remains to be elucidated. In the introduction,

we have mentioned a number of pathways involved in the intra-S-delay, but it was beyond our possibilities to examine the details of replication control in our cell lines. Nevertheless, the experiments presented here show that p53 does play a role for the progress of cells through the S-phase after X-ray exposure, at least with cells irradiated in S-phase itself.

Acknowledgement

We thank D. Dittmann for excellent technical assistance. Cultivation, irradiation and BrdU labeling of EA14 and U87 were carried out by M. Groneberg in the Radiobiological Laboratory of the Department of Radiotherapy of the University Clinics, Essen; we are grateful to him and to M. Stuschke for making this part of the study possible.

References

1. Kastan MB, Onyekwere O, Sidransky D, Vogelstein B, Craig RW. Participation of p53 protein in the cellular response to DNA damage. *Cancer Res* 1991; **51:** 6304-11.
2. Kuerbitz SJ, Plunkett BS, Walsh WV, Kastan MB. Wild-type p53 is a cell cycle checkpoint determinant following irradiation. *Proc Natl Acad Sci USA* 1992; **89:** 7491-5.
3. Howard A, Pelc SR. Synthesis of deoxyribonucleic acid in normal and irradiated cells and its relation to chromosome breakage. *Heredity* 1953; **6:** 261-73.
4. Little JB. Delayed initiation of DNA synthesis in irradiated human diploid cells. *Nature* 1968; **218:** 1064-5.
5. Cuddihy AR, Bristow RG. The p53 protein family and radiation sensitivity: Yes or no? *Cancer Met Rev* 2004; **23:** 237-57.
6. Zölzer F, Streffer C. Quiescence in S-phase and G_1 arrest induced by irradiation and/or hyperthermia in six human tumour cell lines of different p53 status. *Int J Radiat Biol* 2000; **76:** 717-25.
7. Terasima T, Tolmach LJ. Variations in several responses of HeLa cells to x-irradiation during the division cycle. *Biophys J* 1963; **3:** 11-33.
8. Zölzer F, Jagetia G, Streffer C. G_2-block after irradiation of cells with different p53 status. *Strahlen Onkol* 2014*;* **190**: 1075-9.
9. Agarwal ML, Agarwal A, Taylor WR, Stark GR. p53 controls both the G_2/M and the G_1 cell cycle checkpoints and mediates reversible growth arrest in human fibroblasts. *Proc Natl Acad Sci USA* 1995; **92:** 8493-7.
10. Stewart N, Hicks GG, Paraskevas F, Mowat M. Evidence for a second cell cycle block at G_2/M by p53. *Oncogene* 1995; **10:** 109-15.
11. Bunz F, Dutriaux A, Lengauer C, Waldman T, Zhou S, Brown JP, et al. Requirement for p53 and p21 to sustain G_2 arrest after DNA damage. *Science* 1998; **282:** 1497-501.
12. Solberg Landsverk K, Patzke S, Rein ID, Stokke C, Lyng H, De Angelis PM, Stokke T. Three independent mechanisms for arrest in G_2 after ionizing radiation. *Cell Cycle* 2011; **10:** 819-29.
13. Taylor WR, Stark GR. Regulation of the G2/M transition by p53. *Oncogene* 2001; **20:** 1803-15.
14. Stark GR, Taylor WR. Control of the G2/M transition. *Mol Biotech* 2006; **32:** 227-48.
15. Busse PM, Bose SK, Jones RW, Tolmach LJ. The action of caffeine on X-irradiated HeLa cells. III. Enhancement of X-ray-induced killing during G_2 arrest. *Radiat Res* 1978; **76:** 292-307.
16. Powell SN, DeFrank JS, Connell P, Eogan M, Preffer F, Dombkowski D, et al. Differential sensitivity of p53(-) and p53(+) cells to caffeine-induced radiosensitization and override of G_2 delay. *Cancer Res* 1995; **55:** 1643-8.
17. Musk SR. Reduction of radiation-induced cell cycle blocks by caffeine does not necessarily lead to increased cell killing. *Radiat Res* 1991; **125:** 262-6.
18. Schwartz JL, Cowan J, Grdina DJ, Weichselbaum RR. Attenuation of G2-phase cell cycle checkpoint control is associated with increased frequencies of unrejoined chromosome breaks in human tumor cells. *Radiat Res* 1996; **146:** 139-43.
19. Iliakis G, Wang Y, Guan J, Wang H. DNA damage checkpoint control in cells exposed to ionizing radiation. *Oncogene* 2003; **22:** 5834-47.
20. Painter RB, Young BR. Radiosensitivity in ataxia-telangiectasia: a new explanation. *Proc Natl Acad Sci USA* 1980; **77:** 7315-7
21. Larner JM, Lee H, Hamlin JL. S phase damage sensing checkpoints in mammalian cells. *Cancer Surv* 1997; **29:** 25-45.
22. Morgan SE, Lovly C, Pandita TK, Shiloh Y, Kastan MB. Fragments of ATM which have dominant-negative or complementing activity. *Mol Cell Biol* 1997; **17:** 2020-9.
23. Fei P, El-Deiry WS. P53 and radiation responses. *Oncogene* 2003; **22:** 5774-83.
24. Bartek J, Lukas C, Lukas J. Checking on DNA damage in S phase. *Nature Rev Mol Cell Biol* 2004; **5:** 792-804.
25. Liu WF, Yu SS, Chen GJ, Li YZ. DNA damage checkpoint, damage repair, and genome stability. *Acta Gen Sin* 2006; **33:** 381-90.
26. Lee AY, Chiba T, Truong LN, Cheng AN, Do J, Cho MJ, et al. Dbf4 is direct downstream target of ataxia telangiectasia mutated (ATM) and ataxia telangiectasia and Rad3-related (ATR) protein to regulate intra-S-phase checkpoint. *J Biol Chem* 2012; **287:** 2531-43.
27. Falck J, Petrini JH, Williams BR, Lukas J, Bartek J. The DNA damage-dependent intra-S phase checkpoint is regulated by parallel pathways. *Nature Gen* 2002; **30**, 290-4.
28. Willis N, Rhind N. Regulation of DNA replication by the S-phase DNA damage checkpoint. *Cell Div* 2009; **4:** 13.
29. Dai Y, Grant S. New insights into checkpoint kinase 1 in the DNA damage response signaling network. *Clin Cancer Res* 2010; **16:** 376-83.
30. Yazdi PT, Wang Y, Zhao S, Patel N, Lee EY, Qin J. SMC1 is a downstream effector in the ATM/NBS1 branch of the human S-phase checkpoint. *Genes Dev* 2002; **16:** 571-82.
31. Luo H, Li Y, Mu JJ, Zhang J, Tonaka T, Hamamori Y, et al. Regulation of intra-S phase checkpoint by ionizing radiation (IR)-dependent and IR-independent phosphorylation of SMC3. *J Biol Chem* 2008; **283:** 19176-83.
32. Zhou XY, Wang X, Hu B, Guan J, Iliakis G, Wang Y. An ATM-independent S-phase checkpoint response involves CHK1 pathway. *Cancer Res* 2002; **62:** 1598-603.
33. Sørensen CS, Syljuåsen RG, Falck J, Schroeder T, Rönnstrand L, Khanna KK, Zhou BB, Bartek J, Lukas J. Chk1 regulates the S phase checkpoint by coupling the physiological turnover and ionizing radiation-induced accelerated proteolysis of Cdc25A. *Cancer Cell* 2003; **3:** 247-58.
34. Cho YJ, Liang P. Killin is a p53-regulated nuclear inhibitor of DNA synthesis. *Proc Natl Acad Sci USA* 2008; **105:** 5396-401.
35. Cho YJ, Liang P. S-phase-coupled apoptosis in tumor suppression. *Cell Mol Life Sci* 2008; **68:** 1883-96.
36. Demidova AR, Aau MY, Zhuang L, Yu Q. Dual regulation of Cdc25A by Chk1 and p53-ATF3 in DNA replication checkpoint control. *J Biol Chem* 2009; **284:** 4132-9.
37. Vigneron A, Cherier J, Barré B, Gamelin E, Coqueret O. The cell cycle inhibitor p21waf1 binds to the myc and cdc25A promoters upon DNA damage and induces transcriptional repression. *J Biol Chem* 2006; **281:** 34742-50.
38. Zhu Y, Alvarez C, Doll R, Kurata H, Schebye XM, Parry D, Lees E. Intra-S-phase checkpoint activation by direct CDK2 inhibition. *Mol Cell Biol* 2004; **24:** 6268-77.

39. Weininger J, Guichard M, Joly AM, Malaise EP, Lachet B. Radiosensitivity and growth parameters in vitro of three human melanoma cell strains. *Int J Radiat Biol* 1978; **34:** 285-90.

40. Fogh J, Bean MA, Brüggen J, Fogh H, Fogh JM, Hammar SP, et al. Comparison of a human tumor cell line before and after growth in the nude mouse. In: Fogh J, Giovanella B, editors. *The nude mouse in experimental and clinical research.* New York: Academic Press; 1978. p. 215-45.

41. Zölzer F, Hillebrandt S, Streffer C. Radiation induced G_1-block and p53 status in six human cell lines. *Radiother Oncol* 1995; **37:** 20-8.

42. Albino AP, Vidal MJ, McNutt NS, Shea CR, Prieto VG, Nanus DM, et al. Mutation and expression of the p53 gene in human malignant melanoma. *Melanoma Res* 1994; **4:** 35-45.

43. Böhnke A, Westphal F, Schmidt A, El-Awady RA, Dahm-Daphi J. Role of p53 mutations, protein function and DNA damage for the radiosensitivity of human tumour cells. *Int J Radiat Biol* 2004; **80:** 53-63.

44. Binder AB, Serafin AM, Bohm LJ. Abrogation of G(2)/M-phase block enhances the cytotoxicity of daunorubicin, melphalan and cisplatin in TP53 mutant human tumor cells. *Radiat Res* 2000; **154:** 640-9.

45. Stuschke M, Budach V, Sack H. Radioresponsiveness of human glioma, sarcoma, and breast cancer spheroids depends on tumour differentiation. *Int J Radiat Oncol Biol Phys* 1993; **27:** 627-36.

46. Wurm R, Ketel B, Schröder G, Sinn B, Schlenger L, Wolf G, et al. Strahlenempfindlichkeit nach kombination von bestrahlung und koffein. *Strahlenther Onkol* 1997; **173:** 614.

47. Zölzer F, Uma Devi P, Streffer C. Determination of potential doubling times in human melanoma cell cultures subjected to irradiation and/or hyperthermia by flow cytometry. *Radiat Res* 1994; **138:** 451-9.

48. Zölzer F, Streffer C, Pelzer T. Induction of quiescent S-phase cells by irradiation and/or hyperthermia. I. Time and dose dependence. *Int J Radiat Biol* 1993; **63:** 69-76.

49. Begg AC, Moonen L, Hofland I, Dessing M, Bartelink H. Human tumour cell kinetics using a monoclonal antibody against iododeoxyuridine: intratumour sampling variations. *Radiother Oncol* 1988; **11:** 337-47.

50. Zölzer F, Streffer C. G_2-phase delays after irradiation and/or heat treatment as assessed by two-parameter flow cytometry. *Radiat Res* 2001; **155:** 50-6.

51. Zhou J, Prives C. Replication of damaged DNA in vitro is blocked by p53. *Nucl Acid Res* 2003; **31:** 3881-92.

52. Mirzayans R, Aubin RA, Bosnich W, Blattner WA, Paterson MC. Abnormal pattern of post-γ-ray DNA replication in radioresistant fibroblast strains from affected members of a cancer-prone family with Li-Fraumeni syndrome. *Br J Cancer* 1995; **71:** 1221-30.

research article

Intercalated chemotherapy and erlotinib for advanced NSCLC: high proportion of complete remissions and prolonged progression-free survival among patients with EGFR activating mutations

Matjaz Zwitter[1,2], Karmen Stanic[1], Mirjana Rajer[1], Izidor Kern[3], Martina Vrankar[1], Natalija Edelbaher[4], Viljem Kovac[1]

[1] Institute of Oncology Ljubljana, Ljubljana, Slovenia
[2] Faculty of Medicine, University of Maribor, Maribor, Slovenia
[3] University Hospital for Pulmonary Diseases Golnik, Golnik, Slovenia
[4] Department of Pulmonary Medicine, University Clinical Centre Maribor, Maribor, Slovenia

Radiol Oncol 2014; 48(4): 361-368.

Received 25 August 2014
Accepted 8 September 2014

Correspondence to: Assist. Prof. Viljem Kovač, M.D, Ph.D., Institute of Oncology Ljubljana, Zaloska 2, 1000 Ljubljana, Slovenia.
Phone: +386 1 5879 522; Fax: +386 1 5879 400; E-mail address: vkovac@onko-i.si

Disclosure: No potential conflicts of interest were disclosed.

Background. Pharmaco-dynamic separation of cytotoxic and targeted drugs might avoid their mutual antagonistic effect in the treatment of advanced non-small cell lung cancer (NSCLC).

Patients and methods. Eligible patients were treatment-naive with stage IIIB or IV NSCLC. In addition, inclusion was limited to never-smokers or light smokers or, after 2010, to patients with activating epidermal growth-factor receptor (EGFR) mutations. Treatment started with 3-weekly cycles of gemcitabine and cisplatin on days 1, 2 and 4 and erlotinib on days 5 to 15. After 4 to 6 cycles, patients continued with erlotinib maintenance.

Results. Fifty-three patients were recruited into the trial: 24 prior to 2010 (of whom 9 were later found to be positive for EGFR mutations), and 29 EGFR mutation-positive patients recruited later. Unfavourable prognostic factors included stage IV disease (51 patients - 96%), performance status 2–3 (11 patients - 21%) and brain metastases (15 patients - 28%). Grade 4 toxicity included 2 cases of neutropenia and 4 thrombo-embolic events. The 15 EGFR negative patients had 33% objective response rate, median progression-free survival (PFS) 6.0 months and median survival 7.6 months. Among 38 EGFR positive patients, complete response (CR) or partial response (PR) were seen in 16 (42.1%) and 17 (44.7%) cases, respectively. PET-CT scanning was performed in 30 patients and confirmed CR and PR in 16 (53.3%) and 9 (30.0%) cases, respectively. Median PFS for EGFR mutated patients was 21.2 months and median survival was 32.5 months.

Conclusions. While patients with EGFR negative tumors do not benefit from addition of erlotinib, the intercalated schedule appears most promising for those with EGFR activating mutations.

Key words: Non-small cell lung cancer, EGFR activating mutations; gemcitabine; cisplatin; erlotinib; intercalated therapy; metabolic response

Introduction

Discovery of activating epidermal growth-factor receptor (EGFR) mutations as strong predictors of response to targeted therapy with tyrosine-kinase inhibitors (TKIs) has dramatically changed the therapeutic options for a subset of patients with non-small cell lung cancer (NSCLC). Several ran-

domised trials of first-line treatment have confirmed superiority of TKIs gefitinib, erlotinib or afatinib over platinum-based doublets[1-3] and led to registration of these drugs for first-line treatment of metastatic EGFR-mutated NSCLC.

After a median interval of 9 to 14 months, the majority of EGFR positive patients treated with TKIs experience a relapse. While cytotoxic drugs or a different TKI may lead to a second remission, long-term prognosis is unfavourable.

To date, there have been few successful attempts to prevent or delay the development of resistance to TKIs and to extend time to progression.[4] Four large randomized trials on non-selected population of patients with all histologic types showed overlapping curves of progression-free survival (PFS) and overall survival (OS) with chemotherapy and concomitant TKI, as compared to chemotherapy alone.[5-8] Due to this negative experience, few researchers believe that further attempts to combine the two classes of drugs are justified.

To address the issue of the optimal schedule for combination of chemotherapy with TKIs, we should understand why simultaneous therapy with both classes of drugs failed. An explanation may be in the fact that TKIs cause cell cycle arrest and accumulation of cells in G1, leading to their lesser sensitivity to cytotoxic drugs.[9,10] Mutual antagonistic effect of cytotoxic drugs and gefitinib has been confirmed on lung cancer cell lines harbouring sensitizing EGFR mutations.[11]

Pharmacodynamic separation of chemotherapy and of targeted drugs has been proposed for their synergistic activity. Observations on NSCLC cell lines showed that the sequence of cytotoxic drugs and TKIs is crucial for optimal result.[12] Compared to single-agent docetaxel, docetaxel followed by erlotinib resulted in significantly enhanced apoptosis. However, in the reverse sequence of erlotinib followed by docetaxel, a reduction of apoptosis was observed. An interval of 6 days without erlotinib was found to be sufficient to allow cells to re-enter the cycle and to restore their sensitivity to chemotherapy.[13]

Here we present experience from a Phase II clinical trial of intercalated therapy with chemotherapy and erlotinib for treatment-naive patients with advanced adenocarcinoma of the lung. The trial started in 2005 when testing for EGFR mutations was not yet available. To enrich the proportion of patients with tumors sensitive to erlotinib, the initial protocol limited inclusion to never-smokers or light smokers. In 2009, testing for EGFR became available. Analysis of archived biopsy samples for the initial cohort of 24 patients revealed a clear and statistically significant difference in response, PFS and OS in favour of EGFR positive patients. While EGFR wild type patients had response rate of 30% and median time to progression of 6 months, all patients with EGFR activating mutations responded to treatment, with 21.5 months as median time to progression.[14] An amendment to the protocol was therefore made and all additional patients had to be positive for activating mutations of EGFR.

The primary objectives of the trial were progression-free survival and response to treatment; secondary endpoints were treatment toxicity and overall survival. At the time of amendment, metabolic response was added as an additional secondary objective.

Patients and methods

Eligibility criteria

Patients eligible for the trial were chemo-naive with non-squamous lung carcinoma; had stage III B unsuitable for chemo-radiotherapy with curative intent or stage IV; had measurable disease; and had adequate parameters of hematological, liver, renal and cardiac function to receive platinum-based chemotherapy. Patients with asymptomatic untreated brain metastases, and patients in stable neurological status after treatment for brain metastases with surgery and/or radiotherapy were eligible.

In addition to the above criteria, the initial protocol limited inclusion to never-smokers or light smokers with a history of less than 10 pack-years. An amendment made in September 2010 replaced this limitation by confirmed activating mutations of EGFR.

All patients were fully informed and provided written consent to participate in the trial.

Initial diagnostics

Within four weeks prior to treatment, the extent of the disease was determined by chest X-ray and CT scanning of the chest, upper abdomen and brain. Since 2010, PET-CT scanning was included in the initial diagnostics and in evaluation of response to treatment.

EGFR status was assessed by EGFR mutation analysis. To test for EGFR mutations, genomic DNA was extracted from formalin-fixed, paraffin-embedded tumor tissue sections. Quantification of extracted DNA was done on Qubit Fluorometer

(Invitrogen, Carlsbad, USA). To detect EGFR gene activating mutations, the first 10 patients were tested with TheraScreen EGFR29 Mutation Kit (DxS Diagnostics, Qiagen, Manchester, UK) and afterwards withCobas 4800 (Roche Molecular Systems, Pleasanton, USA).

Treatment

The treatment started with four to six cycles of intercalated chemotherapy and erlotinib according to the following schedule:

Day 1: gemcitabine 1250 mg/m^2

Day 2: cisplatin 75 mg/m^2, with appropriate hydration and antiemetics

Day 4: gemcitabine 1250 mg/m^2

Days 5-15: erlotinib 150 mg daily

The cycle was repeated on day 22.

Standard criteria for dose reduction, delay or omission of cytotoxic drugs were observed. Cisplatin was replaced by carboplatin at AUC 5 in case of grade 2-3 nausea or vomiting or in case of grade 1 nephrotoxicity. The intercalated phase of treatment was terminated for patients with any grade 4 hematological toxicity, grade ≥2 nephrotoxicity or any other grade ≥3 non-hematological toxicity, in which case the treatment would continue with maintenance erlotinib.

Immediately after the last cycle, patients continued with maintenance erlotinib 150 mg daily until progression or unacceptable toxicity. In case of grade ≥2 skin toxicity, local antibiotics and/or vitamin K1 cream were applied[15] and reduction of the dose of erlotinib was considered.

Response, time of progression, and follow-up

Definitions of complete response (CR), partial response (PR), stable disease (SD) and progression followed the RECIST criteria.[16] The first evaluation was done during the third cycle, with confirmation of response during the 5th cycle.

Metabolic response to treatment was an additional secondary endpoint. PET-CT scanning was performed prior to treatment and repeated at 6 months after commencing the treatment. Control PET examination included all initial sites of disease, with measurement of corresponding maximal standard uptake value (SUV). Appearance of any new lesion or increase in SUV of a previously known lesion together with ≥ 20% increase in its size was declared as progression. For partial remission, all previously known lesions should either disappear or show at least a 50% reduction of uptake. Patients between progression and partial response were classified as stable disease. Finally, normalisation of PET-CT and disappearance of all lesions with initially increased SUV was required to declare a CR.[17,18]

Statistical planning

In the initial study protocol, the sample size was calculated on the basis of expected median PFS of 10 months with the intercalated schedule, to be compared with 6 months as PFS for the combination of gemcitabine and cisplatin. Planning for the sample size was reviewed in 2010 when TKIs became the new standard first-line treatment for EGFR mutated patients. Taking 20 months as the expected PFS for the intercalated regimen, 35 patients with EGFR mutations were needed for a 80% power to confirm, at the one-sided 0.10 significance level, a difference to the reported 12 months as median PFS for monotherapy with erlotinib.[19]

Ethical considerations

The investigators strictly followed the Helsinki Declaration and the European Council Convention on Protection of Human Rights in Bio-Medicine (Oviedo 1997). The protocol was approved by the Institutional Review Board Committee (Institute of Oncology, Ljubljana) and by the National Committee for Medical Ethics. The trial was registered with the European Medicines Agency, EudraCT Number: 2010-023362-44.

Results

The first cohort of 24 patients selected on the basis of histologic type and smoking history was recruited between September 2005 and July 2010. Among these patients, 9 were later found to be positive for EGFR mutations. After that date and until October 2013, additional 29 patients with EGFR activating mutations entered the trial.

The series includes 28 women and 25 men. All patients were Caucasians. While the majority of patients were in fair general condition, 8 patients had performance status (PS) 2 and additional 3 patients had PS 3. Two patients had stage IIIB unsuitable for treatment with radiotherapy with

TABLE 1. Demographics, prognostic factors, extent of disease and type of EGFR mutations

		All 53 patients	EGFR mutated 38 patients	EGFR wild type 15 patients [a]
AGE	median	57	61	45
	range	25 – 74	37 – 74	25 – 73
GENDER	male	25	17	8
	female	28	21	7
SMOKING	never smoker	33	24	9
	light smoker (< 10 pack years)	11	5	6
	smoker	9	9	0
PERFORMANCE STATUS	ECOG PS 0	12	10	2
	1	30	20	10
	2	8	6	2
	3	3	2	1
STAGE	III B	2	1	1
	IV	51	37	14
SITE(S) OF METASTATIC DISEASE	bone	35	24	11
	distant lung	25	18	7
	pleura and pericardium	24	16	8
	liver and/or suprarenal	17	11	6
	brain (after whole-brain radiotherapy)	15	13 [b]	2
	distant lymph nodes and/or soft tissues	14	10	4
NUMBER OF METASTATIC SITES	1	14	10	4
	2	17	14	3
	3 or more	22	14	8
TYPE OF EGFR MUTATION	Exon 19 deletion [c]	25	25	n. a.
	G719X [c]	4	4	n. a.
	L858R	9	9	n. a.
	S 768i	1	1	n. a.

EGFR = epidermal growth factor receptor
[a] Includes 3 patients for whom ERGF status could not be determined
[b] Includes 1 patient with asymptomatic untreated multiple brain metastases
[c] One patient had deletions and G719X mutation

curative intent; all other patients had stage IV disease. Demographics, sites of metastatic disease and types of EGFR mutations are presented in Table 1.

Treatment delivery and acute toxicity

The actual number of cycles of intercalated therapy was from 1 to 6 (median: 4 cycles).

During the induction phase of the treatment, 6 patients had grade 4 toxicity: two had grade 4 neutropenia and 4 developed deep vein thrombosis, in 3 cases followed by pulmonary embolisms. These 6 patients continued treatment with TKI maintenance. Due to grade 2 – 3 nausea, vomiting or asthenia, additional 4 patients received only 3 cycles of intercalated therapy and continued with monotherapy with erlotinib. During the maintenance phase of the treatment, the only serious and common side effect was skin toxicity, with grades 2 and 3 in 16 and 14 patients, respectively (Table 2).

Response to treatment, progression-free survival, second-line treatment and survival

All patients were evaluable for response and no patient has been lost to follow-up. Due to significant differences between EGFR wild-type and mutated disease, these two groups of patients will be presented separately.

TABLE 2. Treatment toxicity

		All 53 patients	EGFR mutated 38 patients	EGFR wild type 15 patients [a]
	Grade	INDUCTION/ MAINTENANCE	INDUCTION/ MAINTENANCE [b]	INDUCTION/ MAINTENANCE [c]
Anemia	2	14/2	11/2	3/0
	3	1/0	1/0	
Neutropenia	2	15/0	12/0	3/0
	3	5/0	4/0	1/0
	4	2/0	2/0	
Thrombocytopenia	2	4/0	3/0	1/0
	3	2/0	2/0	
Nephotoxicity	2	2/0	1/0	1/0
Skin toxicity [d]	2	11/16	8/11	3/5
	3	4/14	3/13	1/1
Nausea/vomiting	2	6/0	4/0	2/0
Asthenia	2	2/2	1/2	1/0
Thrombo-embolic events	2	1/0	1/0	
	4	4/0	4/0	
Diarrhea	2	5/2	3/1	2/1

EGFR = epidermal growth factor receptor
[a] Includes 3 patients for whom EGFR status could not be determined
[b] All 38 patients continued with maintenance erlotinib
[c] 11 patients continued with maintenance erlotinib
[d] Leading to reduced daily dose of erlotinib to 100 mg (14 patients), 75 mg (6 patients) or 50 mg (5 patients)

EGFR wild-type or unknown (15 patients)

Among patients with EGFR wild-type tumors, 5 patients had PR, 8 had minimal response or stable disease and 2 had progression. Remissions were short-lived with median PFS 6.0 months (95% confidence interval [CI] 3.9 – 8.1). The most frequent sites of progression were intrathoracic disease (11 patients), bone (5) or brain (3). Eight patients did not receive further systemic treatment; other options were continuation with erlotinib (5 patients) or chemotherapy (2). Median survival was 7.6 months (95% CI 5.0 – 10.2).

EGFR activating mutations (38 patients)

Radiologic assessment confirmed CR in 16 (42.1%) and PR in 17 (44.7%), for an overall response of 86.8%. Of the remaining five patients, four patients had minimal response or stable disease, and one had progression. Waterfall plot with the best response is shown in Figure 1.

PET-CT at baseline and after 6 months was performed in 30 patients. Complete remission was documented in 16 patients (53.3%) and PR in 9 patients (40.7%).

Median PFS for all EGFR mutant patients was 21.2 months (95% CI 15.3 – 27.1 months) (Figure 2). No significant difference in PFS was seen when comparing patients with exon 19 deletions to those with other mutations (data not shown).

The most frequent sites of progression were bone (10), lung (10), brain (6), liver (3), or distant lymph nodes (3). Two patients with brain metastases and one patient with diffuse progression in the liver did not receive additional systemic treatment. In 17 patients, treatment with erlotinib continued beyond progression. Other choices were gefitinib or afatinib (8 patients) or different combinations of cytotoxic chemotherapy (6 patients); more than one treatment option per patient may apply.

Median survival for patients with EGFR activating mutations was 32.5 months (95% CI 21.2 – 43.7). Patients with initial performance status 0-1 had longer OS, when compared to those with PS 2-3 (34.8 months, 95% CI 22.0 – 47.7 *vs* 21.1 months, 95% CI 9.1 – 33.1; p = 0.08). At the close-out date (April 22, 2014), 20 patients are alive, of whom 10 are still in complete remission and continue with maintenance erlotinib.

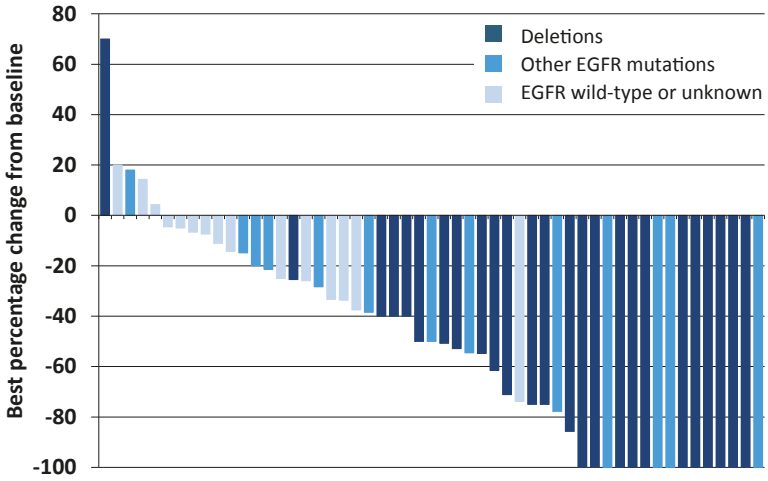

FIGURE 1. Waterfall plot of best percentage change in tumor size (sum of longest diameters).

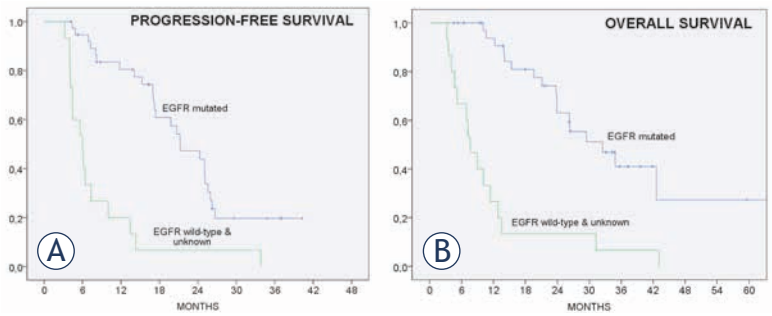

FIGURE 2. Progression-free and overall survival of treated patients (n = 53).

A Progression-free survival for epidermal growth-factor receptor (EGFR) wild-type patients (median 6.0 months, 95% confidence interval [CI] 3.9 – 8.1) and for patients with EGFR activating mutations (median 21.2 months, 95% CI 15.3 – 27.1)

B Overall survival for EGFR wild-type patients (median 7.6 months, 95% CI 5.0 – 10.2) and for patients with EGFR activating mutations (median 32.5 months, 95% CI 21.2 – 43.7).

Discussion

The concept of pharmacodynamic separation of cytotoxic drugs and TKIs for patients with advanced NSCLC has been tested in several clinical trials. Six trials enrolled patients in progression after chemotherapy[20-24] or after TKI[25], with no convincing evidence regarding the advantage of intercalated therapy over conventional choices of second-line therapy. This negative experience is not unexpected: it is reasonable to assume that patients in progression after prior systemic therapy are less likely to respond to a schedule including the category of drugs to which resistance already developed.

Among trials on treatment-naive patients, the closest resemblance to our approach was a US-UK trial of paclitaxel and carboplatin on day 1 and erlotinib on days 2 to 15 of a 3-weekly cycle in the intercalated treatment arm, compared to monotherapy with erlotinib.[26] Yet, this trial recruited only 15 patients with EGFR activating mutations of whom only 6 were randomised to the intercalated treatment, a figure too small for any meaningful conclusion.

FASTACT[27] and FASTACT 2[28] trials demonstrated that erlotinib offers no benefit over chemotherapy alone for EGFR wild-type patients, while those with activating mutations clearly benefit from addition of erlotinib. In hindsight, the design of these two trials was suboptimal for two reasons. First, in the intercalated schedule, timing of erlotinib on days 15 to 28 of a 4-weekly cycle is – in our opinion – questionable. To avoid TKI-induced cell cycle arrest in G1 of the mitotic cycle resulting in putative chemoresistance, »wash-out« period for TKI should be before, rather than after the next application of cytotoxic drugs. The second concern is the choice of chemotherapy alone for the control group. While chemotherapy was indeed the standard treatment for advanced NSCLC some years ago, we now have clear evidence of superiority of TKIs for EGFR mutated patients. Thus, superior survival in the intercalated arm is not unexpected and cannot provide an answer to its potential advantage over treatment with TKI alone.

We would now like to offer comments on our trial with selection of patients, schedule, side effects, response to treatment and future perspectives.

Patients recruited in our trial were all chemo-naive. Factors predicting sensitivity to TKIs were considered in defining the inclusion criteria: smoking status for the first period and EGFR mutations for the second period of recruitment. In other aspects, the population of patients may be considered as prognostically unfavourable, with inclusion of 37% of patients in PS 2-3, 96 % in stage IV, and 74% with 2 or more metastatic sites. In addition, 28% of patients had brain metastases, a frequent metastatic site in EGFR mutated NSCLC.[29] All our patients were Caucasians. These factors should be considered when comparing the experience to other similar trials.

In the cytotoxic part of our schedule, gemcitabine and cisplatin were applied on days 1, 2 and 4. Such a compressed schedule was chosen in order to gain four more days for erlotinib. According to a report from Hangzhou, China, a similar platin-based doublet with gemcitabine on days 1 and 5 has been found active and well tolerated.[30] Myelotoxicity after chemotherapy and skin toxicity in the period of maintenance treatment were expected and man-

ageable. Due to 4 cases of grade 4 thrombo-embolic events, routine thromboprophylaxis with low-molecular weight heparin is recommended.

Regarding efficacy, two very distinct groups emerge. Although the number of EGFR wild-type patients was small, it is clear that the objective response rate (33%), median PFS (6.0 months) and median OS (7.6 months) are not superior to the experience with platinum-based doublets alone. On the other hand, the intercalated regimen for EGFR mutated patients is very promising. In a population of patients including those with poor prognostic factors, high proportion of complete or partial responses (42.1% and 44.7%, respectively), long median PFS (21.2 months) and OS (32.5 months) were recorded – figures which are well above most results reported so far for Caucasian patients. According to several clinical studies and to a survey of routine clinical practice, overall response rate to TKIs as monotherapy is around 70% with less than 10% complete remissions, and median PFS is between 9 and 14 months.[19,31]

Two explanations are offered for the high efficacy of the intercalated therapy. First, this schedule combines three drugs with proven activity, different mechanisms of action, and different toxicity profiles and at the same time applies the principle of pharmaco-dynamic separation to avoid their mutual antagonistic effect. Second, incorporation of erlotinib into the chemotherapy schedule fills the gaps between individual applications of cytotoxic drugs and thus prevents repopulation of the tumor which may be among the decisive factors for failure of standard chemotherapy schedules for solid tumor.[32]

In conclusions, addition of erlotinib to the doublet of gemcitabine and cisplatin in an intercalated schedule was of no benefit to EGFR wild-type patients. On the other hand, the experience for patients with EGFR mutated advanced NSCLC is very promising. The real value of the concept of intercalated therapy will be established in a randomised trial against monotherapy with a TKI as the current standard of treatment for patients with advanced EGFR mutated NSCLC.

Acknowledgments

Supported by grant 2010-I/761 from The Ministry of Science, Education and Sport, Republic of Slovenia.

The authors thank all patients and their families for their cooperation, nurses from the Outpatient Department and Day Hospital for their help in conducting the trial and to dr. Minka Urbančič for valuable comments and for language editing.

References

1. Mok TS, Wu YL, Thongprasert S, Yang CH, Chu DT, Saijo N, et al. Gefitinib or carboplatin-paclitaxel in pulmonary adenocarcinoma. *N Engl J Med* 2009; **361:** 947-57.
2. Rosell R, Moran T, Queralt C, Porta R, Cardenal F, Camps C, et al. Screening for epidermal growth factor receptor mutations in lung cancer. *N Engl J Med* 2009; **361:** 958-67.
3. Sequist LV, Yang JC-H, Yamamoto N, O'Byrne K, Hirsh V, Mok T, et al. Phase III study of afatinib or cisplatin plus pemetrexed in patients with metastatic lung adenocarcinoma with EGFR mutations. *J Clin Oncol* 2013; **31:** 3327-34.
4. Ratti M, Tomasello G. Emerging combination therapies to overcome resistance in EGFR-driven tumors. *Anti-Cancer Drugs* 2014; **25:** 127-39.
5. Giaccone G, Herbst RS, Manegold C, Scagliotti G, Rosell R, Miller V, et al. Gefitinib in combination with gemcitabine and cisplatin in advanced non-small-cell lung cancer: a phase III trial – INTACT 1. *J Clin Oncol* 2004; **22:** 777-84.
6. Herbst RS, Giaccone G, Schiller JH, Natale RB, Miller V, Manegold C, et al. Gefitinib in combination with paclitaxel and carboplatin in advanced non-small-cell lung cancer: a phase III trial – INTACT 2. *J Clin Oncol* 2004; **22:** 785-94.
7. Herbst RS, Prager D, Herman R, Fehrenbacher L, Johnson BE, Sandler A, et al. TRIBUTE: a phase III trial of erlotinib hydrochloride (OSI-774) combined with carboplatin and paclitaxel chemotherapy in advanced non-small-cell lung cancer. *J Clin Oncol* 2005; **23:** 5892-9.
8. Gatzemeier U, Pluzanska A, Szczesna A, Kaukel E, Roubec J, De Rosa F, et al. Phase III study of erlotinib in combination with cisplatin and gemcitabine in advanced non–small-cell lung cancer: The Tarceva Lung Cancer Investigation Trial. *J Clin Oncol* 2007; **25:** 1545-52.
9. Gandara DR, Gumerlock PH. Epidermal growth factor receptor tyrosine kinase inhibitors plus chemotherapy: case closed or is the jury still out? *J Clin Oncol* 2005; **23:** 5856-8.
10. Reck M. Beyond the TRIBUTE trial: integrating HER1/EGFR tyrosine kinase inhibitors with chemotherapy in advanced NSCLC. *Future Oncol* 2006; **2:** 47-51.
11. Tsai CM, Chen JT, Chiu CH, Lai CL, Hsiao SY, Chang KT. Combined epidermal growth factor receptor (EGFR)-tyrosine kinase inhibitor and chemotherapy in non-small-cell lung cancer: chemo-refractoriness of cells harboring sensitizing-EGFR mutations in the presence of gefitinib. *Lung Cancer* 2013; **82:** 305-12.
12. Mahaffey CM, Davies AM, Lara PN Jr, Pryde B, Holland W, Mack PC, et al. Schedule-dependent apoptosis in K-ras mutant non-small-cell lung cancer cell lines treated with docetaxel and erlotinib: rationale for pharmacodynamic separation. *Clin Lung Cancer* 2007; **8:** 548-53.
13. Davies AM, Ho C, Lara PN Jr, Mack P, Gumerlock PH, Gandara DR. Pharmacodynamic separation of epidermal growth factor receptor tyrosine kinase inhibitors and chemotherapy in non-small-cell lung cancer. *Clin Lung Cancer* 2006; **7:** 385-8.
14. Zwitter M, Rajer M, Kovac V, Kern I, Vrankar M, Smrdel U. Intermittent chemotherapy and erlotinib for non-smokers or light smokers with advanced adenocarcinoma of the lung: A phase II clinical trial. *J Biomed Biotechnol* 2011; **2011:** 185646.
15. Ocvirk J, Heeger S, McCloud P, Hofheinz RD. A review of the treatment options for skin rash induced by EGFR-targeted therapies: Evidence from randomized clinical trials and a meta-analysis. *Radiol Oncol* 2013; **47:** 166-75.
16. Therasse P, Arbuck SG, Eisenhauer EA, Wanders J, Kaplan RS, Rubinstein L, et al. New guidelines to evaluate the response to treatment in solid tumors. European Organization for Research and Treatment of Cancer, National Cancer Institute of the United States, National Cancer Institute of Canada. *J Natl Cancer Inst* 2000; **92:** 205-16.

17. Young H, Baum R, Cremerius U, Herholz K, Hoekstra O, Lammertsma AA, et al. Measurement of clinical and subclinical tumour response using [^{18}F]-fluorodeoxyglucose and positron emission tomography: review and 1999 EORTC recommendations. *Eur J Cancer* 1999; **35:** 1773-82.

18. Skoura E, Datseris IE, Platis I, Oikonomopoulos G, Syrigos KN. Role of positron emission tomography in the early prediction of response to chemotherapy in patients with non–small-cell lung cancer. *Clin Lung Cancer* 2012; **13:** 181-7.

19. Rosell R, Carcereny E, Gervais R, Vergnenegre A, Massuti B, Felip E, et al. Erlotinib versus standard chemotherapy as first-line treatment for European patients with advanced EGFR mutation-positive non-small-cell lung cancer (EURTAC): a multicentre, open-label, randomised phase 3 trial. *Lancet Oncol* 2012; **13:** 239-46.

20. Aerts JG, Codrington H, Lankheet NAG, Burgers S, Biesma B, Dingemans AM, et al. A randomized phase II study comparing erlotinib versus erlotinib with alternating chemotherapy in relapsed non-small-cell lung cancer patients: The NVALT-10 study. *Ann Oncol* 2013; **24:** 2860-5.

21. Lee DH, Lee JS, Kim SW, Rodrigues-Pereira J, Han B, Song XQ, et al. Three-arm randomised controlled phase 2 study comparing pemetrexed and erlotinib to either pemetrexed or erlotinib alone as second-line treatment for never-smokers with non-squamous non-small cell lung cancer. *Eur J Cancer* 2013; **49:** 3111-21.

22. Li T, Piperdi B, Walsh WV, Kim M, Gucalp R, Haigentz M, et al. Randomized phase II study of pharmacodynamic separation (PDS) of pemetrexed (Pem) and erlotinib (Erl) versus pem alone in patients (pts) with advanced non-small cell lung cancer (NSCLC). [Abstract]. *J Clin Oncol* 2013; **31(15 Suppl):** No. 8097.

23. Minami S, Kijima T, Hamaguchi M, Nakatani T, Koba T, Takahashi R, et al. Phase II study of pemetrexed plus intermittent erlotinib combination therapy for pretreated advanced non-squamous non-small cell lung cancer with documentation of epidermal growth factor receptor mutation status. *Lung Cancer* 2013; **82:** 271-5.

24. Sangha R, Davies AM, Lara PN, Mack PC, Beckett LA, Hesketh PJ, et al. Intercalated erlotinib-docetaxel dosing schedules designed to achieve pharmacodynamic separation: results of a phase I/II trial. *J Thorac Oncol* 2011; **6:** 2112-9.

25. Yoshimura N, Okishio K, Mitsuoka S, Kimura T, Kawaguchi T, Kobayashi M, et al. Prospective assessment of continuation of erlotinib or gefitinib in patients with acquired resistance to erlotinib or gefitinib followed by the addition of pemetrexed. *J Thorac Oncol* 2013; **8:** 96-101.

26. Hirsch FR, Kabbinavar F, Eisen T, Martins R, Schnell FM, Dziadziuszko R, et al. A randomized, phase II, biomarker-selected study comparing erlotinib to erlotinib intercalated with chemotherapy in first-line therapy for advanced non-small-cell lung cancer. *J Clin Oncol* 2011; **29:** 3567-73.

27. Mok TS, Wu YL, Yu CJ, Zhou C, Chen YM, Zhang L, et al. Randomized, placebo-controlled, phase II study of sequential erlotinib and chemotherapy as first-line treatment for advanced non-small-cell lung cancer. *J Clin Oncol* 2009; **27:** 5080-7.

28. Wu L, Lee JS, Thongprasert S, Yu CJ, Zhang L, Ladrera G, et al. Intercalated combination of chemotherapy and erlotinib for patients with advanced stage non-small-cell lung cancer (FASTACT 2): a randomised, double blind trial. *Lancet Oncol* 2013; **14:** 777-86.

29. Stanic K, Zwitter M, Hitij NT, Kern I, Sadikov A, Cufer T. Brain metastases in lung adenocarcinoma: impact of EGFR mutation status on incidence and survival. *Radiol Oncol* 2014; **48:** 173-83.

30. Miao L, Fan Y, Huang Z, Lin N, Luo L, Yu H. [Phase II trial of improved regimen with gemcitabine in patients with advanced non-small cell lung cancer]. [Chinese]. *Zhongguo Fei Ai Za Zhi* 2012; **15:** 1-5.

31. Douillard J-Y, Ostoros G, Cobo M, Ciuleanu T, McCormack R, Webster A, et al. First-line gefitinib in Caucasian *EGFR* mutation-positive NSCLC patients: a phase-IV, open-label, single-arm study. *Br J Cancer* 2014; **110:** 55-62.

32. Davis AJ, Tannock JF. Repopulation of tumour cells between cycles of chemotherapy: a neglected factor. *Lancet Oncol* 2000; **1:** 86-93.

research article

Induction gemcitabine in standard dose or prolonged low-dose with cisplatin followed by concurrent radiochemotherapy in locally advanced non-small cell lung cancer: a randomized phase II clinical trial

Martina Vrankar[1], Matjaz Zwitter[1,2], Tanja Bavcar[3], Ana Milic[1], Viljem Kovac[1]

[1] Institute of Oncology Ljubljana, Ljubljana, Slovenia
[2] Faculty of Medicine, University of Maribor, Slovenia
[3] Clinical Radiology Institute, University Medical Centre Ljubljana, Slovenia

Radiol Oncol 2014; 48(4): 369-380.

Received 14 March 2014
Accepted 18 April 2014

Crrespondence to: Martina Vrankar, M.D., Institute of Oncology Ljubljana, Zaloška 2, 1000 Ljubljana, Slovenia. Phone: +386 1 5879 629; Fax: +386 1 5879 400; E-mail: mvrankar@onko-i.si

Disclosure: No potential conflicts of interest were disclosed.

Background. The optimal combination of chemotherapy with radiation therapy for treatment locally advanced non-small cell lung cancer (NSCLC) remains an open issue. This randomized phase II study compared gemcitabine in two different schedules and cisplatin - as induction chemotherapy, followed by radiation therapy concurrent with cisplatin and etoposid.

Patients and methods. Eligible patients had microscopically confirmed inoperable non-metastatic non-small cell lung cancer; fulfilled the standard criteria for platin-based chemotherapy; and signed informed consent. Patients were treated with 3 cycles of induction chemotherapy with gemcitabine and cisplatin. Two different aplications of gemcitabine were compared: patients in arm A received gemcitabine at 1250 mg/m^2 in a standard half hour i.v. infusion on days 1 and 8; patients in arm B received gemcitabine at 250 mg/m^2 in prolonged 6-hours i.v. infusion on days 1 and 8. In both arms, cisplatin 75 mg/m^2 on day 2 was administered. All patients continued treatment with radiation therapy with 60-66 Gy concurrent with cisplatin 50 mg/m^2 on days 1, 8, 29 and 36 and etoposid 50 mg/m^2 on days 1-5 and 29-33. The primary endpoint was response rate (RR) after induction chemotherapy; secondary endpoints were toxicity, progression-free survival (PFS) and overall survival (OS).

Results. From September 2005 to November 2010, 106 patients were recruited to this study. No statistically signiffi-cant differences were found in RR after induction chemotherapy between the two arms (48.1% and 57.4%, p = 0.34). Toxicity profile was comparable and mild with grade 3/4 neutropenia as primary toxicity in both arms. One patient in arm B suffered from acute peripheral ischemia grade 4 and an amputation of lower limb was needed. With a median follow-up of 69.3 months, progression-free survival and median survival in arm A were 15.7 and 24.8 months compared to 18.9 and 28.6 months in arm B. The figures for 1- and 3-year overall survival were 73.1% and 30.8% in arm A, and 81.5 % and 44.4% in arm B, respectively.

Conclusions. Among the two cisplatin-based doublets of induction chemotherapy for inoperable NSCLC, both schedules of gemcitabine have a comparable toxicity profile. Figures for RR, PFS and OS are among the best reported in current literature. While there is a trend towards better efficacy of the treament with prolonged infusion of gemcit-abine, the difference between the two arms did not reach statistical significance.

Key words: induction chemotherapy; gemcitabine; non-small cell lung cancer; radiation therapy; concurrent chem-oradiation; randomized clinical trial.

Introduction

Lung cancer remains the most common cause of cancer related deaths in the world. In Europe, approximately 410.000 lung cancer patients were diagnosed and 353.000 individuals were estimated to die from lung cancer in 2012.[1,2] Non-small cell lung cancer (NSCLC) accounts for approximately 85% of all primary lung cancers, of whom about one fourth have locally advanced disease.[3] The standard treatment for patients with surgically unresectable, locally advanced NSCLC includes concurrent radiation therapy and chemotherapy.[4,5] According to a meta-analysis by Auperin *et al.*, concurrent regimens are superior to sequential ones in terms of locoregional control and overal survival.[5,6] Long-term survival rates with these approaches are only in the order of 15%. Considering the fact that with concurrent schedules, the chemotherapeutic agents enhance the tumor´s radiosensitivity and thus improve the local control but have little if any systemic effect, improvement in overall survival can be achieved through better control of distant micrometastases.

Applied either sequentially or in a concurrent schedule, platinum-based chemotherapy with radical radiation therapy is the standard of care for locally advanced NSCLC as well as for small cell lung cancer (SCLC).[7,8] However, the optimal drugs, schedule, sequence and doses of chemotherapy have not been adequately defined.

Gemcitabine is among the standard drugs for the treatment of a variety of tumors, including NSCLC.[9,10] For the usual 30-minute infusion (dose rate 40-60mg/m^2/min), the maximum tolerated dose (MTD) is 1500 mg/m^2 or even higher.[11,12] With infusion lasting for 3, 6 or 24 hours, MTD significantlly falls to 450, 250 and 180 mg/m^2, respectively.[13-15] This phenomenon can be explained by saturation of deoxycytidin kinase, an encyme needed for conversion of gemcitabine into its active form gemcitabine-triphosphate. After a short infusion of a relatively high dose gemcitabine, most of the drug remains unmetabolized. By contrast, prolonged infusion leads to higher intracellular concentration of the active metabolite.[16] Consequently, a lower dose is needed for a comparable activity.

Several phase I and II clinical trials have shown significant antitumor activity of gemcitabine in low-dose in long infusion. The spectrum of diseases includes cancers of the lung, breast, pancreas, gallbladder, bladder, sarcomas, mesotheliomas, refractory leukemias, and refractory Hodgkin´s disease.[14,17] Regarding lung cancer, our group reported favorable experience with gemcitabine in long infusion in combination with cisplatin for metastatic NSCLC.[9,10,18]

After a favorable experience with gemcitabine at a low-dose in prolonged infusion for advanced NSCLC, we here present a phase II randomised trial of induction chemotherapy comparing gemcitabine in two different schedules of application in combination with cisplatin followed by concurrent radiochemotherapy.

Patients and methods

Eligibility criteria

Patients with medically or surgically inoperable citologically or histologically confirmed NSCLC or locall reccurence after previous surgical treatment were eligible for the trial. Patients were required to be 18 years of age or older, have a performance status (PS) of 0-1 based on the Eastern Cooperative Oncology Group, with no evidence of metastatic disease, with no previous chemotherapy or radiation therapy for NSCLC, with no other malignant disease for last three years (except basal cell carcinoma of the skin, carcinoma *in situ* of the cervix or carcinoma of larynx T1N0M0) and have adequate hematological, kidney and liver function. Patients were ineligible if they had malignant pleural or pericardial effusions, evidence of manifest cardial or nevrologic disease or evidence of active infection. All patients were discussed on multidisciplinary thoracic oncology tumor board and considered inoperable due to tumor extent, limited pulmonary function or other comorbidity.

Radiological assessment included chest x-ray, CT scan of the torax, abdomen and brain and technetium-99 bone scan, or FDG-PET-CT examination when available. All studies, including a complete medical history and physical examination, were completed within 2 weeks before study enrollment.

All patients were fully informed and signed a consent to participate in the trial.

The protocol was approved by the Institutional Review Board (Institute of Oncology Ljubljana) and by the National Committee for Medical Ethics, Ministry of Health, Republic of Slovenia.

Treatment

Patients were randomly assigned to one of the two treatment arms. All patients were treated with three 21-day cycles of induction chemotherapy. We compared two different methods of applications

and dosage of gemcitabine, administered as induction chemotherapy: patients in arm A received 1250 mg/m^2 in standard half hour i.v. infusion on days 1 and 8; patients in arm B received gemcitabine 250 mg/m^2 in prolonged 6-hours i.v.infusion on days 1 and 8. In the both arms, cisplatin 75 mg/m^2 on day 2 intravenously was administered.

Within 13–22 days after the last aplication of chemotherapy, all patients continued treatment with radiation therapy concurrent with cisplatin 50 mg/m^2 on days 1, 8, 29 and 36 and etoposide 50 mg/m^2 on days 1–5 and 29–33.

Radiation therapy was administered with a linear accelerator photon beam of 5–10 MV in 2 Gy fractions 5 times weekly to a total dose of 60-66 Gy. Three-dimensional CT-based conformal radiation therapy was used and treatment planning was based on CT scans obtained under normal quiet breathing. The tumor volumes: gross tumor volume (GTV), clinical target volume (CTV), planning target volume (PTV) and organs at risk were delineated. GTV encompassed the primary tumor before chemotherapy and involved lymph nodes determined from diagnostic CT or FDG-PET-CT. CTV was defined as the GTV plus the margin for microscopic extension of the tumor (5 mm) and PTV was defined as CTV plus an additional margin for organ and patient movement (10-15 mm). No elective nodal volumes were included. The dose was prescribed to the isocenter. Tissue heterogeneity correction was performed and the superposition dose calculation algorithm was used. Normal tissue tolerance criteria for the spinal cord, esophagus and lung were specified accordance to Emami normal tissue tolerance tables. Dosimetric parameters were generated from the dose-volume histogram (DVH).

Toxicities were assessed according to Common Terminology Criteria for Adverse Events (CTCAE) version 3.0. The protocol contained guidance for adjustments to adverse events. However, induction chemotherapy should follow schedule with dose reduction or omiting drug application as indicated in protocol. Radiotherapy interruptions or delay were permited for grade 3/4 adverse events.

Treatment assessment

After induction chemotherapy, response of the tumor was assessed by comparing the pre-treatment CT scan with the CT scan of the torax before starting radiation therapy. The response was evaluated according to Response Evaluation Criteria in Solid Tumor (RECIST) criteria version 1.0. In addition, volumetric measurement of tumor on CT scans before and after induction chemotherapy was performed. All three dimensions were measured by a radiologist blinded regarding treatment allocation. The volume was calculated as cuboid shape for each tumor before and after induction chemotherapy, and the percent of response was calculated.

After completion of treatment, patients were evaluated at 6 weeks and every third month thereafter. In addition to clinical exam, chest x-ray and blood tests which were done during every follow-up visit, CT scan of the torax was performed at 5 months after treatment and every year thereafter or earlier if clinically indicated.

Statistical analysis

The primary endpoint of this prospective randomized open-label, phase II trial, was response rate (RR) after induction chemotherapy, and secondary endpoints included progression free survival (PFS), overall survival (OS) and safety profile.

PFS was defined as the time from the beginning of treatment to disease progresion or death. OS was calculated as the time from the start of the treatment to death from any cause. Censoring was defined as the time from the beginning of treatment to the last contact with the patient and for alive patients, as the time from the beginning of treatment to the end of follow-up (October 2013).

Overall and progression-free survival curves were estmated by using Kaplan-Meier method and log-rank test. Chi-square test was used to compare distribution of discrete variable values between the two arms. Mann-Whitney U test was used to compare continuous variables. Z-test for the equality between two proportions was used to evaluate the difference between proportions of patients between arms. A p-value less than 0.05 was considered statistically significant.

Results

Patient characteristics

Between September 2005 and November 2010, a total of 107 patients were randomly assigned to the arm A (53 patients) or the arm B (54 patients). One patient in group A was ineligible due to grade 3 cardial failure immediately after starting the infusion of first application of chemotherapy, so she continued treatment with radiation therapy only. Patient demographics and disease characteristics are listed in Table 1.

TABLE 1. Characteristics of patients in each treatment arm

	ARM A (n = 52) Standard gem – cis	ARM B (n = 54) Low-dose gem - cis	TOTAL	P
Gender				0.42
Male	39	44	83	
Female	13	10	23	
Age				0.41
Median	58	57	57	
Range	42–72	30–77	30–77	
ECOG PS				0.79
0	44	47	91	
1	8	7	15	
Weight loss				0.20
≤ 5 %	41	47	88	
> 5 %	11	6	17	
Histology				0.18
Squamous-cell carcinoma	35	27	62	
Adenocarcinoma	7	16	23	
Large cell carcinoma	4	3	7	
Other& Unspecified	6	8	14	
Stage				0.15
IA	1	0	1	
IB	1	0	1	
IIB	1	2	3	
IIIA	19	31	50	
IIIB	30	21	51	
Reason for inoperability				0.36
Extent of disease	49	52	101	
Functional	3	1	4	
Refuse	0	1	1	
Previous treatment				0.09
No	48	44	92	
Explorative thoracotomy	3	10	13	
Recurrent after lobectomy	1	0	1	

cis = ciplatin; ECOG PS = performance status based on the Eastern Cooperative Oncology Group; gem = gemcitabine; n = number of patients

Most patient had surgically inoperable tumor in stages IIIA and IIIB (94% arm A and 96% arm B). Four patients were inoperable due to poor pulmonary function and 1 patient refused surgical treatment. Most patients had no previous treatment (92% arm A and 82% arm B). Thirteen patients were referred for radiochemotherapy after exploratory thoracotomy and 1 patient had a reccurence 1 year after surgery. The most predominant histological subtype was squamous cell carcinoma (67% arm A and 50% arm B). The differences between the two arms were not statistically significant.

Treatment administered

The treatment delivery for 106 patients in both arms is listed in Table 2. A total of 28 patients (53.8%) in arm A and 24 (44.4%) in arm B received

TABLE 2. Treatment delivery

	ARM A No. of patiens	%	ARM B No. of patiens	%	P
Induction chemotherapy					
3 cycles	28	53.8	24	44.4	0.33
2 cycles	23	44.2	27	50.0	0.55
1 cycle	1	1.9	3	5.6	0.33
Concomitant chemotherapy					
2 cycles	15	28.8	19	35.2	0.48
1 cycle	26	50	24	44.4	0.57
Incomplete 1 cycle	10	19.1	9	16.7	0.92
No chemotherapy	1	1.9	2	3.7	0.39
Radical radiotherapy					
Started radical RT	50	100	53	98.1	0.54
Surgical treatment after induction chemotherapy	0	0	1 (pulmectomy)	1.9	0.32
RT doses >60 Gy	44	84.6	47	87.0	0.72
RT doses >56 Gy	48	92.4	53	98.1	0.16
PARAMETERS OF RADIOTHERAPY	**ARM A**		**ARM B**		
GTV (cm^3)					
Median	123		124		0.98
Range	12–381		11–658		
PTV (cm^3)					
Median	619		626		0.99
Range	133–1282		210–1428		
V5 (%)					
Median	64		61		0.52
Range	21–88		27–86		
V20 (%)					
Median	33		33		0.46
Range	12–56		20–52		
V20 > 40%					
No. of patients	12	24	6	12	0.12
MLD (Gy)					
Median	20		19		0.34
Range	6–30		12–27		
V50oes (%)					
Median	47		42		0.06
Range	15–82		2–68		
MoesD (Gy)					
Median	35		32		0.17
Range	7–52		11–44		

GTV = gross tumor volume; MoesD = mean esophagus dose in Gy; MLD = mean lung dose in Gy; No. = number; PTV = panning target volume; RT = radiotherapy; V5 = volume of lung receiving at least 5 Gy; V20 = volume of lung receiving at least 20 Gy; V50oes = volume of esophagus receiving at least 50 Gy

TABLE 3. Toxicity of induction chemotherapy

	ARM A (n = 52)				ARM B (n = 54)				P*
	Grade 1, 2		Grade* 3,4		Grade 1, 2		Grade* 3,4		
	No.	(%)	No.	(%)	No.	(%)	No.	(%)	
Anemia	47	90.4	**1**	1.9	50	92.6	**0**	0	0.31
Neutropenia	11	21.2	**14**	26.9	13	24.1	**11**	20.4	0.43
Thrombocytopenia	15	28.8	**0**	0	10	18.5	**1**	1.9	0.32
Acute kidney injury	16	30.8	**0**	0	19	35.2	**0**	0	/
Nausea/vomiting	19	36.5	**1**	1.9	20	37.0	**3**	5.6	0.33
Peripheral ischemia	0	0	**0**	0	0	0	**1**	1.9	0.32
Alopecia	Grade 1 11	21.1	**Grade 2 8**	15.4	Grade 1 7	13.0	**Grade 2 23**	42.6	**0.002**

n = number of patients; No. = number; *statistical significance for grade 3, 4

TABLE 4. Hematological and non-hematological toxicity of concurrent radiation and chemotherapy

	ARM A (N = 52)				ARM B (N = 54)				P*
	Grade 1, 2		Grade* 3, 4		Grade 1, 2		Grade* 3, 4		
	No.	(%)	No.	(%)	No.	(%)	No.	(%)	
Anemia	48	92.3	**4**	7.7	53	98.1	**0**	0	0.04
Neutropenia	17	32.7	**15**	28.8	13	24.1	**14**	25.9	0.74
Febrile neutropenia	/	/	**4**	7.7	/	/	**2**	3.7	0.37
Sepsis	/	/	**2**	3.8	/	/	**0**	0	0.15
Pneumonia	0	0	**2**	3.8	0	0	**0**	0	0.15
Thrombocytopenia	24	46.1	**5**	9.6	27	50.0	**0**	0	0.02
Acute kidney injury	21	40.4	**1**	0	20	37.0	**0**	0	0.31
Pericarditis	0	0	**1**	1.9	0	0	**0**	0	0.31
Nausea/vomiting	6	11.5	**3**	5.8	10	18.5	**4**	7.4	0.73
Esophagitis	30	57.7	**9**	17.3	39	72.2	**6**	11.1	0.36
Pneumonitis	1	1.9	**4**	7.7	4	7.4	**1**	1.8	0.16
Neurotoxicity	6	11.5	**0**	0	13	24.1	**0**	0	/
Weight loss									
No			**35**				**36**		0.94
1–5%			**7**				**6**		0.71
6–20%			**8**				**8**		0.93
21–31%			**0**				**2**		0.16

n = number of patients; No. = number; *statistical significance for grade 3, 4

all 3 planned cycles of induction chemotherapy. One patient in arm A and 3 patients in arm B received only one cycle of induction chemotherapy. The dose intensity, measured as mean value of percentage of drug administered was for cisplatin and gemcitabine 87.7% and 89.6% for arm A and 87.2% and 84.7% for arm B, respectively. After induction chemotherapy one patient in arm B undervent surgery and pulmectomy was performed.

In two patients in arm A radiation therapy was initiated with paliative intent due to extent of the tumor. Radical radiation therapy with doses of ≥ 56 Gy was completed in 48 patients (92.4%) in arm A and in 53 patients (98.1%) in arm B. Fifteen

patients (28.8%) in arm A and 19 patients (35.2%) in arm B received 2 planned cycles of concurrent chemotherapy, and to 11 patients in each group no concurrent chemotherapy was given. Main reasons for omitting concurrent chemotherapy were hematological toxicity and esophagitis.

Toxicity

Treatment-related acute toxicities of induction chemotherapy were mild and are listed in Table 3. Grade 3 or 4 adverse events were comparable in both arms. No one had febrile neutropenia or grade 3 or more acute kidney injury. Alopecia was more frequent in arm B (15.4% *vs*. 42.6%, p = 0.004). After second cycle of induction chemotherapy, one patient in arm B suffered from grade 4 acute peripheral ischemia leading to amputation.

Treatment-related acute toxicities of concurrent radiochemotherapy are listed in Table 4. There were statistically significantly higher rates of grade 3/4 anemia and thrombocytopenia in arm A with 7.7% (p = 0.04) and 9.6% (p = 0.02) compared with arm B with no grade 3/4 anemia and thrombocytopenia. Two patients in arm A suffered from sepsis after 20 Gy and 22 Gy of radiaton therapy and first cycle of concurrent chemotherapy. Afterwards, the first patient never continued treatment of lung cancer due to cardial failure leading to his death 3 months later. The second patient developed grade 3 infective pericarditis and glomerulonephritis. During treatment of these complications the brain metastases developed, leading to his death two months after interruption of chest irradiation.

Two patients in arm A died from pneumonia short time after completion of treatment – after 2 weeks and 2 months. In both patients pneumonia was associated with radiation pneumonitis. However, the dose of delivered irradiation was within the restrictions for lung tissue in both cases. An autopsy in one patient revealed aspergiloma and necrosis with some malignant cells at the site of the tumor.

Response and survival

The primary endpoint of the study was RR after induction chemotherapy. All 106 patients in both arms were analyzed for response according RECIST criteria (Table 5). No complete responses were seen. Partial response and stable disease were achieved in 25 patients (48.1%) and 27 patients (51.9%) for arm A, and in 31 patients (57.4%) and 22 patients (40.7%) for arm B, respectively. One patient in arm B had progressive disease.

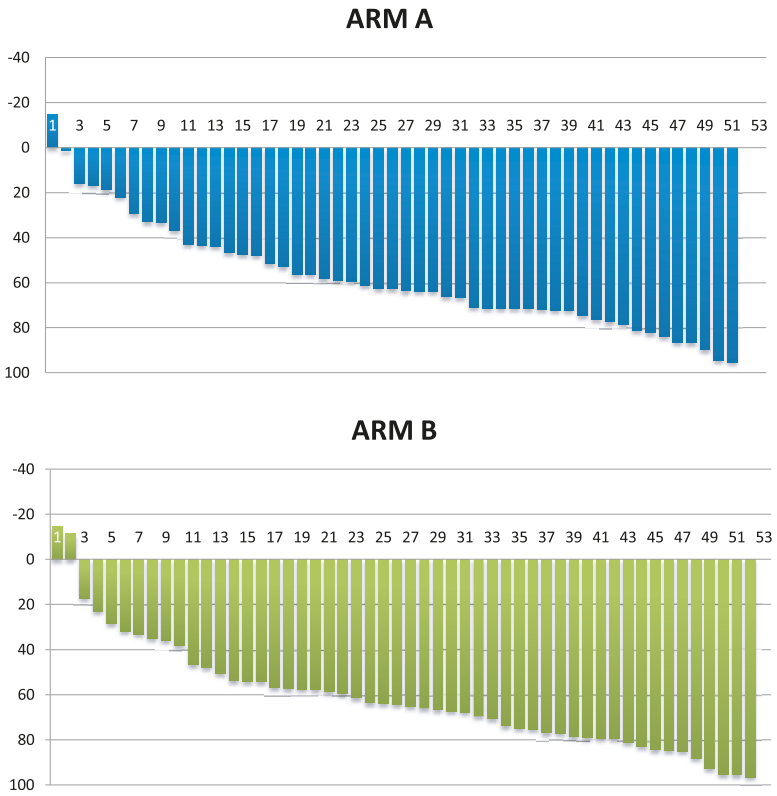

FIGURE 1. Waterfall plot for reduction of the tumor volume after induction chemotherapy for arm A and arm B.

Five month after completion of treatment, 82 patients were evaluable for response according to RECIST. RR was observed in 32 patients (84%) in arm A and in 33 patients (75%) in arm B.

Regarding volumetric measurements, we observed median reduction of the tumor volume for 62.2% in arm A and 64.7% in arm B (p = 0.41) (Figure 1).

The PFS and OS data are shown in Figure 2. No satatistically significant difference in PFS and OS was recognized between the two arms. Median follow-up time of surviving patients was 69.3 months (range 60-72 months). Median PFS was 15.7 months in arm A and 18.9 months in arm B (p = 0.24). The OS in arm A was 24.8 months compared to 28.6 months in arm B (p = 0.18). The OS rates at 1, 2, 3 and 5 years were 73.1%, 51.9%, 32.7% and 19.1% in arm A and 81.5%, 55.6%, 46.2% and 32.2% in arm B, respectively.

Three months after completion of chemo-radiotherapy, one patient in arm B undervent pulmectomy and histologically complete response was

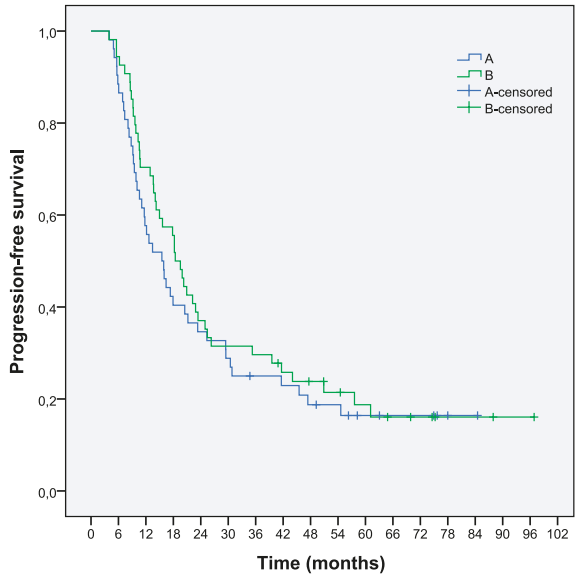

A

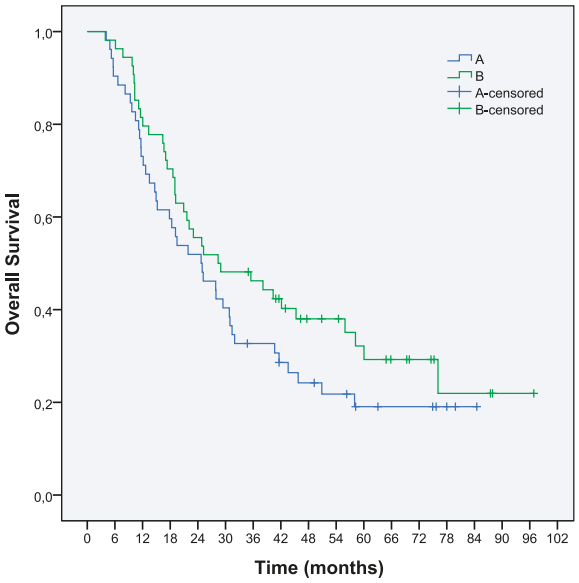

B

FIGURE 2. (A) Progression-free survival and **(B)** overall survival for the two arms.

confirmed. This patient is still alive with no sign of progression.

Three and a half months after completion of treatment one patient in arm A died from pulmonary embolism, confirmed by autopsy.

One patient died from acute lymphatic leukemia two years after the treatment without progresion of lung cancer.

Two patients were affected with second primary cancer, one with new lung cancer six years after first treatment and one with carcinoma of oral cavity also six years after treatment of lung cancer. Both were treated with radiochemotherapy and are still alive.

At the time of last evaluation in October 2013, 28 patients were alive and 19 without disease, 11 and 9 in arm A and 17 and 10 in arm B, respectively.

The sites of initial relapse among 37 patients in arm A were locoregional in 18 patients (48.6%), distant in 12 patients (32.5%) and both locoregional and distant in 7 patients (18.9%), and among 39 patients in arm B locoregional in 21 patients (53.9%), distant in 10 patients (25.6%) and both in 8 patients (20.5%).

Discussion

This prospective randomised phase II trial resulted in the median survival of 24.8 months in arm A and 28.6 months in arm B. Three and 5-year estimated survival rates of 32.7% and 19.1% in arm A and 46.2% and 32.2% in arm B suggest an improved median survival and overall survival in group B compared to group A; however, the difference was not statistically significant. It should be noted that a slight imbalance existed between the two arms. A higher proportion of patients in the arm B had adenocarcinoma histology, was stage III A and previously had explorative thoracotomy. In addition, more patients in arm B received > 56 Gy of radiotherapy, although these differences were not statistically significant.

The primary endpoint of RR after induction chemotherapy revealed no difference between the two groups by RECIST criteria or by volumetric measurement. We conducted volumetric measurement to precisely identifiy differences in the tumor reduction in each groups, however the results are comparable in both groups.

Results of RR after induction chemotherapy in our trial were consistent with some recently published reports. PR and SD in our series were 48.1% and 51.9% in arm A and 57.4% and 40.7% in arm B, respectively. Only one patient in arm B (1.9%) had progressive disease. In the study by Schallier *et al*., with 64 patients constituting the study population, 55% PR was obtained after three cycles of triplet induction chemotherapy regimen of paclitaxel, carboplatin and gemcitabine (PACCAGE).[19] In the study by Hirsh *et al*. of 41 assessable patients who were treated with induction two cycles of carboplatin and gemcitabine 73.1% achieved PR and 24.4% SD.[20] Other publications from recent years showed lower PR and SD of 37% and 50% after two cycles of induction cisplatin and oral vinorelbine[21], PR and SD of 36% and 52% after two cycles of induc-

TABLE 5. Summary of response rates by treatment arm

		ARM A No. of patients	%	ARM B No. of patients	%	P
Response rate after induction chemotherapy-RECIST	CR	0	0	0	0	/
	PR	25	48.1	31	57.4	0.34
	SD	27	51.9	22	40.7	0.25
	PD	0	0	1	1.9	0.32
Response rate after induction chemotherapy-volumetric results	V (cm3) (median) before ChT	145		124		0.55
	V (cm3) (median) after ChT	40.9		28.2		0.26
	Reduction (median, %)	62.6		64.7		0.41
Response 5 months after completion of treatment	CR	18		14		0.33
	PR	14		19		0.36
	SD	1		5		0.10
	PD	5		6		0.80
Median PFS (month)		15.7		18.9		0.24
Median OS (month)		24.8		28.6		0.18
1-year OS (%)		38	73.1	44	81.5	0.30
2-year OS (%)		27	51.9	30	55.6	0.71
3-year OS (%)		17	32.7	24	46.2	0.15
4-year OS (%)		11	24.2	17	38.0	0.43
5-year OS (%)		7	19.1	11	32.2	0.22
Site of the first relapse	No relapse	11	21.2	11	20.4	0.74
	Locoregional	18	48.6	21	53.9	0.51
	Distant	12	32.5	10	25.6	0.56
	Both	7	18.9	8	20.5	0.84
	CNS as the first site of relapse	9	24.3	8	20.5	0.73

ChT = chemotherapy; CNS = central nervous system; CR = complete response; No. = number; OS = overall survival; PD = progressive disease; PFS = progression-free survival; PR = partial response; RECIST = response evaluation criteria in solid tumor; SD = stable disease; V = volume

tion gemcitabine and vinorelbine[22], and PR and SD of 32.1% and 44.6% after two cycles of induction cisplatin and docetaxel.[23]

Compliance to induction chemotherapy in our series was good considering the dose-intensity, with 87% of administered cisplatin in both arms and 89% and 84% of gemcitabine administered in arm A and arm B. However, 53.8% and 44.4% of patients in arm A and arm B received full three cycles of induction chemotherapy. These numbers were quite low but it should be stressed that the schedule of chemotherapy was fixed and aplications of drugs were not delayed but omitted in the case of toxic side effects.

In the concurrent radiochemotherapy the primary objective was completion of radiotherapy without interruption. Dose intensity for arm A and arm B was 61.7% and 67.8% for cisplatin, and 76.4% and 78.9% for etoposide, but only 28.8% and 35.2% of patients in arm A and arm B completed full two cycles of concurrent chemotherapy. The most common reasons for omitting or lowering the doses of concurrent chemotherapy were neutropenia and esophagitis.

Toxicity of induction chemotherapy was mild, and the most frequent grade 3/4 toxicity was neutropenia equally distributed in both arms. In arm B, one case of peripheral ischemia with consequent amputation of lower limb was observed. In recent years, some reports showed possible toxic vascular effects of gemcitabine.[24,25] Among them thrombotic microangiopathy, venous thrombembolism and

acute arterial events (digital ischemia and necrosis, vasculitis) are reported. Vascular events due to gemcitabine seem to be more common in patients with tobacco-associated cancers, as it was also in our case.[24]

Treatment toxicity was more obvious in concurrent radiation therapy and chemotherapy. Grade 3/4 anemia and thrombocytopenia were significantly more common in arm A, whereas alopecia was significantly more common in arm B. Since all patients were treated with the same concurrent chemotherapy, part of the toxicity during radiochemotherapy could be attributed to induction chemotherapy. Alopecia was also recognized as significantly more common toxic effect of low-dose gemcitabine in our previous trial comparing two different schedules of gemcitabine in patients with advanced NSCLC.[9]

Our results with induction low-dose prolonged gemcitabine with median survival of 28.6 months and 3 and 5-year estimated survival of 46.2% and 32.2% are encouraging. Results of meta-analysis based on individual data provided by six randomized trials comparing concurrent and sequental radiochemotherapy in 1205 patients with locally advanced NSCLC demonstrated survival rate of 18.4% at 3 years and 15.1% at 5 years in concurrent group.[6]

In recent years, there were several attempts to improve results of treatment locally advanced NSCLC. Trials with concurrent radiochemotherapy in combination with induction or consolidation chemotherapy using platinum-based combinations report median survival in the range of 13 to 29.5 months[19-23,26-29], 3-year survival in the range of 13% to 39.8%[22,27] and 5-year survival in the range of 12.5% to 22%.[19,26,29]

A recent pooled analysis of 41 phase II/III trials has confirmed that there remains no evidence to suggest that consolidation chemotherapy after concurrent radiochemotherapy improves survival for patients with stage III NSCLC.[30]

Other recent reports on the treatment of locally advanced NSCLC included new drugs such as pemetrexed and cetuximab in combination with radiotherapy and also sequentially.

Median survival of 19.4 months was reported for 40 patients treated with cetuximab concurrently with radiotherapy followed by consolidation therapy with carboplatin and paclitaxel.[31] Among 75 patients, treated with concurrent cetuximab and radiotherapy after docetaxel-cisplatin induction chemotherapy, median survival of 17 months and 3-years OS of 29% were reported.[32] With pemetrexed and cisplatin concurrently with radiotherapy followed by consolidation docetaxel, 28 patients were treated and median survival of 34 months and 1-year survival of 66% was achieved.[33] In a randomized phase II trial of 4 cycles of carboplatin-pemetrexed and concurrent radiotherapy folowed by pemetrexed without or with addition of cetuximab (101 patients), 18-months OS of 58% in the arm without and 54% with cetuximab and median OS of 21.2 months without and 25.2 months with cetuximab were reported.[34]

Another phase III randomized trial of maintenance gefitinib vs. placebo in patients with stage III NSCLC, unselected for EGFR status, who had responded to concurrent radiochemotherapy and consolidation docetaxel demonstrated worse survival in the gefitinib arm. Median survival of 35 months in the control arm compares favourably with results from other phase III studies, although a selection bias must be stressed as patients were randomized following a response to concurrent radiochemotherapy and consolidation chemotherapy.[35]

The most promising results so far have been achieved with trimodality treatment.[36,37] A multicenter phase II trial (CISTAXOL)[36] showed long-term survival of induction chemotherapy with three cycles cisplatin/paclitaxel followed by concurrent radiochemotherapy cisplatin/etoposide and surgery in locally advanced NSCLC. The median survival was 25 months with 5 and 10-year survival rates of 30.2% and 26%, respectively. In spite of nearly two thirds of the 64 patients in the trial in stage IIIB, the R0-resection rate was 50%. However, trimodality treatment is suitable only for a subgroup of patients with locally advanced NSCLC. A larger number of patients is required for any meaningful conclusion concerning the selection of patients for trimodality treatment.

In conclusion, treatment of locally advanced unresectable NSCLC has not significantly progressed in the last decade, in spite of major changes and improvement in treatment of advanced NSCLC. Combined concurrent radiation therapy and chemotherapy with cisplatin-based combinations remains the standard of care for patients in good performance status and no major comorbidities. In comparison with radiation therapy alone, concurrent radiochemotherapy improves local control. However, no trial so far has demonstrated any influence of concurrent chemotherapy to reduce the high risk of systemic failure, probably due to relatively low dose of cytotoxic drugs when applied together with radiation therapy. Contrary to widely held view that there is no clear benefit of additional

chemotherapy before or after concurrent radiochemotherapy, we do believe that systemic control of the disease is of crucial importance for improvement of long-term prognosis. Further trials of induction chemotherapy are therefore warranted, with emphasis on two aspects: individual definition of the optimal schedule of chemotherapy and short gap between completion of chemotherapy and initiation of radiotherapy to avoid repopulation of the tumor cells during this interval.

Our trial compared two cisplatin-based doublets of induction chemotherapy for inoperable NSCLC. Both schedules of gemcitabine had a comparable toxicity profile. Figures for RR, PFS and OS are among the best reported in current literature. In comparison with the standard gemcitabine-cisplatin schedule, the schedule with low-dose gemcitabine in prolonged infusion led to improved long-term survival, but the number of patients is too small for any definitive conclusion. In the future, prognostic and predictive biological and other markers for identify the subgroups of patients for the most optimal schedule of chemotherapy and individualized radiation therapy with isotoxic prescription dose might lead to personalized therapy of patients with inoperable NSCLC.

References

1. Ferlay J, Steliarova-Foucher E, Lortet-Tieulent J, Rosso S, Coebergh JWW, Comber H, et al. Cancer incidence and mortality patterns in Europe: estimates for 40 countries in 2012. *Eur J Cancer* 2013; **49:** 1374-403.
2. Siegel R, Naishadham D, Jemal A. Cancer statistics. *CA Cancer J Clin* 2012; **62:** 10-29.
3. Pfister DG, Johnson DH, Azzoli CG, Sause W, Smith TJ, Baker Jr S, et al. American Society of Clinical Oncology treatment of unresectable non-small cell lung cancer guideline: update 2003. *J Clin Oncol* 2004; **22:** 330-53.
4. O´Rourke N, Roque i Figuls M, Farre Bernardo N, Macbeth F. Concurrent chemoradiotherapy in non-small cell lung cancer. *Cohrane Database Systematic Reviews* 2010; CD002140.
5. Curran WJ Jr, Paulus R, Langer CJ, Komaki R, Lee JS, Hauser S, et al. Sequential vs. concurrent chemoradiation for stage III non-small cell lung cancer: randomized phase III trial RTOG 9410. *J Natl Cancer Inst* 2012; **104:** 79.
6. Aupérin A, Le Péchoux C, Rolland E, Curran WJ, Furuse K, Fournel P, et al. Meta-analysis of concomitant versus sequential radiochemotherapy in locally advanced non-small-cell lung cancer. *J Clin Oncol* 2010; **28:** 2181-90.
7. Kovac V, Smrdel U. Meta-analyses of clinical trials in patients with non-small cell lung cancer. Minireview. *Neoplasma* 2004; **51:** 334-40.
8. Rezonja R, Knez L, Cufer T, Mrhar A. Oral treatment with etoposide in small cell lung cancer - dilemmas and solutions. *Radiol Oncol* 2013; **47:** 1-13.
9. Zwitter M, Kovac V, Smrdel U, Vrankar M, Zadnik V. Gemcitabine in brief versus prolonged low-dose infusion, both combined with cisplatin, for advanced non-small cell lung cancer: a randomized phase II clinical trial. *J Thorac Oncol* 2009; **4:** 1148-55.
10. Zwitter M, Kovac V, Rajer M, Vrankar M, Smrdel U. Two schedules of chemotherapy for patients with non-small cell lung cancer in poor performance status: a phase II randomized trial. *Anticancer Drugs* 2010; **21:** 662-8.
11. Fossela FV, Lipman SM, Shin DM, Tarassoff P, Calayag-Jung M, Perez-Soler R, et al. Maximum-tolerated dose defined for single-agent gemcitabine: a phase I dose-escalation study in chemotherapy-naive patients with advanced non-small-cell lung cancer. *J Clin Oncol* 1997; **15:** 310-6.
12. Touroutoglou N, Gravel D, Raber MN, Plunkett W, Abbruzzese JL. Clinical results of a pharmacodynamically-based strategy for higher dosing of gemcitabine in patients with solid tumors. *Ann Oncol* 1998; **9:** 1003-8.
13. Anderson H, Thacher N, Walling J, Hansen H. A phase I study of a 24 hour infusion of gemcitabine in previously untreated patients with inoperable non-small-cell lung cancer. *Br J Cancer* 1996; **74:** 460-2.
14. Maurel J, Zorrila M, Puertolas T, Antón A, Herrero A, Artal A, et al. Phase I trial of weekly gemcitabine at 3-h infusion in refractory, heavily pretreated advanced solid tumors. *Anticancer Drugs* 2001; **12:** 713-7.
15. Pollera CF, Ceribelli A, Crecco M, Oliva C, Calabresi F. Prolonged infusion gemcitabine: a clinical phase I study at low- (300mg/m^2) and high-dose (875mg/m) levels. *Invest New Drugs* 1997; **15:** 115-21.
16. Cattel L, Airoldi M, Delprino L, Passera R, Milla P, Pedani F. Pharmacokinetic evaluation of gemcitabine and 2´,2´-difluorodeoxycytidine-5´-triphosphate after prolonged infusion in patients affected by different solid tumors. *Ann Oncol* 2006; **17(Suppl 5):** v142-7.
17. Kovac V, Zwitter M, Rajer M, Marin A, Debeljak A, Smrdel U, et al. A phase II trial of low-dose gemcitabine in a prolonged infusion and cisplatin for malignant pleural mesothelioma. *Anticancer Drugs* 2012; **23:** 230-8.
18. Zwitter M, Kovac V, Smrdel U, Kocijancic I, Segedin B, Vrankar M. Phase I-II trial of low-dose gemcitabine in prolonged infusion and cisplatin for advanced non-small cell lung cancer. *Anticancer Drugs* 2005; **16:** 1129-34.
19. Schallier D, Bral S, Ilsen B, Neyns B, Fontaine C, Decoster L, et al. Final overall results of a study with a novel triplet induction chemotherapy regimen (PACCAGE) followed by consolidation radiotherapy in locally advanced inoperable non-small cell lung cancer (NSCLC). *J Thorac Oncol* 2009; **4:** 728-35.
20. Hirsh V, Soulieres D, Duclos M, Faria S, Dell Vecchio P, Ofiara L, et al. Phase II multicenter trial with carboplatin and gemcitabine induction chemotherapy followed by radiotherapy concomitantly with low-dose paclitaxel and gemcitabine for Stage IIIA and IIIB non-small cell lung cancer. *J Thorac Oncol* 2007; **2:** 927-32.
21. Krzakowski M, Provencio M, Utracka-Hutka B, Villa E, Codes M, Kuten A, et al. Oral vinorelbine and cisplatin as induction chemotherapy and concomitant chemo-radiotherapy in stage III non-small cell lung cancer: final results of an international phase II trial. *J Thorac Oncol* 2008; **3:** 994-1002.
22. Leong SS, Fong KW, Lim WT, Toh CK, Yap SP, Hee SW, et al. A phase II trial of induction gemcitabine and vinorelbine followed by concurrent vinorelbine and radiotherapy in locally advanced non-small cell lung cancer. *Lung Cancer* 2010; **67:** 325-9.
23. Descourt R, Vergnenegre A, Barlesi F, Lena H, Fournel P, Falchero L, et al Oral vinorelbine and cisplatin with concurrent radiotherapy after induction chemotherapy with cisplatin and docetaxel for patients with locally advanced non-small cell lung cancer: the GFPC 05-03 study. *J Thorac Oncol* 2011; **6:** 351-7.
24. Grasic Kuhar C, Mesti T, Zakotnik B. Digital ischemic events related to gemcitabine: report of two cases and a systematic review. *Radiol Oncol* 2010; **44:** 257-61.
25. Holstein A, Batge R, Egberts EH. Gemcitabine induced digital ischemia and necrosis. *Eur J Cancer Care (Engl)* 2010; **19:** 408-9.
26. Curran WJ, Paulus R, Langer CR, Komaki R, Lee JS, Hauser S, et al. Sequential vs concurrent chemoradiation for stage III non-small cell lung cancer: randomized phase III trial RTOG 9410. *J Natl Cancer Inst* 2011; **103:** 1452-60.
27. Berghmans T, Van Houtte P, Paesmans M, Giner V, Lecomte J, Koumakis G, et al. A phase III randomized sstudy comparing concomitant radiochemotherapy as induction versus consolidation treatment in patients with locallyy advanced unresectable non-small cell lung cancer. *Lung Cancer* 2009; **64:** 187-93.
28. Senan S, Cardenal F, Vansteenkiste J, Stigt J, Akyol F, De Neve W, et al. A randomized phase II study comparing induction or consolidation chemotherapy with cisplatin-docetaxel, plus radical concurrent chemoradiotherapy with cisplatin-docetaxel, in patients with unresectable locally advanced non-small-cell lung cancer. *Ann Oncol* 2011; **22:** 553-8.

29. Garrido P, Rosell R, Arellano A, Andreu F, Domine M, Perez-Casas A, et al. Randomized phase II trial of non-platinum iduction or consolidation chemotherapy plus concomitant chemoradiation in stage III NSCLC patients: mature results of the Spanish Lung Cancer Group 0008 study. *Lung Cancer* 2013; **81:** 84-90.

30. Tsujino K, Kurata T, Yamamoto S, Kawaguchi T, Kubo A, Isa S, et al. Is consolidation chemotherapy after concurrent chemo-radiotherapy beneficial for patients with locally advanced non-small-cell lung cancer? A pooled analysis of the literture. *J Thorac Oncol* 2013; **8:** 1181-9.

31. Ramalingam SS, Kotsakis A, Tarhini AA, Heron DE, Smith R, Friedland D, et al. A multicenter phase II study of cetuximab in combinaton with chest radiotherapy and consolidation chemotherapy in patients with stage III non-small cell lung cancer. *Lung Cancer* 2013; **81:** 416-21.

32. Hallquist A, Wagenius G, Rylander H, Brodin O, Holmberg E, Loden B, et al. Concurrent cetuximab and radiotherapy after docetaxel-cisplatin induction chemotherapy in stage III NSCLC: satellite-a phase II study from the Swedish Lung Cancer Study Group. *Lung Cancer* 2011; **71:** 166-72.

33. Gadgeel SM, Ruckdeschel JC, Patel BB, Wozniak A, Konski A, Valdivieso M, et al. Phase II study of pemetrexed and cispaltin, with chest radiotherapy followed by docetaxel in patients with stage III non-small cell lung cancer. *J Thorac Oncol* 2011; **6:** 927-33.

34. Govindan R, Bogart J, Stinchcombe T, Wang X, Hodgson L, Kratzke R, et al. Randomized phase II study of pemetrexed, carboplatin, and thoracic radiation with or without cetuximab in patients with locally advanced unresectable non-small-cell lung cancer: Cancer and Leukemia Group B Trial 30407. *J Clin Oncol* 2011; **29:** 3120-5.

35. Kelly K, Chansky K, Gaspar LE, Albain KS, Jett J, Ung YC, et al. Phase-III trial of maitanance gefitinib or placebo after concurrent chemoradiation and docetaxel consolidation in inoperable stage III non-small cell lung cancer. SWOG S0023. *J Clin Oncol* 2008; **26:** 2450-6.

36. Eberhardt WEE, Gauler TC, LePechoux, Stamatis G, Bildat S, Krbek T, et al. 10-year long-term survival (LTS) of induction chemotherapy with three cycles cisplatin/paclitaxel followed by concurrent chemoradiation cisplatin/etoposide/45Gy (1.5Gy bid) plus surgery in locally advanced non-small-cell lung cancer (NSCLC) - a multicenter phase-II trial (CISTAXOL). *Lung Cancer* 2013; **82:** 83-9.

37. Albain KS, Swann RS, Rusch VA, Turrisi AT 3rd, Shepherd FA, Smith C, et al. Radiotherapy plus chemotherapy with or without surgical resection for stage III non-small-cell lung cancer. *Lancet* 2009; **374:** 379-86.

research article

Survival of patients treated with radiation therapy for anaplastic astrocytoma

Christopher A. Barker, Maria Chang, Kathryn Beal, Timothy A. Chan

Department of Radiation Oncology, Memorial Sloan-Kettering Cancer Center, New York, NY, USA

Radiol Oncol 2014; 48(4): 381-386.

Received 17 January 2014
Accepted 10 March 2014

Correspondence to: Christopher A. Barker, M.D., Department of Radiation Oncology, Memorial Sloan-Kettering Cancer Center, 1275 York Avenue, Box 22, New York, New York 10065, USA. Phone: +1 212 639 8168; Fax: +1 212 717 3104; E-mail: barkerc@mskcc.org

Disclosure: No potential conflicts of interest were disclosed.

Background. Anaplastic astrocytoma (AA) represents 7% of primary brain tumors in adults. Patient-, tumor-, and treatment-related factors are thought to be predictive of survival. We retrospectively assessed the association of patient-, tumor-, and treatment-related factors with survival in AA treated with radiotherapy (RT) at our institution.

Patients and methods. Medical records of patients with AA treated with RT between 1987 and 2007 were reviewed. Patient-, tumor-, and treatment-related variables were recorded and used to assign patients to a Radiation Therapy Oncology Group recursive partitioning analysis (RTOG RPA) classification. First use of chemotherapy was recorded. Log-rank tests and Cox regression models were used to assess for an association of patient-, tumor- and treatment-related factors with survival.

Results. One-hundred twenty-six patients were eligible for study. Median age, Karnofsky performance status, and duration of symptoms were 43 years, 90, and 8 weeks. Median radiation dose was 59.4 Gy; 61% of patients underwent tumor resection, and 17% and 41% of patients received temozolomide during and after RT. Median survival was 31 months, and 2-year survival was 58%. RTOG RPA class was associated with survival ($p < 0.001$), but use of temozolomide during or after RT was not ($p > 0.05$).

Conclusions. In this retrospective study with inherent limitations, RTOG RPA classification was associated with survival. Further studies are necessary to confirm or refute this finding.

Key words: anaplastic astrocytoma; radiation therapy; prognosis; Radiation Therapy Oncology Group recursive partitioning analysis (RTOG RPA); temozolomide (TMZ); chemoradiation therapy

Introduction

According to the most recent statistical report of the Central Brain Tumor Registry of the United States, anaplastic astrocytoma (AA, a World Health Organization grade III glioma) is the fourth most common neuroepithelial brain tumor, with an incidence rate of 0.41 per 100,000 person years. This tumor accounts for 7% of all primary brain tumors in adults, with a 2-year survival rate of 43%.[1]

The treatment of patients with AA typically consists of maximal safe resection, followed by external beam radiation therapy (RT). This treatment approach is supported by observational data that suggest that the survival of patients with grade III primary brain tumors is longer after resection (versus biopsy alone).[2] Randomized controlled trials of patients with grade III and IV glioma suggest that RT is associated with longer survival.[3,4]

The survival of patients diagnosed with AA and treated with RT has been associated with patient-, tumor-, and treatment-related factors. The Radiation Therapy Oncology Group (RTOG) conducted the most comprehensive analysis of prognostic factors in the largest group of patients with malignant gliomas (including astrocytomas with anaplastic or atypical foci) enrolled on prospective clinical research protocols and subjected these variables to recursive partitioning analysis (RPA). Six distinct prognostic classes were identified, with 2-year survival rates ranging from 4% to 76%, based on patient age, performance and neurologic

TABLE 1. Criteria for classification of patients with anaplastic astrocytoma to a Radiation Therapy Oncology Group recursive partitioning analysis (RTOG RPA) classification

RTOG RPA Classification	Criteria for assignment to classification			
	Age	Mental status	KPS	Duration of symptoms prior to diagnosis
1	< 50 years	Normal		
2	≥ 50 years		≥ 70	> 3 months
3	< 50 years	Abnormal		
4	≥ 50 years		≥ 70	≤ 3 months
5	≥ 50 years	Normal	< 70	
6	≥ 50 years	Abnormal	< 70	

RTOG RPA = Radiation Therapy Oncology Group recursive partitioning analysis; KPS = Karnofsky performance status.

functional status, mental status, duration of symptoms, extent of surgery, and RT dose.[5]

Given the poor survival rates of patients with AA, chemotherapy is often recommended. However, this point is controversial.[6] A landmark study of patients with glioblastoma (GB, a World Health Organization grade IV glioma) demonstrated an improvement in survival with the use of temozolomide (TMZ, an oral alkylating chemotherapy) during and after RT.[7,8] TMZ and RT have been widely used in the routine treatment of GB and successful outcomes have been reported from retrospective analyses.[9] Because AA often transforms to GB, some have speculated that a similar upfront treatment approach is warranted in AA. Moreover, studies have demonstrated favorable results when TMZ is used for recurrent AA.[10] However, the effect of using TMZ during and after RT for AA has not been well studied.[11]

The goal of this study was to describe the outcome of patients with AA that underwent RT, including an analysis of patient, tumor, and treatment-related factors known to be prognostic in malignant gliomas. In addition, we explored the benefit of TMZ, given during and after RT, to assess for effect on outcome.

Patients and methods

Patients and treatment

This retrospective clinical study was conducted with permission from the institutional review board at our institution. Eligible patients were ≥ 18 years old at the time of histologic diagnosis between 1987 and 2007, and were treated with external beam RT. Patients were identified in electronic institutional databases. Diagnosis of AA was confirmed by a neuropathologist at our institution. Molecular testing for genetic and epigenetic aberrations was not routinely performed during the study time period. Patients with secondary AA, inadequate medical records for review, or who did not receive external beam RT were excluded from study. Age at histologic diagnosis, Karnofsky performance status (KPS), neurologic functional status (able to work or not), mental status (mini-mental status exam score of ≥ 27 or notation of normal mental status), and duration of symptoms prior to histologic diagnosis were recorded. Extent of surgery (biopsy only, or neurosurgeon-determined subtotal or gross total resection), total RT dose (in Gy), and first use of TMZ or other chemotherapy (during and/or after RT) were recorded. Grade ≥ 4 toxicity was assessed using the National Cancer Institute's Common Terminology Criteria for Adverse Events, version 4.0 (CTCAE).

Patient-, tumor-, and treatment-related characteristics were used to assign patients to a RTOG RPA classification.[5,12] The criteria used for assignment to RTOG RPA class are presented in Table 1.

Statistical analysis

Overall survival (OS) was defined as duration of time from the start of RT to death or last follow-up. OS was estimated using Kaplan-Meier methods. Log-rank tests were performed to compare survival between patients that did or did not receive TMZ during RT. Direct Cox regression models (p value limits in and out = 0.05) were built to evaluate the association of RTOG RPA and TMZ use with OS. Three models were built.

Model 1 analyzed the association of survival in patients that received concurrent TMZ during RT (n = 21) vs no TMZ during RT (n = 105)

Model 2 analyzed the association of survival in patients who received concurrent TMZ during RT (n = 21) vs no chemotherapy (TMZ or other) during RT (n = 94)

Model 3 analyzed the association of survival in patients that received TMZ at any time (during or after RT, n = 52) vs no TMZ use (n = 74)

Because the intent of TMZ use after RT could not clearly be defined as adjuvant (i.e., in the absence of disease progression) or salvage (i.e., in the presence of disease progression) therapy, no distinction in the analysis was made for patients that may have received TMZ at time of progression. Hazard ratios (HRs) along with 95% confidence intervals (CIs) were reported. Analyses were carried out using WinSTAT® for Microsoft® Excel (Version 2009.1).

TABLE 2. Baseline patient and treatment-related characteristics of the patients studied (n = 126)

Patient characteristics		N	%
Age (years)	19–30	29	23%
	31–40	25	20%
	41–50	24	19%
	51–60	19	15%
	61–70	19	15%
	71–79	10	8%
KPS	100	9	7%
	90	60	48%
	80	36	29%
	70	11	9%
	60	9	7%
	50	1	1%
Mental status	Normal	101	80%
	Abnormal	25	20%
Symptom duration before diagnosis (weeks)	0–4	48	38%
	5–12	37	29%
	> 12	40	32%
	Unknown	1	1%
Able to work	Yes	44	35%
	No	80	63%
	Unknown	2	2%
Treatment characteristics		**N**	**%**
Extent of surgery	Biopsy	49	39%
	Subtotal resection	50	40%
	Gross total resection	27	21%
RT dose (Gy)	≥ 72	4	3%
	55.8–60.2	110	87%
	≤ 50.4	12	10%
Chemotherapy during RT	None	94	75%
	Temozolomide	21	17%
	Other	11	9%
First chemotherapy after RT	Temozolomide	52	41%
	Other	55	44%
	None	13	10%
	Unknown	6	5%

KPS = Karnofsky performance status; RT = radiation therapy

Results

One-hundred twenty-six patients met the criteria for study. Median follow-up was 28 months. Thirty-six patients were alive at time of last follow-up, and had been followed for a median of 72 months. Median age was 43 years (range, 19–79 years). Median KPS was 90 (range, 50–100). Median duration of symptoms prior to diagnosis was 8 weeks (range 0–312 weeks). Median radiation dose was 59.4 Gy (range, 16–120 Gy). Baseline patient and treatment-related characteristics are presented in Table 2.

Median OS duration was 31 months, and 2-year OS was 58%. Using the aforementioned patient- and treatment-related criteria, patients were assigned to a RTOG RPA class. The median duration of OS and 2-year OS rates by RTOG RPA class for the present cohort are displayed alongside reported data from the RTOG in Table 3. The log-rank test revealed a statistically significant difference in survival among the six classes in the present cohort ($p < 0.001$), as displayed in Figure 1.

The log-rank test revealed no difference in survival between patients that were or were not taking TMZ during RT ($p = 0.28$), as displayed in Figure 2. Median survival of patients receiving TMZ during RT was 19 months, and median survival of patients not receiving TMZ during RT was 33 months; 2-year survival of patients receiving TMZ during was 46%, and 2-year survival of patients not receiving TMZ during RT was 60%.

Cox regression model 1 revealed an association of survival with RTOG RPA class (HR, 1.40; 95% CI, 1.27–1.53; $p < 0.001$), but not use of concurrent TMZ during RT (HR, 1.40; 95% CI, 0.80–2.00; $p = 0.27$). Cox regression model 2 demonstrated an association of survival with RTOG RPA class (HR, 1.35; 95% CI, 1.22–1.49; $p < 0.001$), but not use of concurrent TMZ during RT (HR, 1.34; 95% CI, 0.74–1.95; $p = 0.34$). Similarly, Cox regression model 3 revealed an association of survival with RTOG RPA class (HR, 1.41; 95% CI, 1.28–1.54; $p < 0.001$), but not use of TMZ at any time (HR, 1.09; 95% CI, 0.65–1.54; $p = 0.70$).

Mild-moderate toxicity (CTCAE grade 1–2) was common and consisted of fatigue, alopecia, headaches, nausea, vomiting, cognitive impairment, and disturbances. One patient developed acute lymphoblastic leukemia 4 years after receiving RT followed by carmustine chemotherapy. She died of infectious neutropenia during therapy for acute lymphoblastic leukemia.

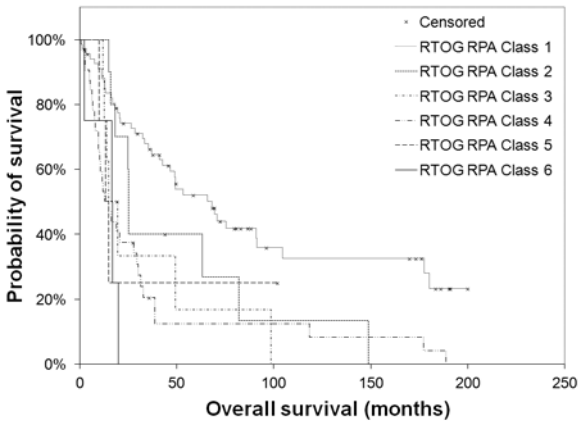

FIGURE 1. Survival of patients with anaplastic astrocytoma treated with radiation therapy, by Radiation Therapy Oncology Group recursive partitioning analysis (RTOG RPA) classification (n = 126). The log-rank test revealed a statistically significant difference in survival by RTOG RPA classification ($p < 0.001$).

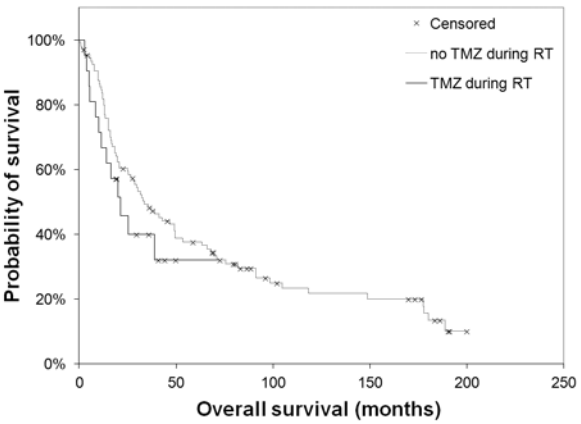

FIGURE 2. Survival of patients with anaplastic astrocytoma treated with radiation therapy, by concurrent use of temozolomide use during radiotherapy (n = 21) or no use of temozolomide during radiotherapy (n = 105). The log-rank test revealed no difference in survival by use or non-use of temozolomide during radiation therapy (RT; $p = 0.28$).

Discussion

In this study, we sought to characterize the outcome of patients with AA treated with RT at our institution. We found that previously reported patient-, tumor-, and treatment-related factors prognostic of survival in patients enrolled on large clinical trials were prognostic in the present cohort. We also attempted to determine the effect of TMZ chemotherapy on the outcome of patients treated for AA. We did not find an association of TMZ with improved survival.

The RTOG RPA classification system, reported by Curran *et al*. in 1993, is a widely used system for assessing prognosis in patients with malignant glioma, being cited over 600 times in the medical literature. Using 20 patient-related, 3 tumor-related, and 6 treatment-related variables, the authors performed an RPA on a group of 1578 patients with malignant glioma, and created a regression tree of prognostic variables that classified patients into six homogenous subsets by survival. Eighteen percent of patients in that analysis harbored an astrocytoma with anaplastic or atypical foci.[5] While the RTOG RPA was validated in another cohort of patients with malignant glioma, to our knowledge the present report is the first describing validation in a retrospective cohort of patient with AA only.[12] The distribution of patients in the present cohort includes more patients with favorable prognoses. However, median and 2-year OS rates were relatively similar except in the poor-prognosis categories (RTOG RPA classes 5 and 6), where the present cohort demonstrated superior survival (albeit in a very small number of patients). In the present study, RTOG RPA class assignment was able to predict a statistically significant difference in survival between the groups. Determining prognosis based on patient-, tumor-, and treatment-related variables is helpful when trying to determine if newer therapies are associated with differences in survival.

Because of the landmark study demonstrating that TMZ use during and after RT improves survival in patients with GB, several studies employing a similar treatment paradigm have been conducted in patients with AA.[8] Kim *et al*. described 33 patients with grade III gliomas treated with TMZ during and after RT. [11] Sixty-five percent of patients in the study were treated for AA. The authors demonstrated the regimen to be safe and well tolerated, with grade ≥3 hematologic toxicity occurring in 15% of patients treated with TMZ during RT, and in 9% of patients treated with TMZ after RT. A specific analysis of the outcomes of patients with AA was not performed.

Combs *et al*. performed a retrospective matched-pair analysis of the outcomes of 60 patients with anaplastic astrocytic tumors treated with RT. Twenty patients who received TMZ during RT were matched to 40 historical controls treated with RT alone. Matching was done based on patient age (<50 years, or ≥50 years), extent of resection (complete, subtotal, or biopsy), and histologic subtype (pure AA, anaplastic oligoastrocytoma, and anaplastic oligodendroglioma). The majority of the patients studied had AA (90%). Median age was 42.4–44.5 years (range, 7–77), with all patients hav-

TABLE 3. Distribution, median and 2-year overall survival of patients by Radiation Therapy Oncology Group (RTOG RPA) classification in the present study, and compared to historical controls from the RTOG database

	Present study				Historical comparison					
					RTOG database (RTOG 74-01, 79-18, 83-02)					
RTOG RPA Class	N	%	Median OS (months)	2-year OS (%)	N	%	Median OS (months)	95% CI	2-year OS (%)	95% CI
1	68	54%	66	73	139	10%	58.6	46.8–108.1	76	68.7–83.3
2	10	8%	25	70	34	2%	37.4	26.2–45.9	68	51.6–83.6
3	8	6%	15	33	175	12%	17.9	15.5–20.6	35	18.6–42.0
4	32	25%	13	37	457	31%	11.1	10.4–11.9	15	12.0–18.0
5	4	3%	13	25	395	27%	8.9	8.3–9.5	6	4.0–8.0
6	4	3%	17	0	263	18%	4.6	4.3–5.3	4	1.8–6.2

RTOG = Radiation Therapy Oncology Group; RPA = recursive partitioning analysis; OS = overall survival; 95% CI = 95% confidence interval

ing KPS ≥70, and 45% having biopsy without tumor resection, thereby representing a cohort very similar to the present study. The authors found median survival of their cohort to be 14 months from time of histologic diagnosis, with 2-year survival of 36%. In their study, extent of surgical resection was not associated with longer survival. The use of TMZ during RT was not associated with longer overall or progression-free survival.[13] The present study corroborates these results, finding no association of TMZ use during or after RT with an improvement in survival.

The present study is limited by several factors. First, the present cohort is relatively small, which limits the power of the analysis. This factor is inherent in retrospective clinical research of a rare disease like AA. It should be noted that this series represents the largest single-institution cohort of AA patients in the contemporary era treated with TMZ. We cannot exclude that bias in the selection of therapy may have led to the observed associations of treatment and outcome in this study. For example, TMZ may have been selected as part of a more aggressive therapeutic regimen for patients with an anticipated worse outcome. By incorporating RTOG RPA into the multivariable analysis, we attempted to minimize this confounding factor. Moreover, additional features prognostic of survival (independent of therapy) were not routinely assessed. Studies have demonstrated that radiographic features (tumor location, size, and ring enhancement), histopathologic features (proliferation rate), and biologic markers (O-6-methylguanine methyltransferase methylation) are also likely to be prognostic of outcome and predictive of response to therapy in this disease.[14–16]

The efficacy of TMZ chemotherapy has been demonstrated in patients with recurrent AA.[10] Many practitioners recommend TMZ during or after RT for AA based on extrapolation from trials in GB with the hope of optimizing the outcome of patients with an otherwise poor long-term prognosis. However, the benefit of using TMZ during or after RT as adjuvant therapy has not been clearly demonstrated. Other studies have suggested that more intensive therapy is not beneficial in patients with AA.[17–18] While potentially controversial, the present findings suggest that TMZ may be best reserved for use in the setting of AA recurrence. The ongoing European Organisation for Research and Treatment of Cancer 26053-22054 CATNON intergroup trial (NCT00626990) will help clarify the appropriate use of TMZ in patients with AA. This 4-arm, multicenter, randomized trial will assess the benefit of TMZ given concurrently with RT, after RT, or both during and after RT in patients with anaplastic gliomas without chromosome 1p/19q deletion. Until further well-controlled studies of this type are reported, the recommendation for TMZ in addition to RT deserves careful discussion between patients and their physicians.

Acknowledgement

This study was supported in part by the Memorial Sloan-Kettering Cancer Center Brain Tumor Center Medical Student Summer Fellowship (M.C.).

References

1. CBTRUS. CBTRUS statistical report: primary brain and central nervous system tumors diagnosed in the United States in 2004-2007. Hinsdale, IL: Central Brain Tumor Registry of the United States; 2011.
2. Laws ER, Parney IF, Huang W, Anderson F, Morris AM, Asher A, et al. Survival following surgery and prognostic factors for recently diagnosed malignant glioma: data from the Glioma Outcomes Project. *J Neurosurg* 2003; **99:** 467-73.
3. Walker MD, Hunt WE, Mahaley MS, Norrell HA, Ransohoff J, Gehan EA. Evaluation of Bcnu and-or radiotherapy in treatment of anaplastic gliomas--cooperative clinical-trial. *J Neurosurg* 1978; **49:** 333-43.
4. Kristiansen K, Hagen S, Kollevold T, Torvik A, Holme I, Stat M, et al. Combined modality therapy of operated astrocytomas grade III and IV. Confirmation of the value of postoperative irradiation and lack of potentiation of bleomycin on survival time: a prospective multicenter trial of the Scandinavian Glioblastoma Study Group. *Cancer* 1981; **47:** 649-52.
5. Curran WJ, Jr., Scott CB, Horton J, Nelson JS, Weinstein AS, Fischbach AJ, et al. Recursive partitioning analysis of prognostic factors in three Radiation Therapy Oncology Group malignant glioma trials. *J Natl Cancer Inst* 1993; **85:** 704-10.
6. Mehta MP, Siker ML, Chakravarti A. Should concomitant and adjuvant treatment with temozolomide be used as standard therapy in patients with anaplastic glioma? *Crit Rev Oncol Hematol* 2006; **60:** 99-111.
7. Stupp R, Hegi ME, Mason WP, van den Bent MJ, Taphoorn MJ, Janzer RC, et al. Effects of radiotherapy with concomitant and adjuvant temozolomide versus radiotherapy alone on survival in glioblastoma in a randomised phase III study: 5-year analysis of the EORTC-NCIC trial. *Lancet Oncol* 2009; **10:** 459-66.
8. Stupp R, Mason WP, van den Bent MJ, Weller M, Fisher B, Taphoorn MJ, et al. Radiotherapy plus concomitant and adjuvant temozolomide for glioblastoma. *N Engl J Med* 2005; **352:** 987-96.
9. Smrdel U, Kovac V, Popovic M, Zwitter M. Glioblastoma patients in Slovenia from 1997 to 2008. *Radiol Oncol* 2014; **48:** 72-9.
10. Yung WKA, Prados MD, Yaya-Tur R, Rosenfeld SS, Brada M, Friedman HS, et al. Multicenter phase II trial of temozolomide in patients with anaplastic astrocytoma or anaplastic oligoastrocytoma at first relapse. *J Clin Oncol* 1999; **17:** 2762-71.
11. Kim YH, Park CK, Cho WH, Kim IA, Moon S, Choe G, et al. Temozolomide during and after radiation therapy for WHO grade III gliomas: preliminary report of a prospective multicenter study. *J Neurooncol* 2011; **103:** 503-12.
12. Scott CB, Scarantino C, Urtasun R, Movsas B, Jones CU, Simpson JR, et al. Validation and predictive power of Radiation Therapy Oncology Group (RTOG) recursive partitioning analysis classes for malignant glioma patients: a report using RTOG 90-06. *Int J Radiat Oncol Biol Phys* 1998; **40:** 51-5.
13. Combs SE, Nagy M, Edler L, Rausch R, Bischof M, Welzel T, et al. Comparative evaluation of radiochemotherapy with temozolomide versus standard-of-care postoperative radiation alone in patients with WHO grade III astrocytic tumors. *Radiother Oncol* 2008; **88:** 177-82.
14. Curran WJ, Scott CB, Horton J, Nelson JS, Weinstein AS, Nelson DF, et al. Does extent of surgery influence outcome for astrocytoma with atypical or anaplastic foci (Aaf)--a report from 3 Radiation-Therapy-Oncology-Group (RTOG) trials. *J Neuro-Oncol* 1992; **12:** 219-27.
15. Compostella A, Tosoni A, Blatt V, Franceschi E, Brandes AA. Prognostic factors for anaplastic astrocytomas. *J Neurooncol* 2007; **81:** 295-303.
16. Graus F, Tortosa A, Vinolas N, Villa S, Verger E, Gil JM, et al. Prognostic pathologic implication of clinical, radiologic, and features in patients with anaplastic gliomas. *Cancer* 2003; **97:** 1063-71.
17. Prados MD, Gutin PH, Phillips TL, Wara WM, Larson DA, Sneed PK, et al. Highly anaplastic astrocytoma--a review of 357 patients treated between 1977 and 1989. *Int J Radiat Oncol Biol Phys* 1992; **23:** 3-8.
18. Laramore GE, Martz KL, Nelson JS, Griffin TW, Chang CH, Horton J. Radiation-Therapy Oncology Group (Rtog) survival-data on anaplastic astrocytomas of the brain: does a more aggressive form of treatment adversely impact survival? *Int J Radiat Oncol Biol Phys* 1989; **17:** 1351-6.

research article

Identification of three anatomical patterns of the spinal accessory nerve in the neck by neurophysiological mapping

Bostjan Lanisnik[1], Miha Zargi[2], Zoran Rodi[3]

[1] Department of Otorhinolaryngology, Cervical and Maxillofacial Surgery, University Medical Center Maribor, Slovenia
[2] Department of Otorhinolaryngology and Cervicofacial Surgery, University Medical Center Ljubljana, Slovenia
[3] Institute of Clinical Neurophysiology, University Medical Center Ljubljana, Slovenia

Radiol Oncol 2014; 48(4): 387-392.

Received 16 August 2013
Accepted 3 September 2013

Correspondence to: Boštjan Lanišnik, M.D., Department of Otorhinolaryngology, Cervical and Maxillofacial Surgery, University Medical Center Maribor, Ljubljanska 5, 2000 Maribor, Slovenia. Phone: +386 2 321 1304; E mail: bostjan.lanisnik@siol.net

Disclosure: No potential conflicts of interest were disclosed.

Background. In spite of preservation of the accessory nerve there is still considerable proportion of patients with partial nerve damage during modified radical neck dissection (MRND).

Methods. The nerve was identified during the surgery and its branches for the trapezius muscle mapped with nerve monitor.

Results. The accessory nerve was mapped during 74 hemineck dissections and three patterns were identified. In type 1 nerve exits at the posterior end of the sternocleidomastoid muscle (SCm) and then it enters the level V (66%). In type 2 the nerve for trapezius muscle branches off before entering the SCm (22%). In type 3 the nerve exits at the posterior part of the SCm and it joins to the cervical plexus (12%). The nerve than exits this junction more medially as a single trapezius branch.

Conclusions. The description of three anatomical patterns in level II and V could help preserving the trapezius branch during MRND.

Key words: spinal accessory nerve; nerve mapping; neck dissection; anatomy; shoulder disability

Introduction

Accessory nerve provides motor supply to sternocleidomastoid and trapezius muscle. If the nerve is damaged during the surgery this results in a trapezius muscle weakness, atrophy and shoulder syndrome. Cranial and middle portions of trapezius muscle are innervated with accessory nerve proper, while caudal portions of the muscle thought to be innervated with fibers originating from C3 and C4 cervical plexus, but some authors believe that contributions from the cervical plexus are purely proprioceptive.[1,2] Anatomy of the accessory nerve in the anterior and posterior triangle of the neck has been comprehensively described in the literature.[3] Even though today the nerve is routinely preserved during neck dissection whenever possible, some authors demonstrate that functional outcomes after the modified radical neck dissection are worse compared to selective neck dissection.[4,5] This is attributed to the dissection of the level V and resection of the cervical roots.[6,7]

In this study we mapped the accessory nerve during modified radical neck dissection type 3, using electrophysiological techniques with the goal to describe surgical anatomy and nerve variations which might be helpful in improving functional outcomes after surgery.

Patients and methods

Forty patients were studied during the neck dissection for head and neck cancer from January 2012 to

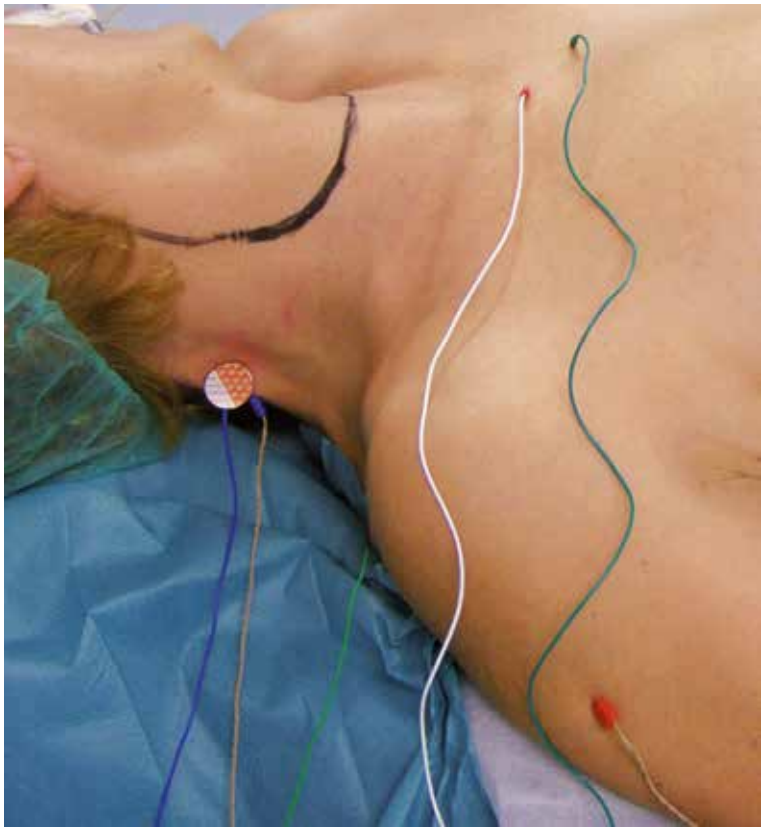

FIGURE 1. Placement of the electrodes in the patient before surgery. Surface electrodes over the trapezius are seen as well as needle electrodes in the trapezius and deltoid muscles. Reference and ground electrodes are placed over the *jugulum*.

January 2013. The aim of the study was to map the course of the accessory nerve, with special consideration to the innervation of the trapezius muscle. The study was designed as a prospective cohort study of patients undergoing first treatment for head and neck cancer without previous surgery or radiation therapy. All patients had N0 or N+ neck that warranted modified radical neck dissection type 3 on one or both sides with preservation of the cervical roots. The study was approved by the Committee for Medical Ethics of the Republic of Slovenia.

Modified radical neck dissection type 3 (MRND) was performed with anterior to posterior dissection technique with preservation of the cervical plexus. The dissection started with elevation of the apron flap. Superficial layers of the deep cervical fascia were incised over the sternocleidomastoid muscle and retracted medially. The muscle was dissected of the fascia to the entrance of the accessory nerve into the muscle. This anatomical point is predictable and is easily identified. The dissection of the accessory nerve continued in the cranial direction, where all branches were preserved. After that, we identified the branch for the trapezius muscle at the posterior margin of the sternocleidomastoid by dissecting the fascia from the muscle with the help of the nerve monitor. Dissection in level V and IIb continued bellow the cervical plexus and accessory nerve, carefully preserving all branches and removing all fatty tissue and fascia. The dissection ended on the alar layer of the deep fascia. Integrity of the accessory nerve was tested continuously during the procedure.

The mapping of the accessory nerve was performed using an intraoperative nerve monitoring device NIM 2.0 (Medtronic Navigation Inc., USA) with bipolar needle and surface electrodes placed in/over the trapezius muscle (registering electrode over the biggest muscle mass and negative electrode over the acromion, Figure 1). A needle electrode was also placed in the deltoid muscle to detect a possible contamination from the stimulation of the brachial plexusSurface electrodes record compound muscle action potentials (CMAP) from a much wider area compared to needle electrodes thus giving better estimation of the number of excitable motor axons innervating the given muscle. On the other hand, bifocally placed needle electrodes record the CMAP only between the needle tips in a localized area of the muscle thus minimizing the risk of recording the action potential from surrounding muscles but at the same time detecting only the smaller fraction of motor axons. Only stimulations with responses recorded on both needle and surface electrodes placed in/over trapezius muscle, and at the same time showing no response in deltoid muscle, were considered to originate from the accessory nerve or its branches.

The nerve was mapped (stimulated) using a hook stimulating electrode that was used to lift up the nerve and prevent the stimulus from spreading in the surrounding tissue. Stimulus current was gradually increased to achieve a supramaximal stimulation. We also stimulated the cervical roots as medially as possible to exclude potential concurrent stimulation of the accessory nerve or its branches. The nerve and roots producing maximal and identical response in the trapezius muscle were followed. The anatomical course of the accessory nerve was recorded.

Results

Mapping of the accessory nerve during 74 modified neck dissections, type 3, was performed in 40

TABLE 1. The table shows frequencies of nerve type combinations in the left and right side of the neck in patients with bilateral modified radical neck dissection

Nerve type combination	No. of patients (%)
Type 1 – Type 1	20 (58.8 %)
Type 2- Type 2	5 (14.7 %)
Type 3- Type 3	2 (5.9 %)
Type 1- Type 3	3 (8.8 %)
Type 1- Type 2	2 (5.9 %)
Type 2- Type 3	2 (5.9 %)

patients. Eighteen patients were treated for oral cavity cancer, 8 for laryngeal cancer, 4 for hypopharyngeal carcinoma, 8 for oropharyngeal cancer, 1 for skin cancer and 1 patient for carcinoma of unknown primary. Mapping of the accessory nerve in 74 dissections resulted in identification of three predictable and recurring anatomical patterns of the accessory nerve.

Type 1 pattern of the accessory nerve was the most common and was found in 49 out of 74 heminecks (66%). In this pattern, the nerve coursed through the sternocleidomastoid muscle, where it divided into the sternocleidomastoid branch and trapezius branch. The latter exited the muscle at its posterior edge and is readily identified in the posterior part of region V and deep to the plane of the cervical roots (Figure 2).

Type 2 pattern was identified in 16 out of 74 heminecks (22%). In this case the branch for the trapezius muscle branched off the common trunk before entering the sternocleidomastoid muscle. The course of this branch is superficial to the cervical roots at least to the level of C4, where it coursed deep and entered region V and the trapezius muscle (Figure 3).

Type 3 is the least common and was found in 9 out of 74 heminecks (12%). It is the most complicated pattern, where the trapezius branch exited at the posterior end of the sternocleidomastoid muscle and joined to the cervical roots at level C3 and/or C4. The trapezius branch then exited from this junction more medially and then it turned deep to the level V (Figure 4).

Thirty-four patients had bilateral modified radical neck dissection. In twenty-seven patients (79%) the same type was found on both sides of the neck. Type 1 was found in 58.8% (20 out of 34) patients, type 2 14.7% (5 out of 34) patients and type 3 in 5.9% (2 out of 34) patients (Table 1). In other 7 patients the nerve types were present in different

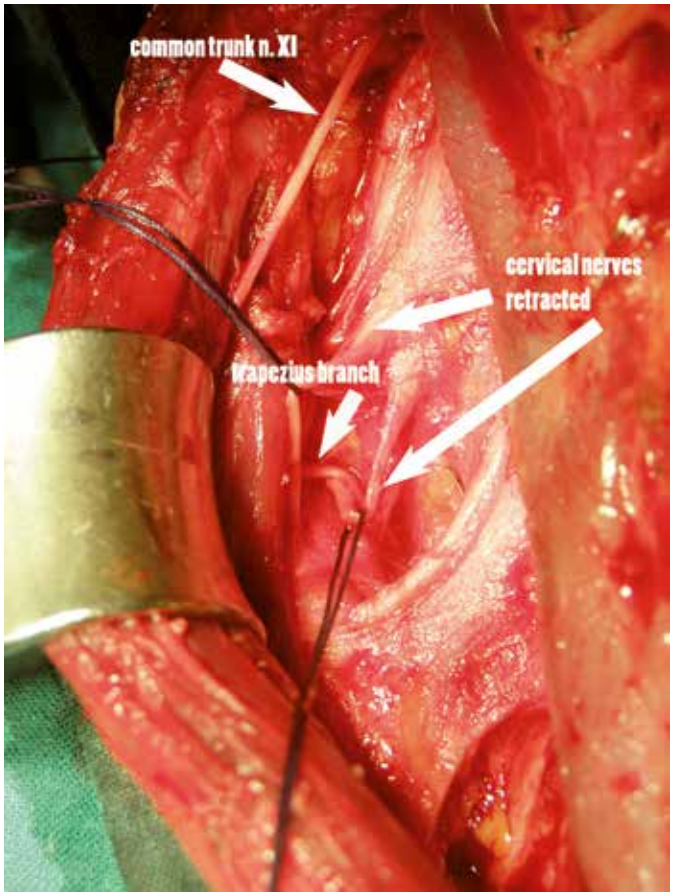

FIGURE 2. In type 1 pattern, a trapezius branch exits at the posterior margin of the sternocleidomastoid muscle, deep to the cervical nerves, and continues to enter level V. Cervical roots are displaced with suture loops for better visualization of the trapezius branch. This pattern was present in 69% of the patients.

combinations: type 1- type 2 in 2 patients (5.9%), type 2-type 3 in 2 patients (5.9%) and type 1-type 3 in 3 patients (8.8%).

In all 40 patients and 74 dissections, we identified a single branch for the trapezius muscle entering region V where it divided into branches for different parts of the muscle.

We couldn't identify the motor response in the trapezius muscle when we stimulated different parts of the cervical roots C2, C3 or C4. If higher currents were used, we could identify the electrical stimulus artifacts on the superficial electrodes when stimulating cervical roots or different tissues of the neck (Figure 5). We identified C2 communication branch in all 74 dissections, but its thickness varied considerably. This branch always led to the trapezius branch and proved to be a reliable marker during the dissection.

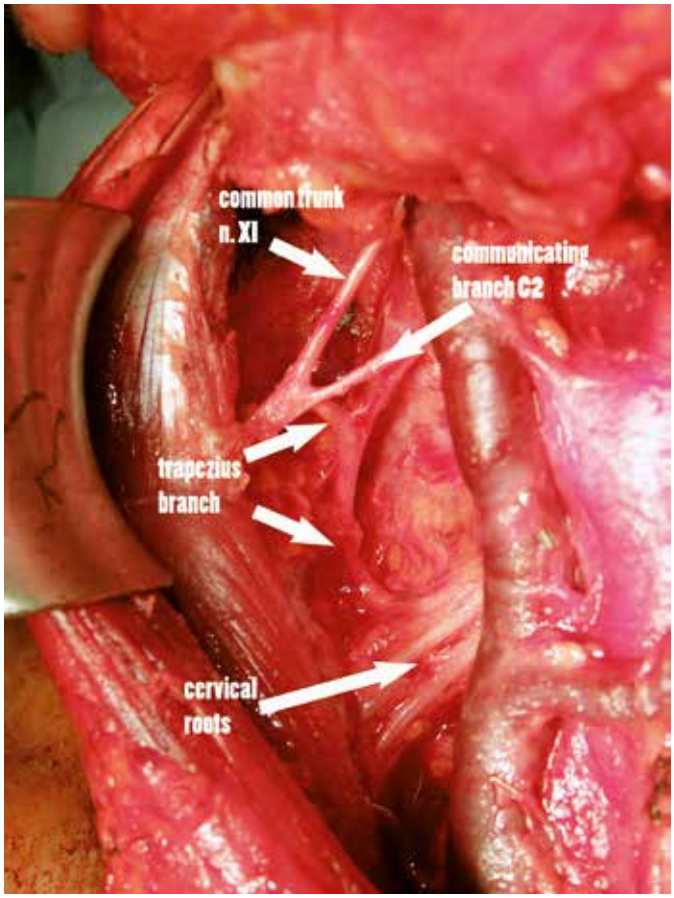

FIGURE 3. In type 2 pattern, a trapezius branch exits the main trunk at level IIa and continues superficial to the cervical nerves in level IIa and enters level V. In this figure, we can see that it is essential to identify this branch early during the dissection in level IIa. This pattern was found in 20% of patients.

Discussion

The anatomical course of the accessory nerve in the neck is described in numerous articles. The main identification point of the nerve is in the posterior triangle, behind the posterior edge of the sternocleidomastoid muscle at Erb's point, which is defined by the exit of the greater auricular nerve from behind the sternocleidomastoid muscle. The accessory nerve can also be identified at the entry point into the sternocleidomastoid muscle. This is the perspective of the nerve identification during modified radical neck dissection. The nerve passes lateral to the jugular vein in the majority of the cases, while medial passage is rare, but the incidence varies in the literature.[3,8]

Even though the accessory nerve is preserved in its superior part during a modified radical neck dissection, significant postoperative shoulder disability can still be observed. This is attributed to the resection of the cervical branches and lymph node dissection in levels IIb and V that leads to damage to branches to the trapezius muscle. Those findings led Kierner *et al.* to conclude that traditional anatomical concepts of the topography of the accessory nerve are not correct. They described a small cranial branch that takes off in the posterior triangle from the main trunk of the accessory nerve and enters into the descending part of the trapezius muscle.[9,10]

Lee *et al.* studied the anatomy of the accessory nerve at level IIb. They found that the nerve passed ventrally to the internal jugular vein in 39.8% of the cases, dorsally in 57.4% and through it in 2.8% of the cases. They also described that in 45.9% of the cases, the nerve sent branches to the sternocleidomastoid muscle without penetrating it, whereas in 54.1% of the cases the nerve passed through the muscle.[11]

Shiozaki *et al.* performed a detailed cadaveric anatomical study with special emphasis on different types of sternocleidomastoid innervation. They described three types: type A is a non-penetrating type; in type B, the nerve partially penetrates the sternocleidomastoid muscle; and in type C, it completely penetrates the muscle. They also described 5 different types of trapezius branches based on the number of branches that innervate the anterior margin of the muscle.[12]

The contribution of the cervical roots to the innervation of the trapezius is still controversial. Current understanding that the trapezius has mixed innervation is based on electromyographical studies of Haas and Solberg from 1962, who stated that the innervation to the trapezius was received from cervical and thoracic branches as well as from spinal accessory nerve.[13] Kierner *et al.* pointed out that their methodology might be questionable, because of the spread of the stimulating current in the posterior triangle, if proper care during the stimulation is not taken. This can lead to false positive results.[10]

After searching the National Library of Medicine database on line (PubMed) we could identify three studies in the last 30 years, where electrophysiological technique was used to address this question. Soo *et al.* used needle detector electrodes in upper, middle and lower part trapezius muscle. They compared the size and pattern of the CMAP if accessory nerve and cervical plexus was stimulated and identified three patterns of motor action potentials. The authors concluded that the trapezius muscle innervation from the cervical plexus is present, but unpredictable and that most important motor input came from accessory nerve.[2]

Pu *et al.* also used electroneuronography to identify the contribution of the cervical plexus to the innervation of the trapezius.[14] They compared CMAP from the accessory nerve, C2, C3 and C4 contributing branches, before and after sectioning the nerve during surgery. They concluded that main motor supply is from the spinal accessory nerve with variable contributions from C2-C4 branches. They also used histochemical staining for acetylcholine esterase activity and found that 0/19 C2 branches, 1/13 C3 branches and 1/14 C4 branches contained motor axons.

Kierner *et al.* used electromyography to identify a small cranial branch that innervates the descending part of the trapezius muscle. This branch takes off in the posterior triangle of the neck medial to the trapezius muscle. The authors could not demonstrate any clinically relevant contribution from the cervical branches to the motor innervation of the trapezius muscle.[10] They described that in about a third of the patients the nerve ran dorsally to the sternocleidomastoid muscle and not through it.

The results of our work, where we mapped the nerve using electrophysiological technique similar to Kierner's *et al.* confirmed some of his observations. We used surface electrodes for detection of the muscle response and we didn't measure the response in different parts of the muscle. The rationale for this decision was the fact that we were mapping the nerve before it branched in the posterior triangle. The branching in the posterior triangle is of great importance in posterolateral dissection. We could identify three major patterns of the accessory nerve in its neck course. In type 1, branches for the trapezius exit the sternocleidomastoid muscle in the area of the Erb point, deep to the cervical plexus and take a course in the posterior triangle as it is usually described in the anatomical dissections.[3,8,15] Type 2 pattern is present when trapezius branches exit the nerve before entering the sternocleidomastoid muscle. This means that the first part of the course is anterior (above the plane) to the cervical plexus and it enters the posterior triangle at various levels, but always bellow C2. This pattern corresponds to the Kierner's *et al.* observation in one third of the patients where the accessory nerve passed through the sternocleidomastoid muscle (22% in our series).[9,10]

The most interesting pattern identified is type 3 where the nerve exits at the posterior surface of the sternocleidomastoid muscle and it joins with the cervical plexus at the C3–4 level. From there, a single branch for the trapezius muscle exits medial to this junction. This medial positioned branch

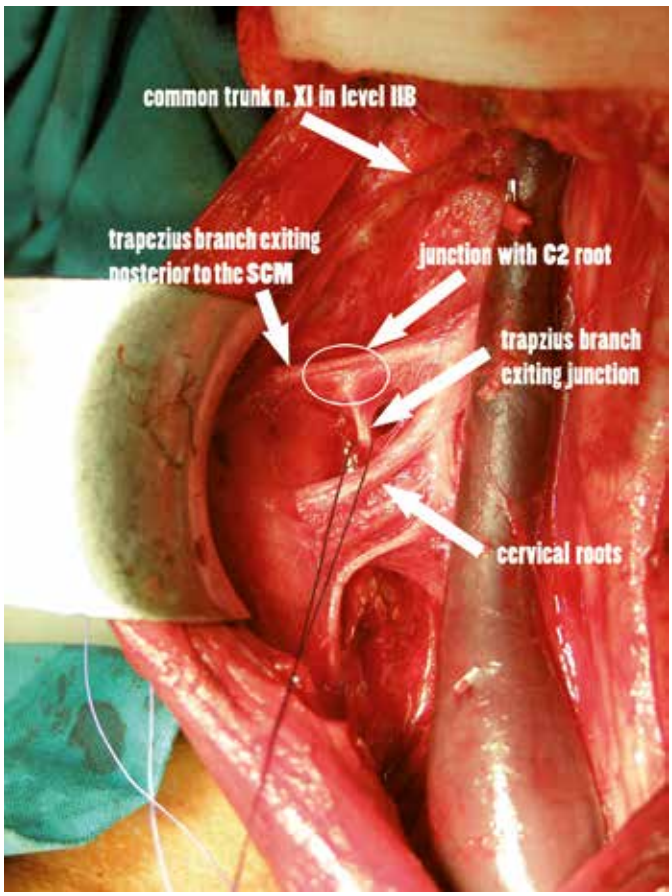

FIGURE 4. Type 3 pattern is more complicated. The trapezius branch is seen exiting at the posterior margin of the sternocleidomastoid muscle and joining with cervical nerves. From this junction, a single branch exits more medially and enters level V (branch is looped with suture). If this type is not recognized, the branch that enters level V might be mistaken for a cervical nerve and cut. This pattern was present in 11% of all patients. SCM-sternocleidomastoid muscle

can be confused for the cervical root and cut during the dissection. This type could also explain the confusion regarding the contribution of the cervical nerves in innervation of the trapezius. When approaching the nerve from a posterior to anterior direction, it is almost impossible to identify the branch that exits from the cervical plexus and innervates the trapezius muscle.

During the modified radical neck dissection the surgeon encounters the accessory nerve from different perspectives. In the beginning of the procedure the nerve is identified at level II before entering into the sternocleidomastoid. If a type 2 division is present, the trapezius branch takes off before entering the sternocleidomastoid muscle (Figure 3). Therefore the trapezius branch is encountered early during the procedure and must be preserved. In type 1, the nerve can be safely identi-

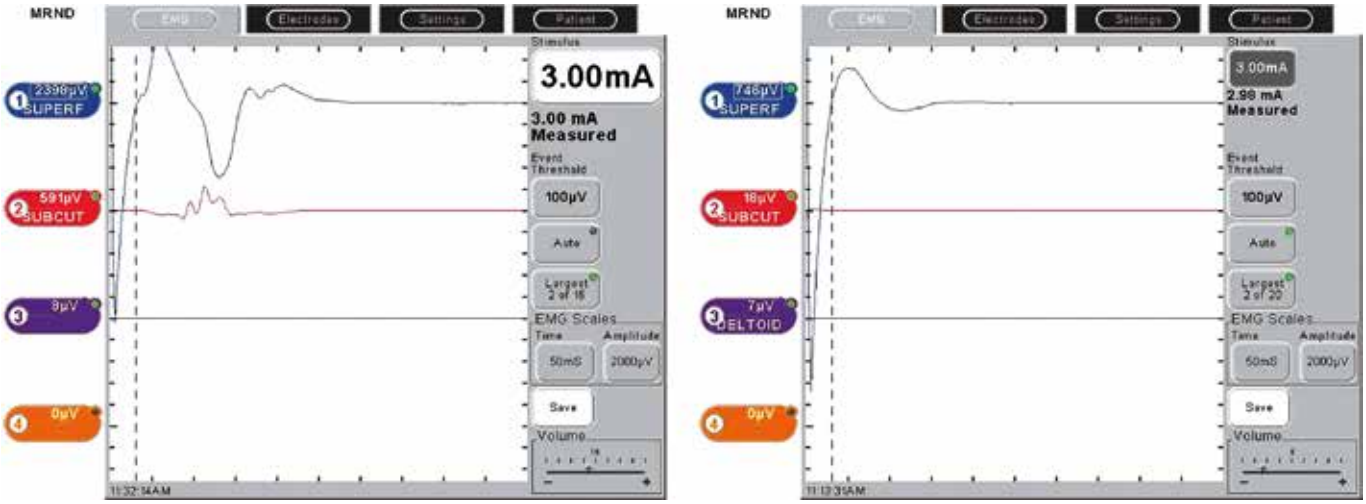

FIGURE 5. The recording of the compound action potential (CMAP) during mapping can be seen on the left side in a patient with type 3 branching. Channel 1 records superficial electrodes while Chanel 2 records from the subcutaneous electrodes. Channel 3 records the CMAP of the deltoid muscle. The left image represent the stimulation of the accessory nerve branches, while the right represents recording while stimulating the cervical branches of C4 where only stimulus artifact and not the CMAP is recorded. Similar results were obtained if we stimulated the C2 communicating branch.

fied behind the posterior edge of the sternocleidomastoid muscle, before passing through level V. Identification of the C2 branch also leads to the trapezius branch and is a safe landmark (Figure 2). In type 3, it is of paramount importance to preserve cervical branches since the branch after exiting from the sternocleidomastoid muscle intermixes with cervical nerves at levels C3 to C4. From there, a single branch exits and enters level V, which can than be safely followed and dissected (Figure 4).

Conclusions

The description of anatomical variations of the accessory nerve in level IIb and V is of clinical importance during neck dissection. Even though the accessory nerve is preserved during modified radical neck dissection, there is still considerable morbidity of the shoulder girdle. We believe that at least some damage to the nerve is inflicted during neck dissection, because the anatomy of the nerve in levels IIb and V is not sufficiently understood by the surgical community.

The description of three different types of trapezius branching patterns might help in its identification and decrease morbidity during neck dissection.

References

1. Brodal A. *Neurological anatomy in relation to clinical medicine.* New York: Oxford University Press; 1981. p. 1053.
2. Soo KC, Strong EW, Spiro RH, Shah JP, Nori S, Green RF. Innervation of the trapezius muscle by the intra-operative measurement of motor action potentials. *Head Neck* 1993; **15:** 216-21.
3. Lloyd S. Accessory nerve: anatomy and surgical identification. *J Laryngol Otol* 2007; **121:** 1118-25.
4. Cheng PT, Hao SP, Lin YH, Yeh AR. Objective comparison of shoulder dysfunction after three neck dissection techniques. *Ann Otol Rhinol Laryngol* 2000; **109:** 761-6.
5. Chepeha DB, Taylor RJ, Chepeha JC, Teknos TN, Bradford CR, Sharma PK, et al. Functional assessment using Constant's Shoulder Scale after modified radical and selective neck dissection. *Head Neck* 2002; **24:** 432-6.
6. Cappiello J, Piazza C, Giudice M, De Maria G, Nicolai P. Shoulder disability after different selective neck dissections (levels II-IV versus levels II-V): a comparative study. *Laryngoscope* 2005; **115:** 259-63.
7. Tsuji T, Tanuma A, Onitsuka T, Ebihara M, Iida Y, Kimura A, et al. Electromyographic findings after different selective neck dissections. *Laryngoscope* 2007; **117:** 319-22.
8. Baring DE, Johnston A, O'Reilly BF. Identification of the accessory nerve by its relationship to the great auricular nerve. *J Laryngol Otol* 2007; **121:** 892-4.
9. Kierner AC, Zelenka I, Heller S, Burian M. Surgical anatomy of the spinal accessory nerve and the trapezius branches of the cervical plexus. *Arch Surg* 2000; **135:** 1428-31.
10. Kierner AC, Burian M, Bentzien S, Gstoettner W. Intraoperative electromyography for identification of the trapezius muscle innervation: clinical proof of a new anatomical concept. *Laryngoscope* 2002; **112:** 1853-6.
11. Lee SH, Lee JK, Jin SM, Kim JH, Park IS, Chu HR, et al. Anatomical variations of the spinal accessory nerve and its relevance to level IIb lymph nodes. *Otolaryngol Head Neck Surg* 2009; **141:** 639-44.
12. Shiozaki K, Abe S, Agematsu H, Mitarashi S, Sakiyama K, Hashimoto M, et al. Anatomical study of accessory nerve innervation relating to functional neck dissection. *J Oral Maxillofac Surg* 2007; **65:** 22-9.
13. Haas E, Sollberg G. Research on the function of the shouder girdle after section of the accessory nerve. *Z Laryngol Rhinol Otol* 1962; **41:** 669-77.
14. Pu YM, Tang EY, Yang XD. Trapezius muscle innervation from the spinal accessory nerve and branches of the cervical plexus. *Int J Oral Maxillofac Surg* 2008; **37:** 567-72.
15. Soo KC, Hamlyn PJ, Pegington J, Westbury G. Anatomy of the accessory nerve and its cervical contributions in the neck. *Head Neck Surg* 1986; **9:** 111-5.

case report

Distant metastasis of rectal adenocarcinoma in a temporary tracheostoma

Robert Sifrer[1], Primoz Strojan[2], Nina Zidar[3], Miha Zargi[1], Ales Groselj[1], Milena Krajinovic[4]

[1] University Department of Otorhinolaryngology and Head and Neck Surgery, Ljubljana, Slovenia
[2] Institute of Oncology Ljubljana, Ljubljana, Slovenia
[3] Institute of Pathology, Faculty of Medicine, Ljubljana, Slovenia
[4] Department of Otorhinolaryngology, General Hospital Novo mesto, Slovenia

Radiol Oncol 2014; 48(4): 393-396.

Received 22 June 2013
Accepted 2 July 2013

Correspondence to: Robert Šifrer, M.D., University Department of Otorhinolaryngology and Head and Neck Surgery, Zaloška 2, 1000 Ljubljana, Slovenia. Phone: +386 1 522 21 94, +386 1 522 48 14; Fax: +386 1 522 26 76; E-mail: robert_sifrer@hotmail.com

Disclosure: No potential conflicts of interest were disclosed.

Background. The temporary tracheostoma's metastases of head and neck cancer had already been reported in the literature. So far, they had been considered as regional dissemination of the malignant disease. We report a case of temporary tracheostoma's metastasis of carcinoma from non-head-and-neck primary site, what has not been reported in the literature, yet. Therefore, it is the first reported case of the systemic dissemination of malignant tumour into temporary tracheostoma.

Case report. Fifty-four-year-old female patient, previously treated for a rectal adenocarcinoma, reported in our office with exophytic pink tissue masses around the temporary tracheostoma. The biopsy and immunohistochemistry findings were consistent with temporary tracheostoma's metastasis of the rectal adenocarcinoma. The patient received palliative radiotherapy and died of systemic progression of the disease.

Conclusions. The patients with history of primary cancer of any origin and exophytic proliferating changes around the tracheostoma require an appropriate diagnostic work-up including a biopsy. The type of treatment depends on the extent of the disease, previous therapy and general condition of the patient.

Key words: temporary tracheostoma; distant metastasis; rectal adenocarcinoma

Introduction

The occurrence of malignant growths in the region of permanent tracheostoma after laryngectomy is well documented in the literature and is usually considered to be a peristomal recurrence of the primary laryngeal carcinoma. It usually affects patients with squamous cell carcinoma arising in the subglottic larynx, malignant infiltration of the thyroid gland, Delphian or paratracheal lymphatic nodes, those with a pre-resection urgent temporary tracheostomy, or incomplete tumour removal with laryngectomy.[1,2] Therefore, some authors prefer urgent laryngectomy over urgent temporary tracheostomy in case of acute respiratory distress due to a laryngeal tumour.[3]

In comparison to permanent tracheostoma, the impairment of the temporary tracheostoma by malignant disease is rare.[4] Only individual case reports on metastasis in temporary tracheostomas, originating from head-and-neck primaries, are available. The problem is usually clinically observed a few months after the completion of treatment, when patients are already decannulated. The clinical picture includes proliferating anterior neck masses with respiratory distress, haemoptysis and haemorrhages.[5,6] Background mechanisms include the continuous shedding and seeding of neoplastic cells from the primary tumour with their implantation in the target area.[4-7] In fact, the metastasis in temporary tracheostoma from the upper aero-

FIGURE 1. Metastasis of colorectal carcinoma in temporary tracheostoma with margins of irradiation field marked on the skin – anterior view.

digestive tract primary carcinoma is a stomal progression of this tumour.

To the best of our knowledge, the metastasis into temporary tracheostoma from a distant primary site has not yet been reported.

Case report

In January 1999, a 54-year-old female was treated by anterior resection of the rectum with anastomosis for a moderately differentiated rectal adenocarcinoma sited 12 cm above the anocutaneous line. In histopathological examination, a 7 × 4 × 0.9 cm tumour and resection margins free of tumour cells were described. The disease stage was pT3pN0M0, Dukes B. The patient was given a course of 50.4 Gy (in 1.8 Gy daily fractions) of postoperative irradiation using 10 MeV linear accelerator photon beams and the four-field box technique until April 1999.

Adhesiolysis, resection of terminal ileum and end-to-end anastomosis were performed in May 2000 and sigmostomy in December 2003 with no signs of local or regional recurrence.

One week after the third surgery, the patient complained of severe hoarseness but was not examined by an otorhinolaryngologist at that time.

In January 2005, multiple pulmonary metastases were diagnosed and the patient was directed to chemotherapy. By October 2005, she had had seven cycles of FOLFIRI regimen (irinotecan, leucovorin, 5-fluorouracil) resulting in a partial remission. At the time of progression in March 2006, a XELOX regimen (capecitabine, oxaliplatin) was introduced. Due to its ineffectiveness, it was replaced with a FOLFIRI-cetuximab combination after the third cycle in June 2006. By March 2007, the patient had received six applications, also without any clinical benefit. As the patient was still in good performance status, the XELOX chemotherapy was re-started, but was terminated after the forth application in July 2007 due to side effects (allergic reaction with dyspnoea during administration of oxaliplatin).

In August 2007, the patient was admitted to the otolaryngology department with a clinical picture of an acute respiratory distress. During the clinical examination, subglottic stenosis was observed. It was of a concentric type and the mucosa covering it was smooth and showed no sign of malignancy, which was confirmed with direct pharyngolaryngoscopy with rigid tracheoscopy. The stenosis was attributed to an orotracheal intubation injury during the last abdominal surgery. An urgent tracheostomy was performed; after the surgical wound healed and the patency of tracheostoma stabilised, the patient was discharged from the hospital with appropriate knowledge on basic care of her tracheostoma.

In February 2008, difficulties with cannula replacements associated with unusual changes around the tracheostoma prompted the patient to visit the ENT office again. After the removal of the cannula, the clinical examination revealed exophytic pink tissue masses, 1.5 × 1.5 cm in size, growing around the left and inferior rim of the tracheostoma in the area of skin transition into tracheal mucosa (Figure 1), mimicking hypertrophic granulations that are usually found in neglected tracheostomas. Due to extent of these changes, a biopsy was performed.

The biopsy sample measured 7 × 5 × 2 mm and consisted of a tumour with abundant necrosis. Histologically, the tumour was composed of atypical glandular tubular structures and islands of tumour cells exhibiting moderate cellular and nuclear pleomorphism, and numerous mitotic figures (Figure 2A). Immunohistochemical analyses showed a diffusely positive reaction for cytokeratin 20 (Figure 2B), and a negative reaction for cytokeratin 7. Morphologic characteristics and the immunophenotypes of the tumour samples from the tracheostoma and the colon were similar, confirming the diagnosis of colon adenocarcinoma metastatic to tracheostoma.

The patient was offered palliative radiotherapy with 10 fractions of 3 Gy/day and an appositional

12 MeV electron beam, covering only the macroscopic disease with margin (Figure 1). At the end of the irradiation course, there was no change in the clinical appearance of the metastasis in the tracheostoma. In May 2008, a CT scan revealed solitary brain metastasis in the left parietal region of 6 cm in diameter with surrounding oedema. She was treated with corticosteroids in addition to whole brain radiotherapy of 20 Gy (4 Gy/day).

The patient died of systemic progression of her malignant disease in June 2008.

Discussion

In this report, we have described a unique case of distant metastasis from a primary tumour other than the head-and-neck squamous cell carcinoma to temporary tracheostoma. Compared to patients with metastatic disease in tracheostomy sites originating from the head and neck primary tumour, several aspects should be emphasized. Metastasis in tracheostoma from head-and-neck cancer is a loco-regional progression of the disease, whereas in our patient the metastasis in the tracheostoma was the consequence of a systemic dissemination of remote malignant disease with haematogenous route of cancer cells spread as the most probable pathogenetic mechanism.

Colorectal cancer can metastasize even 15 years after treatment of the primary tumour.[8] In contrast, the incidence of distant metastases in the larynx is low, ranging from 0.09% to 2% of all malignant lesions in this location.[9,10] The preponderant primaries metastasizing to the larynx are cutaneous melanoma, followed by renal cell, breast and lung carcinomas; metastases of colorectal adenocarcinoma account for only 6% of all secondary laryngeal tumours.[11] The incidence of distant metastases in the trachea is even lower with breast carcinoma, colorectal carcinoma, melanoma, thyroid carcinoma, sarcomas, hepatocellular carcinoma, renal cell carcinomas and esthesioneuroblastoma being reported as origins of metastatic deposits.[12-14] Metastases to the larynx and trachea usually occur *via* a haematogenous route and are seldom lymphogenous.[9,11,12,14] They appear as endolaryngeal and endotracheal lesions and are considered to be locally advanced diseases with unfavourable prognoses.[11,12]

Comparison of histological and immunohistochemical characteristics of primary tumour and the metastasis helps to confirm the diagnosis, as was the case in our patient.[15] Considering the best

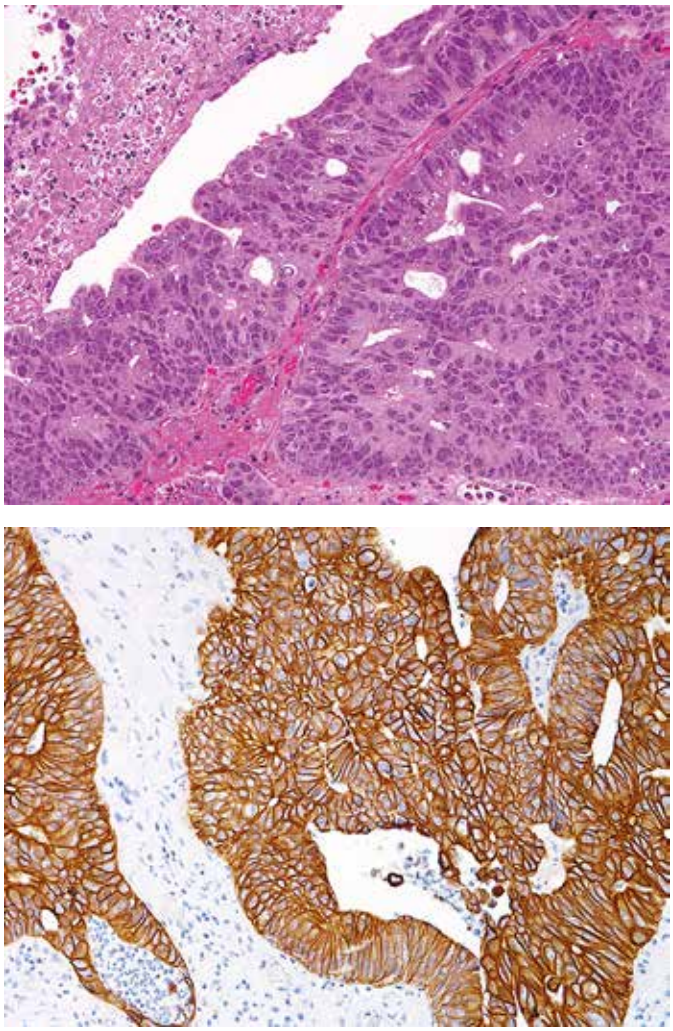

FIGURE 2. Adenocarcinoma metastatic to tracheostoma. **A.** Atypical tubular glandular structures with abundant necrosis, tumour cells show moderate cellular and nuclear polymorphism. **B.** Immunohistochemical reaction for cytokeratin 20 is strongly positive in tumour cells.

treatment option(s) in these patients, one must take into account the extent of the disease in the neck and other body sites (if present), and the patient's general performance and preference(s). Curative treatment scenarios are limited to patients without simultaneous metastases at other sites and depend on eventual previously established therapies.[9-11,15]

The newly created temporary tracheostoma is a surgical wound that heals by second intention. Formation of granulation tissue in the wound is usually abundant, creating a fertile bed for seeded neoplastic cells.[5,7,16] The latter could be explained by a rich vascular network and lack of inflammatory cells found in these granulations, resulting in a good distribution of nutrients and growth factors, and diminished immune reactivity. Accordingly,

we hypothesize that fresh granulations in the recently constructed temporary tracheostoma provided a fertile soil, although at an unusual site, for haematogenously metastasizing neoplastic cells of colorectal adenocarcinoma.

Conclusions

Our case clearly shows that in patients with temporary tracheostoma and history of primary cancer of any origin, including below the clavicles, careful follow-up is required. When exophytic proliferating masses around the tracheostoma are observed, a biopsy is mandatory to exclude malignancy. Unless other distant metastases had already been confirmed, an appropriate diagnostic work-up should be done. If temporary tracheostoma is the only site of metastatic disease, the intent of therapy should be curative; otherwise only palliative measures are indicated. The curative treatment can be surgical, consisting of resection of metastasis with extended laryngectomy, or radiotherapy with the inclusion of visible metastasis and potential sites of eventual microscopic disease in high-dose irradiation volumes. The type of primary treatment depends on the extent of the disease, previous therapy (if any) and the general condition and preferences of the patient.

References

1. Addams GL, Maisel RH. Malignant tumors of the larynx and hypopharynx. In: Cummings WC, Flint PW, Harker LA, editors. *Otolaryngology - head & neck surgery*. Philadelphia: Elsevier Mosby; 2005. p. 2222-83.
2. Barr GD, Robertson AG, Liu KC. Stomal recurrence: a separate entity? *J Surg Oncol* 1990; **44:** 176-9.
3. Griebie MS, Adams GL. "Emergency" laryngectomy and stomal recurrence. *Laryngoscope* 1987; **97:** 1020-4.
4. Halfpenny W, McGurk M. Stomal recurrence following temporary tracheostomy. *J Laryngolo Otol* 2001; **115:** 202-4.
5. Campbell AC, Gleich LL, Barret WL, Gluckman JL. Cancerous seeding of the tracheotomy site in patients with upper aerodigestive tract squamous cell carcinoma. *Otolaryngol Head Neck Surg* 1999; **120:** 601-3.
6. Qureshi SS, Chaukar DA, Dcruz AK. Isolated recurrence of tracheostomy site in non-laryngeal head and neck cancer. *J Postgrad Med* 2006; **52:** 233-4.
7. Armstrong M, Price JC. Tumor implantation in a tracheotomy. Otolaryngol *Head Neck Surg* 1992; **106:** 400-3.
8. Bosmans S, Weynand B, Coche E. Pulmonary metastatic microangiopathy of colon cancer presenting as a tree in bud pattern. *Br J Radiol* 2008; **81:** e11-2.
9. Ferlito A. *Diseases of the larynx*. London: Arnold Publications; 2000.
10. Marioni G, De Filippis C, Ottaviano G, Lorusso M, Staffieri C, Bernini G, et al. Laryngeal metastasis from sigmoid colon adenocarcinoma followed by peristomal recurrence. *Acta Otolaryngol* 2006; **126:** 661-3
11. Sano D, Matsuda H, Yoshida T, Kimura Y, Tanigaki Y, Mikami Y, et al. A case of metastatic colon adenocarcinoma in the larynx. *Acta Otolaryngol* 2005; **125:** 220-2.
12. Mattavelli F, Pizzi N, Pennacchioli E. Esthesioneuroblastoma metastatic to the trachea. *Acta Otorhinolaryngol Ital* 2009; **29:** 164-8.
13. Wood DE. Management of malignant tracheobronchial obstruction. *Surg Clin North Am* 2002; **82:** 621-42.
14. Franklin D, Miller RH, Bloom MG, Easley J, Stiernberg CM. Esthesioneuroblastoma metastatic to the trachea. *Head Neck Surg* 1987; **10:** 102-6.
15. Puxeddu R, Pelagatti CL, Ambu R. Colon adenacarcinoma metastatic to the larynx. *Eur Arch Otorhinolaryngol* 1997; **254:** 353-5.
16. Miller TC, Simental AA, Perez M. Sinonasal adenoid cystic carcinoma seeding to the tracheostomy site. *Laryngoscope* 2006; **116:** 661-2.

case report

Mediastinal teratoma with hydrops fetalis in a newborn and development of chronic respiratory insufficiency

Milanka Simoncic[1], Silvo Kopriva[1], Ziva Zupancic[2], Maja Jerse[3], Janez Babnik[4], Matevz Srpcic[5], Stefan Grosek[1]

[1] Department of Pediatric Surgery and Intensive Care, University Medical Centre Ljubljana, Ljubljana, Slovenia
[2] Institute of Radiology, University Medical Centre Ljubljana, Ljubljana, Slovenia
[3] Institute of Pathology, Faculty of Medicine, Ljubljana, Slovenia
[4] Department of Perinatology, Unit for Neonatal Intensive Care and Therapy, University Medical Centre Ljubljana, Ljubljana, Slovenia
[5] Department of Thoracic Surgery, University Medical Centre Ljubljana, Ljubljana Slovenia

Radiol Oncol 2014; 48(4): 397-402.

Received 28 June 2013
Accepted 24 July 2013

Correspondence to: Prof. Stefan Grosek, M.D., Ph.D., Associate Professor in Paediatrics, Department of Pediatric Surgery and Intensive Care, University Medical Centre Ljubljana, Bohoriceva 20, 1525 Ljubljana, Slovenia. E-mail: stefan.grosek@kclj.si or stefan.grosek@mf.uni-lj.si

Disclosure: No potential conflicts of interest were disclosed.

Background. Mediastinal fetal teratoma can be detected as a mass in the chest during a routine prenatal ultrasound screening. Because of the pressure on mediastinal structures it can be the cause of non-immune hydrops fetalis and polyhydramnion. The development of hydrops fetalis leads to fetal death or premature delivery in most reported cases. Early surgical removal is important, but, the result of treatment depends on the stage of development of mediastinal organs and complications in the postoperative period.

Case report. A 31-year-old *gravida* carrying twins, with spontaneous membrane rupture at 32 weeks gestation underwent urgent caesarean section after antenatal ultrasound revealed severe polyhydramnion and hydrops fetalis in geminus A. The child was intubated immediately after birth due to severe respiratory distress. Ultrasound and X-ray revealed a tumour mass in the right hemithorax. Tumour resection was performed at the age of 7 days. Histology examination revealed an encapsulated immature teratoma. The postoperative course was complicated with respiratory insufficiency which turned into chronic at the age of eight months.

Conclusion. This is the fifth reported child with fetal mediastinal teratoma and severe hydrops fetalis that survived the neonatal period. Additional diagnostic search revealed abnormal course of both pulmonary arteries, which was probably one of the main causes of respiratory insufficiency.

Key words: mediastinal teratoma; non-immune hydrops fetalis; diaphragm paralysis; chronic respiratory insufficiency

Introduction

Mediastinal teratomas are the second most common extragonadal teratomas in children.[1] There are some reports of mediastinal teratomas discovered as a mass in the chest with antenatal ultrasound (US) in fetal life.[2-8] Rapid growth in fetal life can compress lungs, heart and great vessels, which can lead to development of non-immune hydrops fetalis (NIHF).[7] High mortality can be prevented only by an early intervention at the onset of NIHF that dramatically improves deteriorating condition and survival rate of fetuses.[2-4]

If fetus with mediastinal teratoma survives until birth, tumour compression on mediastinal structures usually manifests with severe respiratory distress in newborn.[19-13] Early surgical excision is important, but outcome depends on several additional factors such as lung hypoplasia, the stage of heart development, tracheomalacia and peri- and

FIGURE 1. Geminus A with severe hydrops fetalis was intubated immediately after birth.

FIGURE 2. Chest x-ray after birth demonstrates large round tumour in the right hemithorax. (6 x 7 cm) with deviation of mediastinal structures to the left. Soft tissues of the thoracic wall are oedematous.

postoperative complications.[3,6-8,10] We present a case of mediastinal teratoma in a newborn associated with severe NIHF with several complications after birth and surgical procedure which led to the development of chronic respiratory insufficiency. This is the fifth reported case of a mediastinal teratoma with NIHF in which the newborn survived the neonatal period.

Case report

A 31-year-old *gravida* 2 with twins, *para* 1, was referred to the University Medical Centre Ljubljana because of spontaneous membrane rupture at 32 weeks gestation after an uncomplicated pregnancy. After admission US revealed polyhydramnion and severe NIHF in geminus A. Due to life threatening condition also for healthy geminus B an urgent caesarean section was performed. Geminus A was a boy with Apgar score 3/5 and a birth weight of 3,200 g. He was intubated immediately after birth because of severe NIHF and respiratory distress (Figure 1).

An initial arterial blood gas analysis revealed a respiratory acidosis with a pH of 6.91, $PaCO_2$ 19 kPa and HCO_3 of 13 mmol/l. US revealed anterior mediastinal cystic mass extending into the right and left hemithorax with marked pleural effusion bilaterally. Chest X-ray confirmed a homogenous mass in the anterior right hemithorax with shifting of the mediastinum to the left (Figure 2). Ductus arteriosus with left to right shunt was still patent. Because of pleural effusion pleural puncture was performed, further complicated by pneumothorax. Despite ventilation with high frequent oscillations respiratory acidosis still persisted with PCO2 between 10 and 15 kPa. Due to low blood pressure (mean arterial pressure 4 kPa) and very poor urine output he needed vasoactive support with dopamin and dobutamine. US of the heart showed signs of pulmonary artery hypertension. The diagnosis based on radiological finding was congenital cystic adenomatoid malformation, which needed surgical excision on day seven of life.

Right anterolateral thoracotomy was performed with removal of soft policystic encapsulated tumour without invading into the surrounding structures. Tumour was not connected to respiratory system and lungs were macroscopically normally developed. The surgical specimen measured 55 x 50 mm, weighed 54 g, and was extensively sampled.

Microscopically the tumour was predominantly, in 70%, composed by immature tissue derived from different germinal layers. Cystic areas were alternating with solid tissue. The majority of the tumour was characterized by immature neuroectodermal tissue. The elements of mature glial tis-

sue, ganglion cells and structures of choroid plexus were also randomly interspersed. Mesodermal tissue was represented by mature muscle, bone, adipose tissue, and mature and immature cartilage components with sparsely cellular mesenchymal tissue. The mature components of the tumour were also represented by the microfoci of hepatic differentiation, and pancreatic tissue, as well as sparse elements in the form of skin appendages (Figures 3,4,5). Serum human chorionic gonadotropin and alpha protein were within normal limits, and no further oncologic treatment was necessary.

Hydropic oedemas subsided three days after operation. Urine output and hemodynamic parameters were stable and we discontinued the vasoactive drug support one week after operation. Postoperative course was complicated by a spontaneous pneumothorax on the right side and a sepsis caused by *Staphylococcus epidermidis*. Fifteen days after operation, the newborn still needed support with synchronized intermittent mandatory ventilation. He had multiple spontaneous episodes of oxygen desaturation. We performed diagnostic rigid bronchoscopy with which we excluded changes in the bronchial system. US of the heart showed signs of pulmonary artery hypertension, persistent ductus arteriosus and patent *foramen ovale*. We started treatment with nitric oxide and selective inhibitor of phosphodiesterase type 5, with no improvement. Chest X-ray revealed hyperinflation of the left lung and high position of the diaphragm on the right side (Figure 6).

With electromyography we confirmed phrenic nerve palsy and right diaphragm paralysis. At 50 days of age, a second surgery was performed and the right diaphragm was plicated. He was extubated successfully 1 week after plication. After extubation the cyanosis and tachipnoea were periodically observed with paradoxical movement of the chest. Scintigraphy of the lungs revealed smaller right lung without regional perfusion or ventilation defects.

At 3 months of age, he was referred to the intensive care unit with respiratory distress, intubated and mechanically ventilated. Chest X-ray revealed pneumonia and right lung atelectasis. Computed tomography (CT) scan of the lungs again revealed a high position of the right diaphragm and a consolidation of the right and left lung. Due to multiple failures of weaning from mechanical ventilation and extubation one month after admission the third operation was performed with right diaphragm plication and lung biopsy. Biopsy of the

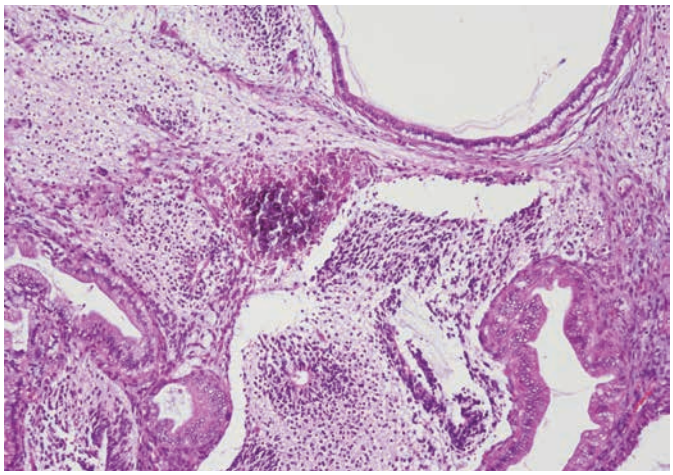

FIGURE 3. Focal calcification and the presence of cystic structures alternating with solid areas composed of mature and immature neural tissue.

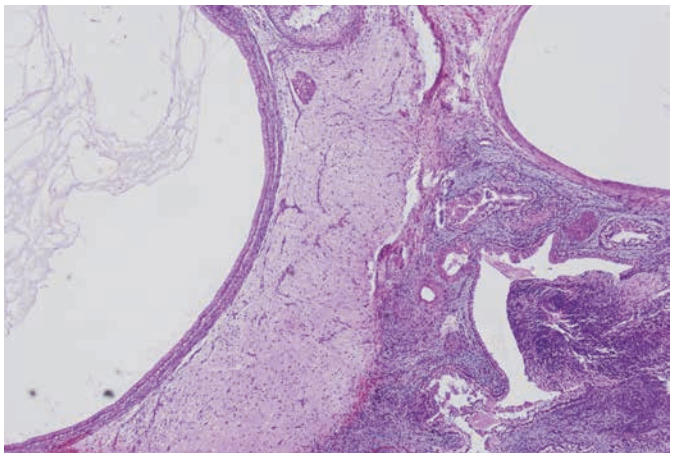

FIGURE 4. Cystic walls lined by columnar and cuboidal epithelium. Solid parts displaying brain tissue comprising of glia cells and primitive neuroepithelium.

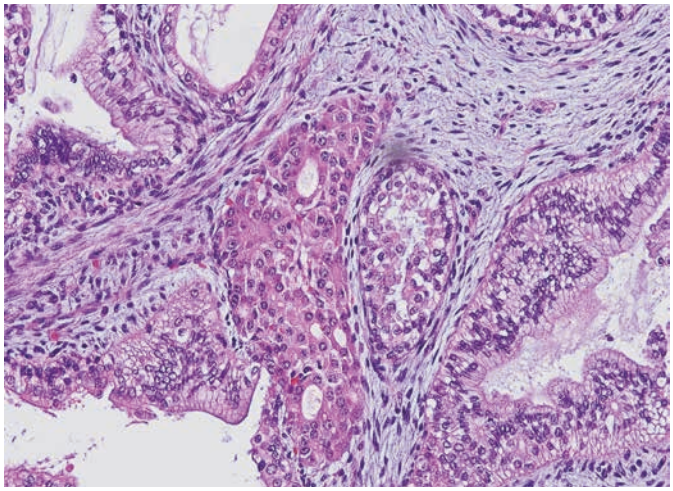

FIGURE 5. Gland-like structure with acinar epithelium resembling pancreatic tissue. Cystic formation embedded in a loose immature stromal tissue.

FIGURE 6. Chest x-ray demonstrates high position of the right diaphragm due to postoperative paralysis.

right lower lung lobe revealed acute interstitial pneumonia and alveolitis. After plication and antibiotic treatment, there was clear but slow improvement. He was extubated one month after plication and was well for one month.

At 6 months of age, he was again referred to the intensive care unit with dyspnoea, tachipnoea, cyanosis and severe respiratory acidosis with $PaCO_2$ 10 kPa. Bronchoscopy revealed narrowing of the left inferior bronchus. US of the heart showed structurally normal heart with the appropriate function of both ventricles. For further assessment of the cardiovascular function heart catheterization was performed, revealing an abnormal course of both pulmonary arteries with signs of pulmonary artery hypertension. Right middle lung lobe was practically without normal right pulmonary vascularisation. With no improvement in respiratory condition one month after treatment we decided for a tracheostomy. He was breathing with nasal continuous positive airway pressure ventilation (CPAP) on Legendair ventilator (Covidien AG™) with the addition of oxygen FiO2 0.25-0.35) after the procedure. We disconnected him from the ventilator in order to evoke spontaneous breathing several times per day.

At 11 months of age, paediatric neurologist made a neurologic assessment. He had severe generalized muscle hypotonia, a convergent strabismus and normal proprioceptive reflexes. Babinski sign was still present. Magnetic resonance imaging (MRI) confirmed atrophic frontal brain changes. We excluded metabolic diseases.

At 1 year of age, the boy was discharged from hospital in a stable clinical respiratory condition with tracheostomy and Legendair ventilator. At the age of 2 years, bronchoscopy revealed massive granulation in trachea just below the tracheostoma. After removal of the granulation the tracheostoma was closed and he is breathing on his own.

Discussion

Mediastinal tumours can be detected before birth by routine antenatal US, most frequently during second and third trimester. With an US we can determine the location of the tumour, pressure on mediastinal structures, cystic or solid tumour components, development of NIHF and polyhydramnion.[14] With fetal MRI we can obtain more precise information about the tumour and its relationship to adjacent structures.[2,4,14] Neonatal outcome depends on the size and location of the tumour, presence of NIHF and early prenatal or perinatal intervention.[12-4,13]

Liang *et al*. evaluated the influence of intrathoracic mass on fetal hemodynamics with Doppler flow velocimetry. They showed in their case that the main changes occurred in the heart and great vessels.[5] On the other hand NIHF indicates that tumour causes intrauterine pressure on the heart and major blood vessels.[7] It is expressed with oedema, ascites, pleural effusion, and hepatomegaly.[2,3] NIHF and polyhydramnion are poor prognostic signs.[3] Pressure in the thorax leads to the development of heart dysplasia and lung hypoplasia with reported death prenatally and after birth.[7,8,15,16] Polyhydramnion develops due to pressure on the oesophagus and decreased swallowing of amniotic fluid.[17]

We found only four reported cases with prenatal identified NIHF caused by mediastinal teratoma, who survived the neonatal period (Table 1).[2-4] In these cases different approaches were used for a successful outcome. In the case by Takayasu *et al*. NIHF resolved immediately after aspiration of the tumour cyst.[4] Merchant *et al.* recommend *in utero* resection of tumour if NIHF develops before 30 weeks gestation. After 30 weeks gestation it is important to evaluate lung development and airway

TABLE 1. Clinical neonatal successfull outcome of fetal mediastinal teratomas with hydrops fetalis

Author/No.	Sex	Imaging	Prenatal procedure	Outcome	Histology
Takayasu[4]	M	US (23 WG): Cystic formation in right anterior mediastinum MRI (29 WG): Cystic/solid mass, NIHF, polyhydramnion	Aspiration of the fetal tumour cyst fluid, Amniocentesis	Hydrops fetalis subsided No RD after birth Resection 30 days after birth NED	Mature teratoma
Giancotti[3]	M	US (29 WG): Anterior mediastinal mass MRI (31 WG): Anterior mediastinal mass, NIHF, polyhydramnion US (32 WG): Rapid growing mass	No	Elective cesarion section (32 WG) RD after birth, resection 1day after birth Left vocal cord/left diaphragm paralysis 18 day after birth diaphragm plication No respiratory problem	Teratoma
Merchant[2]	ND	US (21 WG): Anterior mediastinal mass MRI (22 WG): Anterior mediastinal mass with displacement of the heart, calcification, NIHF	*In utero* resection of the tumour	Preterm labour (25 WG) Bronchopulmonary dysplasia Well at home	Immature teratoma
Merchant[2]	ND	US/MRI (34 WG) Anterior mediastinal mass, calcifications, NIHF, polyhydramnion	Amnioreductions	EXIT procedure with tumour resection Well at home	Immature teratoma
Present case	M	US (33 WG) NIHF, polyhydramnion	No	Urgent cesarion section (33 WG) RD after birth, resection 7 days after birth Chronic respiratory insuficiency 8 month after procedure	Immature teratoma

M = male; MRI = magnetic resonance imaging; ND = no data; NED = no evidence of disease; NIHFb = non-immune hydrops fetalis; RD = respiratory distress; US = ultrasound; WG = weeks gestation

compromise. If the child's airway is compromised we can use *ex-utero* intrapartum treatment (EXIT procedure) to establish ventilation.[2] Giancotti *et al.* reported a prenatally discovered mediastinal tumour with NIHF and resection one day after birth.[3] In our case regular US were normal up to 30 weeks gestation. After spontaneous membrane rupture in 32 weeks gestation severe NIHF in geminus A and polyhydramnion were discovered. This indicates that tumour growth was fast with severe pressure on mediastinal structures.

Mediastinal teratomas without NIHF that were not discovered prenatally presented with severe respiratory distress in a live newborn after birth. In all cases surgery was performed with removal of the tumour, and mortality in this group was low.[9-13]

Postoperative course was complicated with severe tracheomalacia, wound sepsis and chyle leak in the Mogilner *et al*. case.[10] Some authors described diaphragm paralysis with necessary plication after surgery.[3,6] We found only one case in literature with prenatal collapse of the left bronchial system and tracheostomy after surgery at the age of 5 weeks.[6]

Seo *et al.* reported support with extracorporeal membrane oxygenation after surgery, but in this case a congenital cystic adenomatoid malformation, stocker type III (stocker-III CCAM) was later confirmed and the child had profound persistent fetal circulation postoperatively. Other authors do not mention using extracorporeal membrane oxygenation in children with mediastinal teratoma. In our case, the child had in addition to anatomical changes in the pulmonary vessels several risk factors for the development of chronic respiratory insufficiency including diaphragm paralysis, prematurity and several respiratory infections.

Heart catheterization in our case showed that tumour compression in prenatal period had an impact on the anatomy of mediastinal organs.

In conclusion, it is important to decide for early intervention if NIHF develops. Advances in ra-

diologic imaging prenatally and after birth are the main tools for diagnostic evaluation of the disease. In cases when NIHF develops the outcome is mainly unpredictable because short and long term *sequelae* of combined effects of NIHF and teratoma pressure on neighboring organs may develop as we presented with our case.

References

1. Barksdale E, Obokhare I. Teratomas in infants and children. *Curr Opin Pediatr* 2009; **21:** 344-49.
2. Merchant AM, Hedrick HL, Johnson MP, Wilson RD, Crombleholme TM, Howell LJ, et al. Management of fetal mediastinal teratoma. *J Pediatr Surg* 2005; **40:** 228-31.
3. Giancotti A, La Torre R, Bevilacqua E, D'Ambrosio V, Pasquali G, Panici PB. Mediastinal masses: a case of fetal teratoma and literature review. *Clin Exp Obstet Gynecol*. 2012; **39:** 384-7.
4. Takayasu H, Kitano Y, Kuroda T, Kuroda T, Morikawa N, Tanaka H, et. al. Successful management of a large fetal mediastinal teratoma complicated by hydrops fetalis. *J Pediatr Surg* 2012; **45(12):** e21-4.
5. Liang R, Wang P, Chang FM, Chang CH, Yu CH. Prenatal sonographic characteristics and Doppler blood flow study in a case of a large fetal mediastinal teratoma. *Ultrasound Obstet Gynecol* 1998; **11:** 214-8.
6. Dumbell HR, Coleman AC, Pufidin JM, Winship WS. Prenatal ultrasonographic diagnosis and successful management of mediastinal teratoma, A case report. *S Afr Med J* 1990; **78:** 481-3.
7. Froberg MK, Brown RE, Maylock J, Poling E. In utero development of a mediastinal teratoma: a second-trimester event. *Prenat Diagn* 1994; **14:** 884-7.
8. Aksoy F, Sen C, Danisment N. Congenital mediastinal immature teratoma: a case report with autopsy findings. *Turk J Pediatr* 2002; **44:** 76-9.
9. Kuroiwa M, Suzuki N, Takahashi A, Ikeda H, Hatekeyama S, Matsuyama S, et al. Life- threatening mediastinal teratoma in a neonate. *Pediatr Surg Int* 2001, **17:** 235-8.
10. Mogilner JG, Fonseca J, Davies MR. Life-threatening respiratory distress caused by a mediastinal teratoma in a newborn. *J Pediatr Surg* 1992; **27:** 1519-20.
11. Takrouri MS, Al-Qahtani A, Ali AM, Al Shakweer W, Kalou MM, Radwan SM. Management of neonatal massive anterior mediastinal teratoma. A case report. *Middle East J Anesthesiol* 2009; **20:** 461-4.
12. Lakhoo K, Boyle M, Drake DP. Mediastinal teratomas: rewiev of 15 pediatric cases. *J Pediatr Surg* 1993; **28:** 1161-4.
13. Kreller-Laugwitz G, Kobel H, Opermann HF. [Mediastinal teratoma in a newborn infant]. [German]. *Monatsschr Kinderheilkd* 1988; **136:** 270-2.
14. Avni FE, Massez A, Cassart M. Tumours of the fetal body: a review. *Pediatr Radiol* 2009; **39:** 1147-57.
15. Noreen S, Heller DS, Faye-Petersen O. Mediastinal teratoma as a rare cause of hydrops fetalis and death: report of 3 cases. *J Reprod Med* 2008; **53:** 708-10.
16. Kuller JA, Laifer SA, Martin JG, MacPherson TA, Mitre B, et al. Unusual presentation of fetal teratoma. *J Perinatol* 1991; **11:** 294-6.
17. Seo T, Ando H, Watanabe Y, Harada T, Ito F, Kaneko K, et al. Acute respiratory failure associated with intrathoracic masses in neonates. *J Pediatr Surg* 1999; **34:** 1633-7.

research article

Effectiveness of adjuvant trastuzumab in daily clinical practice

Erika Matos, Branko Zakotnik, Cvetka Grasic Kuhar

Institute of Oncology Ljubljana, Department of Medical Oncology, Ljubljana, Slovenia

Radiol Oncol 2014; 48(4): 403-407.

Received 30 August 2013
Accepted 14 October 2013

Correspondence to: Erika Matos, M.D., M.Sc., Institute of Oncology Ljubljana, Department of Medical Oncology, Zaloška 2, SI-1000 Ljubljana, Slovenia. E-mail. ematos@onko-i.si

Disclosure: No potential conflicts of interest were disclosed.

Background. Human epidermal growth factor receptor 2 (HER2) positive breast cancer is an entity with aggressive behaviour. One year of adjuvant trastuzumab significantly improves the disease free survival in the range of 40-50% and reduces the risk of dying from HER2 positive breast cancer by one third. Adjuvant treatment with trastuzumab became available in Slovenia in 2005 and the aim of this study is to explore, if the exceptional results reported in adjuvant clinical trials are achieved also in daily clinical practice.

Patients and methods. An analysis of tumour and patient characteristics, type of treatment and outcome (relapse free and overall survival) of 313 patients (median age 52 years) treated at the Institute of Oncology Ljubljana in years 2005-2009 was performed.

Results. Median follow-up was 4.4 years. Sixty-one patients relapsed and 24 died. Three and four years relapse free survival was 84.2% and 80.8% and the overall survival was 94.4% and 92.5%, respectively. Independent prognostic factors for relapse were tumour grade (HR 2.10; 95% CI 1.07-4.14; p = 0.031) and nodal stage (HR 1.35; 1.16-1.56; p < 0.0001) and for the overall survival nodal stage only (HR 1.36; 1.05-1.78; p = 0.021).

Conclusions. The outcome in patients with adjuvant trastuzumab in daily clinical practice, treated by medical oncologists, is comparable to results obtained in international adjuvant studies.

Key words: breast cancer; trastuzumab, adjuvant; daily clinical practice

Introduction

The most common cancer in women in the developed world as well as in Slovenia is breast cancer (BC).[1] With the introduction of the tumour gene signature the clinical observation that BC is a spectrum of different diseases in terms of prognosis and response to the treatment was confirmed.[2] Using this tool as well as by classical clinico-pathological parameters four types of BCs can be distinguished and human epidermal growth factor receptor 2 (HER2) positive type is one of them, representing about 15% of newly diagnosed invasive BCs.[2-4] It is a unique entity with an aggressive behaviour, characterized by overexpression of HER2 receptor and/or HER2 gene amplification.[3,5] At the beginning of this century, trastuzumab, a humanized monoclonal antibody, that targets HER2 receptor, was approved for the treatment of patients with metastatic HER2-positive BC.[6-8] Given the success of this antiHER2 drug in the metastatic setting, several large, randomized trials were initiated to evaluate its role in the early stage disease. The first results were presented in 2005 and were the basis for the approval of one year adjuvant treatment of patients with HER2 positive BC.[9-11] A significant improvement in disease free survival (DFS) in the range of 40-50% was demonstrated and the risk from dying from BC was reduced by about one third. Reported 4-year DFS and the overall survival (OS) in the trastuzumab arms were 78.6-86% and 89.3-94%, respectively.[12-15] This is the range of benefit seldom achieved in oncology. In the proceeding years new antiHER2 drugs confirmed their activity in metastatic setting; *i.e.* lapatinib, pertuzumab

and trastuzumab-emtansine.[16-18] Adjuvant studies with new antiHER2 drugs are in progress.

The adjuvant treatment with trastuzumab became available in Slovenia in 2005 and the aim of this report is to explore if these exceptional results reported in adjuvant clinical trials are achieved also in daily clinical practice.

Patients and methods

With the approval of the adjuvant trastuzumab treatment the Slovenian HER2 registry was set up. The criteria for the adjuvant treatment with trastuzumab regarding tumour and nodal stage and cardiac function were the same as in pivotal adjuvant trials: tumours larger then 2 cm if node negative disease, any tumour size if node positive disease, performance status zero or one, no serious concomitant cardiac diseases and treatment with adjuvant chemotherapy.[9-11] Data were collected from patient's records. Patients were treated at the Institute of Oncology Ljubljana.

The study was approved by the institutional review board committed.

The main objective of this project was to evaluate the outcome of our real life patient population: relapse free survival (RFS) and OS. We compared our results with the results from randomized studies and other population-based studies.

Statistical analysis

RFS was defined as time elapsed from date of surgery to date of the first relapse (local or distant), date of the last follow-up or date of death without relapse. Patients who died without relapse were censored at time of death. OS was defined as time from surgery to date of death of any cause or date of the last follow-up for patients who were alive. The univariate statistical analysis was performed using Kaplan-Meier method and log-rank test. The multivariate analysis was performed with Cox proportional hazards model. SPSS software version 16 was used for the statistical analysis.

Results

In the 5-year period (2005-2009) 313 patients with HER2 positive BC were treated with adjuvant trastuzumab. The median age of the patients was 52 years (23–76). Median follow-up time was 4.4 years (minimum 0.2 years, maximum 6.9 years). The characteristics of the tumours are presented in Table 1. One hundred and twenty-seven (40%) of patients received an anthracycline-based and 165 (53%) anthracycline- and taxane-based chemotherapy. One hundred and seventy-six (56%) of patients had estrogen receptor (ER) and 130 (42%) of patients had progesterone receptor (PR) positive tumours. All patients with hormone dependent tumours (187 [60%]) were also treated with adjuvant endocrine therapy. Two hundred and seven (66%) patients

TABLE 1. Tumour characteristics of 313 patients

		No.	
Histology	IDC	297	95%
	ILC	6	2%
	Other	10	3%
Tumor grade	I	3	1%
	II	84	27%
	III	220	70%
	Unknown	6	2%
Mitotic index	1	44	14%
	2	94	30%
	3	131	42%
	Unknown	44	14%
Vascular invasion	Present	15	5%
	Absent	186	60%
	Unknown	112	35%
Hormonal receptor status	ER positive	176	56%
	ER negative	137	44%
	PR positive	130	42%
	PR negative	180	58%
	ER and PR negative	126	40%
	Unknown	1	0%
Tumour stage	T1	88	28%
	T2	152	48%
	T3	34	11%
	T4	8	3%
	T4d	25	8%
	Unknown	6	2%
Nodal stage	N0	79	25%
	N1	157	50%
	N2	51	16%
	N3	24	8%
	Unknown	2	1%

ER = estrogen receptor; IDC = invasive ductal carcinoma; ILC = invasive lobular carcinoma; PR = progesterone receptor

TABLE 2. Relapse free survival (univariate analysis)

	HR (95% CI)	P value
Tumour stage	1.25 (1,11-1.40)	< 0.0001
Nodal stage	1.42 (1,23-1.64)	< 0.0001
ER status	1.14 (0,68-1.90)	0.62
PR status	0.82 (0,49-1.36)	0.43
Tumour grade	1.91 (0,98-3.72)	0.059
Mitotic index	1.35 (0,89-2.03)	0.157
Histological type*	1.12 (0,99-1.27)	0.081
Vascular invasion	1.04 (0,98-1.10)	0.162
Chemo – type**	1.29 (0.85-1.98)	0.237

* invasive ductal carcinoma, invasive lobular carcinoma, other types
** anthracycline-based, anthracycline- and taxane-based, other types of chemotherapy; ER = estrogen receptor; PR = progesterone receptor

TABLE 3. Relapse free survival (multivariate analysis). No. of events: 61/313

	HR (95% CI)	P VALUE
Tumour grade	2.10 (1.07-4.14)	0.031
Nodal stage	1.35 (1.16-1.56)	< 0.0001
Tumour stage	1.19 (1.04-1.36)	0.014

TABLE 4. Overall survival (univariate analysis). No. of events: 24/313

	HR (95% CI)	P VALUE
Tumour stage	1.17 (0,94-1,46)	0.155
Nodal stage	1.36 (1,05-1,78)	0.021
ER status	1.22 (0,54-2,80)	0.633
PR status	0.87 (0,39-1,96)	0.733
Tumour grade	2.49 (0,75-8,26)	0.136
Mitotic index	1.63 (0,82-3,24)	0.162
Histological type*	1.12 (0,49-1,35)	0.211
Vascular invasion	1.01 (0,92-1,11)	0.821
Chemo – type**	0.84 (0,40-1,74)	0.632

* invasive ductal carcinoma, invasive lobular carcinoma, other types
** anthracycline-based, anthracycline- and taxane-based, other types of chemotherapy; ER = estrogen receptor; PR = prgesterone receptor

were concomitantly with trastuzumab irradiated to the chest wall, breast and supraclavicular region, according to the international guidelines.[19]

Relapse free survival (RFS)

Sixty-one patients (19.5%) relapsed. Kaplan-Mayer curve for RFS is presented on Figure 1. RFS at 4 years was 80.8%. Tumour stage and grade and nodal stage were found to have a significant impact on RFS in univariate analysis (Table 2). In the multivariate analysis only tumour grade (Hazard ratio [HR] 2.10) and nodal stage (HR 1.35) were found to have independent prognostic role (Table 3).

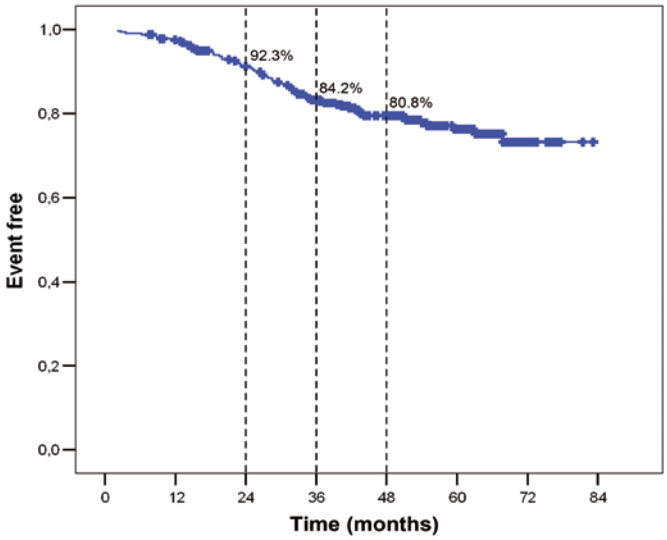

FIGURE 1. Relapse free survival (RFS).

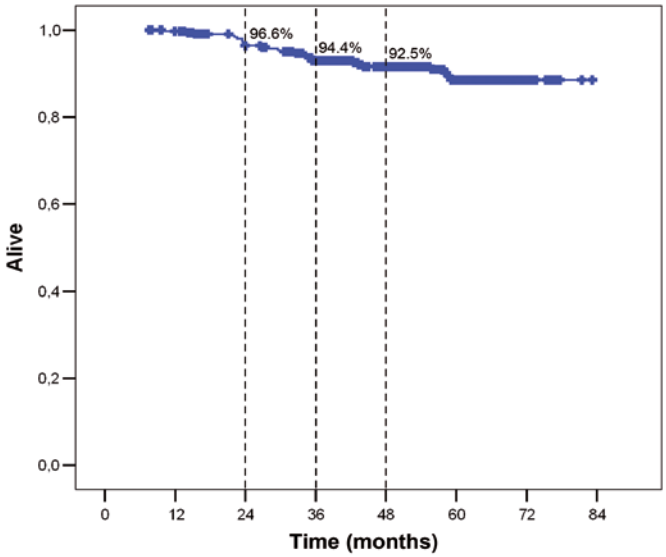

FIGURE 2. Overall survival (OS).

Overall survival (OS)

Twenty-four patients (7.6%) died. Kaplan-Meier survival curve is on Figure 2. OS at 4 years was 92.5%. For OS nodal stage was found to be the only statistically significant factor (HR 1.36) (Table 4).

Discussion

The results of our institutional study are confirming the benefit of one year adjuvant trastuzumab treatment in daily practice. The magnitude of benefit was in the range of randomized studies; RFS at 4 years was 80.8% and OS 92.5%, respectively.

HER2 positive BC is a disease with an aggressive behaviour. Before the era of antiHER2 treatment the estimated 4-5 years OS rate was 75-87%. With the introduction of one year adjuvant trastuzumab the OS of these patients has improved significantly, according to the results of large international studies by about one third.[12-14] In Slovenia, trastuzumab was rapidly implemented in the daily management after the release of these data, in the second half of 2005 already. It is well known that real life population is different to selected study population. In real world patients usually have more concomitant disease, are not as compliant as study population, cardiac follow-up is not done so often; all these factors can consequently result in worse results. The aim of our study was to assess the benefit of one year adjuvant trastuzumab treatment in our real life BC patients and to compare it with the results obtained in randomized clinical studies and other published population-based studies.

In Slovenia with two million inhabitants and about 1200 newly diagnosed BCs yearly at the time of the start of this retrospective observational study we had one comprehensive cancer centre, Institute of Oncology Ljubljana.[20] This is important data since the adjuvant trastuzumab treatment was preceded at this institution only and not many patients were lost from registration and follow up in the database. The median age of 313 patients included in the study was 52 years. This is comparable to international studies in which 50 to 55% of patients were younger then 50 years.[9-14] Our patients had larger tumours compared to patients in international studies if a B-31 part of North American study population is excluded in which node negative patients were not included.[11] Seventy-six percent of patients had tumours T1 and T2 and only 25% of patients had node negative disease. In comparable international studies 80-90% of patients had tumours smaller then 5 cm. Thirty-three and 30% of patients had node negative disease in HERA and BCIRG 006 study, respectively.[9,10] On the contrary, in the Dutch cohort of 479 HER2 positive BC patients 55% had node positive disease.[21] The aggressiveness of this type of BC could be reflected by larger volume of the disease at the first presentation and higher tumour grade. There were 70% of high grade tumours in our population and this is comparable to North American study population.[11] Only 14% of tumours were of low mitotic index. Regarding the hormonal receptor status our cohort of patients did not differ to historical cohorts.[9-11] It is known that about 50% of HER2 positive BCs have positive estrogen and/or progesterone receptors and this was alike in our population.[22]

Adjuvant chemotherapy was as in clinical studies.[9-14] Anthracycline-based chemotherapy was given before trastuzumab, taxane-based chemotherapy concurrently with trastuzumab. More than 90% of patients were treated with either anthracycline- or anthracycline- and taxane-based chemotherapy. Adjuvant endocrine therapy was prescribed according to international guidelines, after adjuvant chemotherapy and concomitantly with adjuvant trastuzumab. Locoregional radiotherapy was delivered to 66% of patients; the dose and the schedule were according to international guidelines.[19]

Tumour grade and nodal involvement were the only independent prognostic factors for the relapse (Table 3). Nodal stage was the only prognostic factors for OS. Also in North American study the tumour and nodal stage were found to be factors significantly important for both, DFS and OS. In that study especially patients with more than 10 lymph nodes involved were at the highest risk and gained the highest absolute improvement with adjuvant trastuzumab.[11,14] Although RFS and DFS are not fully comparable (less events in RFS), the outcome of our non-study population is comparable to the results obtained in the international studies.[12-14] The Dutch retrospective cohort study reports similar results; five years DFS and OS was 81% and 91%, respectively.[21]

Despite indisputable efficacy of adjuvant trastuzumab treatment some questions still remain. One of them, the optimal treatment duration, was mainly resolved after obtaining results of HERA study, which showed that two years of adjuvant treatment was not more effective than one year.[23] Shorter regimens like in FinHER study[24] were not confirmed in PHARE and ShortHER studies.[25,26] St. Gallen consensus 2013 showed almost 100% agreement among panel discussant regarding one year lasting duration of the adjuvant trastuzumab treatment.[19] There are new promising antiHER2 drugs, namely pertuzumab and trastuzumab-emtansine, which have already proven their effectiveness in the metastatic setting and will probably even improve the impressing results of trastuzumab.[17,18]

We think that our results also indicate the advantage of being treated by highly educated specialists (all treating physicians were medical oncologists), in high volume oncological center and with regular cardiac function evaluation. A prospective study of cardiotoxicity of trastuzumab in adjuvant setting is underway at our institution to show putative early and long term side effects.

Conclusions

The prognosis of HER2 positive BC has improved significantly since the introduction of antiHER2 treatment. Our results based on the treatment of real-life BC patients with one year of adjuvant trastuzumab are comparable to the results obtained in international clinical studies.

References

1. Schillani G, Era D, Cristante T, Mustacchi G, Richiardi M, Grassi L, et al. 5-HTTLPR polymorphism and anxious preoccupation in early breast cancer patients. *Radiol Oncol* 2012; **46:** 321-7.
2. Sotiriou C, Pusztai L. Gene-expression signatures in breast cancer. *N Engl J Med* 2009; **360:** 790-800.
3. Slamon DJ, Godolphin W, Jones LA, Holt JA, Wong SG, Keith DE, et al. Studies of the HER-2/neu proto-oncogene in human breast and ovarian cancer. *Science* 1989; **244:** 707-12.
4. Tuzi A, Lombardi D, Crivellari D, Militello L, Perin T, La Grassa M, Massarut S, Veronesi A. Epirubicin and docetaxel as neoadjuvant treatment of hormone receptor positive, HER-2 negative breast cancer: findings from two successive phase II studies. *Radiol Oncol* 2013; **47:** 57-62.
5. Slamon DJ, Clark GM, Wong SG, Levin WJ, Ullrich A, McGuire WL. Human breast cancer: correlation of relapse and survival with amplification of the HER-2/neu oncogene. *Science* 1987; **235:** 177-82.
6. Slamon DJ, Leyland-Jones B, Shak S, Fuchs H, Paton V, Bajamonde A, et al. Use of chemotherapy plus a monoclonal antibody against HER2 for metastatic breast cancer that overexpresses HER2. *N Engl J Med* 2001; **344:** 783-92.
7. Smith IE. Efficacy and safety of Herceptin in women with metastatic breast cancer: results from pivotal clinical studies. *Anticancer Drugs* 2001; **12(Suppl 4):** S3-10.
8. Marty M, Cognetti F, Maraninchi D, Snyder R, Mauriac L, Tubiana-Hulin M, et al. Randomized phase II trial of the efficacy and safety of trastuzumab combined with docetaxel in patients with human epidermal growth factor receptor 2-positive metastatic breast cancer administered as first-line treatment: the M77001 study group. *J Clin Oncol* 2005; **23:** 4265-74.
9. Piccart-Gebhart MJ, Procter M, Leyland-Jones B, Goldhirsch A, Untch M, Smith I, et al. Trastuzumab after adjuvant chemotherapy in HER2-positive breast cancer. *N Engl J Med* 2005; **353:** 1659-72.
10. Slamon D, Eiermann W, Robert N. Phase III randomized trial comparing doxorubicin and cyclophosphamide followed by docetaxel (ACT) with doxorubicin and cyclophosphamide followed by docetaxel and trastuzumab (ACTH) with docetaxel, carboplatin and trastuzumab (TCH) in HER2 positive early breast cancer patients: BCIRG 006 study. [Abstract]. *Breast Cancer Res Treat* 2005; **94(Suppl 1):** A-1.
11. Romond EH, Perez EA, Bryant J, Suman VJ, Geyer CE Jr, Davidson NE, et al. Trastuzumab plus adjuvant chemotherapy for operable HER2-positive breast cancer. *N Engl J Med* 2005; **353:** 1673-84.
12. Gianni L, Dafni U, Gelber RD, Azambuja E, Muehlbauer S, Goldhirsch A, et al. Treatment with trastuzumab for 1 year after adjuvant chemotherapy in patients with HER2-positive early breast cancer: a 4-year follow-up of a randomised controlled trial. *Lancet Oncol* 2011; **12:** 236-44.
13. Slamon D, Eiermann W, Robert N, Pienkowski T, Martin M, Press M, et al. Adjuvant trastuzumab in HER2-positive breast cancer. *N Engl J Med* 2011; **365:** 1273-83.
14. Perez EA, Romond EH, Suman VJ, Jeong JH, Davidson NE, Geyer CE Jr, et al. Four-year follow-up of trastuzumab plus adjuvant chemotherapy for operable human epidermal growth factor receptor 2-positive breast cancer: joint analysis of data from NCCTG N9831 and NSABP B-31. *J Clin Oncol* 2011; **29:** 3366-73.
15. Matos E, Čufer T. Adjuvant treatment of breast cancer patients with trastuzumab. *Radiol Oncol* 2007; **3:** 115-22.
16. Ulhoa-Cintra A, Greenberg L, Geyer CE. The emerging role of lapatinib in HER2-positive breast cancer. *Curr Oncol Rep* 2008; **10:** 10-7.
17. Blumenthal GM, Scher NS, Cortazar P, Chattopadhyay S, Tang S, Song P, et al. First FDA approval of dual anti-HER2 regimen: pertuzumab in combination with trastuzumab and docetaxel for HER2-positive metastatic breast cancer. *Clin Cancer Res* 2013; **19:** 1-6.
18. Ballantyne A, Dhillon S. Trastuzumab emtansine: first global approval. *Drugs* 2013; **73:** 755-65.
19. Goldhirsch A, Winer EP, Coates AS, Gelber RD, Piccart-Gebhart M, Thürlimann B, et al. Personalizing the treatment of women with early breast cancer: highlights of the St Gallen International Expert Consensus on the Primary Therapy of Early Breast Cancer 2013. *Ann Oncol* 2013; **24:** 2206–23.
20. *Cancer in Slovenia 2009.* Ljubljana: Institute of Oncology Ljubljana, Epidemiology and Cancer Registry, Cancer Registry of Republic of Slovenia; 2013.
21. Tjan-Heijnen VCG, Seferina SC, Lobbezoo DJA, Voogd AC, Dercksen MW, van den Berkmortel F, et al. Real-world use and effectiveness of adjuvant trastuzumab in 2665 consecutive breast cancer patients. [Abstract]. *Cancer Res* 2012; **72(24 Suppl):** Nr P5-21-04.
22. Nahta R, O'Regan RM. Therapeutic implications of estrogen receptor signaling in HER2-positive breast cancers. *Breast Cancer Res Treat* 2012; **135:** 39-48.
23. Goldhirsch A, Gelber RD, Piccart-Gebhart MJ, de Azambuja E, Procter M, Suter TM, et al. 2 years versus 1 year of adjuvant trastuzumab for HER2-positive breast cancer (HERA): an open-label, randomised controlled trial. *Lancet* 2013; **382(9897):** 1021-8.
24. Joensuu H, Bono P, Kataja V, Alanko T, Kokko R, Asola R, et al. Fluorouracil, epirubicin, and cyclophosphamide with either docetaxel or vinorelbine, with or without trastuzumab, as adjuvant treatments of breast cancer: final results of the FinHer Trial. *J Clin Oncol* 2009; **27:** 5685-92.
25. Pivot X, Romieu G, Bonnefoi H, Pierga J-Y, Kerbrat P, Guastalla J-P, et al. PHARE Trial results of subset analysis comparing 6 to 12 months of trastuzumab in adjuvant early breast cancer. [Abstract]. *Cancer Res* 2012; **72(24 Suppl):** Nr S5-3.
26. Guarneri V, Frassoldati A, Bruzzi P, D'Amico R, Belfiglio M, Molino A, et al. Multicentric, randomized phase III trial of two different adjuvant chemotherapy regimens plus three versus twelve months of trastuzumab in patients with HER2- positive breast cancer (Short-HER Trial; NCT00629278). *Clin Breast Cancer* 2008; **8:** 453-6.

research article

A method for generating large datasets of organ geometries for radiotherapy treatment planning studies

Nan Hu[1,2,3], Laura Cerviño[2], Paul Segars[4], John Lewis[2], Jinlu Shan[4], Steve Jiang[2], Xiaolin Zheng[3], Ge Wang[1]

[1] Department of Radiation Oncology, Cancer Center,Research Institute of Surgery, Daping Hospital, Third Military Medical University, China
[2] Department of Radiation Oncology, University of California, San Diego, USA
[3] College of Bioengineering, Chongqing University, China
[4] Department of Radiology, Duke University, USA

Radiol Oncol 2014; 48(4): 408-415.

Received: 19 July, 2013
Accepted: 11 October, 2013

Correspondence to: Xiaolin Zheng, College of Bioengineering, Chongqing University, China. E-mail: xlzhengcqu@163.com Ge Wang, Department of Radiation Oncology, Cancer Center, Chongqing Daping Hospital, Third Military Medical University, China. E-mail: dpwangge1968@126.com

Disclosure: No potential conflicts of interest were disclosed.

Background. With the rapidly increasing application of adaptive radiotherapy, large datasets of organ geometries based on the patient's anatomy are desired to support clinical application or research work, such as image segmentation, re-planning, and organ deformation analysis. Sometimes only limited datasets are available in clinical practice. In this study, we propose a new method to generate large datasets of organ geometries to be utilized in adaptive radiotherapy.

Methods. Given a training dataset of organ shapes derived from daily cone-beam CT, we align them into a common coordinate frame and select one of the training surfaces as reference surface. A statistical shape model of organs was constructed, based on the establishment of point correspondence between surfaces and non-uniform rational B-spline (NURBS) representation. A principal component analysis is performed on the sampled surface points to capture the major variation modes of each organ.

Results. A set of principal components and their respective coefficients, which represent organ surface deformation, were obtained, and a statistical analysis of the coefficients was performed. New sets of statistically equivalent coefficients can be constructed and assigned to the principal components, resulting in a larger geometry dataset for the patient's organs.

Conclusions. These generated organ geometries are realistic and statistically representative.

Key words: non-uniform rational B-spline technique; new geometries; statistical shape model; adaptive radiotherapy

Introduction

In recent years, clinical linear accelerators combined with cone-beam computed tomography (CBCT) have become available, and they provide valuable 3D geometric information of patients. This combination offers the advantage of incorporating daily images into the radiotherapy process, such as setup-error correction, dose accumulation[1-4], evaluation and re-planning[5,6], and re-optimization[7,8], which are essential for adaptive radiotherapy (ART).[9-15]

ART integrated with CBCT[16], which uses the daily geometric information to adjust, in each fraction, the treatment plan to the updated patient's anatomy and positioning, significantly improves the accuracy and success of the radiation therapy.[17-19] Image registration between the planning image and daily CBCT images, dose reconstruction, and treatment evaluation were basically employed

to determine whether and how the original plan needs to be adjusted. Plan re-optimization may then be applied, and a new plan is to be worked out for the new fraction of the treatment. It is an optimal compensation of uncertainties, including organ deformation, organ motion and dosimetric errors incurred in previous fractions.

In ART studies of gynecologic cancer, such as 3D organ segmentation, re-planning, and organ shape variation, it is often required the use of large medical geometrical datasets which can represent accurately all cases in a population from which the training set has been sampled. However, usually only limited datasets are available. Sometimes the size of the training dataset was considered to be the most important reason for a relatively high segmentation error.[20] Statistical shape modeling has been proved effective for interpreting objects whose shape can vary.[21] Individual geometric variation can be modeled based on dominating eigen modes of organ deformation.[22] Due to the use of small training datasets, statistical shape models often constrain too much the deformation in medical image applications.[23-24]

The purpose of this work is to develop a novel method to generate large datasets of organ geometries from an actually acquired training dataset of limited size. A statistical shape analysis[25-26] based on the principal component analysis (PCA) was used to determine the major deformation modes present in the training organ geometries. Non-uniform rational B-spline (NURBS) technique, which provides the flexibility to design a large variety of shapes, was also integrated to represent the organ surface. This approach is intended to support various tasks associated with pelvic image processing in adaptive radiotherapy by constructing statistical models of organ deformations and exploiting pelvic organ geometric morphometrics.

Materials and methods

In this section we describe the method we propose to generate new organ geometries based on limited training datasets. First, a set of training images was acquired from daily CBCT scan. Next, surface registration and closest point searching approaches were applied to the training datasets to get the surface points correspondence between different CBCTs. In the following step, a statistical shape analysis to represent the major deformation modes of pelvic organs based on NURBS and PCA was performed; a set of coefficients corresponding to each principal component was obtained. Expectation maximization (EM) algorithm was then used to approximate and estimate the probability density function (PDF) of these coefficients. Finally, by assigning different coefficients from the PDF to the respective principal components, new realistic geometries of the organs can be obtained. A detailed description of each of these steps follows.

Training patient dataset collection and preprocessing

CBCT images have been acquired during the image-guided radiation therapy of gynecologic cancer in a Varian Trilogy treatment machine with on-board imaging system (Varian Medical Systems, Inc., U.S.A.). The on-board imaging system, which consists of a kV x-ray source and a flat panel detector, was installed onto the gantry along an axis orthogonal to the mega voltage beam. The acquired images had 512′512 pixels, with pixel size ranging from 0.5859 to 0.625 mm and slice thickness 2.5 mm. Each CBCT volume consisted of 54 slices.

After the CBCT reconstruction, all the daily images were transferred into Eclipse treatment planning system (TPS) and co-registered. Bladder, rectum, intestines and other organs of interest were extracted from daily CBCT images through manual segmentation, thresholding, and user interaction. Each organ was defined with a series of discrete transverse contours, which are represented by a list of vertices and associated with each of the transverse image slices. The representations of contours for the respective organs were then exported from the TPS and converted to a volumetric binary stack file.

Polygon surface generation

Accurate polygon surface models of anatomical objects have a great impact in various medical applications. They can be used as the basis for computational purposes or morphometrical analysis. In our study, polygon mesh modeling was employed to construct 3D triangular models of the female pelvic organs of interest, and were later converted into NURBS form.

The 3D polygon-surface mesh based on triangles was created from the delineated contours of each organ by using the software IsoSurf (Graham Treece, University of Cambridge, UK.). This software supports extracting triangulated surfaces from blocks of data at varying resolutions, using regularized marching tetrahedra. The original in-

put data to IsoSurf is assumed to be from a stack of parallel images, each of the same size. Here, the binary stack files obtained from the TPS in the previous step were used as the input for isosurf. The set of polygon mesh files was generated for the corresponding organs of all the training images with controllable spatial resolution.

Mesh registration and establishment of point correspondence

A crucial part of our study lies in establishing a point correspondence for all input shapes of each organ, which will be used as the basis for the statistical shape analysis and contribute to new geometries generation. Given the set of N segmented input training surfaces of pelvic organs, for each organ, one of the surfaces was selected as reference surface and the other N-1 training surfaces were set as target surfaces.

An interactive affine registration defined by scaling and translation transformations was initially performed between the reference surface and the N-1 training surfaces, in order to align all the organ shapes into a common coordinate frame. This common coordinate frame can be used to get an appropriate initialization for establishing point correspondence of pelvic organs.

Several approaches could be used to establish mesh-based surface point correspondence. An approach that builds upon the work for surface registration[27] was selected here to find corresponding points on reference surface and the other N-1 training organ surface. This approach was implemented by looking over all the faces, edges, and vertices of the surface meshes to find the closest point on the target surface to each point on the reference image. For this purpose, the point on the reference surface was projected on the corresponding training surface, and the intersection of the line passing through the point that is perpendicular to the surface patches close to projected point was found. The closest point in the target mesh to the intersection was considered the corresponding point. Once point correspondences are established, a topological correlation between the reference surface and target surfaces can be built for the statistical shape analysis.

NURBS generation of the reference surface

In order to determine the organ variation modes based on NURBS representation, NURBS modeling was performed on the reference organ surfaces. Here, NURBS-surface organ models are constructed from the imported polygon mesh models with the Rhinoceros software (McNeel, Seattle, WA, USA), which supports polygon meshes and can be used to create, edit, analyze, and translate NURBS curves, surfaces, and solids.

In Rhinoceros, several contours for each organ were obtained from the input polygon mesh of the reference surface as needed, and then several superior-inferior lines were simultaneously drawn to connect all the contours. NURBS surfaces were then fitted to match the contours by means of the Rhinoceros *loft* function.

NURBS deformation and surface matching

Depending on the displacements of the corresponding surface points, the NURBS representation of the reference surface can be deformed to match the target training surfaces. With this matching procedure, the deformed reference surface will have the same NURBS topology as before, but will have the same shape as the target surface and can, thus, be later used in place of the target surface in the statistical shape analysis.

The surface matching can be expressed as a deformation procedure of NURBS control points based on the displacements of surface points:

$$C2=f(C1,X1\rightarrow X2), \quad [1]$$

where X1 and X2 stand for the corresponding surface points on the reference and target surfaces respectively, and C1 and C2 stand for the corresponding NURBS control points of reference surface and target surfaces respectively.

In order to bring the deformed reference surface closer to the target surface, the deformation procedure was divided into several intermediate steps to avoid the local minima problem:

$$S1\rightarrow S2 \Rightarrow S1\rightarrow S_{11}\rightarrow S_{12}\rightarrow S_{13}\ldots S_{1n-1}\rightarrow S2, \quad [2]$$

where S1 and S2 stand for the reference and target surfaces respectively, and S_{11}, S_{12}, S_{13}, ¼S_{1n-1} stand for the intermediate shapes, which are given by:

$$S_{1j}=S1+(S2-S1)*j/n \quad (j=1,2,3\ldots n-1). \quad [3]$$

n is the total number of substeps, and j is the current working substep. By dividing the deformation in different substeps, the NURBS representation of

the reference surface converges to the target surface.

During every intermediate step, a NURBS warping of the reference organ shape is performed point by point. After one warping step for one control point, both surfaces may coincide at the desired position but may differ at other surface parts. For this reason, the deformation of control points is iterated until a smooth convergence is achieved.

Re-generation of surface points

Organ deformation can be interpreted as the change of organ geometry as given by its shape, and organ shape can be parameterized by the position of a set of surface points. In order to continue with the process and obtain the major deformation modes of the pelvic organs with PCA, a set of surface points is re-sampled from the corresponding NURBS surfaces with controlled precision. This process also provides an accurate approximation of the 3D organ shape with only a few digitized NURBS surface points.

Generating new organ geometries based on the statistical shape analysis

In the statistical shape analysis of pelvic organs, we have represented shapes by means of point distribution models (PDM)[28], which can provide a few-parameter statistical model of organ deformation. The basic idea is to compute the mean shape and to establish, from the training set, the pattern of legal variations in shape. This is done by using PCA to quantitatively determine the major deformation modes present in a training series, which, in our case, were parameterized by sets of corresponding organ surface points. PCA defines a linear transformation that de-correlates the parameter signals of the original shape population by projecting the objects into a linear shape space spanned by a complete set of orthogonal basis vectors. The axes of the shape space are oriented along directions in which the data have its highest variance.[29] Assuming that the corresponding points are located at equivalent positions on different instances of the shape, PCA is used to define a coordinate frame aligned to the principal axes of the data.

Given the training set of size N, PCA was performed on the coordinates of corresponding NURBS surface points $\{t_j=(t_{xj},t_{yj},t_{zj}),\ j=1,\ldots,m\}$, where m is the number of surface points used in the analysis. The PDM constructed from training organ shapes is defined by:

$$X = \bar{X} + Pb = \bar{X} + \sum p_q\ b_q, \quad [4]$$

where X is a 3m-element shape vector, $\bar{X}$ is the mean of the aligned organ shapes $\{X_i, i=1..N\}$ in the training set. P is a matrix containing the first k eigenvectors p_q of the covariance matrix D defined as

$$D = \frac{1}{N-1}\sum_{k=1}^{N}(X_i - \bar{X})(X_i - \bar{X})^T, \quad [5]$$

and b_q is the coefficient in the linear analysis corresponding to eigenvector p_q. D is also involved in the computation of the eigenvalues λ_q and eigenvectors p_q:

$$D \cdot p_q = \lambda_q \cdot p_q \quad [6]$$

By assigning a new set of coefficients b_q to the principal components, new geometries of the organs can be obtained. The new coefficients b_q can be sampled from statistical distributions extracted from the training data. A method reported by Cootes[30] was employed here to analyze the probable density function (PDF) of the coefficients b_q. The PDF was approximated with a mixture of Gaussian distributions derived from the kernel method:

$$p_{mix}(b_q) = \sum_{l=1}^{r} w_l N(b_q : \mu_l, S_l) \quad [7]$$

where $N(b_q : \mu_l, S_l)$ is a PDF of a gaussian with mean μ and covariance S. The Expectation Maximization (EM) algorithm[31] was used to fit such mixture to the given data and then a set of mixture-gaussian functions for the coefficients b_q was obtained.

Once the distribution function of the coefficients is known, its cumulative distribution function (CDF) can be obtained. From the CDF, a series of random coefficients can be generated with Monte-Carlo sampling. Random generation of coefficients is implemented via an inversion method. If u is an uniform random number over the interval (0, 1), then a random number W from a distribution with specified CDF F is obtained using $W = F^{-1}(u)$. The new geometry of the organ was obtained from:

$$X_{new} = \bar{X} + PW \quad [8]$$

where X_{new} stands for the new generated organ shape.

Results

We acquired CBCT images from 10 patients with gynecologic cancer. 15 image sets from different days were acquired for each patient. Bladder, rec-

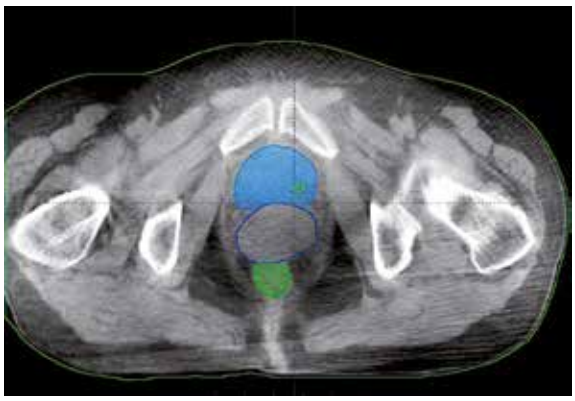

FIGURE 1. Pelvic organs segmented in cone-beam computed tomography (CBCT) images.

FIGURE 2. Polygon surface of pelvic organs. (A) Bladder; (B) Rectum; (C) Intestine.

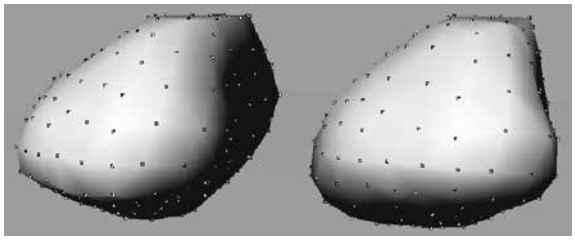

FIGURE 3. Corresponding points on two organ surface.

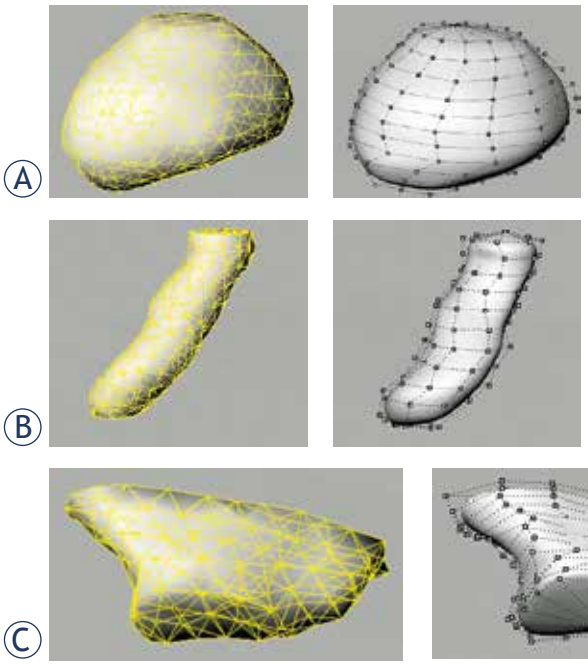

FIGURE 4. Non-uniform rational B-spline (NURBS) representation of pelvic organs converted from polygon meshes. Upper: polygon surfaces represented by triangular meshes. Lower: corresponding NURBS surfaces with control points. **(A)** Bladder; **(B)** Rectum; **(C)** Intestine.

tum, intestines and other organs were contoured in Eclipse TPS (Figure 1). The contours of each organ were exported from TPS for the analysis.

With the contours of each pelvic organ, polygon surfaces were generated with the Isosurf software. Typical examples of triangular meshes for the rectal, the bladder, and the intestines are shown in Figure 2.

Point correspondence was established between the reference surface and the target training surfaces. This correspondence was achieved by a rigid transformation and a closest point search approach. Figure 3 illustrates two different surfaces of the same organ and the corresponding points.

For the reference surfaces, the polygon meshes have been converted into NURBS, which are represented by feature control points, by using the Rhinoceros software. Example NURBS representation of bladder, rectum, and intestines derived from polygon surface are shown in Figure 4. Polygon meshes (left) and NURBS control points (right) are shown.

Figure 5 illustrates the deformation from the NURBS representation of a reference surface to the target surface. Intermediate steps used in the deformation are shown.

Based on the NURBS representation of pelvic organ surface, a set of surface points was re-sampled from the NURBS surface. Figure 6 illustrates the sampled surface points on the NURBS surface of bladder.

PCA was performed on the sampled surface points to capture the major variation modes of the surfaces for the same organ. For the pelvic organs in our study, shape variations have shown to be clearly dominated by only a few eigenvalues, indicating that the geometric variability of the measured organ samples is concentrated in just a few deformation modes. From the statistical shape modeling of pelvic organ, we described the shape variability in the training sets by the first five principal modes, which covered > 90% of the variance in shape change found within the training sets. Figure 7 illustrates the spectra of eigen values of a training dataset.

Figure 8 illustrates the estimation and the corresponding approximation of the PDF of one of the coefficients b_q, which contains a mixture of two gaussian distributions. Random coefficients were generated to match this kind of mixture-gaussian distribution by Monte-Carlo sampling.

Based on the statistical shape analysis of training data sets, new geometries of organs have been generated by a combination of eigenvectors and re-

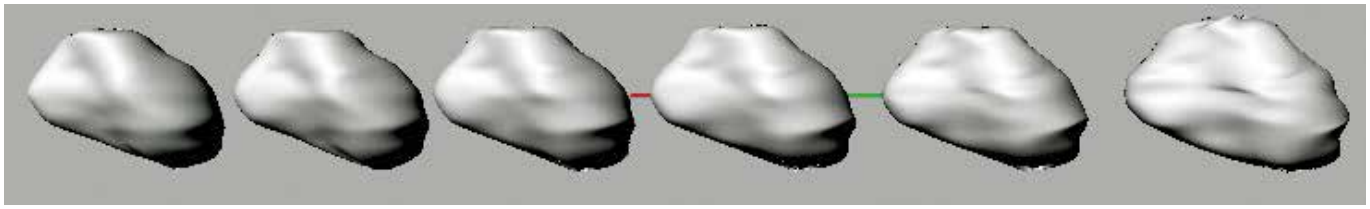

FIGURE 5. Non-uniform rational B-spline (NURBS) surface deformation with intermediate steps.

spective coefficients. Examples of new geometries obtained can be seen in Figure 9.

Discussion

During the course of adaptive radiotherapy, the management of large datasets of organ geometries is a major challenge for clinicians and physicists, not only during image segmentation, but also during the generation of new treatment plans. In this study, we have proposed a novel method to generate large datasets of organ geometries from limited patient data to be used in adaptive radiotherapy. The feasibility of our approach has been illustrated with the construction of new organ shapes from a given limited image set. However, the method itself bypasses the labor of clinical datasets acquisition. Furthermore, the underlying methodology is potentially useful for other medical applications, such as creating a virtual population of anatomical objects for surgical simulation[32-33] or for anatomy education purposes.

The aim of our study has been to derive a realistic model of shape variation via statistical shape modeling, and to obtain new instances of the anatomical representation based on NURBS. This is of particular interest in adaptive radiotherapy, especially due to the increasing demand for on-line organ segmentation, re-planning and re-optimization. Statistical shape modeling can afford an efficient parameterization of the geometric variability of the organ anatomy of patients. The population of variable organs created by our method can be utilized as a data source to support on-line adaptive radiotherapy work. For example, a large number of radiotherapy plans can be generated based on the new geometries. New geometries can also be used to create statistical atlases for segmentation purposes.

Shape representation and shape parameterization are crucial in 3D visualization, image processing, and shape deformation, and determine flexibility, complexity, possible user interactions, and other important issues in various applications.[34] In our study, NURBS has been used for the organ shape representation. NURBS can offer a unified mathematical formulation for representing not only free-

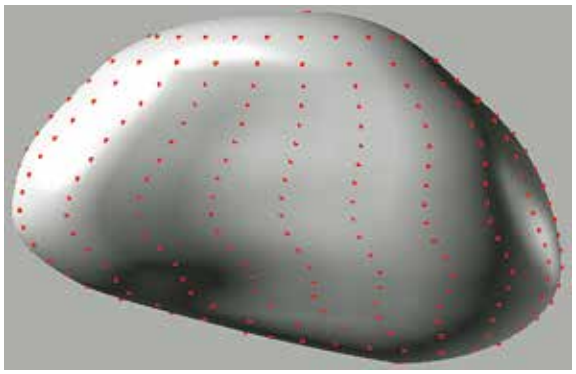

FIGURE 6. Sampling surface points from non-uniform rational B-spline (NURBS) representation of organ.

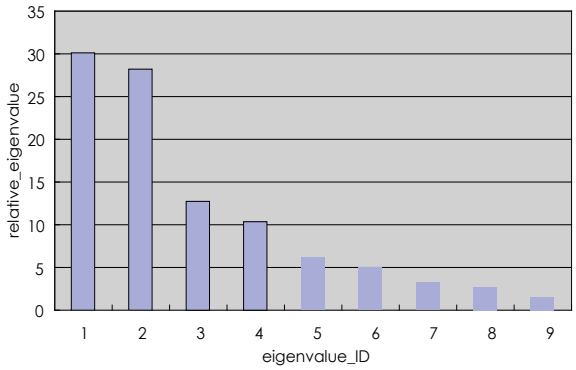

FIGURE 7. Spectra of relative eigenvalues for training datasets (sum of all eigenvalues normalized to 100%).

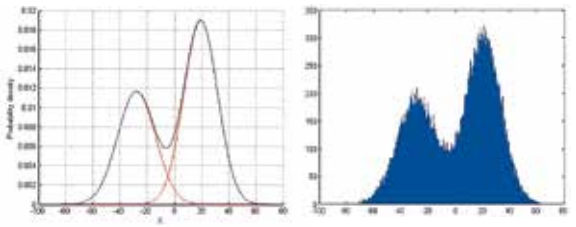

FIGURE 8. Probability density function (PDF) approximation of coefficient and random coefficients generation. **(A)** PDF of coefficient; **(B)** Random generated coefficient.

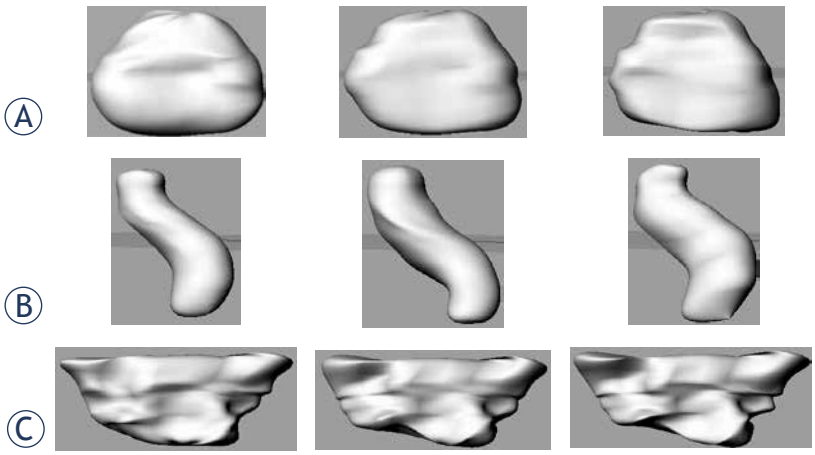

FIGURE 9. New geometries of organs described by statistical shape models after varying the coefficients corresponding to the principal components. **(A)** Generated new geometries of the bladder; **(B)** Generated new geometries of the rectum; **(C)** Generated new geometries of the intestine.

form curves and surfaces, but also standard analytical shapes such as conics, quadrics, and surfaces of revolution.[35] It has been widely used as a free form transformation technique and it provides additional flexibility to design a large variety of shapes. In addition, it can reduce the storage memory in computerized processing in medical applications.

Accurate segmentation is highly desired in the image analysis, which plays an important role in the whole framework proposed in this paper. 2D contours derived from medical images is the bases of 3D geometry of organs, thus the accuracy of segmentation is correlated with the statistical distribution of organ shapes in some way. Based on an experimental simulation, we found that 1-2 mm segmentation errors in 2D images may result in 3-5 mm displacement in 3D organ shapes, deformation modes and geometrical distribution are also affected with the surface error. With more training shapes, the geometrical distribution of organ variation can be presented with more degrees of freedom, even the related effect of segmentation error may be decreased at some resolution level. The segmentation accuracy also can be improved by introducing multi-modality images and registration, which were often utilized to overcome such challenging problems (*i.e.*, low-resolution, blurred boundaries, high noise levels, signal drops, etc.). More realistic representation of organ shape distribution maybe obtained with novel strategy of contour segmentation in the future.

By modifying the position of the control points and separating the deformation into intermediate steps, we have been able to control the surface deformation process. A relatively small deformation step may avoid the local minima problem and guarantee convergence of realistic results. Since B-splines have the feature of local support, iterative warping of control points in the NURBS surface transformation is performed until the desired convergence is reached, which makes the deformed results closer to the target surface.

We have limited our implementation to principal component analysis (PCA), which has shown to be an efficient and effective tool for statistical shape modeling. However, it is possible that some alternative methods might get some improvement in accuracy. The principal geodesic analysis[36] can also be applied in shape representation and may be more accurate in non-linear shape variation studies. An independent component analysis (ICA) is also used in the shape analysis, especially to capture localized variations. Results of constructing a statistical shape model with ICA and PCA for cardiac MR segmentation have been compared, showing that ICA-based model yielded more accurate segmentations over PCA-based model.[37]

Although showing promising potential, there is still much work to be done and much to improve in the methodology here proposed. If intensity information can be assigned to the generated geometries, CT-like medical images could be generated for dosimetric calculations. Deformable multi-organ registration technique, often required in radiation therapy, allows various organ shapes to behave differently and maintain the geometric integrity of different organs. More work is, therefore, necessary to statistically analyze the correlation and interactions of multi-organs, which can be used to build multi-organ models and aid deformable registration.

Conclusions

A method for automatic generation of large datasets of organ geometries from a limited set of images has been developed. The generated organ geometries are realistic and statistically representative of anatomical changes. We have shown that it is possible to capture a major portion of the total shape variability with the first few eigenvectors, and we have validated the creation of new geometric instances based on statistical shape analysis and NURBS representation.

This technique shows potential as a method for application of adaptive radiotherapy in cases with limited patient datasets. Future directions include

exploring intensity models and multi-organ models for dosimetric simulation and deformable registration during adaptive radiotherapy.

Acknowledgments

This research is partly supported by Chinese Scholarship Council.

References

1. Olivera GH, Ruchala K, Lu W, Kapatoes J, Reckwerdt P, Jeraj R, et al. Evaluation of patient setup and plan optimization strategies based on deformable dose registration. *Int J Radiat Oncol Biol Phys* 2003; **57(Suppl):** S188-9.
2. Rietzel E, Chen GT, Choi NC, Willet CG. Four-dimensional image-based treatment planning: target volume segmentation and dose calculation in the presence of respiratory motion. *Int J Radiat Oncol Biol Phys* 2005; **61:** 1535-50.
3. Keall PJ, Joshi S, Vedam SS, Siebers JV, Kini VR, Mohan R. Four-dimensional radiotherapy planning for DMLC-based respiratory motion tracking. *Med Phys* 2005; **32:** 942-51.
4. Yadav P, Ramasubramanian V, Paliwal BR. Feasibility study on effect and stability of adaptive radiotherapy on kilovoltage cone beam CT. *Radiol Oncol* 2011; **45:** 220-6.
5. Vargas C, Martinez A, Kestin LL, Yan D, Grills I, Brabbins DS, et al. Dose-volume analysis of predictors for chronic rectal toxicity after treatment of prostate cancer with adaptive image-guided radiotherapy *Int J Radiat Oncol Biol Phys* 2005; **62:** 1297-308.
6. Yang Y, Schreibmann E, Li T, Xing L. Dosimetric evaluation of kV cone-beam CT (CBCT) based dose calculation. *Phys Med Biol* 2007; **52:** 685-705.
7. Wu C, Jeraj R, Lu W, Mackie TR. Fast treatment plan modification with an over-relaxed Cimmino algorithm. *Med Phys* 2004; **31:** 191-200.
8. Wu C, Jeraj R, Olivera GH, Mackie TR. Re-optimization in adaptive radiotherapy. *Phys Med Biol* 2002; **47:** 3181-95.
9. Yan D, Vicini F, Wong J, Martinez A. Adaptive radiation therapy. *Phys Med Biol* 1997; **42:** 123-32.
10. Yan D, Lockman D, Brabbins D, Tyburski L, Martinez A. An off-line strategy for constructing a patientspecific planning target volume in adaptive treatment process for prostate cancer. *Int J Radiat Oncol Biol Phys* 2000; **48:** 289-302.
11. Rehbinder H, Forsgren C, Lof J. Adaptive radiation therapy for compensation of errors in patient setup and treatment delivery. *Med Phys* 2004; **31:** 3363-71.
12. Lam KL, Ten Haken RK, Litzenberg D, Balter JM, Pollock SM. An application of Bayesian statistical methods to adaptive radiotherapy. *Phys Med Biol* 2005; **50:** 3849-58.
13. Marchant TE, Amer AM, Moore CJ. Measurement of inter and intra fraction organ motion in radiotherapy using cone beam CT projection images. *Phys Med Biol* 2008; **53:** 1087-98.
14. Peszyńska-Piorun M, Malicki J, Golusinski W. Doses in organs at risk during head & neck radiotherapy using IMRT and 3D-CRT. *Radiol Oncol* 2012; **46:** 328-36.
15. Matthiesen C, Ramgopol R, Seavey J, Ahmad S, Herman T. Intensity modulated radiation therapy (IMRT) for the treatment of unicentric Castlemans disease: a case report and review of the use of radiotherapy in the literature. *Radiol Oncol* 2012; **46:** 265-70.
16. Oldham M, Letourneau D, Watt L, Hugo G, Yan D, Lockman D, et al. Cone-beam-CT guided radiation therapy: a model for on-line application. *Radiother Oncol* 2005; **75:** 271-8.
17. Mohan R, Zhang X, Wang H, Kang Y, Wang X, Liu H, et al. Use of deformed intensity distributions for on-line modification of image-guided IMRT to account for inter-fractional anatomic changes. *Int J Radiat Oncol Biol Phys* 2005; **61:** 1258-66.
18. Zehtabian M, Faghihi R, Mosleh-Shirazi MA, Shakibafard AR, Mohammadi M, Baradaran-Ghahfarokhi M. A fast model for prediction of respiratory lung motion for image-guided radiotherapy: a feasibility study. *Int J Radiat Res* 2012; **10:** 73-81.
19. Strojan P. Jereb S, Borsos I, But-Hadzic J, Zidar N. Radiotherapy for inverted papilloma: a case report and review of the literature. *Radiol Oncol* 2013; **47:** 71-6.
20. Lötjönen J, Kivisto S, Koikkalainen J, Smutek D, Lauerma K. Statistical shape model of atria, ventricles and epicardium from short- and long-axis MR images. *Med Image Anal* 2004; **8:** 371-86.
21. Cootes TF, Taylor CJ, Cooper D, Graham J. Active shape models - their training and application. *Comput Vis Image Underst* 1995; **61:** 38-59.
22. Söhn M, Birkner M, Yan D, Alber M. Modeling individual geometric variation based on dominant eigenmodes of organ deformation: implementation and evaluation. *Phys Med Biol* 2005; **50:** 5893-908.
23. Lötjönen J, Antila K, Lamminmaki E, Koikkalainen J, Lilja M. Artificial enlargement of a training set for statistical shape models: Application to cardiac images. *Functional imaging and modeling of heart. Proceedings*. Book series: *Lecture notes in computer science* 2005; **3504:** 92-101.
24. Tölli T, Koikkalainen J, Lauerma K, Lötjönen J. Artificially enlarged training set in image segmentation. *Medical image computing and computer-assisted intervention. Proceedings.* PT 1 Book series: *Lecture notes in computer science* 2006; **4190:** 75-82.
25. Dryden I, Mardia K. *Statistical shape analysis.* New York: John Wiley & Sons; 1998.
26. Small C. *The statistical theory of shape.* Berlin: Springer; 1996.
27. Ge Y, Maurer Jr C, Fitzpatrick J. Surface based 3-D image registration using the Iterative Closest Point algorithm with a closest point transform. *Proc SPIE.* Book series: *Lecture notes in computer science* 1996: 358-67.
28. Cootes TF, Hill A, Taylor CJ, Haslam J. The use of active shape models for locating structures in medical images. *Image Vis Comput* 1994; **12:** 355-66.
29. Rajamani KT, Styner MA, Talib H, Zheng G, Nolte LP, MA Gonzalez Ballester MA. Statistical deformable bone models for robust 3D surface extrapolation from sparse data. *Med Image Anal* 2007; **11:** 99-109.
30. Cootes TF, Taylor CJ. A mixture model for representing shape variation. *Image Vis Comp* 1999; **8:** 567-74.
31. McLachlan G, Basford KE. *Mixture models: inference and applications to clustering.* New York: Dekker; 1988.
32. Tendick F, Downes M, Goktekin T, Cavusoglu M, Feygin D, Wu X, et al. A virtual environment testbed for training laparoscopic surgical skills. *Presence: Teleoperators Virt Environ* 2000; **9:** 236-55.
33. Basdogan C, Ho CH, Srinivasan MA. Virtual environments in medical training: graphical and haptic simulation of laparoscopic common bile duct exploration. *IEEE/ASME Trans Mechatronics* 2001; **6:** 269-85.
34. Lorenz C, Krahnstover N. 3D statistical shape models for medical image segmentation. roceedings. *2nd International Conference on 3-D Digital Imaging and Modeling* 1999: 414-23.
35. Xie H, Qin H. Automatic knot determination of NURBS for interactive geometric design. *IEEE International Conference on Shape Modeling and Applications* 2001: 267-76.
36. Fletcher P, Lu C, Pizer S, Joshi S. Principal geodesic analysis for the study of nonlinear statistics of shape. *IEEE Trans Med Imaging* 2004; **23:** 995-1005.
37. Üzümcü M, Frangi AF, Sonka M, Reiber, Lelieveldt. ICA vs. PCA active appearance models: application to cardiac MR segmentation. *Medical image computing and computer-assisted intervention. Proceedings.* PT 1 Book series: *Lecture notes in computer science* 2003; **2878:** 451-8.

special communications

Slovenian experience from diagnostic angiography to interventional radiology

Dusan Pavcnik

Dotter Interventional Institute, Oregon Health Sciences University, Portland, U.S.A

Radiol Oncol 2014; 48(4): 416-425.

Received 27 September 2013
Accepted 25 November 2013

Correspondence to: Dušan Pavčnik, M.D., Ph.D., Dotter Interventional Institute, Oregon Health Sciences University, 630 SW Gaines St, Portland, OR 97239-309, U.S.A. E-mail: pavcnikd@ohsu.edu

Disclosure: No potential conflicts of interests were disclosed.

Background. The purpose of writing this article is to document the important events and people in the first 50 years of diagnostic angiography and interventional radiology in Slovenia. During this period not only did the name of the institutions and departments change, but also its governance.

Conclusions. This depicted the important roles different people played at various times in the cardiovascular divisions inside and outside of the diagnostic and interventional radiology. Historical data show that Slovenian radiology has relatively immediately introduced the new methods of interventional radiology in clinical practice.

Key words: diagnostic angiography; interventional radiology; history

Introduction

Diagnostic angiography is the study of blood vessels in humans and animals by x-ray contrast method. To describe its early development we have to go back to the discovery of x-rays.

In 1896, one year after Roentgen's discovery of x-rays, Haschek and Lindenthal published the first angiogram of an amputated hand using bismuth, lead and barium salts.[1] The injected contrast mixture demonstrated good absorption of the x-rays and demonstrated the huge potential of this new technique. Of course, a suitable safe contrast material had not been invented yet.

Egas Moniz, Reynaldo dos Santos, Moses Swick, Werner Forssmann

The Portuguese physician and neurologist Egas Moniz, a Nobel Prize winner in 1949, in 1927 developed carotid angiography by using needle puncture and injection of 22% sodium iodide.[2] Various forms of carotid angiography remain a fundamental tool, both in diagnosis and interventional procedures on the brain.

Reynaldo dos Santos in 1929, showed that satisfactory opacification of the abdominal aorta and its branches could be obtained by use of translumbar needle and injection of contrast material.[3] In 1929 Werner Forssmann, Nobel Prize winner in 1956, was the first person to introduce a ureteric catheter into his own heart via antecubital vein (self experiment).[4] The same year, Moses Swick reported discovery of an opaque organic iodine contrast media that was significantly less toxic than sodium iodide.[5] It is a remarkable coincidence that these two important radiological developments were reported for the first time in 1929 in the same issue, in the journal Klinische Wochenschrifft: Swick's paper on the first iodinated water soluble contrast medium, Uroselectan[4], and Forssmann's paper on the catheterization of the heart.[5]

The works of Moniz, dos Santos, Swick and Forssmann had great impact on further development of diagnostic angiography.

Seldinger technique, radioopaque catheters and suitable x ray contrast media

With the introduction of the Seldinger technique in 1953, the procedure became safer and user friendly as no sharp or rigid needles needed to remain inside the vascular lumen. "Catheter replacement of the needle in percutaneous arteriography" was the title of his unique technique published in Acta Radiologica.[6] With the development of radioopaque thermoplastic catheters (KIFA) in Sweden[7] and with the availability of suitable intra-arterial contrast media[8], the groundwork of the modern methods of angiography became well establish. Percutaneous transfemoral transcatheter arteriography was just beginning to emerge in 1950s and in 1960s became the widely applied diagnostic method throughout the world, including Slovenia. Miro Košak introduced the concept of angiography in the Slovenian Journal Zdravstveni Vestnik under the name clinical importance of angiography as diagnostic method in therapy.[9]

FIGURE 1. The pioneers of angiography in Slovenia. From left to right: Ivo Obrez, Jože Stropnik, Stanko Hernja and Miro Košak.

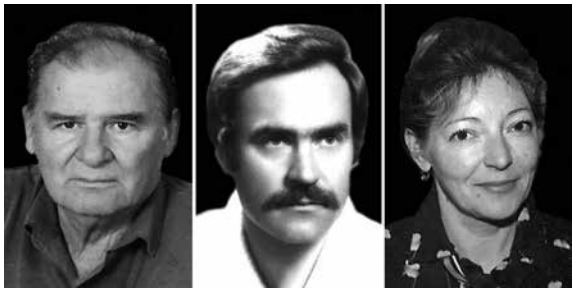

FIGURE 2. The pioneers of angiography in Slovenia. From left to right: Jože Košir, Peter Soklič and Elizabeta Baretić-Kolar.

Ivo Obrez and Jože Stropnik

Ivo Obrez, a native of Novo mesto, Slovenia, earned his medical degree from Ljubljana University School of Medicine in 1955. After finishing a residency in radiology in 1961 in Ljubljana, he led the Department of Roentgenology at the General Hospital Novo mesto until 1965. In the early 1960s he spent part of the year at the Universities of Lund and Stockholm, learning angiographic techniques. There he met Herbert Abrams from Stanford University. By the time he moved to Ljubljana on invitation by Prof Stanko Hernja, he had written 3 scientific articles on angiography[10-12], and co-founded this journal, Radiology and Oncology, at the time the journal of *Radiologia Iugoslavica*.[13] When Ivo Obrez arrived to Ljubljana, he began performing arteriograms, succeeding the surgeon Miro Košak who has done them previously at dislocated fluoroscopic Siemens x ray unit at the Department of Surgery.[9,14] As Ivo Obrez dug into the new tasks, Prof. Hernja and Prof. Košak found resources to support him. The Siemens x-ray apparatus was updated with an image intensifier. With electronic image intensification, the angio procedure could be done in normal light. This led to better visualization of the vascular system and the heart.[12] Pressure injectors and rapid-change film holders allowed multiple images essential for new studies of the cardiovascular and central nervous system. In 1966/67 Dr. Obrez completed a cardiovascular fellowship in Radiology at Stanford in Palo Alto (under prof. Abrams). After his return to Ljubljana, he started performing coronary angiography.[14] Obrez was highly respected by his cardiology peers and trained cardiologists Majda Mazovec, Anton Jagodic, Borut Pust, Andrej Cijan, Peter Rakovec, Darko Zorman and Darja Fettich, pediatric specialist. Dr. Fettich started children heart catheterization in Ljubljana.[14-17] Ivo Obrez also trained many radiology and cardiology fellows in coronary angiography.

Diagnostic cardiovascular angiography

In 1960s was a time of great change in radiology. Prof. Stanko Hernja was determined that his Institute of Roentgenology would contribute to the pace of that change. His commitment included dislocated x-ray unit at the Department of Surgery for enhanced studies of the heart, central nervous system and other vessels. This cardiovascular unit, led by Jože Stropnik, has not been fully equipped with new x-ray equipment. This is why Dr. Stropnik modified homemade cassette changer (Electro-medicina, Ljubljana) for peripheral angiography using five 120 cm long cassettes. Because rotation of the cassettes occurred through

FIGURE 3. The pioneers of angiography in Slovenia. From left to right, upper row: Uroš Vizijak, Marijan Pocajt, Dušan Pavčnik. Lower row: Sead Galijaš, Dušan Tomažič and Jože Matela.

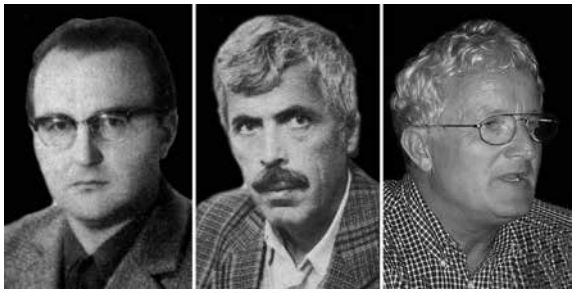

FIGURE 4. Neuroradiologists. From left to right: Martin Čerk, Tomaž Kregar and Miha Škrbec.

the center of the focal spot, there was no blurring. Long leg angiograms showed the vascular system from abdominal aorta to the ankle.[18] His modification has been in use for 30 years. When the Institute of Roentgenology moved to the new University Clinical Centre in 1974, this homemade modification moved with it (Figure 1).

In 1971 Stropnik and Obrez described angiographic diagnostic examination of gastrointestinal bleeding.[19] In early 1970s, Stropnik reported on angiographic image of the liver cirrhosis[20] and on diagnostic importance of variations of celiac trunk.[21] Carotid angiography was performed either by direct injection through a percutaneously inserted needle or by catheter technique. Neuroradiologist Martin Čerk reported on occlusion of internal carotid artery.[22] Čerk, Tomaž Kregar and Miha Škrbec published their own experiences on cerebral angiography.[23] Soklič, Stropnik, Obrez, Košir and Baretić-Kolar published the use of selective angiography in the diagnosis of intraluminal and extraluminal abdominal bleeding. They described that duodenal blood supply originates both from the celiac and superior mesenteric arteries. It was often necessary to inject each artery separately in order to demonstrate the site of bleeding.[24] Jože Košir and Nataša Budihna compared isotope venography with conventional venogram in patients with deep vein thrombosis of the limb.[25] Jurij Us and Jože Košir investigated the potential of the internal mammary artery angiography for the diagnosis of the breast diseases (Figure 2).[26] Other people like Uroš Vizijak from Celje, Marijan Pocajt, Dušan Tomažic and Jože Matela from Maribor, Jože Kocijančič from Murska Sobota, and Dušan Pavčnik and Sead Galijaš from Nova Gorica have to be given credit for the development of angiography in Slovenia as well (Figures 3, 4).

Interventional radiology

Charles Dotter, the father of interventional radiology (IR), was the first to perform angioplasty on a peripheral artery. In his most famous case, Dotter used a guide wire and Teflon coaxial catheters to dilate a superficial femoral artery stenosis in an 82 year old woman with limb ischemia and gangrene who refused amputation. He was successful, the patient was ambulatory for the remainder of her life. That event changed the practice of medicine in the world[27,28]; however it took quite a while for angiographers to change diagnostic thinking and to develop interventional technique and devices. In 1976, Grüntzig reported on percutaneous transluminal angioplasty (PTA) balloon catheters for iliac and peripheral arteries stenosis and in 1979 on coronary balloon catheters for coronary angioplasty.[29,30]

After successful experimental and clinical reports of Drs. Rösch, Baum and Nussbaum in the early 1970s, selective vasoconstrictive infusions became a useful technique for stopping both arterial and venous gastro intestinal bleeding.[31] Rösch reported: "When we could not stop bleeding from a gastric ulcer in a coagulopathic young patient with vasoconstrictive infusions, we selectively embolized the gastro-duodenal artery with autologous blood clot". The publication of this case together with experimental studies was the basis for the wide use of embolization for treatment of arterial gastrointestinal bleeding.[32]

The goals of selective or local thrombolysis are to relieve an acute vascular obstruction by thrombus and unmask the underlying pathology. Charles Dotter started selective thrombolysis in 1972 to treat complications of angiography and PTA.[33]

Transcatheter device technology began in the 1970s with work of Porstmann in occluding patent ductus arteriosus[34], King and Rashkind in closing atrial septal defect[35,36], and Gianturco and his associates in occluding blood vessels.[37] In the 1980s, Palmaz and coworkers extended Dotter's late 1960s concept[38] by introducing balloon expandable stent, to treat stenotic vascular lesions.[39] Caesar Gianturco conceived a spring like zig zag stent made of stainless steel and described his experimental results in 1985.[40] The largest proliferation of device technology started in 1990s.

The transjugular intrahepatic portosystemic shunt (TIPS) is a percutaneous alternative to surgical portosystemic shunts that was conceived in the late sixties by Josef Rösch. A TIPS is a side-to-side shunt of determined diameter designed to function as a partial shunt that preserves a portion of portal flow to the liver.[41]

FIGURE 5. The pioneers of interventional radiology. From left to right: Ivo Obrez, Miloš Šurlan and Dušan Pavčnik.

FIGURE 6. The pioneers of interventional radiology. From left to right: Janko Klančar, Pavle Berden and Jernej Knific.

FIGURE 7. The pioneers of interventional radiology. From left to right: Marijan Jereb, Jurij Us and Erika Brenčič.

IR in Slovenia

Between 1969 and 1980 Slovenian radiologists issued many reports and published papers on interventional radiology procedures. Auersperg, Us-Krasovec and Obrez introduced the use of selective intra-arterial chemotherapy and reported its complication.[42,43] Obrez reported experimental study on temporary occlusion of the renal artery and its effects and significance.[44] Obrez and Kubicka reported simultaneous infusion of vasopressin into two arteries to control massive colonic hemorrhage using a new catheter.[45,46] Marijan Jereb published the usefulness of needle biopsy in chest lesions of different sizes and locations. Direct puncture technique proved to be an invaluable aid in the diagnosis of chest lesions.[47] Jurij Us reported on aspiration biopsy of the retroperitoneal lymph nodes in 1977.[26] In 1980, Obrez made an attempt to define the present status of IR at home and abroad. He stated that IR occupies a unique place in medicine. Obrez performed the first PTA of superficial femoral artery in 1978.[48,49] In Ljubljana University Clinical Centre, Miro Košak was the head of cardiovascular surgery and we all knew it. He respected Ivo Obrez because of his knowledge, catheter skills and clinical judgment. Košak offered surgical stand by to radiologists when performing balloon angioplasty procedures including PTA of femoral, iliac or renal artery.[49] Viktor Videčnik, Elizabeta Baretić-Kolar and Miloš Šurlan reported on thrombolytic therapy for femoro-popliteal occlusions. The lysis has been helped by streptokinase and urokinase. The underlying stenoses were treated by PTA (Figures 5, 6, 7).[50]

Drainage of retroperitoneal and pelvic abscesses and fluid collections

You can help save a life by draining an abscess percutaneously in a septicaemic patient using image guidance and a small catheter, particularly in postoperative patients. Success of abscess drainage depends upon complete evacuation of the cavity, con-

FIGURE 8. Interventional radiologists. From left to right: Tomaž Ključevšek, Dimitrij Kuhelj and Peter Popovič.

FIGURE 9. Interventional radiologists. From left to right: Tomaž Šeruga, Zoran Milošević and Vladka Salapura.

FIGURE 10. From left to right: Alexander Margulis, Mrs. Abrams, Ivo Obrez, Herbert Abrams and Hedvig Hricak on the occasion of Joint meeting and postgraduate course organized by Ivo Obrez and ECA, ESCVIR and ASCVIR in Dubrovnik in 1983.

trol of an underlying condition and prevention of reaccumulation. We published our results in 1984.[51]

Biliary system

Obrez and coworkers reported on percutaneous biliary drainage (PBD) in 1980.[52] Percutaneous transhepatic cholangiography was usually part of interventional procedure as percutaneous biliary drainage. There was continuing evaluation of different technique for draining the gallbladder and obstructed hepatic biliary ducts. Catheters and plastic prosthesis could serve as channels to keep open ducts that were blocked. One of common complication was replacement of dislodged catheter. However; the role of PBD was also changing with the development of interventional endoscopy.[53]

Percutaneous urinary interventions

Relief of acute urinary obstruction was the most common intervention performed by radiologist.[54] Percutaneous access to the kidney has also been used to remove stones, or to place antegrate ureteral stents when retrograde stenting by urologist failed.[55] Miloš Šurlan reported treatment of renal cysts with percutaneous alcohol ablation.[56] The development of extracorporeal lithotripsy and ureteroscopy has limited the number and variety of percutaneous procedure performed in urinary tract.

Embolotherapy

No single embolic agent is universally applicable to all clinical situations. Ivo Obrez reported the use of gelatin sponge and coils for renal tumor treatment in 1978.[57] Prior to performing an embolization, several factors must be considered. These include the desired level of occlusion, the desired duration of occlusion, the relevant vascular anatomy and the available embolic material.[57] Martin Čerk reported embolization of anteriovenous malformation by occluding anterior and middle cerebral artery in 1979. He used gelatin sponge.[58,59] Various embolic materials have been used clinically to control hemorrhage[60], relieve pain, inhibit tumor growth, and facilitate resection by reducing vascularity and tumor bulk. Janko Klančar described embolotherapy of kidney tumors.[61] Other applications of embolotherapy were reported by Pavel Berden on ablation of tumors using absolute ethanol[62], by Rok Cesar on palliative and preoperative treatment of bone tumors[63], by Miloš Šurlan on chemoembolization of malignant liver tumors[64] and Dušan Pavčnik on venous impotence and percutaneous embolization treatment (Figures 8, 9).[65]

Endoluminal stenting

The era of stenting in Slovenia started with the use of self expanding Gianturco Z stents in 1989. Pavčnik

and Šurlan reported that three patients with stenosis of the tracheobronchial tree and one with the obstruction of *vena cava superior* were treated with self expanding stents.[66] While this initial results with the stents were encouraging, these stents should be viewed as a first generation device. In early 1990s we used Palmaz stent, Strecker stent and Wallstent in the arterial system including peripheral, iliac and renal arteries. We published our results recommending predilatation and those lesions have to be covered from healthy to healthy segments.[65-70]

In 1993, the first TIPS was created by the self expanding Wallstent in Ljubljana. Creation of this shunt resulted in a decrease of 18 mmHg in portal pressure. The main advantage of Wallstent was its extreme flexibility. Being encouraged by this result, Pavčnik and Šurlan attempted TIPS in additional patients with severe cirrhosis and variceal hemorrhage.[71] Peter Popovič *et al.* reported TIPS versus endoscopic sclerotherapy in the elective treatment of recurrent variceal bleeding (Figures 10-15).[72]

Heart, aorta and *inferior vena cava*

In 1979 Obrez travelled to Zurich to see Andreas Grüntzig performing coronary angioplasty. He was the first one to do percutaneous transluminal coronary angioplasty (PTCA) in Slovenia in 1980.[73] In 1986 Institute of Roentgenology opened a new Catheterization Laboratory with the state of the art Siemens C-arm cardio angiography. For many years coronary angiography, coronary interventions and pediatric heart procedures were performed in this laboratory. We published our experience after 50 PTCA.[74] Pavčnik and Kranjec performed PTCA of acute coronary occlusion followed by intracoronary and intravenous thrombolysis. They introduced this coronary therapy into Slovene medicine in 1989.[75] Pavčnik, Cijan, Bricelj and Robida reported results on transcatheter balloon valvuloplasty of pulmonary, mitral and aortic valves. Authors described valvuloplasty in congenital and acquired valve disease. From 1987 to 1993 we performed thirteen pulmonary, twenty-six mitral and five aortic valve dilatations.[76,77]

Dušan Pavčnik, Pavle Berden and Mirta Koželj published case report of the transcatheter occlusion of patent ductus arteriosus using Rashkind double umbrella. After two years follow up our two patients were free of symptoms.[78]

In 1995 we reported two cases with inoperable descending thoracic aortic aneurysm. Both patients underwent an intraluminal bypass of the descending thoracic aneurysm with a stent graft. Stent grafts were constructed from Gianturco-Rösch stents and a soft Dacron graft at the Dotter Institute laboratory.[79] First patient with gigantic aneurysm developed two late complications during a 7 years follow-up. He was additionally treated with two endografts.[80] In 2010 Dimitrij Kuhelj *et al.* published risk of deterministic effects during endovascular aortic stent graft implantation.[81]

In 1994 we reported the case of young patient with two symptomatic transient ischemic attacks due to arterio-venous fistula. Patient underwent

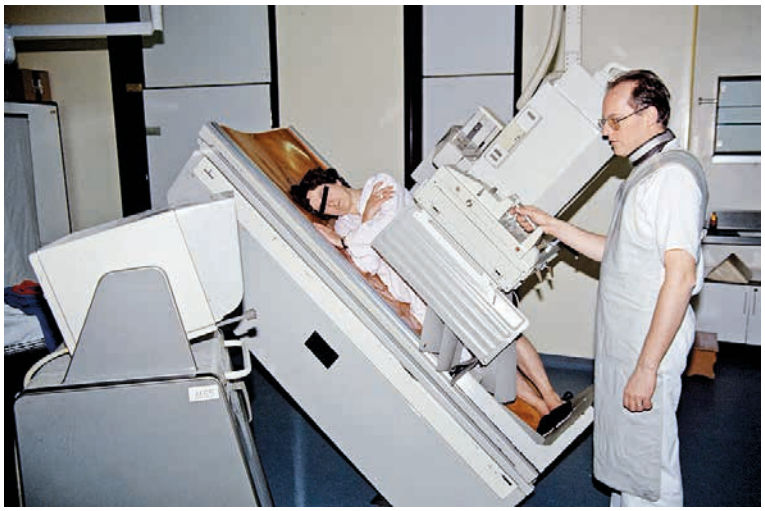

FIGURE 11. Siemens Sireskop (1974-1980s). With electronic image intensification, examination could be made in normal light and recorded on x-ray film or videotape. Maks Kadivec is performing a neuro-radiological procedure. Similar Siemens unit (next door) modified with rapid-change film holder (portable puck) allowed multiple images essential for studies of the cardiovascular system (1964 – early 1990s). There was as well modified homemade cassette changer ("boben") for peripheral angiography.

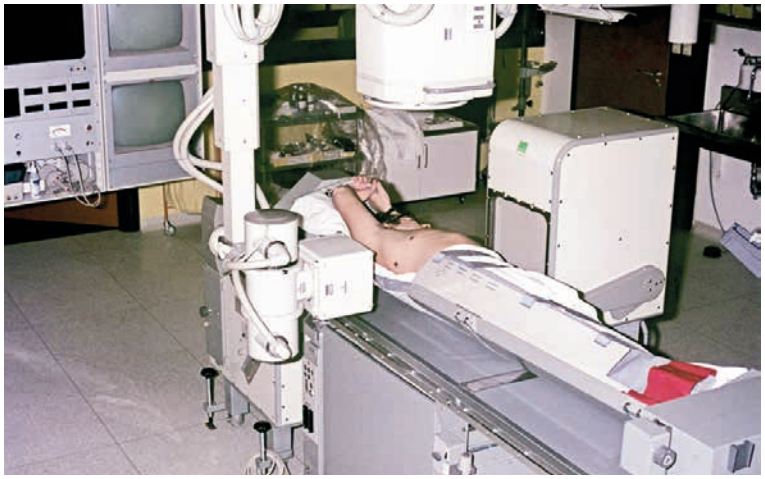

FIGURE 12. Tridoros-Siemens Elema angiocardiographic unit with Schönander rapid-change film holders (1974–1986).

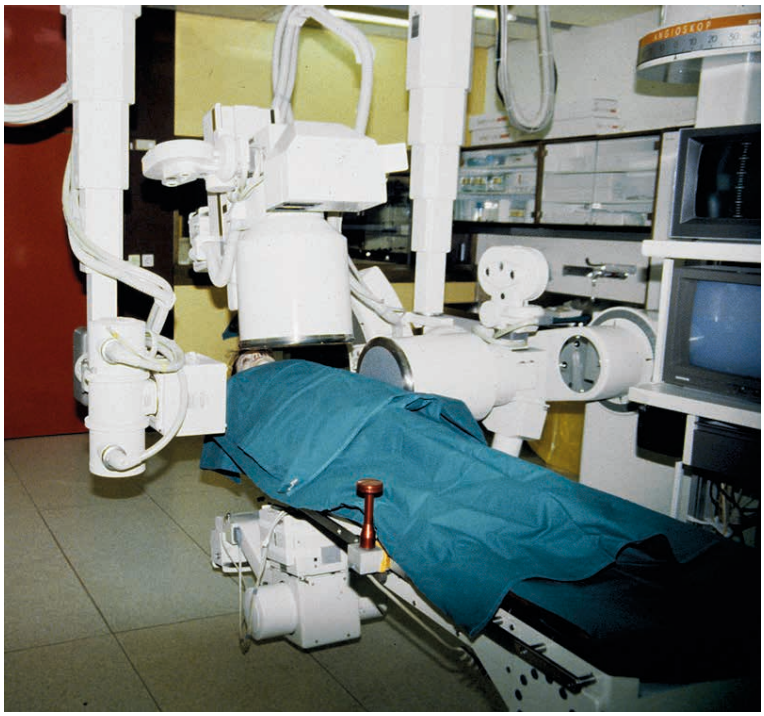

FIGURE 13. Bi-plane Angioskop for coronary cine-angiography (1986–2008).

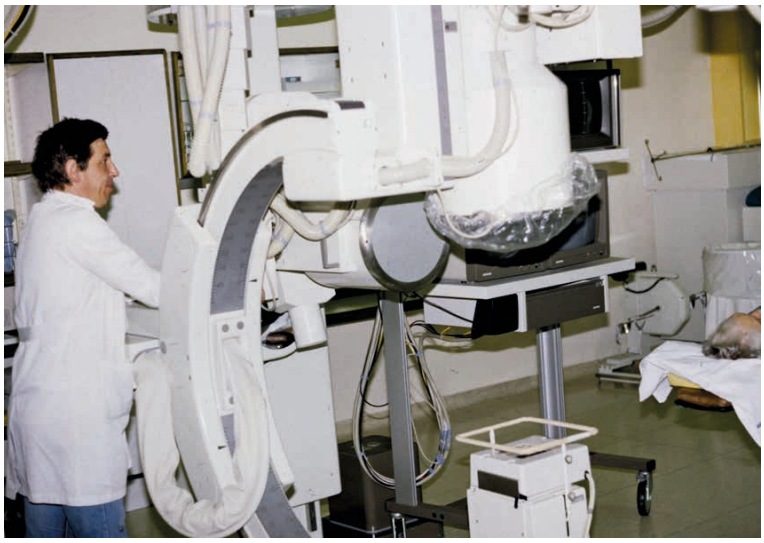

FIGURE 14. Angioskop-the state of the art bi plane Siemens C-arm digital subtraction and cine- angiography (1986–2008) (Jaka Regvart, Radiol. Ing.).

transcatheter closure of the shunt with Gianturco coils. Patient developed transient pleurisy few days after embolization. Percutaneous transcatheter occlusion of pulmonary anteriovenous fistula has become the treatment of choice replacing surgical intervention.[82] Vladka Salapura, Tomaž Ključevšek, Dimitrij Kuhelj and Peter Popovič reported on *inferior vena cava* (IVC) filters in 2008.[83]

Tomaž Šeruga in 2004 and Zoran Milošević in 2007 reported transcatheter treatment of aneurysms in cerebral circulation using coils. Šeruga detached electrolytically detachable platinum coils.[84,85] In 2010 Vladka Salapura *et al.* reported study: Infrapopliteal run-off and the outcome of femoropopliteal percutaneous transluminal angioplasty in Vasa.[86] In 2013 Dimitrij Kuhelj *et al.* published about percutaneous mechanical thrombectomy of superior mesenteric artery embolism.[87]

Ivo Obrez

Prof. Obrez rose through the academic ranks. He became associate professor in 1972 and a full professor in 1984. He was named director of the Institute of Roentgenology in Ljubljana in 1974. Through his book chapters, articles, lectures and trainees from Slovenia and former Yugoslavia, Dr Obrez has dominated the specialty for more than two decades. His impact on the field of angiography and IR was important not only in Slovenia and former Yugoslavia but also in Europe. He supported demand for people and equipment and, in turn, expected service and quality. He worked very closely with surgeons and his cardiology colleagues at University Clinical Center in Ljubljana. His philosophy was to try to prevent turf battles and collaborate. Dr Obrez returned to the United States as visiting professor in 1972 at Stanford, in 1978/79 and in 1981 at Harvard (Brigham and Women's Hospital) in Boston. Ivo Obrez was the Executive Committee member when European College of Angiography (ECA) joined forces with the European Society of Cardiovascular and Interventional Radiology (ESCVIR), to form CIRSE in 1985. In 1983 Obrez was the Meeting Chairman for the joint meeting (ECA, ESCVIR and American ASCVIR) in Dubrovnik (Figure 10). Ivo Obrez died of pancreatic cancer in 1989.

Conclusions

Author reviewed the Slovenian experience from diagnostic angiography to IR. He reviewed briefly the beginning of interventional vascular radiology and the origins of IR's major interventional vascular and non vascular procedures. After these beginnings, many interventionalists contributed to further improvement or modifications of these procedures. In 1995, The author moved to Portland, Oregon. He is currently Director and Professor of Research at the Dotter Interventional Institute,

Oregon Health and Science University. He has published over 120 scientific publications including 5 studies in Slovenian journal Radiology and Oncology.[87-91]

Historical data show that Slovenian radiology has relatively immediately introduced the new methods of interventional radiology in clinical practice.

FIGURE 15. Philips-Integris C for digital subtraction angiography (1993–2009) (Marijan Klemenc, Radiol. Ing.)

References

1. Haschek E, Lindenthal OT. A contribution to the practical use of the photography according to Röntgen. *Wien Klin Wochenschr* 1896; **9:** 63.
2. Moniz E, Diaz A, Lima A. La radioarteriographie at la topographie cranioencephalique. *J Radiol Electr* 1928; **12:** 72.
3. Dos Santos R, Lamas AC, Pereira-Caldas J. Arteriografia da aorta e dos vasos abdominais. *Med Contemt* 1929; **47:** 93.
4. Forssmann W. Die Sondierung des rechten Herzens. *Klin Wochenschr* 1929; **8:** 2085-7.
5. Swick N. Darstelung der Niere und Harnwege in rontgenbild durch intravenose Einbringung eines neuen Kontrastoffes, des Uroselectans. *Klin Wochenschr* 1929; **8:** 2087-9.
6. Seldinger SI. Catheter replacement of the needle in percutaneous arteriography. *Acta Radiologica* 1953; **39:** 368-76.
7. Ödman P: Percutaneous selective angiography of the main branches of the aorta. *Acta Radiol* 1956; **45:** 1-14.
8. Wallingford VH. The development of organic iodine compounds as x-ray contrast media. *J Am Pharmacol Assoc (scientific Edition)* 1953; **42:** 721-8.
9. Košak M. [Clinical importance of angiography as diagnostic method in therapy]. [Slovenian]. *Zdrav Vestn* 1957; **26:** 45-8.
10. Obrez I. [Serial cerebral angiography with an improvised cassette – our own experiences]. [Slovenian]. *Zdrav Vestn* 1964; **33:** 13-5.
11. Obrez I. [Angiographic diagnostic examination of abdominal organs using Seldinger's method]. [Slovenian]. *Zdrav Vestn* 1965; **34:** 50-6.
12. Obrez I. [Selective renal angiography]. [Slovenian]. *Zdrav Vestn* 1966; **35:** 77-9.
13. Pavčnik D. 60 years of the Slovenian Association of Radiology 1950-2010. *Radiol Oncol* 2009; **43:** 137-43.
14. Obrez I, Stropnik J, Hernja S, Košak M, Jagodic A. [Coronarography]. [Slovenian]. *Zdrav Vestn* 1969; **38:** 135-8.
15. Pust B, Obrez I, Mazovec M, Košak M. [Case of tricuspidal stenosis in rheumatic heart disease]. [Slovenian]. *Zdrav Vestn* 1969; **38:** 165-8.
16. Robida A, Fettich D. [Heart catheterization and angiography in children in Slovenia in years 1963-1984]. [Slovenian]. *Zdrav Vestn* 1986; **55:** 583-5.
17. Cijan A, Obrez I. [Coronarography]. [Slovenian]. *Med Razgl* 1984; **23(Suppl.7):** 191-204.
18. Hernia S. Professor Dr. [Jože Stropnik (1923-1982)]. [Slovenian]. *Zdrav Vestn* 1982; **51:** 510-10.
19. Stropnik J, Obrez I. [Diagnostic angiographic examination of gastrointestinal bleeding]. [Slovenian]. *Zdrav Vestn* 1971; **40:** 283-7.
20. Stropnik J. [Angiographic image of the liver cirrhosis]. [Slovenian]. *Zdrav Vestn* 1972; **41:** 418-20.
21. Stropnik J. [Diagnostic importance of variations of celiac trunk]. [Slovenian]. *Zdrav Vestn* 1975; **44:** 505-7.
22. Denišlič M, Černk M. [Supraclinoid occlusion of internal carotid artery]. [Slovenian]. In: Lokar J, editor. *Zbornik 5. kongresa neurologov in psihiatrov Jugoslavije.* Portorož, October 1–4, 1976. Ljubljana; 1976. p. 148-9.
23. Černk M, Kregar T, Škrbec M. Aplasia arteriae carotis interne dex. In: *12. kongres radiologa Beograd 1984. Zbornik sažetaka*. 1984. p. 148.
24. Soklič P, Stropnik J, Obrez I, Košir J, Baretić-Kolar E. [Roentgenologic diagnosis of the hemorrhage of digestive tract]. [Croatian]. *Radiol Iugoslav* 1976; **10:** 471-4.
25. Budihna N, Košir J. [Interpretation of 99 MTC MAA venography in comparison with x-ray venography in patients with the deep vein thrombosis of lower limbs]. [Slovenian]. In: *14. jugoslovenski sastanak o medicini. Kratki sadrzaji radova*. Beograd; 1976. p. 61.
26. Us J. [*Memories at the radiologic diagnostics, 1967 do 1994*]. [Slovenian]. Ljubljana: Self-publishing; 2010.
27. Dotter CT. Cardiac catheterization and angiographic techniques of the future. *Cesk Radiol* 1965; **19:** 217-36.
28. Dotter CT, Judkins MP. Transluminal treatment of atherosclerotic obstructions: Description of a new technique and preliminary report of its applications. *Circulation* 1964; **30:** 654-70.
29. Grüntzig A, Mahler F, Kumpe D, Brunner U, Meier W. [Experiences with Dotter's percutaneous recanalization of chronic arterial occlusions]. [German]. *Schweiz Med Wochenschr* 1976: **106:** 422-4.
30. Grüntzig A, Senning A, Siegenthaler WA. Nonoperative dilation of coronary artery stenosis. Percutaneous transluminal coronary angioplasty. *N Engl J Med* 1979; **301:** 61-8.
31. Rösch J, Keller FS, Kaufman JA. The birth, early years and future of interventional radiology. *J Vasc Intervent Radiol* 2003; **14:** 841-53.
32. Rösch J, Dotter CT, Brown MT. Selective arterial embolization. A new method for control of acute gastrointestinal bleeding. *Radiology* 1972; **102:** 303-6.
33. Dotter CT, Rösch J, Seaman AJ. Selective clot lysis with low-dose streptokinase. *Radiology* 1974; **111:** 31-7.

34. Portsmann W, Wierny L, Warnke H. Catheter closure of patent ductus arteriosus: 62 cases treated without thoracotomy. *Radiol Clin North Am* 1971; **9:** 203-18.

35. King TD, Mills NL. Nonoperative closure of atrial septal defect. *Surgery* 1976; **75:** 383-8.

36. Rao PS. History of atrial septal occlusion devices. In: Rao PS, Kern MJ, editors. *Catheter based devices: for the treatment of non-coronary cardiovascular disease in adults and children.* Philadelphia, PA: Lippincott Williams & Wikins; 2003. p. 3-9.

37. Gianturco C, Anderson JH, Wallace S. Mechanical devices for arterial occlusion. *Am J Roentgenol Radium Ther Nucl Med* 1975: **124:** 428-35.

38. Dotter CT. Transluminally placed coiled endarterial tube grafts. *Invest Radiol* 1969; **4:** 329-32.

39. Palmaz JC, Sibbitt RR, Tio FO. Expandable intraluminal vascular graft: feasibility study. *Surgery*1986; **99:** 199-205.

40. Wright KC, Wallace S, Charnsangavej C, Carrasco CH, Gianturco C. Percutaneous endovascular stents: an experimental evaluation. *Radiology* 1985; **156:** 69-72.

41. Rösch J, Hanafee W, Snow H, Barenfus M, Gray R. Transjugular intrahepatic portacaval shunt; an experimental work. *Am J Surg* 1971; **121:** 588-92.

42. Auersperg M, Us-Krasovec M, Obrez I. Problems in intra-arterial chemotherapy. I. Drug dilution. *Neoplasma* 1969; **16:** 579-83.

43. Erjavec M, Auersperg M, Obrez I. Radioactive isotopes in the control of intra-arterial chemotherapy. *Radiobiol Radiother*1971; **12:** 219-25.

44. Obrez I, Abrams HL. Temporary occlusion of the renal artery: effects and significance. *Radiology* 1972; **104:** 545-56.

45. Kubicka RA, Obrez I, Levin DC**.** Simultaneous infusion of vasopressin into two arteries. Control of massive colonic hemorrhage. *JAMA* 1979; **241:** 725-6.

46. Obrez I. A "wire-whip" catheter for selective catheterization of aortic branches. *Cardiovasc Radiol* 1978; **25:** 193-7.

47. Jereb M. The usefulness of needle biopsy in chest lesions of different sizes and locations. *Radiology* 1980; **134:** 13-5.

48. Obrez I, Soklič P, Baretić-Kolar E, Brenčič E. [Interventional (therapeutic) radiology]. [Slovenian]. *Zdrav Vestn* 1980; **49:** 633-40.

49. Obrez I, Baretić-Kolar E, Soklič P. [Percutaneous transluminal angioplasty. The possibility and results]. [Slovenian]. *4. konferenca o aterosklerozi in arterijski trombozi. Zbornik.* Ljubljana; 1980. p. 139-42.

50. Videčnik V, Baretić-Kolar E, Šurlan M. [Locally fibrinolytic treatment of peripheral obliterative arteriopathy]. [Slovenian]. *Zdrav Vestn* 1983; **52:** 165-9.

51. Obrez I, Šurlan M, Pavčnik D. [Percutaneous drainage of abscesses in abdomen]. [Slovenian]. *Zdrav Vestn* 1984; **53:** 569-73.

52. Obrez I , Brenčič E, Baretić-Kolar E, Soklič P. [Percutaneous transhepatic cholangiography and drainage of the biliary tract]. [Croatian]. *15. kongres hirurga Jugoslavije. Sažetci.* Ljubljana; 1980. p. 38.

53. Pavčnik D, Obrez I, Šurlan M, Brenčič E. [Results of percutaneous transhepatic biliary drainage at the patients with obstructive icterus]. [Slovenian]. *Zdrav Vestn* 1984; **53:** 581-3.

54. Šurlan M, Obrez I, Pavčnik D. [Percutaneous nephrostomy]. [Slovenian]. *Zdrav Vestn* 1984; **53:** 575-80.

55. Šurlan M, Pavčnik D, Janež J. Percutaneous removal of renal stones. *Radiol Iugosl* 1986; **20:** 223-6.

56. Šurlan M, Šušteršič J, Pavčnik D, Obrez I. [Treatment of renal cyst with alcohol ablation]. [Serbian]. In: Petronić V, editor. *9. kongres urologa Jugoslavije sa internacionalnim učešćem: zbornik radova.* Beograd: Urološka klinika Kliničkog centra MF; 1986. p. 350-4.

57. Obrez I. [Interventional radiology]. [Slovenian]. *5. sodobna interna medicina*. Ljubljana; 1979. p. 172-4.

58. Čerk M. [Embolization of anterior and middle cerebral artery with Gealfomom at head arteriovenous malformation. 1]. [Slovenian]. *Angioclub*. Ljubljana; 1979.

59. Čerk M. [Embolization of head and neck arteriovenous malformation and meningiomas at Unit for Neurodiagnostics of the Institute of Radiology, University Clinical Centre Ljubljana]. [Slovenian]. In: Pavčnik D, Šurlan M, editors. *Intervencijska radiologija v onkologiji. 6. jugoslovanski simpozij o intervencijski radiologiji in v onkologiji*. Ljubljana; 1989. 43-35.

60. Soklič P. Percutaneous transhepatic vein embolization at hemorrhage of esophageal varices. [Slovenian]. [*6. sodobna interna medicina*]. Ljubljana; 1980. p. 191-9.

61. Klančar J, Šurlan M, Pavčnik D, Obrez I. [Embolotherapy of inoperable kidney tumors]. [Croatian]. In: Mašković J, Boschi S, Stanić I, editors. In: *Intervencijska radiologija*. Split: ZLH, Podružnica Split, Sekcija za radiologiju; 1986; 315-21.

62. Berden P, Pavčnik D, Šurlan M. [Treatment of liver metastases of renal cell carcinoma with percutaneous aplication of absolute ethanol]. [Slovenian]. In: Pavčnik D, Šurlan M, editors. *Intervencijska radiologija v onkologiji. 6. jugoslovanski simpozij o intervencijski radiologiji v onkologiji*. 1989. p. 86-7.

63. Cesar R, Vidmar-Bračika, Pavčnik D, Šurlan M. [Embolizaion of bone tumors]. [Slovenian]. In: Pavčnik D, Šurlan M, editors. *Intervencijska radiologija v onkologiji. 6. jugoslovanski simpozij o intervencijski radiologiji v onkologiji*. 1989. p. 180-1.

64. Šurlan M, Gadzijev E, Pavčnik D, Pleskovič L, Klančar J. Contemporary treatment of malignant liver tumors. [Slovenian]. In: [Pavčnik D, Šurlan M, editors. Intervencijska radiologija v onkologiji]. [Slovenian]. *Intervencijska radiologija v onkologiji. 6. jugoslovanski simpozij o intervencijski radiologiji v onkologiji*. 1989. p. 68-70.

65. Pavčnik D, Šurlan M. [Cavernosography and treatment of zdravljenje venous impotence]. [Slovenian]. *Radiol Iugosl* 1990; **24:** 25-7.

66. Pavčnik D, Šurlan M. Self-expanding metallic stents. *Radiol Iugosl* 1990; **24:** 147-50.

67. Pavčnik D, Šurlan M. [Intravascular stents]. [Slovenian]. *Med Razgl* 1994; **33(Suppl 1):** 111-9.

68. Knific J, Pavčnik D, Klančar J, Berden P, Šurlan M. [Use of intravascular stents for treatment of peripheral occlusive disease]**.** [Slovenian]. *Med Razgl* 1994; **33(Suppl 1):** 121-7.

69. Berden P, Šurlan M, Knific J, Klančar J, Pavčnik D. [The successful recanalization of the peripheral arteries with vascular stents]. [Slovenian]. *Med Razgl* 1994; **33(Suppl 1):** 129-36.

70. Šurlan M, Pavčnik D, Klančar J, Berden P., Knific J. [Percutaneous transluminal renal angioplasty and stenting]. [Slovenian]. *Med Razgl* 1994; **33(Suppl 1):** 157-62.

71. Pavcnik D**,** Surlan M. Transjugular intrahepatic portocaval stents. In: Gadzijev E, Markovic S, Sojar V, editors. *Book of lectures and abstracts. Ljubljana: ALPS-ADRIA Hepatobiliary School.* July 5–6, 1993. Ljubljana: Faculty of Medicine, University Medical Center; 1993. p. 28-30.

72. Popovič P, Štabuc B, Skok P, Šurlan M. TIPS versus endoscopic sclerotherapy in the elective treatment of recurrent variceal bleeding. *J Int Med Res* 2010; **38:** 1121-33.

73. Cijan A. [Coronary angioplasty]. [Slovenian]. *Med Razgl* 1994; **33(Suppl 1):** 169-78.

74. Cijan A, Pust B, Pavčnik D. [The results of PTCA at the first 50 patients with stenosis of coronary occlusions] [Slovenian]. In: *10. radenski dnevi. Strokovni sestanek Kardiološke sekcije Slovenskega zdravniškega društva.* Radenci; 1989. p. 23-4.

75. Kranjec I, Cijan A, Pavčnik D. Intravenous thrombolysis of acute coronary occlusion after percutaneous transluminal angioplasty. In: Benulič T, Serša G, Kovač V, editors. *Advances in radiology and oncology*. Ljubljana: Radiologia Iugoslavica; 1992. p. 30-4.

76. Pavčnik D, Cijan A, Bricelj V. Transcatheter balloon valvuloplasty. *Radiol Oncol* 1993; **27:** 175-9.

77. Robida A, Pavčnik D. Perforation of the heart in a newborn with critical pulmonary valve stenosis during balloon valvuloplasty. *Int J Cardiol* 1990; **26:** 111-2.

78. Pavčnik D, Berden P, Koželj M. Transcatheter occlusion of patent ductus arteriosus in adults. *Radiol Oncol* 1995; **29:** 9-11.

79. Pavčnik D, Keller FS, Cobanoglu A, Uchida B, Timmermans H, Gabrijelčič T, et al. Transfemoral intraluminal stent graft implanted for thoracic aortic aneurysm. *Thorac Cardiovasc Surg* 1995; **43:** 208-11.

80. Šurlan M, Pavčnik D, Gabrijelcic T, Keller FS, Rösch J. Late complications and shape changes of the endografts after gigantic thoracic aortic aneurysm repair during a 7-year follow-up. *Thorac Cardiovasc Surg* 2002; **50:** 104-8.

81. Kuhelj D, Zdesar U, Jevtic V, Skrk D, Omahen G, Zontar D, et al. Risk of deterministic effects during endovascular aortic stent graft implantation. *Br J Radiol* 2010; **83:** 958-63.

82. Pavčnik D. Transcatheter embolization of pulmonary anteriovenous fistula with Gianturco coils. *The Congress of the Hungarian Society of Cardiology*. Balatonfured; 1994.

83. Salapura V, Ključevšek T, Kuhelj D, Popovič P. IVC filters. [Slovenian]. In: Kozak M, Blinc A, editors. *Pogoste žilne bolezni: kako jih preprečujemo, odkrivamo in zdravimo.* Ljubljana: Združenje za žilne bolezni, Slovensko zdravniško društvo; 2008. p. 77-84.

84. Šeruga T, Klein GE. Endovascular treatment of intracranial artery aneurysms in the posterior cerebral circulation. *Wien Klin Wochenschr* 2004; **116(Suppl 2):** 13-8.

85. Milošević Z. [Bioactive coils for the treatment of cerebral aneurysms]. [Slovenian]. In: Tetičkovič E, Žvan B, editors. *Možganska kap - do kdaj*. Maribor: Kapital; 2007. p. 203-7.

86. Salapura V, Blinc A, Kozak M, Jezovnik MK, Pohar Perme M, Berden P , et al. Infrapopliteal run-off and the outcome of femoropopliteal percutaneous transluminal angioplasty. *Vasa* 2010; **39:** 159-68.

87. Kuhelj D, Kavcic P, Popovic P. Percutaneous mechanical thrombectomy of superior mesenteric artery embolism. *Radiol Oncol* 2013; **47:** 239-43.

88. Dušan Pavčnik. 60 years of the Slovenian Association of Radiology 1950-2010. *Radiol Oncol* 2009; **43:** 137-43

89. Kranokpiraksa P, Pavcnik D, Kakizawa H, Uchida BT, Jeromel M, Keller FS, Rösch J. Hemostatic efficacy of chitosan-based bandage for closure of percutaneous arterial access sites: An experimental study in heparinized sheep model. *Radiol Oncol* 2010; **44:** 86-91.

90. Jeromel P, Pavcnik D. Infrahepatic caudal/inferior vena cava interruption with azygos/hemiazygos continuation. Vascular anomaly in swine. *Radiol Oncol* 2010; **44:** 149-52.

91. Pavcnik D, Tekulve K , Uchida B, Luo ZH, Jeromel M, VanAlstine W, et al. Double BioDisk: a new bioprosthetic device for transcatheter closure of atrial septal defects- a feasibility study in adult sheep. *Radiol Oncol* 2012; **46:** 89-96.

92. Luo ZH, Chung A, Choi GB, Lin YH, Pang H, Uchida BT, Pavcnik D, Jeromel M, Keller FS, Rösch J. Iodine based radiopacity of experimental blood clots for testing of mechanical thrombectomy devices. *Radiol Oncol* 2013; **47:** 1-5

Radiol Oncol 2014; 48(4): 331-338.
doi:10.2478/raon-2014-0011

Natančnost pozitronske emisijske tomografije z ^{18}F-deoksiglukozo in računalniške tomografije pri ugotavljanju razširjenosti na novo odkritega raka nosnega žrela. Sistematični pregled in metaanaliza

Vellayappan BA, Soon YY, Earnest A, Zhang Q, Koh WY, Tham IWK, Lee KM

Izhodišča. Želeli smo ovrednotiti vlogo pozitronske emisijske tomografije z 18F-deoksiglukozo in računalniške tomografije (FDG-PET/CT) pri ugotavljanju razširjenosti raka nosnega žrela. Da bi ocenili natančnost preiskave FDG-PET/CT pri ugotavljanju zamejitve novoodkritih rakov nosnega žrela, smo naredili sistematični pregled literature in metaanalizo dosegljivih podatkov.

Metode. Pregledali smo različne biomedicinske podatkovne baze in konferenčne zbornike. Določili smo skupne občutljivosti in specifičnosti, diagnostična razmerja obetov (DRO) in s pomočjo hierarhičnega regresijskega modela izdelali zaključne krivulje ROC (receiver operating characteristic).

Rezultati. Našli smo 15 ustreznih kliničnih raziskav, ki so skupaj vključevale 851 bolnikov. 5 jih je obravnavalo primarni tumor (T), 9 področne bezgavke (N) in 7 oddaljene zasevke (M). Ocena kombinirane občutljivosti za FDG-PET/CT za razvrstitev T je bila 0,77 (95 & interval zaupanja [CI] 0,59–0,95). Kombinirana občutljivost za razvrstitev N je bila 0,84 (95 % CI 0,76–091), specifičnost 0,90 (95 & CI 0.83–0.97), DRO 82,4 (23,2–292,6) in indeks Q* 0,90. Za razvrstitev M je bila ocena kombinirane občutljivosti 0,87 (95 & CI 0,74–1,00), specifičnost 0,98 (95% CI 0,96–1,00), DRO 120,9 (43,0–340,0) in indeks Q* 0,89.

Zaključki. Pri na novo ugotovljenem raku nosnega žrela je bila raziskava z FDG-PET/CT primerno natančna za opredelitev N in M, ne pa tudi za razvrstitev T. Preiskava s FDG-PET/CT bi morala biti skupaj z magnetnoresonančnim slikanjem nosnega žrela del rutinskih zamejitvenih preiskav.

Radiol Oncol 2014; 48(4): 339-347.
doi:10.2478/raon-2014-0018

Iskanje primarnih tumorjev pri bolnikih z nevroendokrinimi tumorji (NET) neznanega izvora in klinično sumljivih NET. Ovrednotenje preiskav Ga-68 DOTATOC PET/CT in In-111 DTPA oktreotid SPECT/CT

Schreiter NS, Bartels AM, Froeling V, Steffen I, Pape UF, Beck A, Hamm B, Brenner W, Röttgen R

Izhodišča. Namen raziskave je bil ovrednotiti klinično učinkovitost preiskav Ga-68 DOTATOC PET/CT in In-111 DTPA oktreotid SPECT/CT za ugotavljanje primarnih tumorjev pri bolnikih z nevroendokrinimi tumorji neznanega izvora (NETUP) ali za ugotavljanje klinično sumljivih primarnih nevroendokrinih tumorjev (SNET).

Bolniki in metode. V letih med 2006 in 2009 smo v raziskavo vključili 123 bolnikov. Pri 52 bolnikih smo naredili preiskavo z Ga-68 DOTATOC PET/CT-jem (33 bolnikom z NETUP-om in 19 s SNET-om) in pri 71 bolnikih preiskavo z In-111 DTPA oktreotid SPECT/CT-jem (50 bolnikom z NETUP-om in 21 s SNET-om). Bolnikom smo diagnozo potrdili histopatološko ali pa s sledenjem bolezni.

Rezultati. Pri 123 bolnikih smo skupaj odkrili 21 primarnih tumorjev. Pri skupini bolnikov z NETUP-om, kjer smo uporabili Ga-68 DOTATOC, smo odkrili primarne tumorje pri 15 bolnikih (45,5 %). Pri skupini bolnikov, kjer smo uporabili In-111 DTPA oktreotid pa smo primarni tumor odkrili pri 4 bolnikih (8 %) ($p<0.001$). Pri skupini bolnikov s SNET-om, smo odkrili samo 2 primarna tumorja z metodo Ga-68 DOTATOC. Pri bolnikih z NETUP-om je bilo možno odkriti primarne tumorje statistično značilno bolj pogosto kot pri bolnikih s SNET-om ($p = 0,01$). 14 bolnikov smo operirali.

Zaključki. Preiskavo z Ga-68 DOTATOC PET/CT-om v večji meri priporočamo kot preiskavo z In-111 DTPA oktreotid SPECT/CT-om, kadar iščemo primarne NET pri bolnikih z NETUP-om. Pri bolnikih s SNET-om pa je potrebno to preiskavo uporabljati pazljivo.

Radiol Oncol 2014; 48(4): 348-353.
doi:10.2478/raon-2014-0007

Pomen sonoelastografije, sive skale in barvne dopplerske ultrazvočne preiskave pri opredelitvi malignosti vozličev v ščitnici

Tatar IG, Kurt A, Yilmaz KB, Doğan M, Hekimoglu B

Izhodišča. Ultrazvočna preiskava je neinvazina metoda, ki jo pogosto uporabljamo v diagnostičnem postopku obravnave ščitničnih vozličev. Namen raziskave je bil oceniti uporabnost sonografskih in elastosonografskih parametrov pri ugotavljanju malignosti teh vozličev.

Bolniki in metode. Ultrazvočno smo ovrednotili 150 ščitničnih vozličev z elastosonografijo, s sivo skalo in z dopplersko tehniko. S citološko analizo smo odkrili 141 benignih in 9 malignih vozličev.

Rezultati. Orientacija vozličev je bil edini sonografski parameter statistično značilno povezan z malignostjo (p = 0,003). Z elastosonografsko analizo (razmerje elastičnosti) smo ugotovili, da je pri ugotavljanju malignosti najboljša razmejitvena vrednost 1,935 (p = 0,000). Senzitivnost je bila 100 %, specifičnost 76 %, negativna napovedna vrednost 100 %, pozitivna napovedna vrednost 78,5 % in stopnjo natančnosti78 %. Ugotovili smo statistično značilno odvisnost med vrednostjo elastičnosti in malignostjo (0,001). Večina benignih vozličev je imelo vrednost 2 in 3, noben ni imel vrednosti 5. Nasprotno, noben maligni vozlič ni imel vrednosti 1 in 2, večina je imela vrednost 5.

Zaključki. Elastosonografske parametre bo potrebno upoštevati v diagnostičnem postopku obravnave ščitničnih vozličev.

Radiol Oncol 2014; 48(4): 354-360.
doi:10.2478/raon-2014-0032

Različen razvoj tumorskih celic v fazi S celičnega ciklusa glede na njihov status p53

Zölzer F, Mußfeldt T, Streffer C

Izhodišča. Regulacija kontrolnih točk pri prehodu celic v fazi S je kompleksna, predvsem po izpostavitvi celic ionizirajočemu sevanju. Nejasna je vloga proteina p53. Namen študije je bil proučiti razvoj obsevanih tumorskih celic v fazi S, v odvisnosti od statusa p53 teh celic.

Materiali in metode. V raziskavi smo uporabili tri pare tumorskih celičnih linij. Vsaka je imela funkcionalen in okvarjen p53. Takoj po obsevanju smo celice označili z bromdeoksiuridinom (BrdU), nato smo jih inkubirali v gojišču brez označevalca ter s pomočjo pretočne citometrije sledili njihov razvoj v fazi S celičnega ciklusa.

Rezultati. Pri celicah z okvarjenim p53 je bil prehod v fazi S celičnega ciklusa upočasnjen vsaj za nekaj ur, pri celicah z normalnim p53 pa je bil prehod neoviran ali celo nekoliko pospešen.

Zaključki. Rezultati raziskave nedvoumno kažejo na vlogo p 53 pri razvoju celic v fazi S celičnega ciklusa po obsevanju. Natančen mehanizem delovanja, kako je regulirana iniciacija in podvajanje DNA pri obsevanih celicah, pa še ni znano.

Radiol Oncol 2014; 48(4): 361-368.
doi:10.2478/raon-2014-0038

Izmenična kemoterapija in erlotinib pri bolnikih z nedrobnoceličnim rakom pljuč. Velik delež popolnih odgovorov na zdravljenje ter podaljšano preživetje brez znakov bolezni pri bolnikih, ki so imeli aktivirajoče mutacije

Zwitter M, Stanič K, Rajer M, Kern I, Vrankar M, Edelbaher N, Kovač V

Izhodišča. Pri bolnikih z nedrobnoceličnim rakom pljuč se lahko s farmakodinamičnim ločevanjem citostatikov in tarčnih zdravil izognemo njihovemu medsebojnemu antagonističnemu delovanju. Primarni cilj klinične raziskave je bil ugotoviti odgovor na zdravljenje in preživetje brez napredovanja bolezni pri bolnikih, ki so izmenično prejemali kemoterapijo in erlotinib; sekundarni cilj pa ugotoviti stranske učinke zdravljenja in celokupno preživetje bolnikov.

Bolniki in metode. V prospektivno klinično raziskavo smo vključili bolnike s stadijem IIB in IV nedrobnoceličnega raka pljuč, ki še niso bili zdravljeni s kemoterapijo. Bolniki so bili nekadilci ali pretekli lahki kadilci, od leta 2010 pa smo vključevali le tiste, kjer smo dokazali aktivirajoče mutacije na receptorjih epidermalnega rastnega dejavnika (EGFR). Bolniki so prejemali kemoterapijo na 3 tedne: gemcitabin 1. in 4., cisplatin na 2. dan ter erlotinib od 5. do 15. dne vsakega kroga kemoterapije. Po 4 do 6 krogih je bolnik prejemal vzdrževalni odmerek erlotiniba.

Rezultati. V raziskavi smo zdravili 53 bolnikov: 24 pred letom 2010 (kasneje smo ugotovili, da jih je 9 imelo mutacije EGFR) ter 29 bolnikov po letu 2010, ki so vsi imeli aktivirajoče mutacije EGFR. Bolniki so imeli tudi neugodne napovedne dejavnike za preživetje: bolezen v stadiju IV (51 bolnikov, 96 %), stanje splošne zmogljivosti 2–3 (11 bolnikov, 21 %) in možganske zasevke (15 bolnikov, 28%). Toksičnost stopnje 4 smo videli pri 2 bolnikih z nevtropenijo in 4 s tromboembolijo. Pri 15 bolnikih, ki niso imeli mutacije EGFR, smo ugotovili 33 % objektivnih odgovorov, srednje preživetje brez napredovanja bolezni je bilo 6,0 mesecev in srednje celokupno preživetje 7,6 mesecev. Pri 38 bolnikih, ki pa so imeli mutacije EGFR, smo ugotovili popoln ali delen odgovor na zdravljenje v 16 (42,1 %) in 17 (44,7 %) primerih. Preiskavo PET-CT smo naredili pri 30 bolnikih in potrdila je popoln ali delen odgovor na zdravljenje v 16 (53,3 %) in 9 (30,0 %) primerih. Srednje preživetje brez napredovanja bolezni pri bolnikih z mutacijami EGFR je bilo 21,2 mesecev, srednje celokupno preživetje pa 32,5 mesecev.

Zaključki. Bolnikom, pri katerih nismo dokazali mutacij EGFR, nismo uspeli izboljšati učinka zdravljenja z dodajanjem erlotiniba. Nasprotno pa so rezultati izmeničnega zdravljenja s kemoterapijo in erlotinibom ohrabrujoči pri bolnikih z mutacijami EGFR.

Radiol Oncol 2014; 48(4): 369-380.
doi:10.2478/raon-2014-0026

Zdravljenje bolnikov z lokalno napredovalim nedrobnoceličnim rakom pljuč. Uvodna kemoterapija z gemcitabinom v standardnem odmerku ali v nižjem odmerku in v podaljšani infuziji ter s cisplatinom, ki ji je sledila sočasna kemoradioterapija. Klinična randomizirana raziskava II. faze

Vrankar M, Zwitter M, Bavčar T, Milić A, Kovač V

Izhodišča. Zdravljenje lokalno napredovalega nedrobnoceličnega raka pljuč ter optimalna kombinacija kemoterapije in obsevanja ostaja odprto vprašanje. V randomizirani klinični raziskavi II. faze smo v uvodni kemoterapiji primerjali učinkovitost dveh različnih shem aplikacije gemcitabina s standardno dozo cisplatina, nato smo bolnike radikalno obsevali in jih sočasno zdravili s cisplatinom in etoposidom.

Bolniki in metode. Bolniki, primerni za vključitev v raziskavo, so imeli mikroskopsko potrjen neoperabilen nemetastatski nedrobnocelični pljučni rak; izpolnjevali so kriterije za zdravljenje s kemoterapijo na osnovi platine; podali so podpisano soglasje za sodelovanje v raziskavi. Zdravili smo jih s tremi krogi uvodne kemoterapije z gemcitabinom in cisplatinom. Primerjali smo dve različni shemi aplikacije gemcitabina: bolniki v roki A so prejeli gemcitabin v odmerku 1250 mg/m^2 v standardni polurni intravenski infuziji 1. in 8. dan kemoterapije; bolniki v roki B pa so prejeli gemcitabin v odmerku 250 mg/m^2 v daljši 6-urni intravenski infuziji prav tako 1. in 8. dan. V obeh rokah so bolniki 2. dan prejeli cisplatin v odmerku 75 mg/m^2. Vsi bolniki so nadaljevali zdravljenje z obsevanjem s 60-66 Gy sočasno s cisplatinom v odmerku 50 mg/m^2 1., 8., 29. in 36. dan obsevanja ter etoposidom 50 mg/m^2 1.-5. in 29.-33. dan obsevanja. Primarni cilj raziskave je bil ugotoviti odgovor na zdravljenje (RR) po uvodni kemoterapiji; sekundarni cilj pa so bili ugotavljanje stranskih učinkov zdravljenja, preživetja brez napredovanja bolezni (PFS) in celokupnega preživetja (OS).

Rezultati. Od septembra 2005 do novembra 2010 smo v raziskavo vključili 106 bolnikov. Po uvodni kemoterapiji nismo našli statistično značilnih razlik v RR med obema rokama (48,1 % in 57,4 %, p = 0,34). Stranski učinki uvodne kemoterapije so bili blagi in primerljivi v obeh rokah. Najpogosteje smo ugotavljali nevtropenijo stopnje 3/4. En bolnik v roki B je utrpel akutno periferno ishemijo stopnje 4, zaradi česar je bila potrebna amputacija spodnjega uda. Srednji čas spremljanja bolnikov je bil 69,3 mesecev; PFS in OS v roki A sta bila 15,7 in 24,8 mesecev, v roki B pa 18,9 in 28,6 mesecev. Eno- in tri-letno celokupni preživetji sta bili 73,1 % in 30,8 % v roki A ter 81,5 % in 44,4 % v roki B.

Zaključki. Pri uvodni kemoterapiji z dvema različnima shemama aplikacije gemcitabina in standardno dozo cisplatina za zdravljenje neoperabilnega nemetastatskega nedrobnoceličnega raka pljuč smo ugotovili primerljive stranske učinke. Učinkovitost zdravljenja, ki smo jo določali z RR, PFS in OS, je med najvišjimi poročanimi v literaturi. Opazili smo težnjo boljše učinkovitosti zdravljenja s podaljšano infuzijo gemcitabina, vendar je število bolnikov premajhno za zaznavanje statistično pomembne razlike.

Radiol Oncol 2014; 48(4): 381-386.
doi:10.2478/raon-2014-0019

Preživetje bolnikov z anaplastičnim astrocitomom po obsevanju

Barker CA, Chang M, Beal K, Chan TA

Izhodišča. Med primarnimi možganskimi tumorji odraslih je 7 % anaplastičnih astrocitomov (AA). Predvidevajo, da je preživetje bolnikov odvisno od tumorja, bolnika in od zdravljenja. V raziskavi smo retrospektivno ocenili povezanost med tumorjem, bolnikom in zdravljenjem ter med preživetjem.

Bolniki in metode. Pregledali smo podatke bolnikov z AA, ki smo jih med letoma 1987 in 2007 zdravili z obsevanjem v Memorial Sloan-Kettering Cancer Centru v New Yorku. Beležili smo spremenljivke, povezane s tumorjem, bolnikom in zdravljenjem ter jih uporabili za porazdelitev bolnikov v skupine po RTOG RPA (*Radiation Therapy Oncology Group recursive partitioning analysis*). Zabeležili smo tudi prvo uporabo kemoterapije. Testi log-rank in regresijski modeli Cox so bili uporabljeni za oceno povezave med dejavniki tumorjev, bolnikov in zdravljenja s preživetjem.

Rezultati. Sto šestindvajset bolnikov je bilo primernih za raziskavo. Srednja starost je bila 43 let, stopnja splošne zmogljivosti po Karnofskem 90 in trajanje simptomov 8 tednov. Srednja doza obsevanja je bila 59,4 Gy. 61% bolnikov smo operirali, 17% bolnikov je prejelo temozolomid med obsevanjem ter 41% po obsevanju. Srednje preživetje je bilo 31 mesecev, 2-letno preživetje pa 58%. RTOG RPA razredi so bili povezani s preživetjem ($p < 0,001$), ne pa tudi prejemanje temozolomida med in po obsevanju ($p > 0,05$).

Zaključki. V raziskavi, omejeni z retrospektivnim pristopom, je bila RTOG RPA razdelitev povezana s preživetjem. Potrebne so nadaljnje klinične raziskave o vplivu zdravljenja s temozolamidom na preživetje.

Radiol Oncol 2014; 48(4): 387-392.
doi:10.2478/raon-2013-0069

Identifikacija treh anatomskih variant XI. možganskega živca z elektrofiziološkim kartiranjem

Lanišnik B, Žargi M, Rodi Z

Izhodišča. Čeprav med modificirano radikalno disekcijo ohranimo XI. možganski živec, ima precejšen delež bolnikov težave z gibljivostjo ramenskega obroča.

Metode. V raziskavi smo med modificirano radikalno disekcijo kartirali XI. možganski živec s pomočjo nevrofizioloških metod.

Rezultati. Živec smo nadzorovali med 74 disekcijami vratu in identificirali tri anatomske variacije. Živec lahko vstopi v sternokleidomastoidno mišico (mSCM) in iz nje izstopi na zadnji meji v regiji V. Govorimo o tipu 1 in smo ga našli pri 66 % disekcij vratu. Če se veja za trapezno mišico odcepi pred vstopom v sternokleidomastoidno mišico, govorimo o tipu 2 delitve. Ta tip je bil prisoten pri 22 % disekcij. Če se veja za trapezno mišico pojavi za zadnjim robom sternokleidomastoidne mišice ter se pomeša s cervikalnim pleksusom, se iz njega odcepi kot ena veja in vstopi regijo V, govorimo o tipu 3. Je najredkejši, našli smo ga v 12 %.

Zaključki. Opis treh anatomskih variacij XI. možganskega živca je lahko v pomoč pri disekciji vratu in pri tem zmanjšanju možnosti medoperativne poškodbe.

Radiol Oncol 2014; 48(4): 393-396.
doi:10.2478/raon-2013-0079

Oddaljeni zasevek rektalnega žleznega raka v začasni traheostomi

Šifrer R, Strojan P, Zidar N, Žargi M, Grošelj A, Krajinović M

Izhodišča. Zasevke v začasni traheostomi iz raka glave in vratu so v literaturi že opisovali. Do sedaj so jih pripisovali regionalnemu zasevanju malignega tumorja. Poročamo o primeru zasevka v začasni traheostomi iz primarne lokalizacije izven glave in vratu. Takšen primer do sedaj v literaturi še ni bil opisan. Prikazujemo prvi primer sistemskega zasevanja malignega tumorja v začasno traheostomo.

Prikaz primera. Štiriinpetdesetletna bolnica, ki so jo predhodno zdravili zaradi rektalnega žleznega raka, je prišla na pregled v našo ambulanto zaradi eksofitičnih, rožnatih tkivnih sprememb okrog začasne traheostome. Izvidi biopsije in imunohistokemičnih preiskav so pokazali, da je zaseval rektalni rak v začasno traheostomo. Bolnico smo paliativno obsevali. Umrla je zaradi sistemskega napredovanja bolezni.

Zaključki. Bolniki z anamnezo primarnega raka katere koli lokalizacije in z eksofitičnimi, proliferativnimi tkivnimi spremembami okrog traheostome zahtevajo primerno diagnostično obravnavo, ki vključuje biopsijo. Način zdravljenja je odvisen od razširjenosti bolezni, predhodnega zdravljenja in splošnega zdravstvenega stanja bolnika.

Radiol Oncol 2014; 48(4): 397-402.
doi:10.2478/raon-2013-0080

Mediastinalni teratom novorojenčka s fetalnim hidropsom in razvojem kronične respiratorne insuficience

Simončič M, Kopriva S, Zupančič Ž, Jerše M, Babnik J, Srpčič M, Grosek Š

Izhodišča. Mediastinalne teratome lahko v neonatalnem obdobju odkrijemo naključno med rednimi ultrazvočnimi pregledi. Zaradi pritiska na mediastinalne strukture lahko povzročijo neimuni fetalni hidrops in polihidramnij. V večini primerov razvoj fetalnega hidropsa vodi v smrt zarodka ali prezgodnji porod. Zgodnja kirurška odstranitev je pomembna, vendar je rezultat zdravljenja odvisen od stopnje razvoja mediastinalnih organov in zapletov v pooperativnem obdobju.

Prikaz primera. 31-letno nosečnico z bihoriatnimi dvojčki smo v 33. tednu nosečnosti sprejeli v porodnišnico po spontanem razpoku jajčnih ovojev. Naredili smo urgentni carski rez, ker smo ultrazvočno ugotovili polihidramnij in obsežni fetalni hidrops pri plodu A. Dvojček A je bil zaradi hude dihalne stiske intubiran takoj po rojstvu. Ultrazvočno in rentgensko smo v desnem hemitoraksu potrdili tumorsko maso veliko 4 x 6 cm. V starosti sedmih dni smo naredili operativni poseg z resekcijo tumorja. Patomorfološko smo potrdili kongenitalni nezreli mediastinalni teratom. Pooperativno obdobje se je zapletlo z respiratorno insuficienco, ki se je v 8. mesecu starosti razvila v kronično obliko.

Zaključki. Predstavljeni primer novorojenčka z mediastinalnim teratomom in hudim neimunim fetalnim hidropsom je peti primer v literaturi, ki je kljub visoki smrtnosti ob takšni bolezni preživel neonatalno obdobje. Ob razvoju kronične respiratorne insuficience smo diagnosticirali spremenjen potek obeh pljučnih arterij, ki je verjetno z drugimi dejavniki povzročil končno respiratorno stanje.

Radiol Oncol 2014; 48(4): 403-407.
doi:10.2478/raon-2013-0081

Učinkovitost dopolnilnega zdravljenja s trastuzmabom v klinični praksi

Matos E, Zakotnik B, Gražič Kuhar C

Izhodišča. Rak dojke s prekomerno izraženostjo receptorjev za humani epidermalni rastni dejavnik 2 ali pomnožitvijo njihovega gena (HER2 pozitiven rak) je agresivna bolezen. Pri bolnicah, ki imajo takšen rak, enoletno dopolnilno zdravljenje s trastuzumabom izboljša preživetje brez bolezni za 40–50 %. Za eno tretjino zmanjša tveganje za smrt. Dopolnilno zdravljenje s trastuzumabom smo v Sloveniji uvedli že v letu 2005. Namen tega prispevka je prikazati, da v vsakodnevni praksi dosegamo enako dobre rezultate, kot v dopolnilnih kliničnih študijah.

Bolnice in metode. V analizo smo vključili 313 bolnic (srednja starost 52 let), ki smo jih zdravili na Onkološkem inštitutu v Ljubljani od leta 2005 do 2009. Analizirali smo značilnosti bolnic, tumorjev, njihovo zdravljenje in izhod bolezni (preživetje brez ponovitve bolezni in celokupno preživetje).

Rezultati. Srednji čas spremljanja bolnic je bil 4,4 leta. Bolezen se je ponovila pri 61 bolnicah, 24 bolnic je umrlo. Triletno preživetje brez ponovitve bolezni je bilo 84,2 %, štiriletno 80,8 %. Triletno celokupno preživetje je bilo 94,4 %, štiriletno 92,5 %. Neodvisna napovedna dejavnika za preživejte brez bolezni sta bila stopnja malignosti tumorja (razmerje tveganj [HR] 2,1; 95 % interval zaupanja [CI] 1,07–4,14; p = 0,031) in prizadetost bezgavk (HR 1,35; 95 % CI 1,16–1,56; p < 0,0001), za celokupno preživetje pa samo prizadetost bezgavk (HR 1,36; 95 % CI 1,05–1,78; p = 0,021).

Zaključki. Naši rezultati izhajajo iz vsakodnevne klinične prakse enoletnega dopolnilnega zdravljenja s trastuzumabom. Bolnice, ki jih zdravijo internisti onkologi, imajo izhod zdravljenja primerljiv rezultatom mednarodnih raziskav in potrjujejo učinkovitost dopolnilnega zdravljenja.

Radiol Oncol 2014; 48(4): 408-415.
doi:10.2478/raon-2014-0003

Metoda za tvorbo velikih zbirk podatkov o geometriji organov za raziskave načrtovanja obsevanj

Nan Hu, Laura Cerviño, Paul Segars, John Lewis, Jinlu Shan, Steve Jiang, Xiaolin Zheng, Ge Wang

Izhodišča. Vse več uporabljamo adaptivno radioterapijo, zato potrebujemo pri kliničnem in raziskovalnem delu velike zbirke podatkov o geometriji organov. Ti temeljijo na anatomiji bolnikov. Za raziskovanja kot so n. pr. segmentacija slik, ponovno načrtovanje obsevanja, analiza deformacij organov so v kliniki včasih na voljo le omejene zbirke podatkov.

Materiali in metode. V raziskavi smo predlagali novo metodo za oblikovanje velikih zbirk podatkov o geometriji organov za potrebe adaptivne radioterapije. Študijske podatke o obliki organov, dnevno pridobljene s koničnožarčnim CT-jem, smo poravnali v skupnem koordinatnem sistemu in kot referenčno površino izbrali eno izmed študijskih površin. Izdelali smo statistični oblikovni model organov, ki je temeljil na točkovnem ujemanju med površinami in podatki pridobljenimi s t. i. tehniko NURBS. Analizo glavne komponente smo naredili na vzorčenih površinskih točkah, ki naj bi predstavljale najpomembnejše variante pri vsakem organu. Ustvarili smo zbirko glavnih komponent in ustreznih koeficientov, ki predstavljajo deformacijo površine organa, in naredili statistično analizo koeficientov.

Rezultati. Tvorba novih zbirk statistično primerljivih koeficientov in njihovo dodeljevanje glavnim komponentam je možno in omogoča oblikovanje večjih geometrijskih zbirk podatkov o organih bolnikov.

Zaključki. Razvili smo metodo za avtomatsko tvorbo velikih zbirk podatkov o bolnikovi geometriji iz omejene slikovne podatkovne zbirke. Tako nastale geometrije organov so realne in statistično verodostojne.

Radiol Oncol 2014; 48(4): 416-425.
doi:10.2478/raon-2014-0023

Slovenska pot od diagnostične angiografije do intervencijske radiologije

Pavčnik D

Izhodišča. Namen članka je dokumentirati pomembne dogodke in ljudi v prvih 50 letih diagnostične angiografije in intervencijske radiologije v Sloveniji. V tem obdobju se niso zamenjala le imena bolnišnic in oddelkov, temveč tudi njihovo vodstvo.

Zaključki. Sestavek poudarja pomembno vlogo ključnih oseb za razvoj diagnostične angiografije in intervencijske radiologije v Sloveniji. Zgodovinski podatki kažejo, da je slovenska radiologija sorazmerno hitro uvajala sodobno interventno radiologijo v klinično prakso.

Fundacija "Docent dr. J. Cholewa"
je neprofitno, neinstitucionalno in nestrankarsko
združenje posameznikov, ustanov in organizacij, ki želijo
materialno spodbujati in poglabljati raziskovalno
dejavnost v onkologiji.

Dunajska 106
1000 Ljubljana

IBAN: SI56 0203 3001 7879 431

Activity of "Dr. J. Cholewa" Foundation for Cancer Research and Education – a report for the final quarter of 2014

The Dr. J. Cholewa Foundation for Cancer Research and Education is a non-profit, non-political and non-government organisation that helps professionals, institutions and other individuals and organisations obtaining at least part of financial funds primarily for cancer research and education in the Republic of Slovenia. Financial support for qualified individuals and organisations interested in theoretical and practical problems in cancer has resulted in a number of publications and projects.

The Foundation continues to provide financial support to "Radiology and Oncology", an international scientific journal that is edited, published and printed in Ljubljana, Slovenia. "Radiology and Oncology" publishes scientific research articles, reviews, case reports, short reports and letters to the editor about research and studies in experimental and clinical oncology, supportive therapy, experimental and clinical research in radiology, radiophyics, prevention and early diagnostics of different types of cancer. It is an open access journal available in pdf format with an important Science Citation Index Impact factor. All the abstracts in "Radiology and Oncology" are available in Slovenian and the journal can thus provide sufficient scientific information from various fields of high quality cancer research to interested lay public in Slovenia.

High quality research demands a certain amount of financial support and many excellent ideas cannot be carried into effect for the simple lack of it. The Dr. J. Cholewa Foundation for Cancer Research and Education is thus constantly evaluating ways to intensify financial support to all interested in the fight against cancer in the Republic of Slovenia. As already experienced before and especially in the last two years, efforts to organise scientific and other meetings of specific interest in cancer research and cancer education may result in very effective dissemination of specific knowledge among professionals and lay public. This activity will thus continue to form an ever more important part in expanding Foundation's activities in the future.

Borut Štabuc, MD, PhD
Tomaž Benulič, MD
Viljem Kovač, MD, PhD
Andrej Plesničar, MD, MSc

TANTUM VERDE®

Lajšanje bolečine in oteklin pri vnetju v ustni votlini in žrelu, ki nastanejo zaradi okužb in stanj po operaciji in kot posledica radioterapije (t.i. radiomukozitis).

CSC ANGELINI

Imetnik dovoljenja za promet
CSC Pharma d.o.o.
Jana Husa 1a
1000 Ljubljana

www.tantum-verde.si

Tantum Verde 1,5 mg/ml oralno pršilo, raztopina

Kakovostna in količinska sestava
1 ml raztopine vsebuje 1,5 mg benzidaminijevega klorida, kar ustreza 1,34 mg benzidamina. V enem razpršku je 0,17 ml raztopine. En razpršek vsebuje 0,255 mg benzidaminijevega klorida, kar ustreza 0,2278 mg benzidamina. En razpršek vsebuje 13,6 mg 96 odstotnega etanola, kar ustreza 12,728 mg 100 odstotnega etanola, in 0,17 mg metilparahidroksibenzoata (E218).

Terapevtske indikacije
Samozdravljenje: lajšanje bolečine in oteklin pri vnetju v ustni votlini in žrelu, ki so lahko posledica okužb in stanj po operaciji. Po nasvetu in navodilu zdravnika: lajšanje bolečine in oteklin v ustni votlini in žrelu, ki so posledica radiomukozitisa.

Odmerjanje in način uporabe
Uporaba 2- do 6-krat na dan (vsake 1,5 do 3 ure). Odrasli: 4 do 8 razprškov 2- do 6-krat na dan. Otroci od 6 do 12 let: 4 razprški 2- do 6-krat na dan. Otroci, mlajši od 6 let: 1 razpršek na 4 kg telesne mase; do največ 4 razprške 2 do 6-krat na dan.

Kontraindikacije
Znana preobčutljivost za zdravilno učinkovino ali katerokoli pomožno snov.

Posebna opozorila in previdnostni ukrepi
Pri manjšini bolnikov lahko resne bolezni povzročijo ustne/žrelne ulceracije. Če se simptomi v treh dneh ne izboljšajo, se mora bolnik posvetovati z zdravnikom ali zobozdravnikom, kot je primerno. Zdravilo vsebuje aspartam (E951) (vir fenilalanina), ki je lahko škodljiv za bolnike s fenilketonurijo. Zdravilo vsebuje izomalt (E953) (sinonim: izomaltitol (E953)). Bolniki z redko dedno intoleranco za fruktozo ne smejo jemati tega zdravila. Uporaba benzidamina ni priporočljiva za bolnike s preobčutljivostjo za salicilno kislino ali druga nesteroidna protivnetna zdravila. Pri bolnikih, ki imajo ali so imeli bronhialno astmo, lahko pride do bronhospazma. Pri takih bolnikih je potrebna previdnost.

Medsebojno delovanje z drugimi zdravili in druge oblike interakcij
Pri ljudeh raziskav o interakcijah niso opravljali.

Nosečnost in dojenje
Tantum Verde z okusom mentola 3 mg pastile se med nosečnostjo in dojenjem ne smejo uporabljati.

Vpliv na sposobnost vožnje in upravljanja s stroji
Uporaba benzidamina lokalno v priporočenem odmerku ne vpliva na sposobnost vožnje in upravljanja s stroji.

Neželeni učinki
Bolezni prebavil Redki: pekoč občutek v ustih, suha usta.
Bolezni imunskega sistema Redki: preobčutljivostna reakcija.
Bolezni dihal, prsnega koša in mediastinalnega prostora Zelo redki: laringospazem.
Bolezni kože in podkožja Občasni: fotosenzitivnost. Zelo redki: angioedem.

Rok uporabnosti
4 leta. Zdravila ne smete uporabljati po datumu izteka roka uporabnosti, ki je naveden na ovojnini. Posebna navodila za shranjevanje Za shranjevanje pastil niso potrebna posebna navodila. Plastenko z raztopino shranjujte v zunanji ovojnini za zagotovitev zaščite pred svetlobo. Shranjujte pri temperaturi do 25°C. Shranjujte v originalni ovojnini in nedosegljivo otrokom.

XGEVA®: PRVI IN EDINI ZAVIRALEC LIGANDA RANK, KI PREPREČUJE ZAPLETE KOSTNIH ZASEVKOV

SUPERIORNO PREPREČEVANJE.[1] TARČNO DELOVANJE.[1] SUBKUTANO INJICIRANJE.[1]

- Zdravilo XGEVA® je indicirano za preprečevanje zapletov kostnih zasevkov pri odraslih s kostnimi zasevki solidnih tumorjev.
- Priporočen odmerek zdravila XGEVA® je 120 mg v enkratni subkutani injekciji, enkrat na 4 tedne.[1]

XGEVA®
(denosumab)
NATANČEN. MOČAN. DOKAZAN.

XGEVA® 120 mg raztopina za injiciranje (denosumab) – SKRAJŠAN POVZETEK GLAVNIH ZNAČILNOSTI ZDRAVILA
Samo za strokovno javnost. Pred predpisovanjem si preberite celoten povzetek glavnih značilnosti zdravila.
▼Za to zdravilo se izvaja dodatno spremljanje varnosti. Poročati je potrebno o vseh domnevnih neželenih učinkih zdravila.
SESTAVA ZDRAVILA: Ena viala vsebuje 120 mg denosumaba v 1,7 ml raztopine (70 mg/ml). Pomožne snovi s prepoznavnim delovanjem: 1,7 ml raztopine vsebuje 78 mg sorbitola (E420). **TERAPEVTSKE INDIKACIJE:** Preprečevanje skeletnih dogodkov (patoloških zlomov, obsevanja kosti, kompresije hrbtenjače ali operacije kosti) pri odraslih s kostnimi metastazami solidnih tumorjev. **ODMERJANJE IN NAČIN UPORABE:** Priporočeni odmerek zdravila XGEVA® je 120 mg enkrat na 4 tedne v enkratni subkutani injekciji v stegno, trebuh ali nadlaket. Vsi bolniki morajo prejemati dodatek vsaj 500 mg kalcija in 400 i.e. vitamina D dnevno, razen če ima bolnik hiperkalciemijo. *Bolniki z okvaro ledvic:* Prilagoditev odmerka ni potrebna. Izkušnje pri bolnikih na dializi ali s hudo okvaro ledvic (očistek kreatinina < 30 ml/min) so omejene. *Bolniki z okvaro jeter:* Varnost in učinkovitost denosumaba nista raziskani. *Starejši bolniki (stari ≥ 65 let):* Prilagoditev odmerka ni potrebna. *Pediatrični bolniki:* Uporaba zdravila XGEVA® ni priporočljiva za pediatrične bolnike (stare < 18 let), ker njegovi učinkovitost in varnost pri teh bolnikih nista dokazani. Za subkutano uporabo. Zdravilo XGEVA® mora aplicirati zdravstveni delavec. **KONTRAINDIKACIJE:** Preobčutljivost na zdravilno učinkovino ali katero koli pomožno snov. Huda, nezdravljena hipokalciemija. **POSEBNA OPOZORILA IN PREVIDNOSTNI UKREPI:** Vsi bolniki morajo prejemati dodatek kalcija in vitamina D, razen če ima bolnik hiperkalciemijo. Obstoječo hipokalciemijo je treba odpraviti še pred začetkom zdravljenja z zdravilom XGEVA®. Hipokalciemija se lahko pojavi kadarkoli med zdravljenjem z zdravilom XGEVA®. Najpogosteje se pojavi v prvih 6 mesecih zdravljenja. Bolniki s hudo okvaro ledvic (očistek kreatinina < 30 ml/min) ali na dializi imajo večje tveganje za pojav hipokalciemije, tem bolnikom je priporočljivo kontrolirati koncentracijo kalcija. Če se med prejemanjem zdravila XGEVA® pojavi hipokalciemija, je lahko potrebno dodatno dodajanje kalcija. Bolniki z aktivnimi zobnimi boleznimi ali boleznimi čeljustnice morajo pred zdravljenjem z zdravilom XGEVA® opraviti zobozdravstveni pregled, vključno z ustreznimi preventivnimi zobozdravstvenimi ukrepi. Med zdravljenjem se morajo bolniki izogniti invazivnim zobozdravstvenim posegom, če je to mogoče, ter skrbeti za dobro ustno higieno. Bolnike, pri katerih med zdravljenjem z zdravilom XGEVA® obstaja sum na osteonekrozo čeljustnice ali se jim ta razvije, mora zdraviti zobozdravnik ali ustni kirurg. Pri takšnih bolnikih lahko obsežna zobna operacija za zdravljenje osteonekroze čeljustnice stanje še poslabša. Preden zdravnik predpiše zdravilo XGEVA® bolniku z neugodnimi dejavniki tveganja za osteonekrozo čeljustnice in če se med zdravljenjem z zdravilom XGEVA® pojavi osteonekroza čeljustnice, je treba narediti individualno oceno koristi in tveganja. Atipični zlomi stegnenice se lahko pojavijo že ob majhni poškodbi ali celo brez poškodbe, in sicer v subtrohanternem in diafiznem predelu stegnenice. Za te dogodke so značilni specifični radiografski izvidi. O njih so poročali tudi pri bolnikih z določenimi sočasnimi bolezenskimi stanji (npr. s pomanjkanjem vitamina D, revmatoidnim artritisom, hipofosfatazijo) in med uporabo določenih zdravil (npr. difosfonatov, glukokortikoidov, zaviralcev protonske črpalke). Ti dogodki so se pojavili tudi brez antiresorpcijskega zdravljenja. Podobni zlomi, opisani v zvezi z difosfonati, so pogosto obojestranski, zato je treba pri bolnikih, ki se zdravijo z denosumabom in so imeli zlom srednjega dela stegnenice, opraviti tudi pregled druge stegnenice. Pri bolnikih, pri katerih obstaja sum na atipičen zlom stegnenice, je treba razmisliti o prenehanju uporabe zdravila XGEVA® ob vrednotenju bolnika glede na individualno oceno koristi in tveganja. Bolnikom je treba naročiti, da morajo med zdravljenjem z zdravilom XGEVA® zdravniku poročati o novi ali nenavadni bolečini v stegnu, kolku ali dimljah. Bolnike s takšnimi simptomi je treba preiskati glede nepopolnega zloma stegnenice. Bolniki, zdravljeni z zdravilom XGEVA®, sočasno ne smejo prejemati drugih zdravil, ki vsebujejo denosumab (za indikacije pri osteoporozi), in difosfonatov. Bolniki z redko prirojeno motnjo intolerance za fruktozo ne smejo uporabljati zdravila XGEVA®. **INTERAKCIJE:** Študij medsebojnega delovanja niso izvedli. V kliničnih preskušanjih sočasna kemoterapija in/ali hormonsko zdravljenje ali predhodna intravenska izpostavljenost difosfonatom niso klinično pomembno spremenili najmanjše koncentracije denosumaba v serumu in farmakodinamike denosumaba (N-telopeptid v urinu, prilagojen na kreatinin, uNTx/Cr). **POVZETEK NEŽELENIH UČINKOV:** Zelo pogosti (≥ 1/10): dispneja, driska. Pogosti (≥ 1/100 do < 1/10): hipokalciemija, hipofosfatemija, ekstrakcija zoba, hiperhidroza, osteonekroza čeljustnice. Redki (≥ 1/10.000 do < 1/1.000): preobčutljivost na zdravilo, anafilaktična reakcija, atipični zlom stegnenice. **FARMACEVTSKI PODATKI:** Shranjujte v hladilniku (2 °C - 8 °C). Ne zamrzujte. **NAČIN IN REŽIM PREDPISOVANJA TER IZDAJE ZDRAVILA:** Predpisovanje in izdaja zdravila je le na recept s posebnim režimom – ZZ. **IMETNIK DOVOLJENJA ZA PROMET:** Amgen Europe B.V., Minervum 7061, NL-4817 ZK Breda, Nizozemska. **Dodatna pojasnila lahko dobite v lokalni pisarni:** Amgen zdravila d.o.o., Šmartinska 140, SI-1000 Ljubljana. **DATUM ZADNJE REVIZIJE BESEDILA:** 24. oktober 2013. **DATUM PRIPRAVE INFORMACIJE:** Julij 2014. Podrobne informacije o zdravilu so objavljene na spletni strani Evropske agencije za zdravila http://www.ema.europa.eu/.
Literatura: 1. Povzetek glavnih značilnosti zdravila XGEVA® (denosumab), Amgen 2013.

SLO-DO-AMG-008-2014-JUL

AMGEN®

Predstavljamo GIOTRIF®

Stopimo na novo raven učinkovitosti v prvi liniji

- Prvi registrirani **ireverzibilni zaviralec družine ErbB**[1]
- **Giotrif® je prvo zdravilo,** ki signifikantno **izboljša preživetje** v 1.liniji zdravljenja napredovalega EGFR M+ NSCLC v primerjavi s kemoterapijo.[2]

GIO 08/september 2014 "Samo za strokovno javnost"

*N=345. PFS=progression free survival

Literatura: 1. Sequist LV, Yang JCH, Yamamoto N, O Byrne K, Hirsh V, Mok T, et.al. Phase III study of afatinib or cisplatin plus pemetrexed in patients with metastatic lung adenocarcinoma with EGFR mutations. JCO 2013; 31: 3327-34. **2.**Afatinib OS analysis. ASCO abstract and oral presentation, Chicago 2014. **3.** Na spletnih straneh Zavoda za zdravstveno zavarovanje Slovenije objavljeno e-gradivo: Spremembe list zdravil in živil, 10.9.2014 dostopno na http://www.zzzs.si/zzzs/info/egradiva.nsf/

SKRAJŠAN POVZETEK GLAVNIH ZNAČILNOSTI ZDRAVILA

GIOTRIF 20 mg filmsko obložene tablete, GIOTRIF 30 mg filmsko obložene tablete, GIOTRIF 40 mg filmsko obložene tablete, GIOTRIF 50 mg filmsko obložene tablete

▼ Za to zdravilo se izvaja dodatno spremljanje varnosti.

Kakovostna in količinska sestava: ena filmsko obloženo tableta vsebuje 20 mg (30 mg/ 40 mg/ 50 mg) afatiniba (v obliki dimaleata). Vsebuje laktozo. **Terapevtske indikacije:** kot monoterapija je indicirano za zdravljenje odraslih bolnikov, ki se še niso zdravili z zaviralcem receptorja za epidermalni rastni dejavnik (EGFR) TK z lokalno napredovalim ali metastaznim nedrobnoceličnim pljučnim rakom (NSCLC) z aktivacijsko(imi) mutacijo(ami) EGFR. **Odmerjanje in način uporabe:** zdravljenje z zdravilom GIOTRIF mora uvesti in nadzorovati zdravnik, ki ima izkušnje z uporabo zdravil za zdravljenje raka. Pred začetkom zdravljenja z zdravilom GIOTRIF je treba določiti stanje mutacije EGFR z dobro validirano in robustno metodologijo, da bi se izognili lažno negativnim ali lažno pozitivnim ocenam. *Odmerjanje*: priporočeni odmerek zdravila je 40 mg enkrat na dan. Zdravljenje z zdravilom GIOTRIF naj traja, dokler bolezen ne začne napredovati ali do tedaj, ko bolnik zdravila več ne prenaša. Odmerek je možno tudi povečati, pri bolnikih, ki zdravljenje dobro prenašajo, oziroma zmanjšati pri tistih, pri katerih se pojavijo simptomatične neželene reakcije. Največji dnevni odmerek je 50 mg. Bolnikom, katerim smo odmerek kdaj prej zmanjšali, ga ne smemo povečati. Zdravila bolniki ne smejo jemati ob jedi. Zaviralce P-gp je treba dajati z zamikom. Zdravljenje z zdravilom GIOTRIF ni priporočljivo za bolnike s hudo ledvično ali hudo jetrno okvaro in za pediatrično populacijo. *Za natančnejša navodila glede odmerjanja glejte Povzetek glavnih značilnosti zdravila.***Kontraindikacije**: preobčutljivost za afatinib ali katero koli pomožno snov, nosečnost in dojenje. Ženske v rodni dobi morajo med zdravljenjem in še najmanj 1 mesec po zadnjem odmerku uporabljati ustrezno kontracepcijo.**Posebna opozorila in previdnostni ukrepi:** driska, s kožo povezanimi neželeni dogodki (izpuščaj, akne, bulozna, mehurjasta in eksfoliativna kožna obolenja; Stevens-Johnsonov sindrom), ženski spol, manjša telesna masa, obstoječa ledvična okvara, intersticijska pljučna bolezen in podobne neželene reakcije (pljučna infiltracija, pnevmonitis, akutni sindrom dihalne stiske, alergijski alveolitis), huda jetrna okvara, keratitis, bolniki s tveganjem za srčna obolenja in bolnikih z boleznimi, ki lahko vplivajo na LVEF; sočasno zdravljenju z močnimi induktorji P-gp, redka dedna motnja neprenašanja galaktoze, laponska oblika pomanjkanja laktaze ali malabsorpcija glukoze/galaktoze. Zdravilo GIOTRIF ima blag vpliv na sposobnost vožnje in upravljanja s stroji. **Interakcije:** močni zaviralci P-gp (tudi, toda ne samo, ritonavir, ciklosporin A, ketokonazol, itrakonazol, eritromicin, verapamil, kinidin, takrolimus, nelfinavir, sakinavir in amiodaron) in BCRP, močni induktorji P-gp (tudi, a ne samo, rifampicin, karbamazepin, fenitoin, fenobarbital ali šentjanževka), substrati Pgp, peroralni substrati za BCRP (tudi, a ne samo, rosuvastatina in sulfasalazina) in hrana. **Neželeni učinki:** Zelo pogosti: paronihija, zmanjšan tek, epistaksa, driska, stomatitis, izpuščaj, akneiformni dermatitis, pruritus in suha koža. Pogosti: cistitis, dehidracija, hipokaliemija, disgevzija, konjunktivitis, suho oko, rinoreja, dispepsija, heilitis, povečanje alanin-aminotransferaze, povečanje aspartat-aminotransferaze, sindrom roke in noge, mišični krči, ledvična okvara/ ledvična odpoved, pireksija in zmanjšanje telesne mase. Občasni: keratitis in intersticijska pljučna bolezen. **Način in režim izdaje:** Rp/Spec. **Imetnik dovoljenja za promet:** Boehringer Ingelheim International GmbH, Binger Strasse 173, D-55216 Ingelheim am Rhein, Nemčija. **Za podrobnejše informacije glejte** Povzetek glavnih značilnosti zdravila 09/2013.

NOVO
GIOTRIF®
(afatinib) tablete
DVIGNITI PRIČAKOVANJA

UKREPAJMO
ONKOLOGIJA BOEHRINGER INGELHEIM

Boehringer Ingelheim

ERBITUX®
CETUXIMAB

See the difference

Individualizirano zdravljenje za bolnike z metastatskim kolorektalnim rakom

Merck Serono Onkologija | *Ključ je v kombinaciji*

Erbitux 5 mg/ml raztopina za infundiranje
Skrajšan povzetek glavnih značilnosti zdravila

Sestava: En ml raztopine za infundiranje vsebuje 5 mg cetuksimaba in pomožne snovi. Cetuksimab je himerno monoklonsko IgG_1 protitelo. **Terapevtske indikacije:** Zdravilo Erbitux je indicirano za zdravljenje bolnikov z metastatskim kolorektalnim rakom z ekspresijo receptorjev EGFR in nemutiranim tipom RAS v kombinaciji s kemoterapijo na osnovi irinotekana, kot primarno zdravljenje v kombinaciji s FOLFOX in kot samostojno zdravilo pri bolnikih, pri katerih zdravljenje z oksaliplatinom in zdravljenje na osnovi irinotekana ni bilo uspešno in pri bolnikih, ki ne prenašajo irinotekana. Zdravilo Erbitux je indicirano za zdravljenje bolnikov z rakom skvamoznih celic glave in vratu v kombinaciji z radioterapijo za lokalno napredovalo bolezen in v kombinaciji s kemoterapijo na osnovi platine za ponavljajočo se in/ali metastatsko bolezen. **Odmerjanje in način uporabe:** Zdravilo Erbitux pri vseh indikacijah infundirajte enkrat na teden. Pred prvo infuzijo mora bolnik prejeti premedikacijo z antihistaminikom in kortikosteroidom najmanj 1 uro pred uporabo cetuksimaba. Začetni odmerek je 400 mg cetuksimaba na m^2 telesne površine. Vsi naslednji tedenski odmerki so vsak po 250 mg/m^2. **Kontraindikacije:** Zdravilo Erbitux je kontraindicirano pri bolnikih z znano hudo preobčutljivostno reakcijo (3. ali 4. stopnje) na cetuksimab. Kombinacija zdravila Erbitux s kemoterapijo, ki vsebuje oksaliplatin, je kontraindicirana pri bolnikih z metastatskim kolorektalnim rakom z mutiranim tipom RAS ali kadar status RAS ni znan. **Posebna opozorila in previdnostni ukrepi:** Pojav hude reakcije, povezane z infundiranjem, zahteva takojšnjo in stalno ukinitev terapije s cetuksimabom. Če pri bolniku nastopi blaga ali zmerna reakcija, povezana z infundiranjem, lahko zmanjšate hitrost infundiranja. Priporočljivo je, da ostane hitrost infundiranja na nižji vrednosti tudi pri vseh naslednjih infuzijah. Če se pri bolniku pojavi kožna reakcija, ki je ne more prenašati, ali huda kožna reakcija (≥ 3. stopnje po kriterijih CTCAE), morate prekiniti terapijo s cetuksimabom. Z zdravljenjem smete nadaljevati le, če se je reakcija izboljšala do 2. stopnje. Če ugotovite intersticijsko bolezen pljuč, morate zdravljenje s cetuksimabom prekiniti, in bolnika ustrezno zdraviti. Zaradi možnosti pojava znižanja nivoja elektrolitov v serumu se pred in periodično med zdravljenjem s cetuksimabom priporoča določanje koncentracije elektrolitov v serumu. Pri bolnikih, ki prejemajo cetuksimab v kombinaciji s kemoterapijo na osnovi platine, obstaja večje tveganje za pojav hude nevtropenije. Takšne bolnike je potrebno skrbno nadzorovati. Pri predpisovanju cetuksimaba je treba upoštevati kardiovaskularno stanje in indeks zmogljivosti bolnika in sočasno dajanje kardiotoksičnih učinkovin kot so fluoropirimidini. Če je diagnoza ulcerativnega keratitisa potrjena, je treba zdravljenje s cetuksimabom prekiniti ali ukiniti. Cetuksimab je treba uporabljati previdno pri bolnikih z anamnezo keratitisa, ulcerativnega keratitisa ali zelo suhih oči. Cetuksimaba ne uporabljajte za zdravljenje bolnikov s kolorektalnim rakom, če imajo tumorje z mutacijo RAS ali pri katerih je tumorski status RAS neznan. **Interakcije:** Pri kombinaciji s fluoropirimidini se je v primerjavi z uporabo fluoropirimidinov, kot monoterapije, povečala pogostnost srčne ishemije, vključno z miokardnim infarktom in kongestivno srčno odpovedjo ter pogostnost sindroma dlani in stopal. V kombinaciji s kemoterapijo na osnovi platine se lahko poveča pogostnost hude levkopenije ali hude nevtropenije. V kombinaciji s kapecitabinom in oksaliplatinom (XELOX) se lahko poveča pogostnost hude driske. **Neželeni učinki:** Zelo pogosti (≥ 1/10): hipomagneziemija, povečanje ravni jetrnih encimov, kožne reakcije, blage ali zmerne reakcije povezane z infundiranjem, mukozitis, v nekaterih primerih resen. Pogosti (≥ 1/100 do < 1/10): dehidracija, hipokalciemija, anoreksija, glavobol, konjunktivitis, driska, navzeja, bruhanje, hude reakcije povezane z infundiranjem, utrujenost. **Posebna navodila za shranjevanje:** Shranjujte v hladilniku (2 °C - 8 °C). **Pakiranje:** 1 viala z 20 ml ali 100 ml raztopine. **Način in režim izdaje:** Izdaja zdravila je le na recept-H. **Imetnik dovoljenja za promet:** Merck KGaA, 64271 Darmstadt, Nemčija.

Datum zadnje revizije besedila: junij 2014.

Pred predpisovanjem zdravila natančno preberite celoten Povzetek glavnih značilnosti zdravila.

Samo za strokovno javnost.

Podrobnejše informacije so na voljo pri predstavniku imetnika dovoljenja za promet z zdravilom:
Merck d.o.o., Ameriška ulica 8, 1000 Ljubljana, tel.: 01 560 3810, faks: 01 560 3830, el. pošta: info@merck.si

www.merckserono.net
www.Erbitux-international.com

PM-ONC-04/2014 /29.08.2014

Merck Serono

Merck Serono is a division of Merck

MERCK

ORION PHARMA

Building well-being

dexdor®
in odvajanje od mehanske ventilacije

dexdor® izboljša obravnavo pacienta in izid zdravljenja:

- *Ohranja mirnega in sodelujočega pacienta;* [1, 2]
- *Izboljša pacientovo komunikacijo;* [1, 2]
- *Olajša ekstubacijo.* [1, 2]

dexdor®
dexmedetomidine

Miren Sodelujoč Pacient

1. Riker RR, Shehabi Y, Bokesch PM, Ceraso D, Wisemandle W, Koura F, et al. Dexmedetomidine vs midazolam for sedation of critically ill patients: a randomized trial. JAMA. 2009;301(5):489-99.
2. Jakob SM, Ruokonen E, Grounds RM, Sarapohja T, Garratt C, Pocock SJ, et al. Dexmedetomidine vs midazolam or propofol for sedation during prolonged mechanical ventilation: two randomized controlled trials. JAMA. 2012;307(11):1151-60.

Instructions for authors

The editorial policy

Radiology and Oncology is a multidisciplinary journal devoted to the publishing original and high quality scientific papers and review articles, pertinent to diagnostic and interventional radiology, computerized tomography, magnetic resonance, ultrasound, nuclear medicine, radiotherapy, clinical and experimental oncology, radiobiology, radiophysics and radiation protection. Therefore, the scope of the journal is to cover beside radiology the diagnostic and therapeutic aspects in oncology, which distinguishes it from other journals in the field.

The Editorial Board requires that the paper has not been published or submitted for publication elsewhere; the authors are responsible for all statements in their papers. Accepted articles become the property of the journal and, therefore cannot be published elsewhere without the written permission of the editors.

Submission of the manuscript

The manuscript written in English should be submitted to the journal via online submission system Editorial Manager available for this journal at: **www.radioloncol.com**.

In case of problems, please contact Sašo Trupej at saso.trupej@computing.si or the Editor of this journal at gsersa@onko-i.si

All articles are subjected to the editorial review and when the articles are appropriated they are reviewed by independent referees. In the cover letter, which must accompany the article, the authors are requested to suggest 3-4 researchers, competent to review their manuscript. However, please note that this will be treated only as a suggestion; the final selection of reviewers is exclusively the Editor's decision. The authors' names are revealed to the referees, but not vice versa.

Manuscripts which do not comply with the technical requirements stated herein will be returned to the authors for the correction before peer-review. The editorial board reserves the right to ask authors to make appropriate changes of the contents as well as grammatical and stylistic corrections when necessary. Page charges will be charged for manuscripts exceeding the recommended length, as well as additional editorial work and requests for printed reprints.

Articles are published printed and on-line as the open access (**www.degruyter.com/view/j/raon**).

All articles are subject to 700 EUR + VAT publication fee. Exceptionally, waiver of payment may be negotiated with editorial office, upon lack of funds.

Manuscripts submitted under multiple authorship are reviewed on the assumption that all listed authors concur in the submission and are responsible for its content; they must have agreed to its publication and have given the corresponding author the authority to act on their behalf in all matters pertaining to publication. The corresponding author is responsible for informing the coauthors of the manuscript status throughout the submission, review, and production process.

Preparation of manuscripts

Radiology and Oncology will consider manuscripts prepared according to the Uniform Requirements for Manuscripts Submitted to Biomedical Journals by International Committee of Medical Journal Editors (www.icmje.org). The manuscript should be written in grammatically and stylistically correct language. Abbreviations should be avoided. If their use is necessary, they should be explained at the first time mentioned. The technical data should conform to the SI system. The manuscript, excluding the references, tables, figures and figure legends, must not exceed 5000 words, and the number of figures and tables is limited to 8. Organize the text so that it includes: Introduction, Materials and methods, Results and Discussion. Exceptionally, the results and discussion can be combined in a single section. Start each section on a new page, and number each page consecutively with Arabic numerals.

The Title page should include a concise and informative title, followed by the full name(s) of the author(s); the institutional affiliation of each author; the name and address of the corresponding author (including telephone, fax and E-mail), and an abbreviated title (not exceeding 60 characters). This should be followed by the abstract page, summarizing in less than 250 words the reasons for the study, experimental approach, the major findings (with specific data if possible), and the principal conclusions, and providing 3-6 key words for indexing purposes. Structured abstracts are preferred. Slovene authors are requested to provide title and the abstract in Slovene language in a separate file. The text of the research article should then proceed as follows:

Introduction should summarize the rationale for the study or observation, citing only the essential references and stating the aim of the study.

Materials and methods should provide enough information to enable experiments to be repeated. New methods should be described in details.

Results should be presented clearly and concisely without repeating the data in the figures and tables. Emphasis should be on clear and precise presentation of results and their significance in relation to the aim of the investigation.

Discussion should explain the results rather than simply repeating them and interpret their significance and draw conclusions. It should discuss the results of the study in the light of previously published work.

Charts, Illustrations, Images and Tables

Charts, Illustrations, Images and Tables must be numbered and referred to in the text, with the appropriate location indicated. Charts, Illustrations and Images, provided electronically, should be of appropriate quality for good reproduction. Illustrations and charts must be vector image, created in CMYK color space, preferred font "Century Gothic", and saved as .AI, .EPS or .PDF format. Color charts, illustrations and Images are encouraged, and are published without additional charge. Image size must be 2.000 pixels on the longer side and saved as .JPG (maximum quality) format. In Images, mask the identities of the patients. Tables should be typed double-spaced, with a descriptive title and, if appropriate, units of numerical measurements included in the column heading. The files with the figures and tables can be uploaded as separate files.

References

References must be numbered in the order in which they appear in the text and their corresponding numbers quoted in the text. Authors are responsible for the accuracy of their references. References to the Abstracts and Letters to the Editor must be identified as such. Citation of papers in preparation or submitted for publication, unpublished observations, and personal communications should not be included in the reference list. If essential, such material may be incorporated in the appropriate place in the text. References follow the style of Index Medicus. All authors should be listed when their number does not exceed six; when there are seven or more authors, the first six listed are followed by "et al.". The following are some examples of references from articles, books and book chapters:

Dent RAG, Cole P. In vitro maturation of monocytes in squamous carcinoma of the lung. *Br J Cancer* 1981; **43:** 486-95.

Chapman S, Nakielny R. *A guide to radiological procedures*. London: Bailliere Tindall; 1986.

Evans R, Alexander P. Mechanisms of extracellular killing of nucleated mammalian cells by

macrophages. In: Nelson DS, editor. *Immunobiology of macrophage.* New York: Academic Press; 1976. p. 45-74.

Authorization for the use of human subjects or experimental animals

When reporting experiments on human subjects, authors should state whether the procedures followed the Helsinki Declaration. Patients have the right to privacy; therefore the identifying information (patient's names, hospital unit numbers) should not be published unless it is essential. In such cases the patient's informed consent for publication is needed, and should appear as an appropriate statement in the article. Institutional approval and Clinical Trial registration number is required.

The research using animal subjects should be conducted according to the EU Directive 2010/63/EU and following the Guidelines for the welfare and use of animals in cancer research (Br J Cancer 2010; 102: 1555 – 77). Authors must state the committee approving the experiments, and must confirm that all experiments were performed in accordance with relevant regulations.

These statements should appear in the Materials and methods section (or for contributions without this section, within the main text or in the captions of relevant figures or tables).

Transfer of copyright agreement

For the publication of accepted articles, authors are required to send the License to Publish to the publisher on the address of the editorial office. A properly completed License to Publish, signed by the Corresponding Author on behalf of all the authors, must be provided for each submitted manuscript.

The non-commercial use of each article will be governed by the Creative Commons Attribution-NonCommercial-NoDerivs license.

Conflict of interest

When the manuscript is submitted for publication, the authors are expected to disclose any relationship that might pose real, apparent or potential conflict of interest with respect to the results reported in that manuscript. Potential conflicts of interest include not only financial relationships but also other, non-financial relationships. In the Acknowledgement section the source of funding support should be mentioned. The Editors will make effort to ensure that conflicts of interest will not compromise the evaluation process of the submitted manuscripts; potential editors and reviewers will exempt themselves from review process when such conflict of interest exists. The statement of disclosure must be in the Cover letter accompanying the manuscript or submitted on the form available on **www.icmje.org/coi_disclosure.pdf**

Page proofs

Page proofs will be sent by E-mail to the corresponding author. It is their responsibility to check the proofs carefully and return a list of essential corrections to the editorial office within three days of receipt. Only grammatical corrections are acceptable at that time.

Open access

Papers are published electronically as open access on **www.degruyter.com/view/j/raon**, also papers accepted for publication as E-ahead of print.

kapsule
SUTENT®
sunitinibijev malat

Vsak dan šteje

za bolnike z napredovalim karcinomom ledvičnih celic

28. september	15. december	**30. april**	2. avgust
Jesenski festival	Zimske počitnice	**Družinsko srečanje**	Začetek kuharskega tečaja

BISTVENI PODATKI IZ POVZETKA GLAVNIH ZNAČILNOSTI ZDRAVILA

SUTENT 12,5 mg, 25 mg, 37,5 mg, 50 mg trde kapsule
Sestava in oblika zdravila: Ena kapsula vsebuje 12,5 mg, 25 mg, 37,5 mg ali 50 mg sunitiniba (v obliki sunitinibijevega malata). **Indikacije:** Zdravljenje neizrezljivega in/ali metastatskega malignega gastrointestinalnega stromalnega tumorja (GIST) pri odraslih, če zdravljenje z imatinibom zaradi odpornosti ali neprenašanja ni bilo uspešno. Zdravljenje napredovalega/metastatskega karcinoma ledvičnih celic (MRCC) pri odraslih. Zdravljenje neizrezljivih ali metastatskih, dobro diferenciranih nevroendokrinih tumorjev trebušne slinavke (pNET), kadar gre za napredovanje bolezni pri odraslih (izkušnje z zdravilom Sutent kot zdravilom prve izbire so omejene). **Odmerjanje in način uporabe:** Terapijo mora uvesti zdravnik, ki ima izkušnje z uporabo zdravil za zdravljenje rakavih bolezni. *GIST in MRCC:* Priporočeni odmerek je 50 mg peroralno enkrat na dan, 4 tedne zapored; temu sledi 2-tedenski premor (Shema 4/2), tako da celotni ciklus traja 6 tednov. *pNET:* Priporočeni odmerek je 37,5 mg peroralno enkrat na dan, brez načrtovanega premora. *Prilagajanje odmerka*: Odmerek je mogoče prilagajati v povečanjih po 12,5 mg, upoštevaje individualno varnost in prenašanje. Pri GIST in MRCC dnevni odmerek ne sme preseči 75 mg in ne sme biti manjši od 25 mg; pri pNET je največji odmerek 50 mg na dan, z možnimi prekinitvami zdravljenja. Pri sočasni uporabi z močnimi zaviralci ali induktorji CYP3A4 je treba odmerek ustrezno prilagoditi. *Pediatrična populacija:* Uporaba sunitiniba ni priporočljiva. *Starejši bolniki (≥ 65 let):* Med starejšimi in mlajšimi bolniki niso opazili pomembnih razlik v varnosti in učinkovitosti. *Okvara jeter:* Pri bolnikih z jetrno okvaro razreda A in B po Child-Pughu prilagoditev odmerka ni potrebna; pri bolnikih z okvaro razreda C sunitinib ni bil preizkušen, zato njegova uporaba ni priporočljiva. *Okvara ledvic:* Prilagajanje začetnega odmerka ni potrebno, nadaljnje prilagajanje odmerka naj temelji na varnosti in prenašanju pri posameznem bolniku. *Način uporabe:* Zdravilo Sutent se uporablja peroralno, bolnik ga lahko vzame s hrano ali brez nje. Če pozabi vzeti odmerek, ne sme dobiti dodatnega, temveč naj vzame običajni predpisani odmerek naslednji dan. **Kontraindikacije:** Preobčutljivost na zdravilno učinkovino ali katerokoli pomožno snov. **Posebna opozorila in previdnostni ukrepi:** *Bolezni kože in tkiv:* obarvanje kože, gangrenozna pioderma (običajno izgine po prekinitvi zdravljenja), hude kožne reakcije (multiformni eritem (EM), Stevens-Johnsonov sindrom (SJS) in toksična epidermalna nekroliza (TEN)). Če so prisotni znaki EM, SJS ali TEN, je treba zdravljenje prekiniti. *Krvavitve* v prebavilih, dihalih, sečilih, možganih; najpogosteje epistaksa; krvavitve tumorja, včasih s smrtnim izidom. **Pri bolnikih, ki se sočasno zdravijo z antikoagulanti**, se lahko **redno spremlja celotna krvna slika** (trombociti), **koagulacijski faktorji** (PT / INR) in opravi **telesni pregled**. *Bolezni prebavil:* poleg diareje, navzee/bruhanja, bolečine v trebuhu, dispepsije, stomatitisa/bolečine v ustih in ezofagitisa tudi hudi zapleti (včasih s smrtnim izidom), vključno z gastrointestinalno perforacijo. *Hipertenzija:* pri bolnikih s hudo hipertenzijo, ki je ni mogoče urediti z zdravili, je priporočljivo začasno prenehanje zdravljenja. *Hematološke bolezni:* zmanjšanje števila nevtrofilcev, trombocitov, anemija. *Bolezni srca in ožilja:* srčno-žilni dogodki, vključno s srčnim popuščanjem, kardiomiopatijo in motnjami v delovanju miokarda, v nekaterih primerih s smrtnim izidom. Sunitinib povečuje tveganje za pojav kardiomiopatije. *Podaljšanje intervala QT:* previdna uporaba pri bolnikih z znano anamnezo podaljšanja intervala QT, tistih, ki jemljejo antiaritmike, in tistih z relevantno, že obstoječo srčno boleznijo, bradikardijo ali elektrolitskimi motnjami. *Venski in arterijski trombembolični dogodki*; arterijski včasih s smrtnim izidom. *Dogodki na dihalih:* dispneja, plevralni izliv, pljučna embolija ali pljučni edem; redki primeri s smrtnim izidom. *Moteno delovanje ščitnice:* bolnike je treba med zdravljenjem rutinsko spremljati glede delovanja ščitnice vsake 3 mesece. *Pankreatitis*, tudi resni primeri s smrtnim izidom. *Hepatotoksičnost*, nekateri primeri s smrtnim izidom. *Holecistitis*, vključno z akalkuloznim in emfizemskim holecistitisom. *Delovanje ledvic:* primeri zmanjšanega delovanja ledvic, odpovedi ledvic in/ali akutne odpovedi ledvic, v nekaterih primerih s smrtnim izidom. *Fistula:* če nastane fistula, je treba zdravljenje s sunitinibom prekiniti. *Oteženo celjenje ran:* pri bolnikih, pri katerih naj bi bil opravljen večji kirurški poseg, je priporočljiva začasna prekinitev zdravljenja s sunitinibom. *Osteonekroza čeljustnic:* pri sočasnem ali zaporednem dajanju zdravila Sutent in intravenskih bisfosfonatov je potrebna previdnost; invazivni zobozdravstveni posegi predstavljajo dodatni dejavnik tveganja. *Preobčutljivost/angioedem. Motnje okušanja. Konvulzije:* obstajajo poročila, nekatera s smrtnim izidom, o preiskovancih s konvulzijami in radiološkimi znaki sindroma reverzibilne posteriorne levkoencefalopatije. *Sindrom lize tumorja*, v nekaterih primerih s smrtnim izidom. *Okužbe:* **hude okužbe z ali brez nevtropenije** (okužbe **dihal**, **sečil**, **kože in sepsa**), **vključno z nekaterimi s smrtnim izidom**; redki primeri nekrotizitajočega fasciitisa, vključno s prizadetostjo presredka, ki so bili včasih smrtni. *Hipoglikemija*: če se pojavi simptomatska hipoglikemija, je treba zdravljenje s sunitinibom začasno prekiniti. Pri sladkornih bolnikih je treba redno preverjati raven glukoze v krvi in, če je treba, prilagoditi odmerek antidiabetika. **Medsebojno delovanje z drugimi zdravili:** (Študije so izvedli le pri odraslih.) Zdravila, ki lahko zvečajo koncentracijo sunitiniba v plazmi (ketokonazol, ritonavir, itrakonazol, eritromicin, klaritromicin ali sok grenivke). Zdravila, ki lahko zmanjšajo koncentracijo sunitiniba v plazmi (deksametazon, fenitoin, karbamazepin, rifampin, fenobarbital, *Hypericum perforatum* oz. šentjanževka). **Plodnost, nosečnost in dojenje:** Zdravila Sutent ne smemo uporabljati med nosečnostjo in tudi ne pri ženskah, ki ne uporabljajo ustrezne kontracepcije, razen če možna korist odtehta možno tveganje za plod. Ženske v rodni dobi naj med zdravljenjem z zdravilom Sutent ne zanosijo. Ženske, ki jemljejo zdravilo Sutent, ne smejo dojiti. Neklinični izsledki kažejo, da lahko zdravljenje s sunitinibom poslabša plodnost samcev in samic. **Vpliv na sposobnost vožnje in upravljanja s stroji:** Sutent lahko povzroči omotico. **Neželeni učinki:** Najbolj resni neželeni učinki (nekateri s smrtnim izidom) so: odpoved ledvic, srčno popuščanje, pljučna embolija, gastrointestinalna perforacija in krvavitve (npr. v dihalih, prebavilih, tumorju, sečilih in možganih). Najpogostejši neželeni učinki (ki so se pojavili pri vsaj 20 % bolnikov v registracijskih preskušanjih) so: zmanjšan apetit, motnje okušanja, hipertenzija, utrujenost, prebavne motnje (npr. driska, slabost, stomatitis, dispepsija in bruhanje), sprememba barve kože in sindrom palmarno-plantarne eritrodisestezije. Med najbolj pogostimi neželenimi učinki so hematološke motnje (nevtropenija, trombocitopenija, anemija in levkopenija). Ostali zelo pogosti (≥ 1/10) neželeni učinki so: hipotiroidizem, nespečnost, omotica, glavobol, dispneja, epistaksa, kašelj, bolečina v trebuhu, zaprtje, obarvanje kože, izpuščaj, spremembe barve las, suha koža, bolečine v udih, artralgija, bolečine v hrbtu, vnetje sluznice, edem, pireksija. **Način in režim izdaje:** Predpisovanje in zdaja zdravila je le na recept, zdravilo pa se uporablja samo v bolnišnicah. Izjemoma se lahko uporablja pri nadaljevanju zdravljenja na domu ob odpustu iz bolnišnice in nadaljnjem zdravljenju. **Imetnik dovoljenja za promet:** Pfizer Limited, Ramsgate Road, Sandwich, Kent, CT13 9NJ, Velika Britanija. **Datum zadnje revizije besedila:** 24.07.2014
Pred predpisovanjem se seznanite s celotnim povzetkom glavnih značilnosti zdravila.

SUT-09-14 Samo za strokovno javnost

Pfizer Luxembourg SARL, GRAND DUCHY OF LUXEMBOURG 51, Avenue J.F. Kennedy, L-1855
PFIZER, Podružnica Ljubljana, Letališka cesta 3c, 1000 Ljubljana, Slovenija

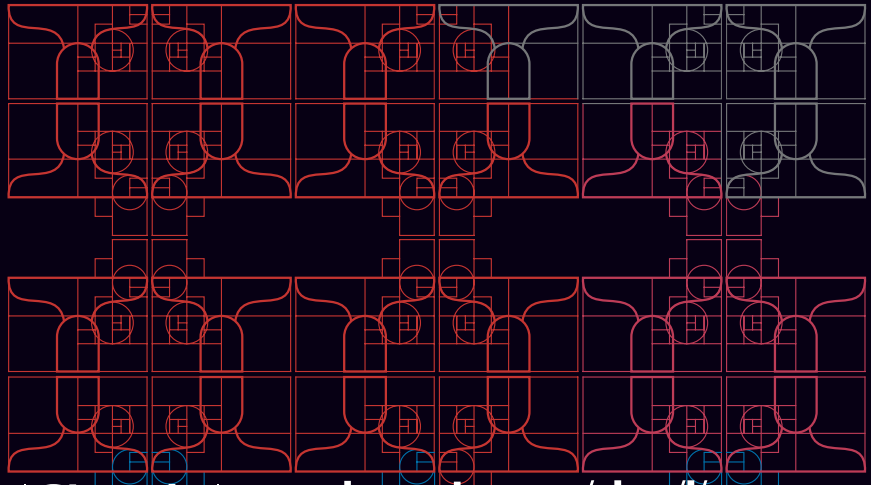

Radiology and Oncology | Ljubljana | Slovenia | www.degruyter.com/view/j/raon

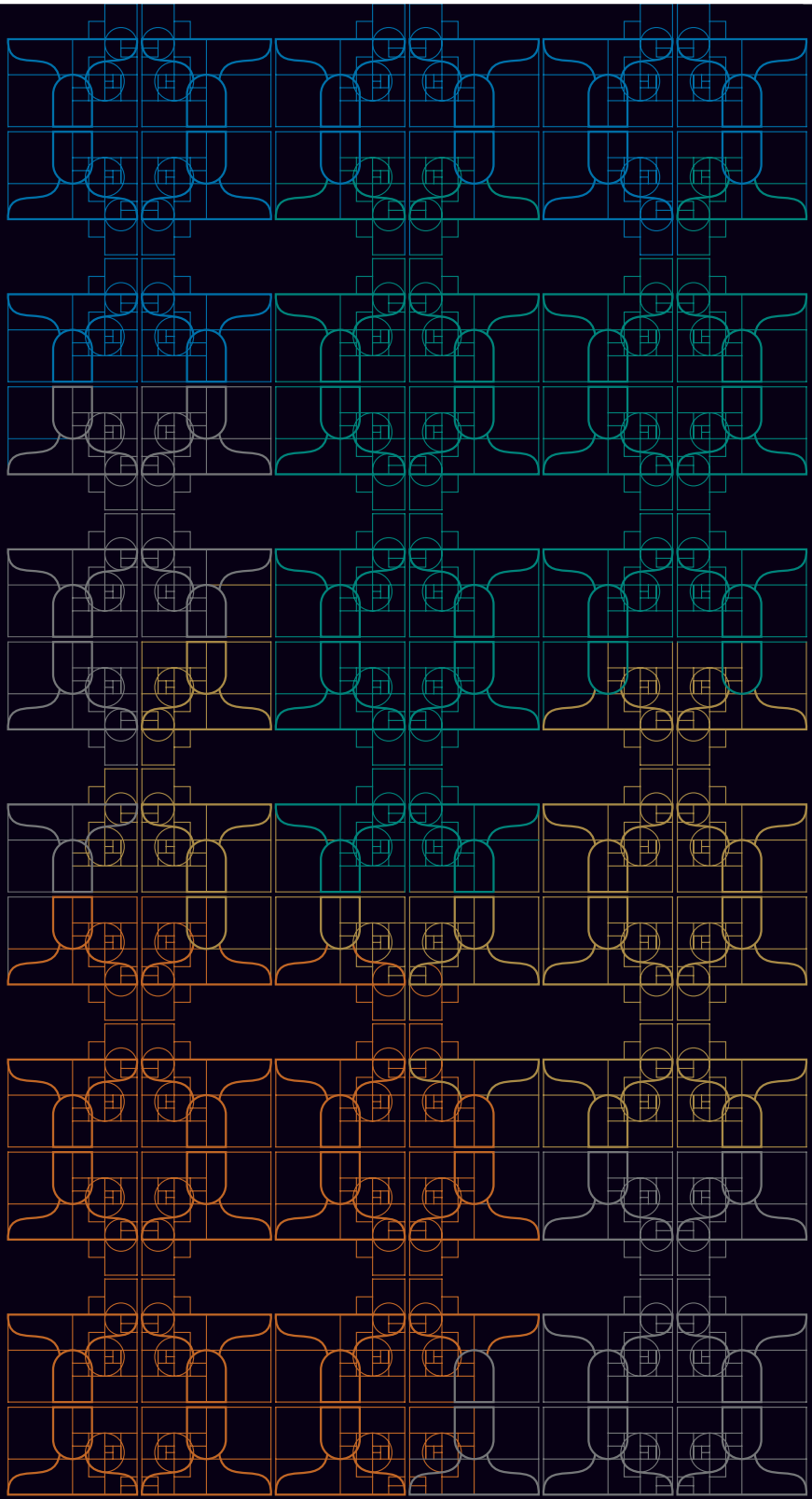

ISSN 1318 - 2099